Determination of Near Surface Hydraulic Conductivity from Infiltration Measurements

A thesis submitted

in partial fulfillment of the requirements

for the degree of

Doctor of Philosophy

by

Biplab Ghosh

Indian Institute of Technology Guwahati

Department of Civil Engineering

Guwahati - 781 039,

Assam, India

January 2020

Dedicated

To

My Mother for her Support and Encouragement

Throughout My Life

CERTIFICATE

This is to certify that the thesis entitled **"Determination of Near Surface Hydraulic Conductivity from Infiltration Measurements"**, submitted by **Mr. Biplab Ghosh**, to the Indian Institute of Technology Guwahati, India, for the award of the degree of Doctor of Philosophy in Civil Engineering, is a record of bonafide research work carried out by him under my guidance and supervision. The work embodied in this thesis has not been submitted for any other degree or diploma. In my opinion, the thesis is up to the standard of fulfilling the requirements of the doctoral degree as prescribed by the regulations of this Institute.

IIT Guwahati
Date:

Dr. Sreeja Pekkat
Associate Professor
Department of Civil Engineering
Indian Institute of Technology Guwahati
Guwahati-781039

STATEMENT

I do hereby declare that the matter embodied in this thesis is the result of investigations carried out by me in the Department of Civil Engineering, Indian Institute of Technology Guwahati, Assam, India. In keeping with the general practice of reporting scientific observations, due acknowledgements have been made wherever the work described is based on the findings of other investigators.

IIT Guwahati
Date:

Mr. Biplab Ghosh
Research Scholar
Department of Civil Engineering
Indian Institute of Technology Guwahati

Acknowledgements

It is my great pleasure to thank each and every one who helped directly or indirectly to complete my research work and made this thesis possible. I owe my deepest gratitude to all of them.

The first and foremost gratitude goes to my supervisor **Dr. Sreeja Pekkat** for her valuable guidance throughout the research work. I thank her for encouragement, patience towards research and support, which enabled me to develop a better understanding of the subject leading to the present this thesis. I would like to thank her for precious time taken to discuss thoroughly on the topic and make me what I am today.

I would also like to acknowledge my sincere gratitude to my doctoral committee members **Prof. A. K. Sarma, Prof. D. Bandyopadhyay, Dr. Abhishek Kumar** for their advices and suggestions throughout my research work.

I would like to thankfully acknowledge Indian Institute of Technology Guwahati, India for the financial support extended for performing this research work under Startup Research Grant program vide the project no. SG/CE/P/SP/2.

I would also like to express my sincere gratitude to Prof. Sreedeep S., Civil Engineering Department, IIT Guwahati, for his timely suggestions and encouragement.

I am grateful to my friends, **Mr. Nilanjan Mandal, Mr. Ardhedhu S Choudhury** for their support in making my stay at IIT Guwahati comfortable.

Deep heartedly, I thank my **mother** for her encouragement and motivation at each and every step.

Biplab Ghosh

Abstract

Infiltration characterize the water entry into the soil during rainfall and irrigation. It is an important parameter for the hydrological modelling of catchment. There are different methodologies adopted in the field that can induce variability in infiltration characterization. Such variabilities and the possible factors need to be studied in detail. The conventional and established ring infiltrometers suffers the limitations of being heavy, less portable, cumbersome and time consuming procedure and requires huge quantity of water. Disc infiltrometers are recent development for measuring infiltration characteristics with relative ease due to its portability and less requirement of water. The difference in measurement philosophy, working principle and mathematical formulations has resulted in conflicting observations on the measurement response of different infiltrometers.

There is a need for critical assessment of measurement variability associated with infiltrometer measurements under different field conditions, soil type and mathematical formulations. Not many studies exist in the literature that investigates the role of soil and infiltrometer related parameters on disc infiltrometer measurements. This is specifically true for the soil and field specific conditions of Indian subcontinent. There are no clear appraisals or there are contrasting findings in the literature on the variability induced in hydraulic characterization based on infiltrometer measurements.

This research work deals with laboratory and field evaluation of disc infiltrometer for gaining more confidence in field infiltration measurements. To gain more confidence in portable and simple mini disc infiltrometer (MDI), the measurements were compared with the results of conventional infiltrometer and permeameters. The utility of disc infiltrometer for determining spatial and temporal variation of infiltration characteristics in the field were demonstrated. The influence of short-term and long-term MDI measurements on hydraulic characterization was investigated. The influence of initial soil compaction state on infiltration characteristics was studied to check the possibility of a correlation between soil specific parameters and infiltration. The moisture and pressure head variation that happens in the subsurface during infiltration beneath MDI was studied using controlled laboratory column set up. Based on the results from this study, the appropriateness of different infiltration equations for defining hydraulic characteristics based on MDI measurements were evaluated.

Keywords: Infiltration, field measurement, laboratory measurement, mini disc infiltrometer, tension infiltrometer, double ring infiltrometer, permeameter, hydraulic conductivity, spatial interpolation, infiltration equations

Contents

List of Tables

List of Figures

Nomenclature

A_1	dimensionless van Genuchten parameter
A_2	dimensionless van Genuchten parameter
C_1	constant related to hydraulic conductivity (L/T)
C_2	constant related to hydraulic conductivity ($L/T^{1/2}$)
D	water diffusivity (L^2/T)
h_0	applied negative disc tension (L)
I	cumulative infiltration(L)
i	infiltration rate (L/T)
i_i	initial infiltration rate(L/T)
i_f	final quasi-steady state infiltration rate(L/T)
K	hydraulic conductivity(L/T)
K_s	saturated hydraulic conductivity(L/T)
K_{h_0}	near saturated near surface hydraulic conductivity(L/T)
l	pore-connectivity parameter
n	van Genuchten parameter representing pore-size distribution index
q	flux (L^3/T)
Q	steady-state flux (L^3/T)
r_0	radius of circular pond/ disc (L)
r	correlation coefficient
S	Sorptivity ($L/T^{1/2}$)
S_e	effective saturation
t	time (T)

t_f	time at which infiltration rate approaches the final quasi-steady state infiltration rate (T)
w	gravimetric water content
Z	gravity head (L)
α	van Genuchten parameter representing air entry value (1/L)
α_t	Gardner's parameter
γ	dry density (M/L^3)
γ_w	unit weight of water (M/L^3)
θ	volumetric water content
θ_r	residual volumetric water content
θ_s	saturated volumetric water content
λ_c	macroscopic capillary length (L)
ψ	suction head (L)

Abbreviations

DRI	Double ring infiltrometer
TI	Tension disc infiltrometer
MDI	Mini-disc Infiltrometer
GP	Guelph Permeameter
CHP	Constant head Permeameter
PI	Pressure Infiltrometer
SFH	Simplified falling head Infiltrometer
BB	Bottomless bucket method for measuring Infiltration
AM	Arithmetic Mean
SD	Standard Deviation
CV	Coefficient of Variation
1D	One Dimension
2D	Two Dimension
3D	Three Dimension
ANN	Artificial Neural Network
USCS	Unified Soil Classification System
SCS	Soil Conservation Service
GIS	Geographic Information System
ASTM	American Society for Testing and Materials
SP	Poorly graded sand
CL	Lean clay of low plasticity
MH	High plasticity silt
ML	Low plasticity silt
SA	Sand
RS	Red soil
P	Precipitation
E	Evaporation
ET	Evapotranspiration
GLUE	Generalized likelihood uncertainty estimation

BEST	Beerkan Estimation of Soil Transfer parameters
SWCC	Soil water characteristic curve
RMSE	Root mean square error
MSE	Mean square error
AEV	Air entry value
BAp	Bland-Altman plot
LoA	Limits of agreement
DL	Differentiated Linearization method
MLR	Multiple-Linear Regression
ANOVA	One-way analysis of variance
SS	Sum of squares
SSB	Sum of squares between groups
SSW	Sum of squares within groups
MSB	Mean of squares between groups
MSW	Mean of square within groups
W-G	Wooding-Gardner method
W-R	Weir's Refinement method
vG-Z	van- Genuchten Zhang method
W-S	White and Sully method
S-W	Simunek-Wooding method
H	Haverkamp method
A	Ankeny method
Z-I	Zhang method –I method
Z-II	Zhang method –II method
K-E	Kriging-Exponential spatial interpolation method
K-S	Kriging-Spherical spatial interpolation method
K-C	Kriging-Circular spatial interpolation method
K-L	Kriging-Linear spatial interpolation method
IDW	Inverse Distance Weighted Method for spatial interpolation
NNM	Natural Neighbor Method for spatial interpolation
SM	Spline Method for spatial interpolation
TM	Trend interpolation Method

Chapter 1

Introduction

1.1. General

Infiltration is the property of the soil that defines the entry of water into the subsurface at the ground during precipitation or irrigation process. It is an important soil-atmosphere boundary characteristic that significantly governs the hydrological cycle. The knowledge of infiltration is mandatory for hydrological modelling of runoff, irrigation management, watershed modelling, water balance studies in cover system and estimation of plant available water in the root zone. At catchment level, infiltration is one of the dominant parameters for determining flooding and drought conditions. The process of infiltration is complex and governed by multiple factors such as the soil texture, compaction state, gradation, plasticity characteristics, water retention characteristics, vegetative cover and the presence of preferential pathways (Loaiciga and Huang, 2007; Dagadu and Nimbalar, 2012 Assouline, 2013; Zhou, et al., 2015). These factors will influence infiltration characterization using different methodologies in different soils and climatic conditions.

There are different methodologies adopted for infiltration characterization such as single ring infiltrometer and double ring infiltrometer under constant and falling positive pressure head (or negligible head), disc infiltrometers under controlled negative head, Philip's dune infiltrometer (Munoz-Carpena, et al., 2002). The conventional and established ring infiltrometers suffer the limitations of being heavy, less portable, cumbersome and time consuming procedure and requires huge quantity of water. This limits its use in performing extensive infiltration measurements with adequate repetitions on catchment scale and on difficult grounds. Disc infiltrometers are recent developments for measuring infiltration characteristics corresponding to near saturated conditions with relative ease and are based on both transient and steady-state conditions. The advantage of this instrument is its portability, less water requirement, non-destructive and non-intrusive procedure causing minimal soil disturbance. It also permits extensive spatial-temporal measurements in the field with adequate repetitions. It is obvious from the literature that the measurement philosophy, working principle, mathematical formulations, and representative soil volume is different for infiltrometers. There are conflicting

observations on the measurement response of different infiltrometers reported in the literature (Morbidelli, et al., 2017).

1.2. Motivation of the Research

A need for critical assessment of measurement variability associated with infiltrometer measurements under different field conditions, soil type and mathematical formulations has motivated this study. Not many studies exist in the literature that understands the systemic influence of soil and infiltrometer related parameters on disc infiltrometer measurements. While there is quite a few evaluation of infiltration measurements reported in the literature (Nestingen, et al., 2018), not many studies exist for the soil and field specific conditions of Indian subcontinent. There are no clear appraisals or contrasting findings in the literature on the variability induced in hydraulic characterization based on infiltrometer measurements (Verbist, et al., 2013). This would create inconsistency when different infiltration measurement data sets are used as inputs in the same project.

It is felt that a detailed evaluation of instruments like mini disc infiltrometer is required for gaining confidence in infiltration measurements. Both short-term and long-term measurements need to be evaluated under controlled laboratory conditions. This will help to formulate a method for rapidly determining infiltration characteristics from short-term measurements, which will give identical results of long-term measurements. The influence of initial soil compaction state on infiltration need to be studied systematically. There is a need to check the possibility of a correlation between soil specific parameters and infiltration. The moisture and pressure head variation that happens in the subsurface during infiltration is important to understand subsurface moisture dynamics of a particular soil. Such an effort is also essential for verifying the numerical model used for defining flow in variably saturated soil. It is also of interest to evaluate whether the infiltration characteristics obtained using disc infiltrometer conforms to the prediction from infiltration models reported in the literature.

To gain more confidence in portable and simple disc infiltrometer measurements, it is important to compare the results of disc infiltrometer with conventional methods like double ring infiltrometer in the field and ensure the repeatability of measurements. The role of boundary tension head set in the disc infiltrometer on infiltration characteristics need to be understood in detail. Based on the above understanding, the utility of disc

infiltrometer for determining spatial and temporal variation of infiltration characteristics in the field need to be demonstrated. Motivation to fulfil these research needs is the basis of this research work, which has been organized as follows.

1.3. Organization of the Thesis

The thesis is organized into the following chapters:

Chapter 1 introduces the topic of research, motivation and need of the research and structure of the thesis.

Chapter 2 provides a review of literature relevant to the research area followed by critical appraisal and gaps in the research. Based on this, the objective and scopes of the research are listed.

Chapter 3 describes the study area, which is in the sub-basin of river Brahmaputra, Assam, north-east India. The measurement methodologies for soil hydraulic characteristics adopted in this study are discussed in this chapter.

Chapter 4 discusses the field studies pertained to the comparison of mini disc infiltrometer measurements with conventional double ring infiltrometer, tension disc infiltrometer for identical initial conditions and two different seasons. The chapter also analyzes the hydraulic conductivity determined from infiltrometers and Permeameters.

Chapter 5 demonstrates the utility of mini disc infiltrometer for determining seasonal and spatial variability of infiltration characteristics in the study area.

Chapter 6 investigates the appropriateness of nine steady state and transient mathematical equations for determining hydraulic conductivity based on mini disc infiltrometer measurements. The influence of short-term and long-term measurements on near saturated and saturated hydraulic conductivity based on mini disc infiltrometer measurements is presented as last part of this chapter.

Chapter 7 presents the laboratory investigation for investigating the influence and sensitivity of soil fraction, negative pressure head and initial compaction condition on infiltration characteristics. This chapter also presents multi-linear regression and ANN model for predicting hydraulic conductivity based on the known initial conditions.

Chapter 8 presents the controlled laboratory experiments with instrumented column and numerical modelling using Hydrus software for studying flow beneath mini disc infiltrometer.

Chapter 9 enlists the major conclusions from this research work, followed by major contributions and future scope of the research.

Chapter 2

Literature Review

2.1. General

Infiltration or the entry of water into the soil from the ground surface characterizes the fractioning of rain/ irrigation water into runoff, soil storage and groundwater recharge (Hillel, 1998; Corradini, et al., 2000; Mishra, et al., 2003; De Luca and Cepeda, 2016). The quantification of infiltration is mandatory for watershed modelling and estimating water and pollutant transport in the porous media (Jiang, et al., 2005; Chahinian, et al., 2006; Bean, et al., 2007; Pitt, et al., 2008; Assouline, 2013; Brown and Borst, 2014; Zhou, et al., 2015; Angulo-Jaramillo, et al., 2016; Alizadehtazi, et al., 2016; Lee, et al., 2016). The plant available water in the root zone is decided by the quantity of water infiltration (Hillel, 1998; van Dam and Feddes, 2000; Garg, et al., 2017). Accurate measurement of infiltration is necessary for water balance modeling related to hydrological projects (Lee, et al., 2016).

The infiltrated water moves downward under gravity and spread laterally under sorptive or capillary force (Philip, 1957; Zhang, 1997; Webb, et al., 2003; Dagadu and Nimbalar, 2012). Infiltration capacity is a mandatory input for various hydrological projects such as irrigation management, nutrient leaching, artificial recharge of aquifers, groundwater recharge, water and solute transport through soils, drainage and flood modeling (Chow, et al., 1988; van Genuchten, et al., 1996; Revol, et al., 1997; Hillel, 1998; Burian, et al., 1999; Mishra, et al., 2003; Lu and Likos, 2004; Chu and Marino, 2005; Lin and Wei, 2006; Loaiciga and Huang, 2007). Determination of water infiltration is necessary for the efficient design of drainage layer in landfill cover system (Yamsani, et al., 2016; Merino-Martín, et al., 2017) and permeable pavement systems (Brown and Borst, 2014).

In this chapter a detailed review of infiltration, determination of soil hydraulic properties with conventional methods and disc infiltrometer, seasonal variability of infiltration in different soil condition, laboratory and field studies on infiltration are carried out.

2.2. Determination of Infiltration

The general hydrologic water budget in terms of infiltration is represented by Eq. 2. 1.

$$F = B_I + P - E - T - ET - S - R - I_A - B_0 \quad (2.\ 1)$$

where F is the cumulative depth of infiltration; B_I is the boundary input; P is the precipitation; E is the evaporation; ET is the evapotranspiration.; S is the storage through retention or detention area; R is the surface runoff; I_A is the initial abstraction and B_0 is the boundary output.

Different equations used for determining infiltration differ by their mathematical representation and parameters involved. Infiltration models are used for calculating the infiltration rate and different infiltration modeling approaches are described in the following sections:

2.2.1. Theoretical Equations

The theoretical equations are based on the flow of water through unsaturated soil. The Richards' equation (Richards, 1931; Chow, et al., 1988), which describes water flow in variably saturated soil. This non-linear equation given by Eq. 2. 2 can be used for determining the infiltration rate.

$$\frac{\partial \theta}{\partial t} = \frac{\partial}{\partial z}\left(D\frac{\partial \theta}{\partial z} + K \right) \quad (2.\ 2)$$

where θ is the water content; D is the soil water diffusivity; z is the gravity head, and K is the hydraulic conductivity.

The physical basis for infiltration process is provided by the Richards equation, which is developed based on the Darcy's equation of flow in porous media and the mass conservation principle. Darcy's flux (q) is given by Eq. 2. 3.

$$q = -K\frac{\partial h}{\partial z} \quad (2.\ 3)$$

$$h = \psi + z \quad (2.\ 4)$$

where h is the total head, and Ψ is the suction head.

The continuity equation is given by Eq. 2. 5

$$\frac{\partial \theta}{\partial t} + \frac{\partial q}{\partial z} = 0 \quad (2.\ 5)$$

Using Eq. 2. 3 and 2. 5, Richards' equation is derived in the form given by Eq. 2. 2.

2.2.1.1. Green-Ampt Equation

Green and Ampt have developed an infiltration equation in the year 1911, to get an exact analytical solution based on Darcy's law (Chow, et al., 1988). This equation can be used to calculate cumulative infiltration and rate of infiltration. The Green-Ampt equation has two conditions based on the ponded depth i) when ponded depth is neglected (Eq. 2. 6) and (ii) when ponded depth is taken into account (Eq. 2. 8).

$$F(t) = Kt + \Psi \Delta\theta \ln\left[1 + \frac{F(t)}{1 + \Psi \Delta\theta}\right] \tag{2. 6}$$

$$f(t) = K\left(\frac{\Psi \Delta\theta}{F(t)} + 1\right) \tag{2. 7}$$

When ponded depth is considered ($t>t_p$) the equation takes the form as follows:

$$F(t) = K(t - t_0) + (\Psi - h_p)\Delta\theta \ln\left(1 + \frac{F(t)}{(\Psi - h_p)\Delta\theta}\right) \tag{2. 8}$$

where $F(t)$ is the cumulative infiltration; K is the hydraulic conductivity; Ψ is the wetting front soil suction head; θ is the water content; $f(t)$ is the infiltration rate; h_p is the ponded depth; t is the time at which the infiltration rate is calculated; t_0 is the initial time at which infiltration starts and t_p is the time to ponding.

2.2.1.2. Philip's Equation

Philip has solved the Richards equation under less restricted condition (Philip, 1957) using the Boltzmann transformation to convert the differential equation into an ordinary equation. By solving the ordinary equation, the equation for cumulative infiltration $F(t)$ was obtained and further, differentiating this will give the equation for rate of infiltration $f(t)$. It was assumed that the hydraulic conductivity (K) and soil water diffusivity (D) vary when moisture content changes. Philip's equation for cumulative infiltration is represented by Eq. 2. 9.

$$F(t) = St^{1/2} + Kt \tag{2. 9}$$

The infiltration rate equation is obtained by differentiating Eq. 2. 9 and is given by Eq. 2. 10.

$$f(t) = \frac{1}{2} St^{-1/2} + K \tag{2. 10}$$

where S is the sorptivity and t is the time after the beginning of infiltration.

2.2.2. Empirical Equations

2.2.2.1. Horton's Equation

One of the earliest infiltration equations was developed by Horton in the year 1933 (Chow, et al., 1988), who observed that infiltration begins at some rate f_0 and exponentially decreases until it reaches a constant rate *fc*.

$$f(t) = f_c + (f_0 - f_c)e^{-kt} \quad (2.\ 11)$$

where *f(t)* is the infiltration at time *t*; *fc* is the constant infiltration rate, f_0 is the initial infiltration rate at time t = 0 and *k* is the decay constant.

The main limitation of this equation is that Horton's equation assumes that the rate of rainfall, *R*, is more than the infiltration rate throughout the rain.

2.2.2.2. Kostiakov Equation

It is an empirical equation which is less restrictive because it does not require the assumptions regarding soil surface and soil profile conditions that the physically based equations require. Kostiakov (1932)) proposed a simple empirical power equation based on curve fitting from field data.

$$f = K_k t^{-a} \quad (2.\ 12)$$

where *f* is the infiltration rate; *t* is the time after infiltration starts, and K_k and α are constants, which depend on the type of soil and initial conditions.

The Kostiakov equation is widely used because of its simplicity, ease of determining the two constants from measured infiltration data and reasonable fit to infiltration data for many soils over short periods. The major flaws of this equation are that it predicts infiltration capacity to be infinite at *t* equals zero and approaches zero for long times, while actual infiltration rates approach a steady value (Chow, et al., 1988)

Mezencev (1948) proposed a modification to Kostiakov's equation by adding a constant to the equation that represents the final infiltration rate when the soil becomes saturated after prolonged infiltration.

$$f = K_k t^{-a} + f_c \quad (2.\ 13)$$

where f_c is the steady-state infiltration rate.

The Kostiakov and modified Kostiakov equations tend to be the preferred models used for irrigation infiltration, probably because it is less restrictive to the mode of water application than some other models.

2.3. Review on Mathematical Equations for Infiltration Analysis

Infiltration is a complex phenomenon, depending on soil and rainfall properties and initial and boundary conditions within the flow domain (Assouline, 2013). Vertical infiltration in layered soils was studied by many researchers (Fok, 1970; Hachum and Alfaro, 1980; Samani, et al., 1989), particularly using analytical and numerical methods (Hanks and Bowers, 1962; Whisler and Clute, 1966; Srivastava and Yeh, 1991; Romano, et al., 1998; Corradini, et al., 2000) and through experimental methods (Stauffer and Dracos, 1986; Serrano, 1990). From these literatures, it can be inferred that the transient procedure of infiltration is intricate because of the non-linearity of soil water characteristics and several boundary and initial conditions. The hysteretic behavior of the soil water interaction further increased the complexity. Efforts were made to comprehend the physics of infiltration and to advance measurement procedures of infiltration in the previous few decades.

Infiltration is effectively a two-phase flow system, where infiltrating water also displaces pore air (Faybishenko, 1999; Hillel, 1998). This displacement occurs readily, and therefore infiltration only needs to be studied purely in terms of the water phase dynamics. However, studies have shown that the air phase can have a significant influence on infiltration, either as entrapped air ahead of the wetting front, or as encapsulated air bubbles in the transmission zone (Constantz, et al., 1988; Faybishenko, 1999; Wang, et al., 2009).

Soil hydraulic characteristics were initially presented by Darcy in the year of 1856 for saturated soils and extended to unsaturated soils (Buckingham, 1907; Richards, 1931), where the solution necessities the information of the soil hydrological properties which can be attained from the curves of water retention and hydraulic conductivity. Philip (1969) provided the definition of sorptivity (S) as the proportionality constant between cumulative intakes into the unsaturated soil and the square root of time for one-dimensional sorption in the absence of gravity. Philip's two-term infiltration equation was used to determine soil sorptivity and soil hydraulic conductivity using cumulative infiltration data from the double ring and tension infiltrometers. In this state, the sorptivity (S) and the hydraulic conductivity (K) for different land slopes and water pressure heads were calculated by fitting Philip's equation to cumulative infiltration data. It was noted that the hydraulic conductivity (K) and sorptivity coefficient (S) were reduced with an increase

in tension (Raoof, et al., 2009). The sorptivity coefficient was increased and the hydraulic conductivity was decreased with the increase in slope gradient.

Warrick (1992) explored the relationship of sorptivity and microscopic capillary length. The results were significant for parameter estimation including applications related to the time of ponding and disc infiltrometers. Zhang (1997) used a two-term infiltration equation to determine soil sorptivity and hydraulic conductivity from cumulative infiltration data from the disc infiltrometer. Sorptivity and hydraulic conductivity were estimated for various soils along with different radii and tensions of the disc infiltrometer and initial infiltration conditions.

Several instruments were developed for the determination of the sorptivity and hydraulic conductivity of the soil based on infiltration such as, single or double ring infiltrometers under constant head (Bouwer, 1986; Wu, et al., 1997; Bodhinayake, et al., 2004; Fatehnia, et al., 2016), disc infiltrometers under controlled suction head (Warrick, 1992; Angulo-Jaramillo, et al. 2000; Vandervaere, et al., 2000), and falling head ring infiltrometers (Elrick, et al., 1995; Angulo-Jaramillo, et al., 2003). The flow rate into the soil from a single ring infiltrometer is a combination of both vertical and horizontal flow (Tricker, 1978). Reynolds and Elrick (1990) considered the infiltration process of a single ring as a three-dimensional (3D) problem. Marshall and Stirk (1950) showed that infiltration rates measured using single ring infiltrometers decreased as the ring diameter increased. Touma, et al. (2007) examined the estimation of sorptivity and saturated hydraulic conductivity form single ring infiltration data in the case of a small ring diameter, driven 0.4–0.5 cm into the soil to prevent lateral loss of water and under negligible positive water head. To do this, vertical one-dimensional (1D) and single ring cumulative infiltration data were generated numerically for soils with known hydrologic properties. Their analysis was based on an equation given by Haverkamp, et al. (1994) between the cumulative infiltration from a circular 3D source and that corresponding to 1D flow. Using several 1D physically based infiltration functions and a least square nonlinear optimization technique (Marquardt, 1963), it was concluded that single ring infiltration tests are suitable for the determination of sorptivity and saturated hydraulic conductivity, and are reliable for hydrological modeling purposes.

Double ring infiltrometers are widely used for in situ determination of soil hydraulic conductivity (Bouwer, 1986; Dirk, et al., 1999). A buffer ring was used to minimize the lateral movement from the inner ring on which the measurements were made

to obtain the 1D vertical infiltration capacity. Burgy and Luthin (1956) reported that there is no significant difference in the results of infiltration measured by single ring infiltrometers of 15 cm diameter and double ring infiltrometers with 15 cm inner ring and 30 cm outer ring diameter. Swartzendruber and Olson (1961a, b) conducted a series of double ring infiltration experiments with different sizes of outer rings to determine the buffer effect for sandy soil. It was found that the buffering brings the actual infiltration velocity close to 1D infiltration rate and the measurement error because of lateral flow becomes negligible as the diameter of the outer ring increases to 1.2 m. Ahuja (1976) reported that from an inner ring of 30 cm diameter, the lateral flow was practically eliminated when a buffering ring of 90 cm diameter was employed. Wu, et al. (1997), based on numerical data, showed that when the outer ring diameter was increased to 1.2 m, the measured infiltration rates were 20–33% greater than the 1D infiltration rates for three test soils. It becomes clear that the effectiveness of double ring apparatus cannot be judged accurately. There is no scientific consensus about the appropriate ring sizes for inner and outer ring diameter for measuring 1D vertical infiltration using double ring infiltrometers.

The basic concept is that cumulative infiltration data, from both inner and outer ring, can be transformed to a linearized equation for 1D infiltration (Valiantzas, 2010) to estimate the time required for the wetting front to reach the bottom of the cylinders. Subsequently, sorptivity and saturated hydraulic conductivity can be estimated by fitting the aforementioned 1D linearized equation on the double ring cumulative infiltration data (Pollalis and Valiantzas, 2014). From the numerical results, it was found that the proposed method provides parameter estimates for S and Ks of acceptable accuracy for the four selected soils that cover a range of soil spectrum.

One-dimensional water flow in a saturated-unsaturated soil can be measured in the field by a variety of methods. Richards, et al. (1956) presented one of the most common field methods, the unsteady drainage flux method or the instantaneous profile method to determine unsaturated hydraulic conductivity. Similarly, Hillel and Gardner (1970) provided another field method to determine unsaturated hydraulic conductivity which is known as the steady flux method. Transient laboratory methods like outflow or evaporation experiments show little sensitivity to the hydraulic conductivity at near saturated conditions. Wooding (1968) derived a steady state approximation approach

which is the base for most of the methods to estimate hydraulic conductivity using infiltration data with the disc infiltrometer.

The disc infiltrometer is becoming a widely used device for determining soil hydraulic properties in the field. There are several numerical studies which simulate the cumulative infiltration versus time response from a disc infiltrometer, wherein, the initial condition of the soil is important. Tension disc infiltrometer experiments are generally conducted until an apparent steady state is reached because most of the methods of analysis are based on Wooding's solution for steady state flux (Wooding, 1968). However, the time necessary to reach a steady state may be a penalizing aspect for soils with low permeability and the information contained in the transient stages can be lost. Moreover, steady state methods assume homogeneous soil and uniform initial water content which may be unrealistic when the volume of the soil sample is large. Zhang (1997) determined the unsaturated hydraulic conductivity using the disc infiltrometer by considering soil retention function. In the past decades, various numerical schemes such as, finite difference method (Hornung and Messing, 1981), finite element method (Zienkiewicz and Pareck, 1970; Neuman, 1973; Simunek, et al., 1998) and boundary element methods (Brebbia and Walker, 1980) were formulated to solve the Richard's equation.

Several analytical solutions were proposed by researchers (Cho, 1971; Wagenet et al., 1976; van Genuchten, 1980) and unfortunately, analytical solutions for more complex situations like transient water flow are either not available or cannot be derived. In such cases, numerical methods must be employed. Springer and Cundy (1987) described, how to envisage soil hydraulic properties from physical properties like texture for parameterizing physically based models of surface runoff. The overland flow simulations using texture based parameters were significantly different than those from the field based parameters.

Smith (1972) presented a model which is used to study the self-governing influence of soil type, initial soil moisture content, rainfall rate, and rainfall pattern. In this study, a dimensionless formula was formulated to describe the infiltration decay curves for all types of soils, initial conditions, and rainfall rates. Reynolds and Elrick (1991) simulated water movement in unsaturated soils. Hydraulic functions, the soil retention function and the unsaturated hydraulic conductivity function are essential for such simulation. The soil retention function is comparatively easier to measure than the unsaturated hydraulic conductivity function. Beven and Binley (1992) proposed a generalized likelihood

uncertainty estimation (GLUE) procedure which is an inverse modeling method permitting information to be pooled to determine probability distributions of parameters and predicting the models. Kumar, et al. (2010) discussed the GLUE procedure which is used for the calibration of hydrological models.

Haverkamp, et al. (1996) proposed a method that permits synchronized characterization of both the soil hydraulic properties, $h(\theta)$ and $K(\theta)$, distinct from the preceding infiltration-based methods. Lassabatère, et al. (2006) enhanced the procedure to streamline soil hydraulic characterization, which was termed as the Beerkan Estimation of Soil Transfer parameters (BEST). This method deliberates analytic methods for hydraulic characteristic curves and determines their texture dependent shape parameters from the particle-size study by pedo-transfer functions. Structure reliant scale parameters were determined with zero pressure head by 3D field infiltration measurements from the transient infiltration formulation by Haverkamp, et al. (1994). Mubarak, et al. (2009b) used the BEST technique to describe the temporal variability of soil hydraulic characteristics under different conditions. Yilmaz, et al. (2010) stated that the BEST procedure (BEST – slope) may lead to inaccurate values of saturated soil hydraulic conductivity particularly when the steady-state infiltration rate cannot be attained. A revised BEST procedure (BEST-intercept) was proposed to evade negative saturated soil hydraulic conductivity values. Xu, et al. (2012) have shown that the BEST technique and its modified method led to poor presentation while fitting a cumulative infiltration curve and caused low value for sand or wet soils. Bagarello, et al. (2014) suggested a third alternate algorithm (BEST-steady) incorporating the use of the steady-state part of the infiltration. The predictable benefit of BEST-steady method is that the difficulties related to the practice of the transient infiltration data are evaded. Di Prima, et al. (2018) conducted laboratory testing of Beerkan infiltration measurements for evaluating the role of soil sealing on the infiltration of water. Lassabatere, et al. (2019) studied the spatial inconsistency of infiltration and soil hydraulic properties at the field scale. Alagna, et al. (2019) used Beerkan measurements to determine soil hydraulic properties of a crusted loamy soil in a Mediterranean vineyard.

2.4. Comparative Assessment of Infiltration Measurements

Conventionally, infiltration is measured using a single or double ring infiltrometers under constant and falling head (ASTM D 3385). Other instruments used for estimating infiltration characteristics are disc infiltrometers under controlled negative head (Warrick,

1992; Angulo-Jaramillo, et al., 2000; Vandervaere, et al., 2000a, b), falling head ring infiltrometers (Elrick, et al., 1995; Angulo-Jaramillo, et al., 2003; Angulo-Jaramillo, et al., 2016), Philip's dune infiltrometer (Munoz-Carpena, et al., 2002) and lysimeters (Qashu, 1969). The conventional and established single ring and double ring infiltrometers (ASTM D3385) are heavy, less portable, follows cumbersome and time consuming procedure and requires a huge quantity of water. This limits its use in performing extensive infiltration measurements with adequate repetitions on a catchment scale and difficult grounds (McKenzie, et al., 2002). Disc infiltrometers are a recent development for measuring infiltration characteristics corresponding to near saturation conditions with relative ease (Moret Fernández, et al., 2009; Latorre, et al., 2013; Latorre, et al., 2015). The dominant mechanism governing flow is one dimensional in double ring infiltrometer and three-dimensional unsaturated wetting front migration under disc infiltrometer (Latorre, et al., 2013). The measurement philosophy, working principle, mathematical formulations, boundary conditions, and representative soil volume is different for double ring infiltrometer and disc infiltrometers (Haverkamp, et al., 1994; Reynolds, et al., 2002; McKenzie, et al., 2002; David and César, 2009).

In this context, a miniature version of disc infiltrometer, mini disc infiltrometer (MDI), has gained popularity due to its relative ease, high portability, non-invasive and non-intrusive procedure for measuring near surface and near saturated hydraulic conductivity (Dohnal, et al., 2010). Mini disc infiltrometer (MDI) is a handy and easily portable instrument, which is used for quantifying the infiltration based on transient flow of water from disc placed on the soil surface (Loaiciga and Huang, 2007; David and César, 2009; Moret Fernández, et al., 2009; Dagadu and Nimbalar, 2012; Latorre, et al., 2013; Latorre, et al., 2015). The three dimensional flow from the disc to the surrounding unsaturated soil can be used for the determination of near saturated hydraulic conductivity K_{h0} corresponding to a negative pressure head h_0 (Latorre, et al., 2013; Angulo-Jaramillo, et al., 2016). This allows extensive spatio-temporal measurements using MDI in the field with adequate repetitions (David and César, 2009; Latorre, et al., 2015).

Past studies have determined the hydraulic conductivity of vegetated soils and different plant covers using MDI (Homolák, et al., 2009; Gadi, et al., 2017). Researchers have proposed short term transient methods and long term steady state methods for analyzing disc infiltrometer data (Ankeny, et al., 1991; Logsdon and Jaynes, 1993; Jacques, et al., 2002; Angulo-Jaramillo, et al., 2000, 2016). These methods adopt different

assumptions, mathematical formulations and boundary conditions for estimating hydraulic characteristics (David and César, 2009; Haverkamp, et al., 1994; Reynolds, et al., 2002). This may lead to the variability in the determination of surface hydraulic conductivity using MDI (Verbist, et al., 2013). There are comparisons of different infiltrometer results and insightful discussions on the theoretical formulations used for MDI (Angulo-Jaramillo, et al., 2016). Ronayne, et al. (2012) have compared Guelph permeameters with disc infiltrometers and ring infiltrometers. The variabilities in the hydraulic conductivity depending on the measurement techniques are appraised in the literature (Verbist, et al., 2013). Researchers have carried out studies to evaluate different physically based, semi-empirical and empirical infiltration equations in different types of soil (Hsu, et al., 2002; Mishra, et al., 2003; Chahinian, et al., 2006; Sihag, et al., 2017). However, there is no conclusive recommendation on the appropriateness of any particular measurement methodology. This is mainly due to the lack of reference true value for hydraulic conductivity in the field (Morbidelli, et al., 2017).

Infiltrometers measure hydraulic properties of soil based on the cumulative water entry at the soil-atmosphere boundary whereas permeameters is based on the flow of water within the soil mass (Verbist, et al., 2010). There are several established field permeameters, which determines hydraulic conductivity based on the permeation of water that occurs through the soil (ASTM D 5856). Many in-situ methods were developed for determining the saturated hydraulic conductivity which includes, the auger-hole, piezometer methods, and well-pumping tests. From the literature (Morbidelli, et al., 2017), it can be noted that the hydraulic conductivity determined using Guelph permeameter (GP), double ring infiltrometer (DRI) and tension infiltrometer (TI) at field and laboratory scale, DRI grossly overestimated saturated hydraulic conductivity. It was observed that GP overestimated at laboratory scale and underestimated at the field scale, while TI results presented significant error ranging from 24 % to 66 % and the error in the MDI measurements were high as compared to the DRI (Nestingen, et al., 2018).

The purpose of infiltrometers and permeameters is to establish hydraulic characteristics in terms of hydraulic conductivity, sorptivity and matric flow potential (Reynolds, et al., 2002; David and César, 2009; Angulo-Jaramillo, et al., 2016). Even though the objective is the same, the philosophy of measurement is different for infiltrometers and permeameters. For infiltrometer, hydraulic characteristics are determined indirectly based on the entry of water into relatively dry soil. The cumulative

infiltration versus time response is analyzed by a steady state or transient method for determining hydraulic conductivity. For disc infiltrometer, this is termed as near saturated hydraulic conductivity (Angulo-Jaramillo, et al., 2016). On the contrary, for permeameters, the hydraulic conductivity is determined directly based on the flow within the soil mass following Darcy's law. It is noted that the initial and boundary conditions, working principle and mathematical formulations are different for infiltrometers and permeameters (Haverkamp, et al., 1994; Reynolds, et al., 2002; Luna-Saez, et al., 2005; David and César, 2009). They also exhibit a difference in terms of flow path dimensionality (1D, 2D or 3D), assumptions, short term or long term observations, theoretical formulations and zone of influence of measurements (Latorre, et al., 2013; Angulo-Jaramillo, et al., 2016).

2.5. Critical Appraisal of the Reviewed Literature

There are conflicting observations on the measurement response of different infiltrometers reported in the literature (Haverkamp, et al., 1994; Reynolds, et al., 2002; McKenzie, et al., 2002; David and César, 2009, Fodor, et al., 2011). There is still a need for critical evaluation of measurement variability among the infiltrometers for various field conditions. While there are quite a few evaluations of infiltration measurements reported in the literature (Vanderlinden, et al., 1998), none exists for the soil specific and field specific conditions in the Indian subcontinent. There are no clear appraisals, or contrasting findings in the literature on the extent of variability between saturated hydraulic conductivity obtained from DRI and near saturated hydraulic conductivity obtained from disc infiltrometers. This would help to appraise the magnitude of hydraulic characteristics when diverse infiltration data sets are used as inputs in different projects. Similarly, there are not many studies that critically evaluate the appropriateness of different mathematical equations for determining hydraulic conductivity based on disc infiltrometer measurements under identical field conditions and different seasons.

It is noted that the comparative studies among infiltrometers and permeameters are not conclusive in the literature and recommend further studies to understand the intra and inter variability of hydraulic conductivity. There are not many studies that critically evaluate the difference in hydraulic conductivity determined from infiltrometers and permeameters. For using these instruments for field measurements, it is mandatory to appraise the variability induced by these measurement procedures. It is noted that the

studied on field measurements evaluating the influence of procedural differences on hydraulic conductivity is sparse in the literature (Morbidelli, et al., 2017). The lack of quantifications of the association between hydraulic conductivity and soil compaction state and the soil type is due to cumbersome, arduous infiltration measurement techniques along with difficult to reach controlled field compaction conditions (Pitt, et al., 2008; Serrano, 1990). The quantification of the relationship between infiltration characteristics of a catchment and initial conditions and soil type is missing in the literature. There is a need for critical evaluation of the variability in infiltration measurements to explore the quantitative relationship and sensitivity of soil types and initial compaction state on soil hydraulic characteristics.

The relatively new mini disc infiltrometer (MDI) needs to be critically analyzed for throwing more insights on the appropriateness of different methodologies and mathematical analysis reported in the literature (Ankeny, et al., 1991; Haverkamp, et al., 1994; David and César, 2009; Angulo-Jaramillo, et al., 2016). More efforts are needed to add clarity to the MDI measurement methodology for determining infiltration characteristics of the catchment. This is mainly due to the handy experimental procedure and ease of using MDI in the field. Systematic laboratory studies with different soil types need to be carried out to quantify the influence of soil fraction, initial water content and dry density on infiltration, which is otherwise difficult to capture from conventional double ring infiltrometer and field measurements. The utility of disc infiltrometer for determining temporal and spatial variability of infiltration characteristics in the field need to be demonstrated. No studies are reported that explore the flow process that happens beneath the disc infiltrometer through carefully planned laboratory experiments and numerical simulation.

2.6. Objective and Scopes of the Research Work

The objective of the research is to evaluate the disc infiltrometer methodology and the associated mathematical equations for determining the near surface hydraulic conductivity from the infiltration characteristics of the soil. Following are the scopes of the work to meet this objective:

1. Field investigation of infiltration characteristics for a study area located in the sub-catchment of river Brahmaputra, north-east India.

i. Comparison of infiltration characteristics for the study area using conventional infiltrometers and permeameters with identical initial conditions for two different seasons.

ii. Studying the spatial and temporal variation of infiltration characteristics in the field measured using MDI.

2. Investigation on time dependent infiltration measurements and equations for determining hydraulic conductivity.

   i. Evaluation of steady and transient state mathematical equations for analysing MDI measurements in the field.

   ii. Study the influence of transient and steady state (short and long term) MDI measurements on near saturated and saturated hydraulic conductivity determination.

3. Laboratory investigation of infiltration characteristics for different soil types.

   i. Systematic laboratory studies with different soil types to quantify the influence of soil type, initial water content and dry density (initial compaction state) on infiltration.

   ii. Investigation of flow beneath MDI by performing controlled experiments and numerical simulation.

Chapter 3

Methodology and Study Area

3.1. General

In this chapter, the measurement methodologies for soil hydraulic characteristics and the detailed description of the study area where the infiltration experiments are carried out are discussed.

3.2. Measurement Methodology

There are several well-established infiltrometers and permeameters for measuring in-situ hydraulic conductivity. Infiltrometers measure hydraulic conductivity based on water entry into an unsaturated soil at soil-atmosphere boundary where as permeameters measure flow of water from one point to the other within the soil mass. This difference in measurement philosophy along with the methods of analysis involved in the measurement may result in varying estimates of in-situ hydraulic conductivity. In this study, infiltration characteristics were measured in the field using conventional Double Ring Infiltrometer (DRI), two disc infiltrometers (Mini Disc Infiltrometer, MDI and Tension Infiltrometer, TI) and Guelph Permeameter (GP) and in the laboratory, the constant head permeameter (CHP) is used for determining the saturated hydraulic conductivity of soils. The following sections discuss the theoretical background and working principle of different measurement methodologies adopted in this study.

3.2.1. Double Ring Infiltrometer (DRI)

The double ring infiltrometer consists of an inner and outer ring, which need to be inserted into the ground using a 3.6 kg hammer (ASTM D 3385). The diameter of the outer ring is 60 cm, and that of the inner ring is 30 cm with an annular space of 30 cm as shown in Fig. 3. 1. The weight of the DRI is 22.7 kg which makes it inconvenient for extensive use in the field. Each ring is supplied with a constant ponding depth of 5 cm. The infiltration rate is determined by the quantity of water that infiltrates into the soil per unit area per unit time. The volume of water added to the inner ring to maintain constant head is the measure of the volume of water that infiltrated into the soil. The volume of water infiltrated into the soil is converted to an incremental infiltration rate and plotted as a function of time.

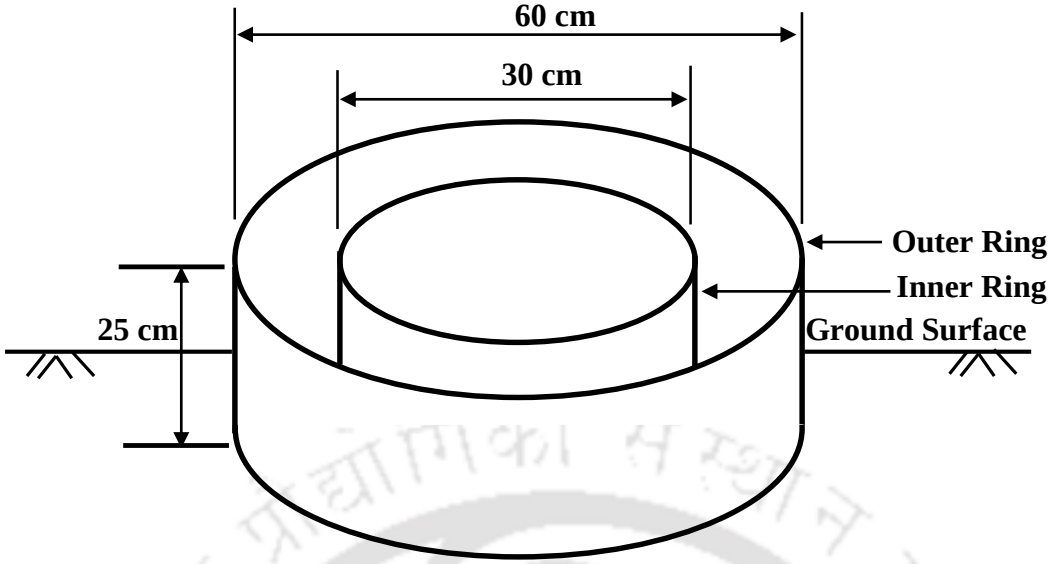

Fig. 3. 1 Schematic representation of double ring infiltrometer

Theoretically, a steady state infiltration rate is achieved once the soil becomes saturated. The time required to achieve steady state generally increases with fine soil texture (Angulo-Jaramillo, et al., 2016). The measurements were conducted for 1 hour within which the soil at all the stations attained a steady state infiltration rate. The field saturated hydraulic conductivity (K_s) can be estimated when water flow rate in the inner ring approaches a quasi-steady state (Angulo-Jaramillo, et al., 2016). The detailed procedure for measuring DRI is outlined in the literature (ASTM D 3385).

The flow of water from the inner cylinder of DRI is one-dimensional. At steady state condition, the flow of water from the infiltrometer is essentially under gravity force. Hence, the steady state infiltration rate can be approximated as the saturated hydraulic conductivity, K_s (Angulo-Jaramillo, et al., 2016; Reynolds, et al., 2002). The limitation of DRI is that the hammering or jacking of heavy rings into the ground can result in the destruction of soil structure causing the infiltration rate to be underestimated or overestimated and thus deviating from the true value of the saturated hydraulic conductivity (Angulo-Jaramillo, et al., 2016; McKenzie, et al., 2002). A cohesionless soil can undergo densification due to insertion, and a compacted soil can get destabilized affecting the preferential flow at the boundary.

3.2.2. Tension Infiltrometer (TI)

The tension infiltrometer (TI) is a disc infiltrometer in which the head causing flow at the disc (soil surface) can be adjusted between 0 mm to -200 mm (Tension Infiltrometer, 2825K1). Unlike DRI, the main advantage of TI is that the disc need not be inserted into the ground for the measurement of infiltration. This would avoid disturbance to the soil structure in which infiltration studies are conducted. It consists of a water reservoir through which the water infiltrates and a constant head Marriot bubbler tube to control the negative head at which water flows out of the disc as shown in Fig 3. 2. Due to the tension applied on the disc, water infiltrates into the underlying soil at a slower rate than ponded water head on the soil surface (as in DRI). TI measures the volume of water entering into the soil per unit time through the porous disc.

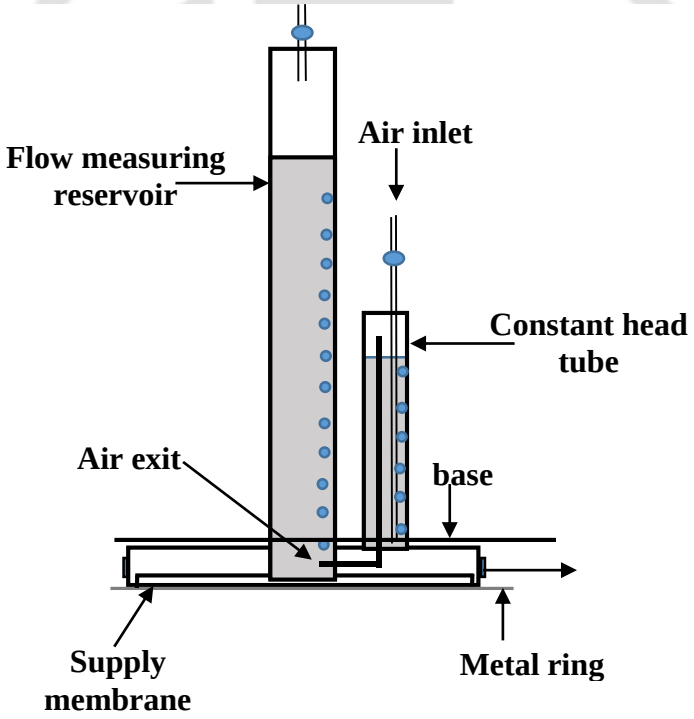

Fig. 3. 2 Schematic diagram of the tension infiltrometer

The methodology for determining $K(h_0)$ from the tension infiltrometer is based on the mathematical formulation for unconfined infiltration from a shallow pond proposed by (Wooding, 1968) and as given by Eq. 3. 1. The equation represents the steady state flow rate as a function of hydraulic conductivity given by Eq. 3. 1.

$$Q_{h_0} = \pi r^2 K_{h_0}\left[1+\frac{4}{\pi r\alpha_t}\right] \quad (3.\ 1)$$

where Q_{h_0} is the flow rate (mm^3/h), K_{h_0} is the hydraulic conductivity (mm/h) for the tension h_0 applied on the disc, and α_t is Gardner's parameter which represents the sorptivity number of the soil (McKenzie, et al., 2002). If α_t for a given soil is known, then K_{h_0} can be determined for the measured Q_{h_0} in the field using Eq. 3. 1.

Gardner proposed a relationship between the unsaturated hydraulic conductivity K_{h_0} and soil matric potential h_0 (Gardner, 1958) given by Eq. 3. 2.

$$K_{h_0} = K_s e^{\alpha_t h_0} \quad (3.\ 2)$$

where K_s is the saturated hydraulic conductivity.

Alternately, if α_t is unknown, as was the case for this study, a two hydraulic head was used to estimate K_{h_0} (Ankeny, et al., 1991; Angulo-Jaramillo, et al., 2016; McKenzie, et al., 2002). In this method, Q_{h_0} is determined corresponding to two tension heads h_1 and h_2, simultaneously as in Eq. 3. 3 and 3. 4, which can be further used to develop Eq. 3. 5 for determining α_t.

$$Q_{h_1} = \pi r^2 K_s e^{\alpha_t h_1}\left[1+\frac{4}{\pi r\alpha_t}\right] \quad (3.\ 3)$$

$$Q_{h_2} = \pi r^2 K_s e^{\alpha_t h_2}\left[1+\frac{4}{\pi r\alpha_t}\right] \quad (3.\ 4)$$

$$\alpha_t = \frac{\ln Q_{h_2} / \ln Q_{h_1}}{(h_2 - h_1)} \quad (3.\ 5)$$

For consistency, h_1 and h_2 are taken as zero and 6 cm, respectively, for all the locations in this study with Q_{h_2} measured before Q_{h_1} in order to maintain the wetting sequence. With α_t determined as stated above, it is possible to calculate K_{h_0} or K_s from Eqs. 3.1 and 3.3 or 3.4 respectively. It may be noted that the determination of K_{h_0} or K_s using TI is dependent on α_t, which is not readily known for the soils. Therefore, any error in α_t would influence the accuracy of hydraulic conductivity determined using TI.

3.2.3. Mini Disc Infiltrometer (MDI)

Mini disc infiltrometer (MDI) is a handy and easily portable instrument, which is used for quantifying the infiltration based on transient flow of water from disc placed on the soil surface (Loaiciga and Huang, 2007; David and César, 2009; Moret Fernández, et al., 2009; Dagadu and Nimbalar, 2012; Latorre, et al., 2013 and Latorre, et al., 2015). The three-dimensional flow from the disc to the surrounding unsaturated soil can be used for the determination of near saturated hydraulic conductivity (K_{h_0}) corresponding to a negative pressure head (h_0) (Latorre, et al., 2013; Angulo-Jaramillo, et al., 2016). The MDI can be used to perform extensive point measurements with adequate repetitions in a given catchment due to its portability and less water requirement.

MDI (Meter Group, 2018) is a miniature form of tension infiltrometer and ideal for field measurement due to its compact size and a limited quantity of water requirement. The total length of MDI is 32.7 cm, with an adjustable suction range of 0.5 cm to 7 cm. It has two chambers, which are filled with water. The upper chamber (bubbling chamber) controls the suction applied at the disc. In this study, the measurement was performed with 0.5, 2, 4 and 6 cm tension heads. Water for infiltration is stored in the lower chamber. There is a sintered, porous, stainless steel disc at the bottom of the lower chamber through which water infiltrates, having a thickness of 0.3 cm and a diameter of 4.5 cm as shown in Fig 3. 3. MDI has low capacity water reservoir made of small diameter tube which allows accurate measurements of water levels. This necessitates short term measurements and transient state approach for analyzing infiltration data as discussed below. For long term measurements, water reservoir needs to be filled intermittently resulting in discontinuities in infiltration measurements.

The volume of water that infiltrates into the soil corresponding to different time intervals are observed, and a graph was plotted between the square root of time on the x-axis and cumulative infiltration on the y-axis. A polynomial as given by Eq. 3. 6 is fitted to the data points (Zhang, 1997a),

$$I = C_1\sqrt{t} + C_2 t \qquad (3.\ 6)$$

where, C_1, and C_2 are the parameters related to the soil sorptivity and the hydraulic conductivity; I is the cumulative infiltration and t is the time.

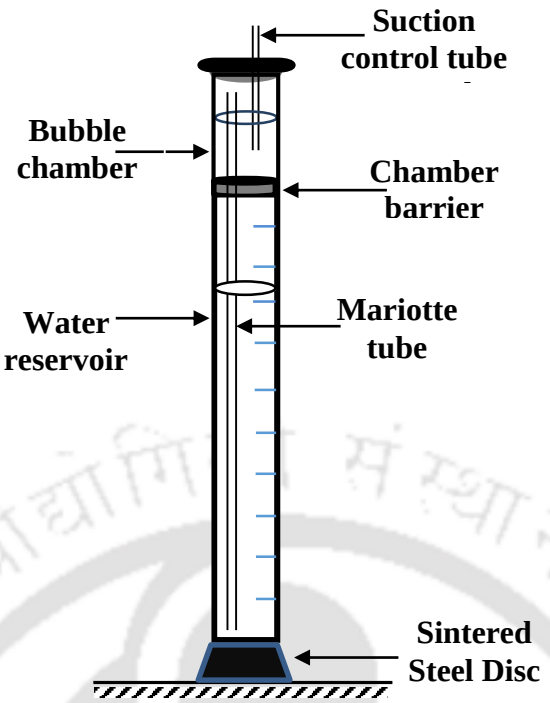

Fig. 3. 3 Schematic diagram of the mini disc infiltrometer

Near Saturated hydraulic conductivity of the soil, K_{h_0} is computed using Eq. 3. 7 (Zhang, 1997a),

$$K_{h_0} = \frac{C_2}{A_2} \tag{3. 7}$$

where, C_2 is the slope of the curve of the cumulative infiltration vs. square root of time, and A_2 is the parameter given by Eq. 3. 8 (Zhang, 1997a),

The volume of water that infiltrates into the soil corresponding to different time intervals are observed, and a graph was plotted between the square root of time on the x-axis and cumulative infiltration on the y-axis. A polynomial as given by Eq. 3. 6 is fitted to the data points (Zhang, 1997a),

$$I = C_1\sqrt{t} + C_2 t \tag{3. 8}$$

where, C_1, and C_2 are the parameters related to the soil sorptivity and the hydraulic conductivity; I is the cumulative infiltration and t is the time.

Near Saturated hydraulic conductivity of the soil, K_{h_0} is computed using Eq. 3. 7 (Zhang, 1997a),

$$K_{h_0} = \frac{C_2}{A_2} \tag{3. 9}$$

where, C_2 is the slope of the curve of the cumulative infiltration vs. square root of time, and A_2 is the parameter given by Eq. 3. 8 (Zhang, 1997a),

$$A_2 = \frac{11.65\left(n^{0.1}-1\right)\exp\left[2.92\left(n-0.19\right)\alpha h_0\right]}{\left(\alpha r_0\right)^{0.91}}, \qquad n \geq 1.9 \tag{3. 10}$$

$$= \frac{11.65\left(n^{0.1}-1\right)\exp\left[7.5\left(n-0.19\right)\alpha h_0\right]}{\left(\alpha r_0\right)^{0.91}}, \qquad n < 1.9$$

n and α are the van Genuchten parameters for the soil (van Genuchten, 1980; Carsel and Parrish, 1988; Zhang, 1997a; Dohnal, et al., 2010), h_0 (≤ 0) is the pressure head applied on the infiltrometer disc, r_0 is the radius of the disc. From the formulation, it is clear that the appropriateness of infiltration characteristics determined using MDI would depend upon the representative van Genuchten parameters of the soil.

3.2.4. Guelph Permeameter (GP)

The Guelph permeameter (GP), which is depicted in Fig. 3. 4, is a bore hole constant head permeameter for measuring field saturated hydraulic conductivity at a depth below the ground surface (15 cm to 75 cm) (Reynolds and Elrick, 1985; Morbidelli, et al., 2017; Salverda and Dane, 1993; Hayashi and Quinton, 2004).

For better comparison with MDI, GP measurements were conducted at a depth of approximately 15 cm. A constant ponding depth of water varying from 5 cm and 10 cm was maintained in the bore hole using Marriott principle. Under constant head, there is a steady-state three dimensional flow of water into the adjacent unsaturated soil. This results in the formation of saturated soil bulb around the ponding depth depending on the type of soil, the radius and head of water in the well. Once the unique bulb is established, the outflow of water from the well reaches a steady-state, which can be measured. The rate of steady state outflow of water was used to determine the field saturated hydraulic conductivity K_s as given by Eq. 3. 9, which is based on single head method.

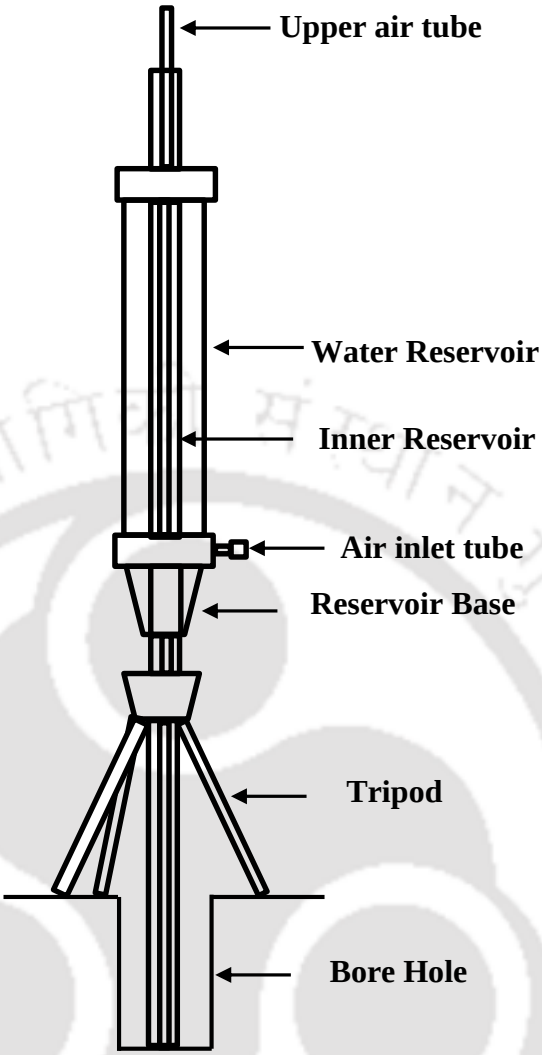

Fig. 3. 4 Schematic representation of guelph permeameter

The details of working methodology and mathematical formulations for GP for the determination of K_s are well established in the literature (Morbidelli, et al., 2017; Elrick and Reynolds, 1992; Reynolds et al., 1985).

$$K_s = \frac{CQ_1}{2\pi H_1^{\,2} + \pi a^2 C + 2\pi\left(\frac{H_1}{a^*}\right)} \tag{3. 11}$$

where, H_1 is the ponding depth, Q_1 is the steady state outflow from the GP, a is the auger hole radius equal to 3 cm, a^* is the capillary length factor and C is the shape factor. The values of a^* and C were estimated based on the soil type (Elrick, et al., 1989).

3.2.5. Constant Head Permeameter (CHP)

The constant head permeameter (CHP) is a well-established method for determining the saturated hydraulic conductivity of soils in the laboratory (ASTM D 5856). The procedure is the direct application of Darcy's law to a one-dimensional, steady flow of water through a saturated column of soil. Undisturbed soil cores could not be extracted from the field due to the presence of significant amount of sand. Therefore, remolded soil was packed in the permeameter to the same initial density and water content prevalent in the field. According to Darcy's law, the volume of water flowing through the cylindrical soil sample in a given time was used to determine saturated hydraulic conductivity (ASTM D 5856). Silicon grease was applied at the boundary of the CHP to avoid any preferential flow.

3.3. Description of the Study Area

The study area is in the sub basin of river Brahmaputra, Assam, North-east India, with its geographic location between 26^{o}11'3.434"N and 26^{o}11'55.122"N Latitude and 91^{o}41'14.324"E and 91^{o}42'10.578"E Longitude. The elevation of the stations vary from 49 m to 97 m above mean sea level. To take into account the spatial variability of infiltration characteristics, the infiltration measurements were performed at 14 locations (designated as S1 to S14) in the study area. The study area details are depicted in Fig 3. 5. The soil surface was bare with no influence of vegetation on the measurements and free from intentional anthropogenic activities.

The near surface soils were characterized for specific gravity, grain-size distribution, field density, and initial moisture content according to the procedure stated in the specific code of practice (ASTM D 854; ASTM D 7928; ASTM D 6938; ASTM D 698; ASTM D 2216; ASTM D2487; IS: 2720). The grain-size distribution was used to classify the soils, was determined based on the Unified Soil Classification System (ASTM D 2487). Different soil parameters of the study area are listed in Table 3. 1. It can be noted from Table 3. 1 that there are four types of soils viz., loamy sand, loam, sand and silt in the study area with varying field density.

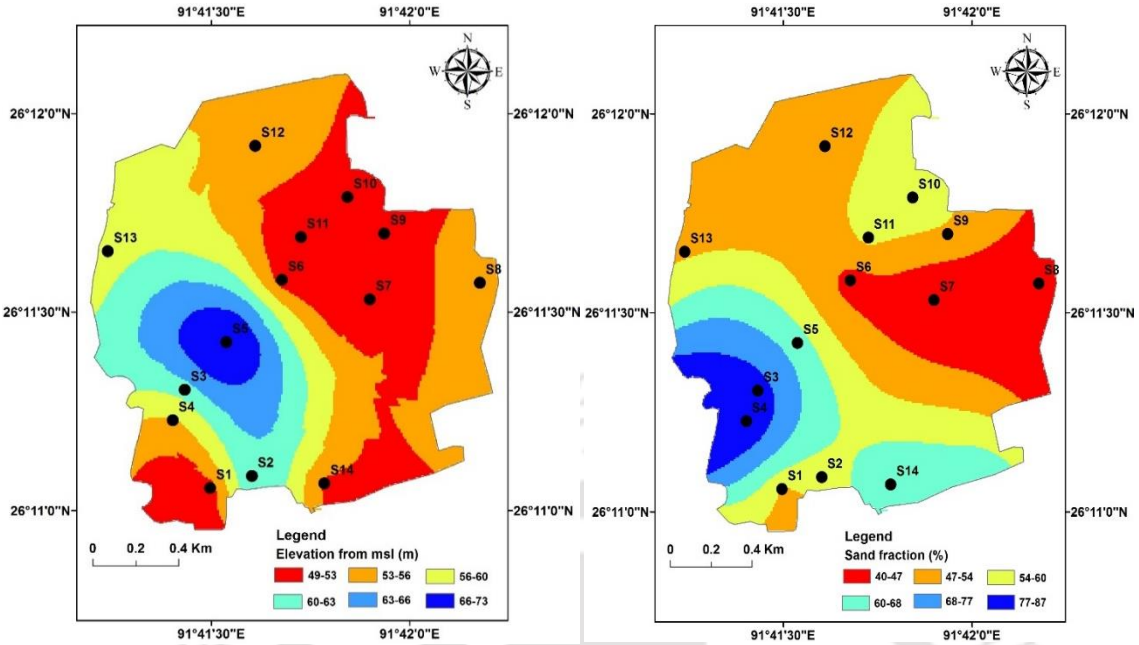

Fig. 3. 5 Layout of the study area with its details of (a) contours and (b) sand fraction

Table 3. 1 Details of soils at different stations of the study area

Station No.	Particle size fraction (%)				Soil Type	USCS *	Field Dry Density (g/cc)	Specific Gravity (G_s)	van Genuchten parameters	
	G*	S*	Si*	C*					α	n
S1	23	53	17	7	Sand	SM	1.74	2.580	0.145	2.68
S2	4	56	34	6	Loamy sand	SM	1.40	2.525	0.124	2.28
S3	2	82	16	0	Sand	SM	1.76	2.410	0.145	2.68
S4	1	87	12	0	Sand	SM	2.02	2.410	0.145	2.68
S5	13	64	15	8	Sand	SM	1.85	2.535	0.145	2.68
S6	2	45	40	13	Loam	MH	1.57	2.560	0.036	1.56
S7	2	40	55	3	Silt	MH	1.42	2.545	0.016	1.37
S8	3	42	53	2	Silt	MH	1.49	2.495	0.016	1.37
S9	2	52	45	1	Loam	SM	1.59	2.495	0.036	1.56
S10	3	59	38	0	Loam	SM	1.71	2.510	0.036	1.56
S11	3	56	38	3	Loam	SM	1.58	2.470	0.036	1.56
S12	3	48	39	10	Loam	SM	1.68	2.505	0.036	1.56
S13	1	53	46	0	Loam	SM	1.67	2.580	0.036	1.56
S14	1	67	25	7	Loamy sand	SM	1.88	2.560	0.124	2.28

*G-Gravel, S sand, Si-silt, C-clay, USCS-Unified Soil Classification System (ASTM D 2487) **(**SM- silty sand; MH- silt of high plasticity, elastic silt)

For understanding the seasonal variability of hydraulic conductivity, the hydraulic conductivity (K_s) has determined from September 2011 to August 2015 in all the 14 stations of the study area. For specific analysis, the experiments were conducted for long time for June 2014, December 2014 and June 2015, which represents wettest and driest month, respectively for the study area. The stations were selected such that the depth of top soil layer at all the locations was more than 1 m avoiding the soil layer effects on infiltration measurements and maintaining homogeneity.

3.4. Details of the Infiltration Measurements

For a particular station with identical initial conditions, infiltration measurements were performed using all the four instruments. A typical lay out of infiltration measurement scheme in the station for a particular station is depicted in Fig. 3. 6. Symbols denote the location of infiltration measurement for each instrument. Similar layout of infiltration measurements was followed for all the 14 stations. It needs to be noted that adequate space was provided to rule out the influence of one measurement over the other. To ensure this, a minimal distance of 0.75 m was maintained between each measurement as shown in Fig. 3. 6.

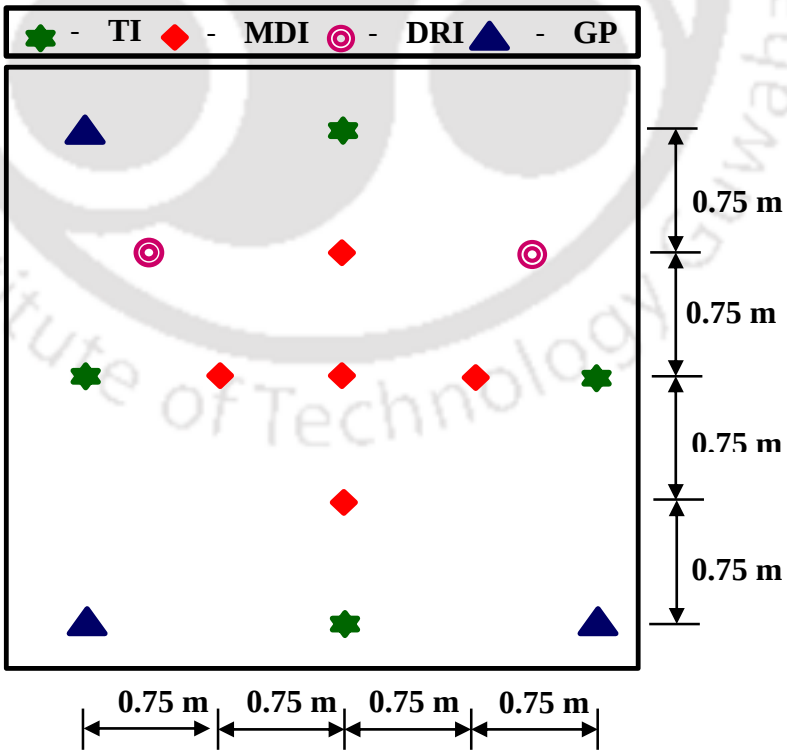

Fig. 3. 6 Lay out of infiltration measurement scheme for a particular station

The measurements using DRI was repeated twice, TI was repeated four times, MDI was repeated 5 times and GP was repeated thrice. It may be noted that a small and compact size of the MDI permitted more repetitions whereas the bulky DRI with less repetitions. Owing to the small disc size, the soil volume contributing to MDI measurement would be least and the maximum for DRI. For a cracked and desiccated soils, this would result in large variability in hydraulic parameters.

For all practical purpose, MDI measurements can be treated as truly point measurements as compared to DRI. In the case of CHP, the soil was remolded and compacted to the same initial condition in the field. It was mainly because of the difficulty in extracting undisturbed cores for the soil prevalent at the station.

Chapter 4

Field Investigations on Infiltration Measurements

4.1. General

Infiltration measurements are important for the hydrological modelling of catchment. Different methodologies adopted for measurements exhibit variability in infiltration characterization, which needs to be studied in detail. This chapter discuss the variability in infiltration measurements under identical field conditions of the study area and its impact on characterizing near surface near saturated hydraulic conductivity.

4.2. Measurement Induced Variability in Infiltration Characteristics

For the evaluation of measurement induced variability, the infiltration characteristics measured in the study area described in Section 3. 3, using double ring infiltrometer (DRI), mini disc Infiltrometer (MDI) and tension disc infiltrometer (TI) are compared. For a particular station with identical initial conditions, infiltration measurements were performed using all the three instruments. For understanding seasonal influence, the measurements conducted in June 2014 and December 2014, which represents wettest and driest month, respectively were selected.

4.2.1. Analysis of Measured Infiltration Curves

The infiltration rate curves for four stations S5, S7, S10, and S14 representing the different soil types are depicted in Fig. 4. 1 for the month of June 2014. It can be noted from Fig. 4. 1 that all the infiltrometers approach a quasi-steady infiltration rate, which is specific for a given infiltrometer, soil type and initial condition. Measured infiltration rate offer an excellent first-hand information of the possible water intake capacity of soils. It is an unambiguous signature of water entry as influenced by soil type, ground surface condition, compaction state and measuring instrument. Four specific features of the measured infiltration rate curve, (a) initial infiltration rate (i_i) or maximum infiltration rate, (b) final quasi-steady state infiltration rate (i_f) or minimum infiltration rate, (c) range of infiltration rate ($i_i - i_f$), and (d) time at which infiltration rate approaches i_f designated as final time (t_f) is used in this study for further evaluation of infiltration variability. For clarity, the above-mentioned features are indicated in Fig. 4. 1 (for S7). It needs to be stated here that these specific features were chosen because they are related to the direct

measurements (close to reality) and are not influenced by any assumptions, mathematical computations or knowledge of soil related parameters that are likely to influence the near saturated hydraulic conductivity (K_{h_0}) determination, as explained in Chapter 3. For a given soil type and initial condition, these parameters are dependent only on the measurement methodology and hence offers better possibility while comparing different infiltrometers.

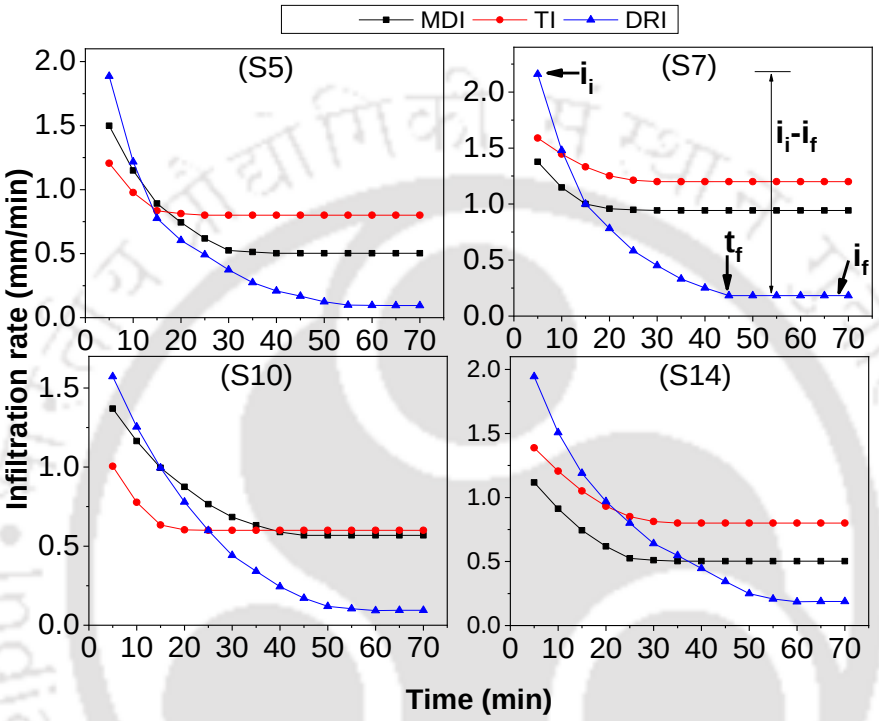

Fig. 4. 1 Infiltration rate curves for selected stations for the month of June 2014

The infiltration rate versus time response of all the 14 stations for two seasons are shown in Fig. 4. 2. For reference, a typical value of steady state infiltration for clay (Pit, et al., 1999) (approximate lower bound) is shown in Fig. 4. 2. It can be noted from Figs. 4. 1 and 4. 2 that the measured infiltration rate versus time follows similar trend for all the cases. However, there is considerable difference in the measured infiltration rate of different infiltrometers. Even though infiltration rate is a quantity normalized by area of infiltration surface, the results still indicate that different infiltrometers portrays different quantity of infiltration for the same initial state of the soil. To appraise the differences in infiltration curves, the specific features of infiltration curve i_i, i_f, and $i_i - i_f$ is plotted for all the 14 stations as shown in Fig. 4. 3.

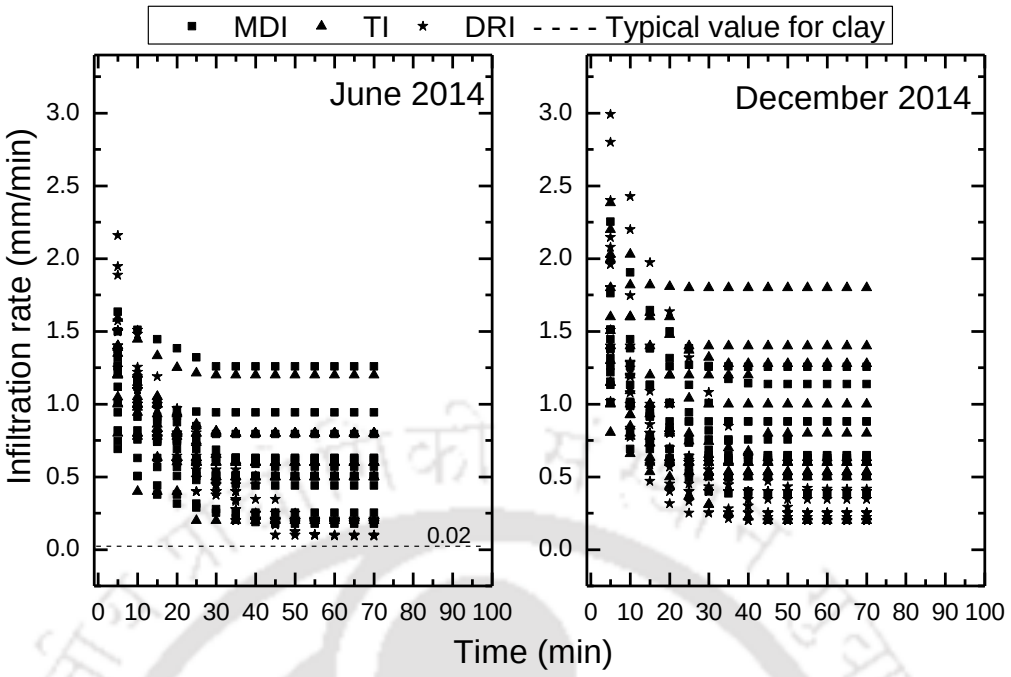

Fig. 4. 2 Infiltration rate for all infiltrometers and stations and two seasons

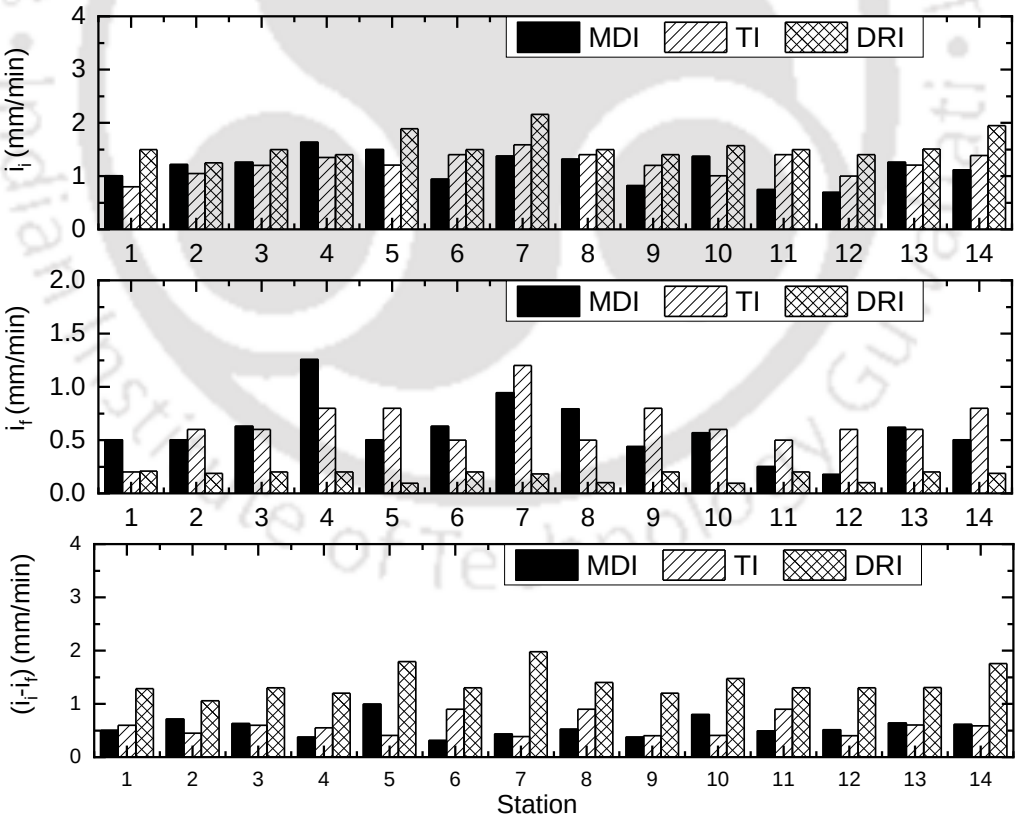

Fig. 4. 3 Comparison of initial infiltration rate (i_i), minimum infiltration rate (i_f) and range of infiltration rate (i_i- i_f) for June 2014

Since both the seasons follow the same trend, the result of only June 2014 is presented here. It is quite explicit that the i_i is highest for DRI while in most of the cases it is comparable for tension disc infiltrometers. This could be mainly due to the positive ponding head and higher infiltration area of DRI as compared to disc infiltrometer. Similarly, the minimum infiltration rate or final infiltration rate (i_f) is minimum for DRI. Due to the tension imposed on the boundary, the final equilibrium infiltration rate is higher than DRI for the disc infiltrometers. Under a positive head causing infiltration, it is found that the i_f approaches to a very low value for DRI for all the stations. While the DRI represents one-dimensional gravity flow with negligible influence of sorptivity on infiltration characteristics and there is a prominent influence of sorptivity on the infiltration characteristics of disc infiltrometer. For a homogenous surface, the resulting initial infiltration rate beneath disc infiltrometer is a trade-off between the tension head imposed on the boundary and the sorptive force existing in the soil. The disturbance of soil during insertion of the ring also contribute to higher initial infiltration in DRI as against zero disturbance in the case of disc infiltrometers. The aerial foot print of both the disc infiltrometers is much lesser than the DRI there by leading to a high cumulative volume of infiltration for the latter. A higher aerial foot print of DRI would result in delayed equilibration and minimal final infiltration. The difference in diameter of both disc infiltrometers did not influence the infiltration characteristics significantly.

This apparently means that the range of infiltration rate is maximum for DRI as shown in Fig. 4. 3. For the same soil type and initial state, the measured infiltration rate response is entirely different for disc infiltrometers and DRI. The reasons for this has been cited in the literature as the inclusion or exclusion of macro pore flow depending on the tension head for disc infiltrometer. However, even for a very marginal or negligible tension (0.05 kPa to 2 kPa), the infiltration rate response is significantly different for disc infiltrometers and DRI. This would result in different scenarios of hydrological response for a given station when these instruments are used simultaneously in a given project. The implication of this variation on infiltration characterization (determination of hydraulic conductivity) is discussed later in this chapter.

Before proceeding to the infiltration characterization, an effort was made to investigate different procedures of normalization of infiltration curves owing to the significant differences in measured infiltration features as discussed above. To start with, it can be noted from Fig. 4.2 that the measured infiltration rate versus time response

exhibits a wide scatter of data while comparing different infiltrometers for the study area. A simple normalization is followed for both infiltration rate and time as shown in Eqs. 4.1 and 4.2.

$$i_{n1} = \frac{i}{i_f} \tag{4. 1}$$

$$t_n = \frac{t}{t_f} \tag{4. 2}$$

where i is the infiltration rate at time t, i_f and t_f are defined earlier, t_n is the normalized time and i_{n1} is the normalized infiltration rate. The plot for i_{n1} versus t_n is depicted in Fig. 4. 4.

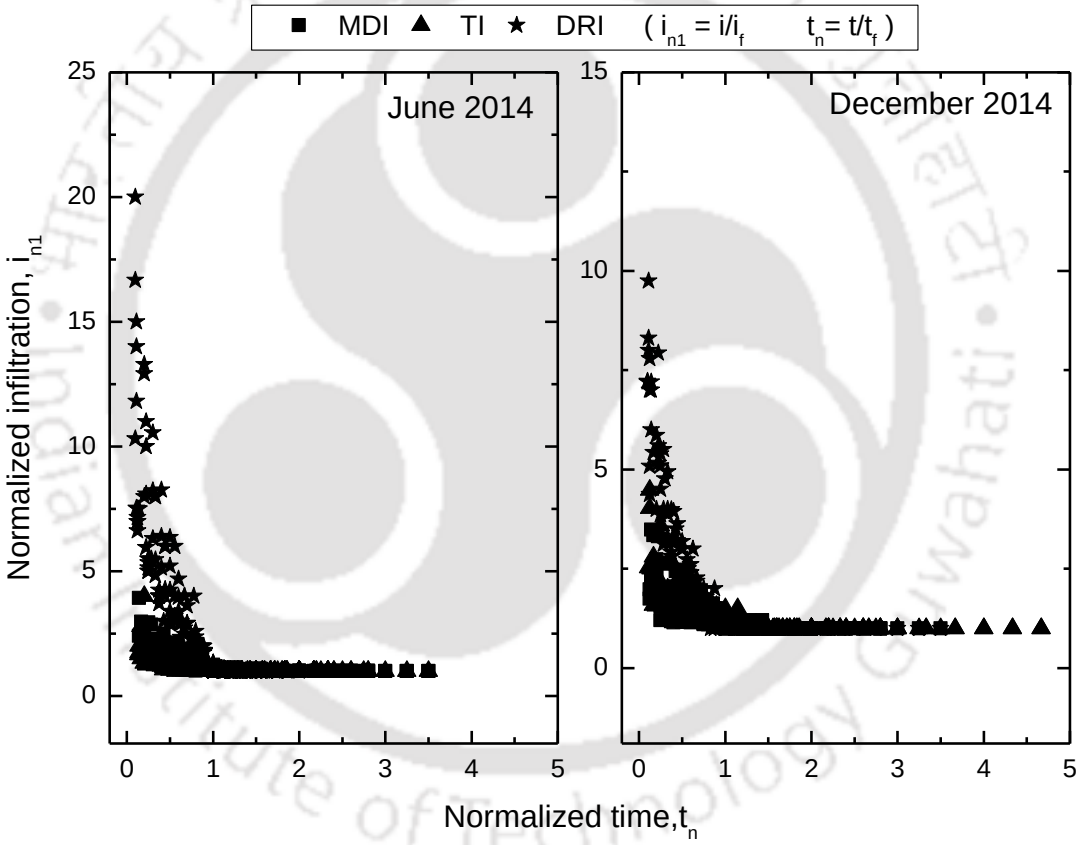

Fig. 4. 4 Simplified normalized infiltration rate versus normalized time for different infiltrometers

It can be noted that the normalization has resulted in considerable refinement in data representation as compared to Fig. 4. 2. However, there is a considerable difference in i_{n1} for DRI due to the influence of i_f (comparatively less for DRI). Therefore, the reference scale of normalized infiltration is quite different for disc infiltrometers and DRI.

To secure the normalized infiltration rate between 1 and 0 an alternate normalization of infiltration rate (i_{n2}) was followed as shown in Eq. 4. 3.

$$i_{n2} = \frac{i - i_f}{i_i - i_f} \tag{4. 3}$$

This normalization is similar to the representation of infiltration rate according to Horton's equation (Chow, et al., 1988) as given by Eq. 4. 4.

$$i_{n2} = \frac{i - i_f}{i_i - i_f} = e^{-k_H t} \tag{4. 4}$$

where k_H is Horton's parameter. To start with, i_{n2} is plotted as a function of time t following Horton's equation as shown in Fig. 4. 5. The depicted result clearly shows the inadequacy of normalization when Eq. 4. 4 is considered.

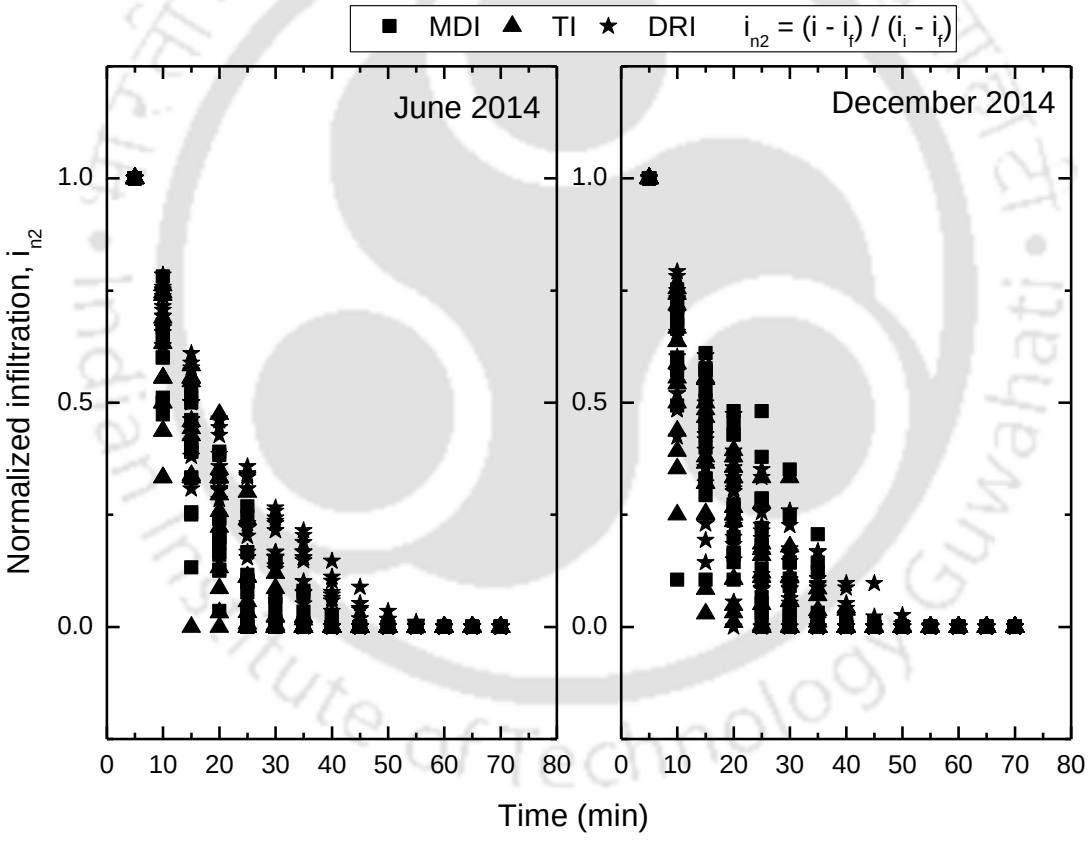

Fig. 4. 5 Normalized infiltration rate similar to Horton's equation versus time for different infiltrometers

An alternate method of normalization was adopted in this study by plotting i_{n2} as a function of normalized time, t_n, as shown in Fig. 4. 6. Horton's form of equation (Eq. 4 .4) is modified by replacing t by t_n and fitted to the data presented in the figure and the

parametric statistics summarized in Table 4. 1. It can be noted that the Horton form of equation cannot capture i_{n2} versus t_n adequately. By trial and error method, other non-linear regression equations were explored, which would efficiently represent the normalized data. It was noted that an asymptotic curve represented by Eq. 4. 5 is a better choice as shown in Fig. 4. 6 and the regression coefficient is listed in Table 4. 1.

$$i_{n2} = A - B * C^{t_n} \tag{4. 5}$$

where *A*, *B* and *C* are empirical asymptotic curve fitting parameters as listed Table 4. 1.

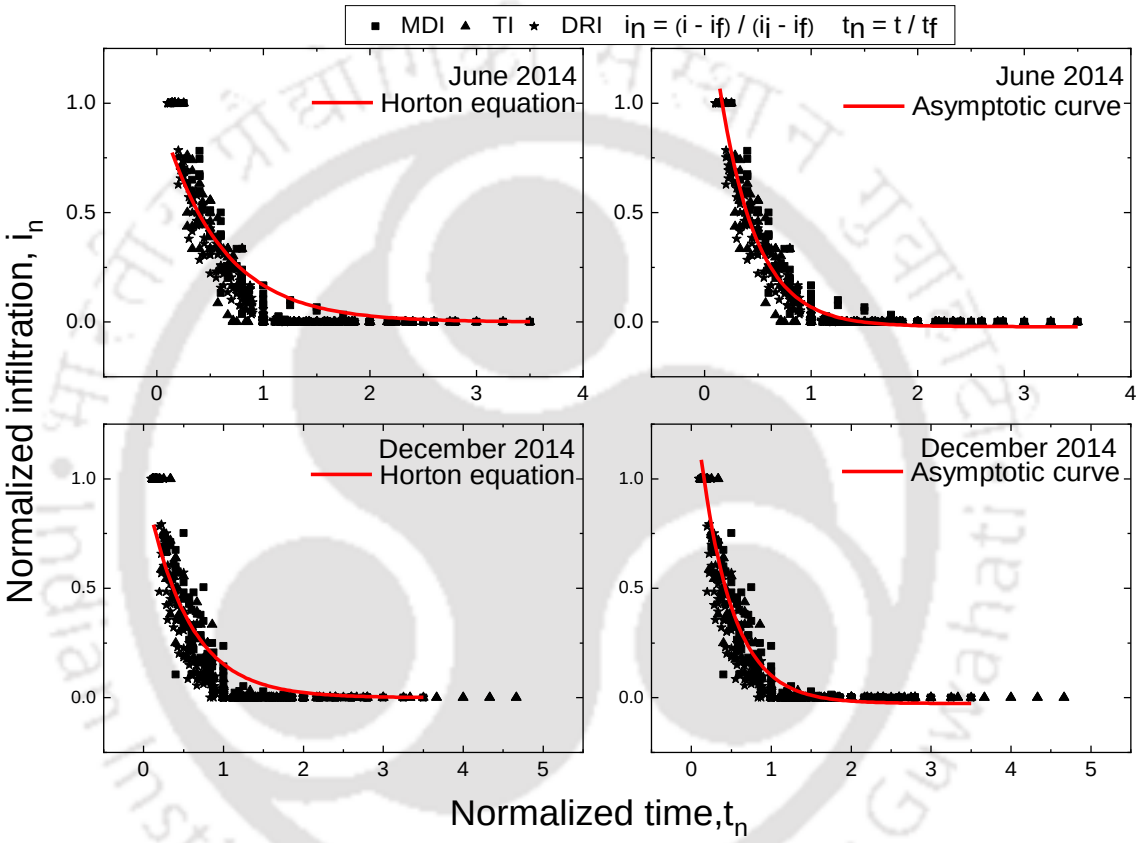

Fig. 4. 6 Normalized infiltration rate versus normalized time for different infiltrometers

Table 4. 1 Summary of parameters for normalized infiltration equation

Equation	Parameter	June 14	December 14
Horton form considering normalized time $\boldsymbol{i_{n2} = e^{-k_H t_n}}$	k_H	1.786	1.874
	R^2	0.8643	0.8623
Asymptotic $\boldsymbol{i_{n2} = A - B * C^{t_n}}$	A	-0.0213	-0.0264
	B	-1.648	-1.515
	C	0.0543	0.0847
	R^2	0.9408	0.9361

The normalization presented in Fig. 4. 6 clearly indicates that the measured response is less influenced by the instrument related bias. The values summarized in Table 4. 1 also indicates that the seasonal variation does not have much influence on the parametrization of normalized infiltration equation (normalized Horton equation and Eq. 4. 5). It is believed that the proposed normalization would alleviate instrument related variabilities while comparing infiltration measurements performed using different infiltrometers under various conditions. However, more studies are needed to evolve a procedure for determining hydraulic conductivity from the normalized curve, which is not attempted in this study. The hydraulic conductivity is determination is based on the general procedure suggested by the manufacturer or as suggested by recommended code procedure, discussed below.

The infiltrometer measures cumulative infiltration and infiltration rate. However, for quantifying infiltration for any hydrological or drainage application needs the infiltration to be expressed as an equation. There are several empirical (eg: Horton's equation) and semi-empirical or physically based equation (for e.g.: Philip's equation, Green-Ampt equation) for quantification. These physically based equations are expressed in terms for hydraulic conductivity (more correctly near surface hydraulic conductivity). Green-Ampt equation is an example, which is mostly applicable for saturated case or ponding head (positive pressure head or near zero pressure head). There are other equations in terms of sorptivity and hydraulic conductivity for near saturated conditions like Philip's equation. For using these infiltration equations in any hydrological model necessitates the knowledge of near surface hydraulic conductivity. Hence, the infiltration measurements need to be quantified in terms of hydraulic conductivity to study the sensitivity and relationship. Hence, irrespective of the infiltrometers used in the field, the hydraulic conductivity determined from the infiltration measurements are discussed in the following section.

4.2.2. Determination of Hydraulic Conductivity from Measured Infiltration

The cumulative infiltration versus time response was used to determine hydraulic conductivity by following the procedures discussed in Chapter 3. It is understood that for all the external factors remaining same, the saturated hydraulic conductivity is a time invariant parameter of the soil. Therefore, an attempt was made to first evaluate the time invariant response of hydraulic conductivity determined using the three infiltrometers for the two seasons as shown in Fig. 4. 7.

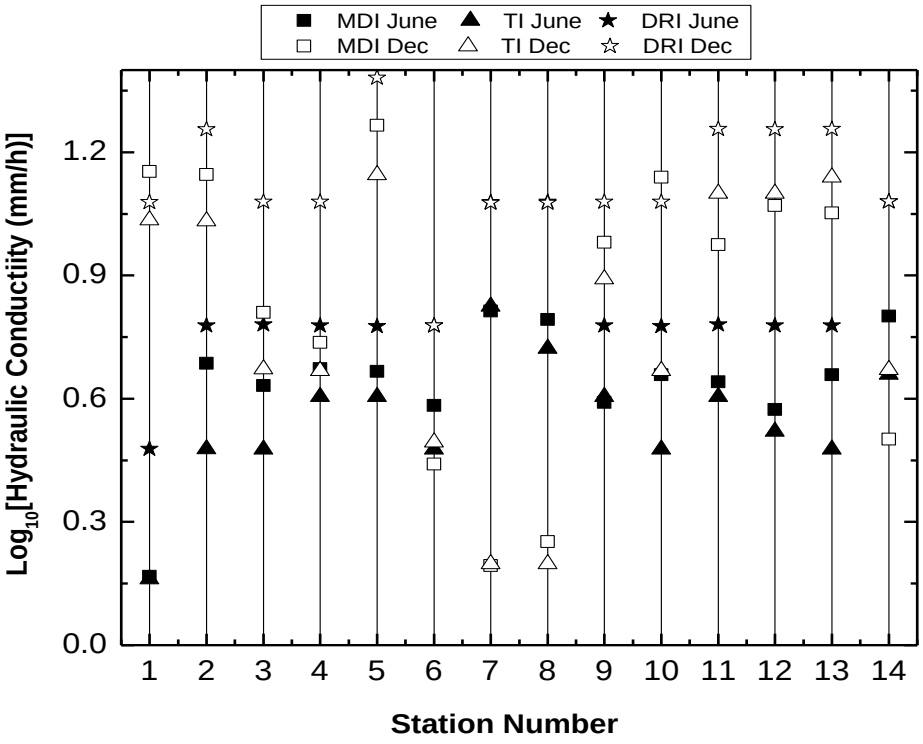

Fig. 4. 7 Time invariance of log transformed hydraulic conductivity determined using infiltrometers

It is well established in the literature that DRI is used to determine field saturated hydraulic conductivity (K_s) and expected to be invariant. It can be noted from the figure that there are marginal differences in K_s determined using DRI for the two seasons. Similarly, K_s measured using DRI in December shows consistently a higher value (marginally) for all the stations as compared to June. These observed differences in DRI measurements can be attributed to surface soil shrinkage and associated cracking due to dry conditions during the summer, soil structural changes due to wetting-drying, and/or unknown anthropogenic activities. Interestingly, it may be noted that both MDI and TI follows similar trend as that of DRI and the results obtained for both the seasons are not significantly different for majority of the cases. For some stations, K_{h_0} of different seasons obtained from disc infiltrometers are much closer than DRI. Irrespective of stations and infiltrometers, the difference in hydraulic conductivity between two seasons is well within one order of magnitude. This is an encouraging observation for ascertaining the utility of disc infiltrometers (with near zero tension head at the boundary) for assessing near surface

near saturated field hydraulic conductivity for the site conditions discussed in this study by following the general measurement and analysis procedures.

4.2.3. Statistical Analysis of Hydraulic Conductivity

The statistical parameters such as the maximum, minimum, arithmetic mean and standard deviation are calculated for the log transformed hydraulic conductivity values measured using disc infiltrometers. And a column plot for measured field hydraulic conductivity using different infiltrometers is depicted in Fig. 4. 8. Only the mean hydraulic conductivity is considered for DRI due to limited number of repetitions (two). Considering the soil variabilities, environmental factors and measurement uncertainties it is explicit from Fig. 4. 8 that the hydraulic conductivity determination using all the infiltrometers are fairly repeatable for all the stations and for varying seasons.

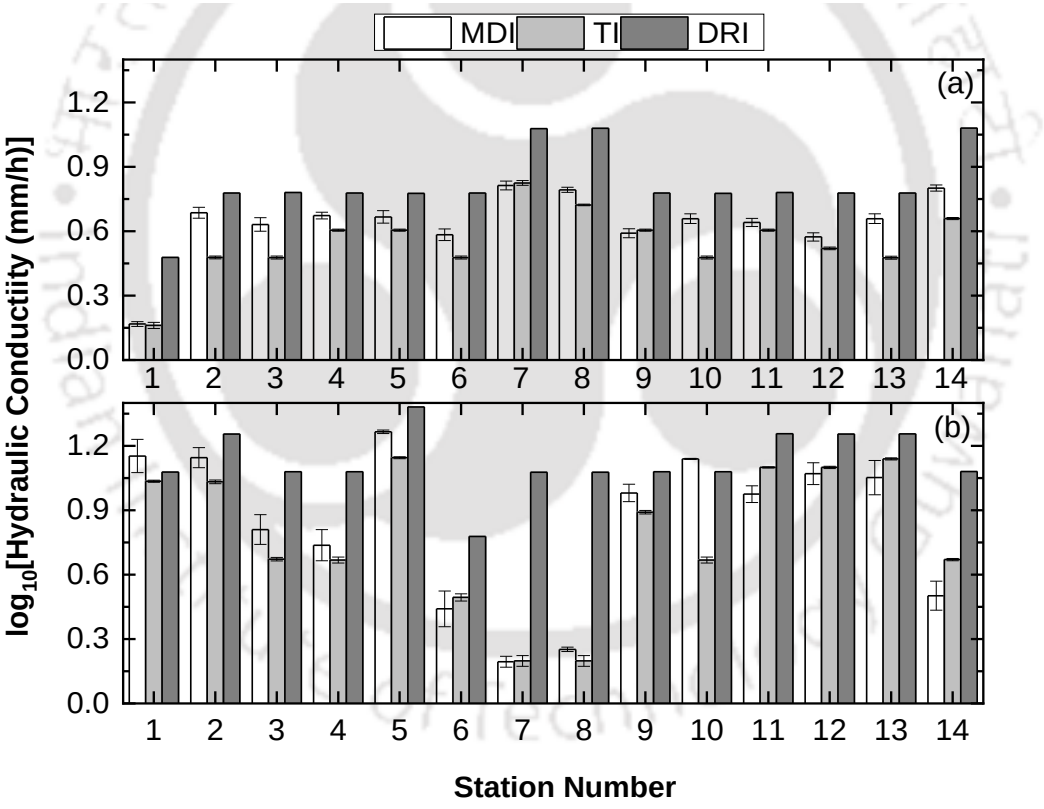

Fig. 4. 8 Statistical representation of hydraulic conductivity (mm/h) from three infiltrometers (a) June 2014 and (b) December 2014 (Box represents the mean; the top and bottom of the whiskers indicate 75th and 25th percentiles, respectively)

Comparison of mean hydraulic conductivity (mm/h) determined using DRI, TI and MDI for all the 14 stations for the month of June and December 2014 along with the initial

water content are presented in Fig. 4. 9. It can be noted from Fig. 4. 9 that there is a fair comparison among the mean hydraulic conductivity determined using all the three infiltrometers. For all the stations, DRI gave marginally higher mean hydraulic conductivity than disc infiltrometers where as both the disc infiltrometers gave nearly identical values. On the contrary, a high mean hydraulic conductivity was noted for DRI measurements for stations 7 and 8 during December 2014. However, for the same stations, the difference was marginal during June 2014. This indicates that the significant difference in mean hydraulic conductivity during December measurements is not associated with the methodology but may be attributed to some local conditions prevalent during the measurements.

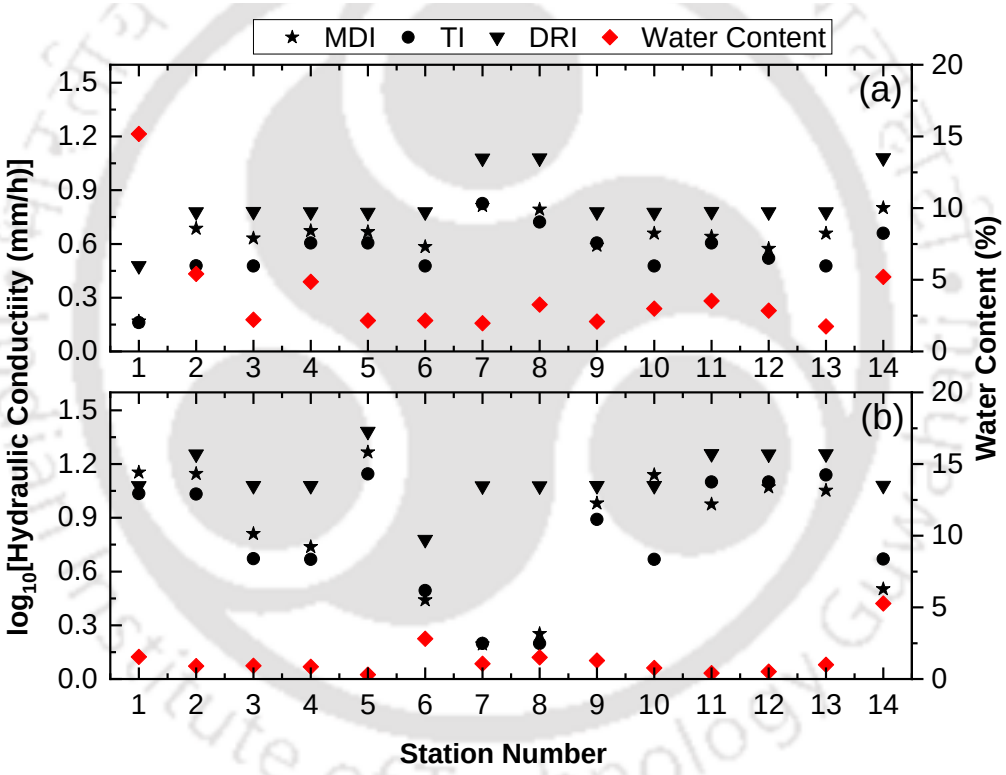

Fig. 4. 9 Influence of initial water content on infiltrometer measurements (a) June 2014 and (b) December 2014

To investigate further, the influence of soil type prevalent at the station on hydraulic conductivity was examined. Table 4. 2 presents the evaluation of statistical significance of parameters such as initial water content, sand, silt and clay on hydraulic conductivity determined using the three infiltrometers.

Table 4. 2 Statistical significance of selected parameters on hydraulic conductivity determined using various infiltrometers

Parameter	June 2014					
	MDI		TI		DRI	
	r	*p* value	*r*	*p* value	*r*	*p* value
w	-0.753	0.002	-0.673	0.008	-0.527	0.05
Sand	0.02	0.93	-0.119	0.69	-0.189	0.52
Silt	0.377	0.18	0.439	0.12	0.479	0.08
Clay	-0.262	0.37	-0.21	0.47	-0.14	0.63
	December 2014					
	MDI		TI		DRI	
	r	*p* value	*r*	*p* value	*r*	*p* value
w	-0.479	0.08	-0.319	0.267	-0.506	0.065
Sand	0.244	0.40	0.181	0.54	0.116	0.69
Silt	-0.411	0.14	-0.366	0.19	-0.139	0.64
Clay	0.002	0.99	0.158	0.59	-0.145	0.62

w: initial water content; *r*: correlation coefficient

Statistical significance was assessed by determining correlation coefficient (*r*) and *p* value for a confidence interval of 0.05. The correlation is considered to be statistically significant if the *p* value is less than 0.05 (null hypothesis of no relationship is rejected) (Bagarello, et al., 2014). It can be noted from the table that initial water content exhibits a negative correlation with hydraulic conductivity and is the only parameter where there is a possibility of statistically significant relationship. Such a negative relationship is expected because a dry soil result in high infiltration. The particle size fraction was found to have statistically insignificant correlation with hydraulic conductivity. Other possibility may be due to higher soil disturbance around the circumference of ring while inserting the double ring, which is more sensitive for fine-grained silts. The presence of macropores or some preferential flow at these stations during measurements may increase the infiltration from DRI. The effect of these factors need to be considered as localized effects. Since the aerial footprint of these instruments vary significantly, it is possible that the adjacent locations where the disc infiltrometer measurements were performed was not influenced by macropores or preferential pathways.

Statistical comparison of mean hydraulic conductivity was performed by t-test using IBM SPSS statistics (version 20) with details of null hypotheses (significance level of 5 %) listed in Table 4. 3. The proposed null hypothesis is rejected if the corresponding *p* value is less than the significance level of 0.05. H1 and H4 results indicate that the mean

hydraulic conductivity values from MDI and TI are similar for both the seasons. According to null hypothesis, the mean hydraulic conductivity values from both MDI and TI is statistically different from DRI values. It can be noted that the hydraulic conductivity determined by MDI and TI are approximately half to two-thirds of DRI values. This is consistent with the Philip parameter A (Philip, 1957), which was reported to be close to 0.30 reported in Sharma, et al. (1980), Christianson, et al. (2016) and 0.67 as reported in Youngs, (1968).

Table 4. 3 Statistical analysis of mean hydraulic conductivity obtained from three infiltrometers using t-test

S. No.	Hypothesis	Null Hypothesis	*p* values
1	H1	Set of mean hydraulic conductivity values from MDI and TI are similar in the month of June, 2014	**0.141**
2	H2	Set of mean hydraulic conductivity values from MDI and DRI are similar in the month of June, 2014	0.005*
3	H3	Set of mean hydraulic conductivity values from DRI and TI are similar in the month of June, 2014	0.001*
4	H4	Set of mean hydraulic conductivity values from MDI and TI are similar in the month of Dec, 2014	**0.700**
5	H5	Set of mean hydraulic conductivity values from MDI and DRI are similar in the month of Dec 2014	0.011*
6	H6	Set of mean hydraulic conductivity values from DRI and TI are similar in the month of Dec, 2014	0.002*

* denotes a statistically significant difference ($p<0.05$): bold values indicate the null hypothesis has failed to reject

The statistical variability is further quantified in terms of arithmetic mean (AM), standard deviation (SD) and coefficient of variation (CV) of mean hydraulic conductivity determined using three infiltrometers and listed in Table 4. 4. For better representation, the mean hydraulic conductivity from different infiltrometers is plotted with the respective mean hydraulic conductivity obtained from three infiltrometers (K_{ave}) along with ±25 % error bar as shown in Fig. 4. 10. It may be noted from the Table 4. 4 that the coefficient of variation is high for the results obtained, which is similar to the outcome of *t*-test in Table 4. 3. Figure 4. 10 depicts that except for three cases, the variability of hydraulic conductivity is within ± 25% of the mean value. From the literature, it is clear that the range of variation in hydraulic conductivity is quite wide in orders of magnitude for soils

(Pit, et al., 1999; Warrick and Nielsen, 1980; Whitaker, et al., 2003; Touma, et al., 2007; Woltemade, 2010).

Table 4. 4 Statistics of mean hydraulic conductivity determined using different infiltrometers

Station No.	Mean $\log_{10}$[Hydraulic conductivity (mm/h)]					
	June 2014			December 2014		
	AM	SD	CV (%)	AM	SD	CV (%)
S1	0.27	0.18	67.2	1.09	0.06	5.5
S2	0.65	0.15	23.8	1.14	0.11	9.7
S3	0.63	0.15	24.1	0.85	0.21	24.3
S4	0.69	0.09	12.7	0.83	0.22	26.6
S5	0.68	0.09	12.7	1.26	0.12	9.4
S6	0.61	0.15	24.9	0.57	0.18	31.8
S7	0.91	0.15	16.5	0.49	0.51	103.9
S8	0.86	0.19	21.8	0.51	0.49	96.8
S9	0.66	0.10	15.9	0.98	0.09	9.6
S10	0.64	0.15	23.6	0.96	0.26	26.6
S11	0.68	0.09	13.7	1.11	0.14	12.7
S12	0.62	0.14	21.8	1.14	0.10	8.7
S13	0.64	0.15	23.8	1.15	0.10	8.9
S14	0.85	0.21	25.3	0.75	0.30	39.6

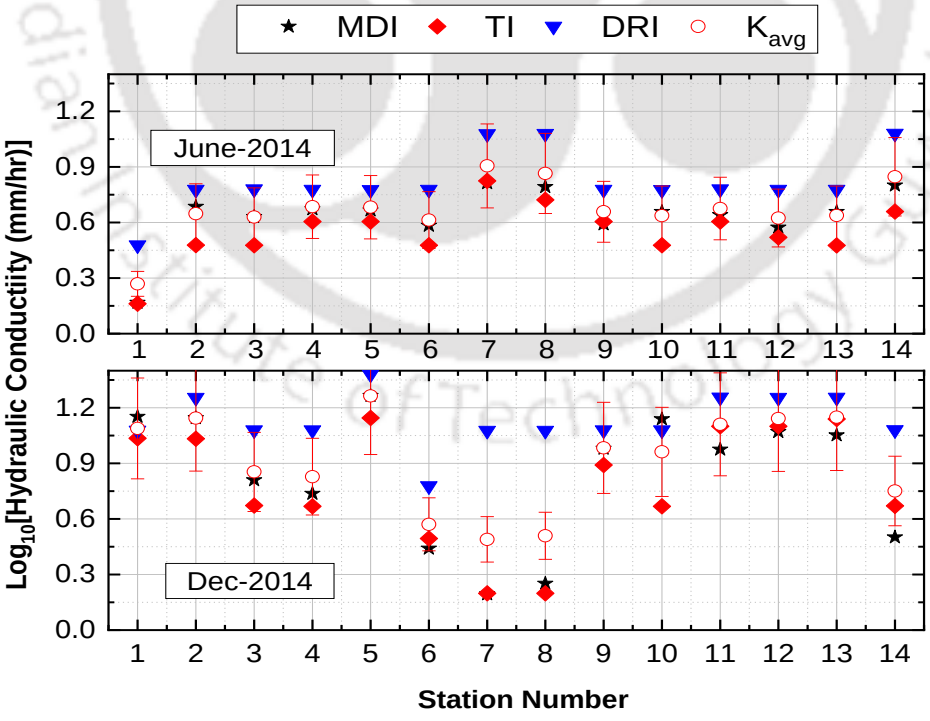

Fig. 4. 10 Comparison of hydraulic conductivity obtained using the three infiltrometers with mean (K_{ave}) value and ±25% error bar

Given such a wide variation and taking into account the number of factors affecting the determination of hydraulic conductivity, the variability of ±25% from the mean value can still be considered reasonable. The study clearly demonstrates the usefulness of disc infiltrometers vis-à-vis DRI for rigorous and repeatable measurements for establishing infiltration characteristics at catchment scale.

4.2.4. Comparison of Infiltration Measurements Reported in the Literature

Hydraulic conductivity from DRI was observed to be 7 to 13 times higher than TI in the absence of sand contact layer and 12 to 33 times higher than TI in the presence of sand contact layer (Köhne, et al., 2011). Similar findings were endorsed by other researchers for agricultural soils (Reynolds, et al., 2002; Verbist, et al., 2013), except for low-permeability soils where results were similar for DRI and TI methods. In, Vanderlinden, et al. (1998), a comparison of hydraulic conductivity below and outside the olive-canopy was done using four different instruments: constant-head well permeameter, falling-head lined borehole permeameter, twin-rings and disc infiltrometer. The study observed that all the techniques gave higher hydraulic conductivity values under the canopy for falling-head lined borehole permeameter and twin-rings. Outside the canopy, hydraulic conductivity from constant-head well permeameter and twin-rings were significantly higher than falling-head lined borehole permeameter and disc infiltrometer.

Statistically similar estimates of saturated hydraulic conductivity of loamy soil were found in (Alagna, et al., 2016), differing at the most by a factor of three for the results obtained from six infiltrometer techniques such as BEST, the pressure infiltrometer (PI), one-potential experiments with TI, MDI, the simplified falling head (SFH) technique and the bottomless bucket (BB) method. The TI and MDI techniques yielded the highest and similar hydraulic conductivity values among the tested infiltrometer techniques suggesting that macropores were not excluded from the flow process. The study highlighted lower variability of hydraulic conductivity data obtained with the MDI as compared with the other methods. In the case of sloping surfaces, it was found that the hydraulic conductivity estimated from tension infiltrometers were 1.2 to 2 times higher than those from double ring infiltrometers for all slope gradients up to 20% with silt loam soil (Bodhinayake, et al., 2004). A lowest value of the hydraulic conductivity was observed for MDI as compared to Guelph permeameter (Ronayne, et al., 2012). The reviewed comparative studies indicate contrasting observations under different conditions indicating the need for more evaluations. All the studies focused on the comparisons of hydraulic conductivity,

which involves different methods of determination. None of the studies have attempted to compare the direct measured results in terms of infiltration characteristics as shown in this study. This offers a better comparison of instrument related bias exemplifying the importance of this study.

4.2.5. Relationship between Infiltration Characteristics and Hydraulic Conductivity

This study investigated the relationship between the measured infiltration characteristics and hydraulic conductivity determined from different infiltrometer results. For this purpose, hydraulic conductivity obtained from all the infiltrometers for two seasons and 14 stations were plotted together as a function of i_i, i_f, and $i_i - i_f$ as shown in Fig. 4. 11. It can be noted that K_{h_0} exhibit a positive correlation with all the infiltration characteristics. A relatively statistically significant relationship was noted for i_i, and $i_i - i_f$ denoted by Pearson's r indicated on Fig. 4. 11. For a linear relationship passing through origin, K_{h_0} is observed to be 0.089, 0.173 and 0.125 times i_i, i_f and $i_i - i_f$, respectively. There are not many studies that explore the statistical significance of relationship between K_{h_0} and infiltration characteristics in the literature. Such a relationship holds potential for evolving a methodology for determining K_{h_0} from directly measured infiltration characteristics. However, more studies with different types of soil and initial conditions are required to generalize this finding and the correlation.

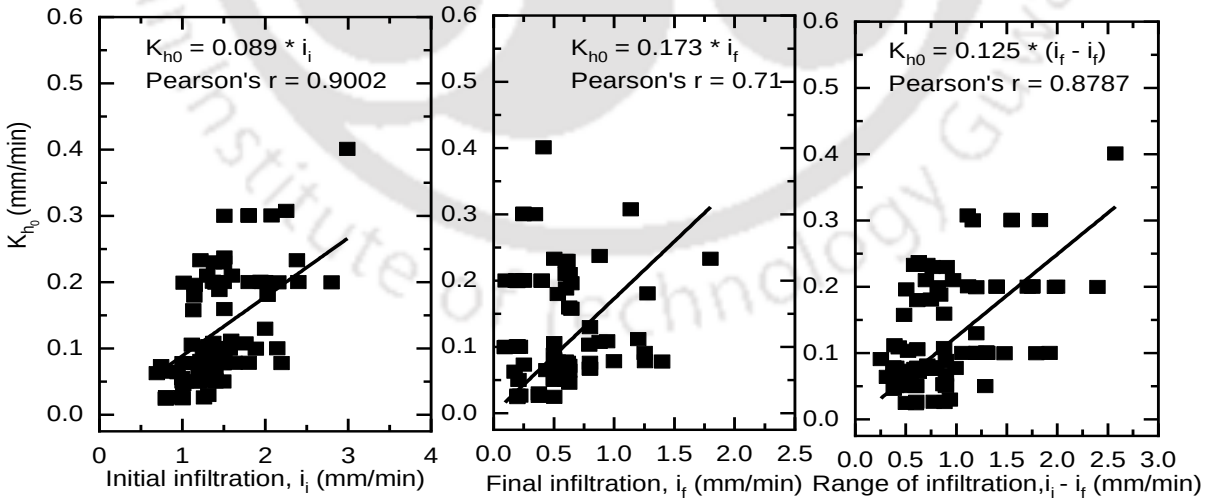

Fig. 4. 11 Relationship between hydraulic conductivity and infiltration characteristics

4.3. Infiltrometers and Permeameters for Measuring Hydraulic Conductivity

For the study of evaluation of infiltrometers and permeameters measurements from 12 different stations of the study area were selected (S1-S6 and S9-S14). Infiltration measurements were conducted for two seasons: in December 2014 representing winter – the driest month and June 2015, which represents monsoon - wettest month for the study area respectively. In the field, it was ensured that the depth of the topsoil layer at all the locations was more than 70 cm avoiding the possibility of soil layer effects on infiltration and maintaining homogeneity. For a particular station, hydraulic conductivity measurements were performed using all the four instruments.

A near zero tension was maintained for disc infiltrometers to avoid the influence of negative head on hydraulic conductivity measurements. The DRI, GP and CHP measurements were performed under constant ponding head conditions. Repeatability studies were first performed for all the five instruments used in this study. One of the challenges in the repeatability study of field measurements is maintaining identical initial conditions. This often gets violated when each measurement is performed sufficiently away from each other for avoiding the zone of influence of individual measurements. It may be noted that MDI being a smaller instrument, five repetitions could be performed at every station without violating the identical initial conditions. TI measurements were performed four times, GP three times and laboratory CHP three times with the same initial moisture content and dry density conditions in the field. DRI repetition could be performed only twice due to the large size of the instrument and cumbersome measurement procedure. More DRI measurements beyond the zone of influence of individual measurements necessitate a larger areal extent, which may violate identical initial condition.

The scatter plot for repeatability studies for infiltrometer and permeameter measurements corresponding to two different seasons are shown in Fig. 4. 12. Qualitatively it can be noted that the infiltrometer measurements exhibited higher scatter in measurements as compared to permeameter results. For quantitative statistical analysis, the data presented in Fig. 4. 12 were log transformed based on the understanding that hydraulic conductivity generally follows log-normal distribution (Bouwer, 1969; Nielsen, et al., 1973; Buckland, 1988).

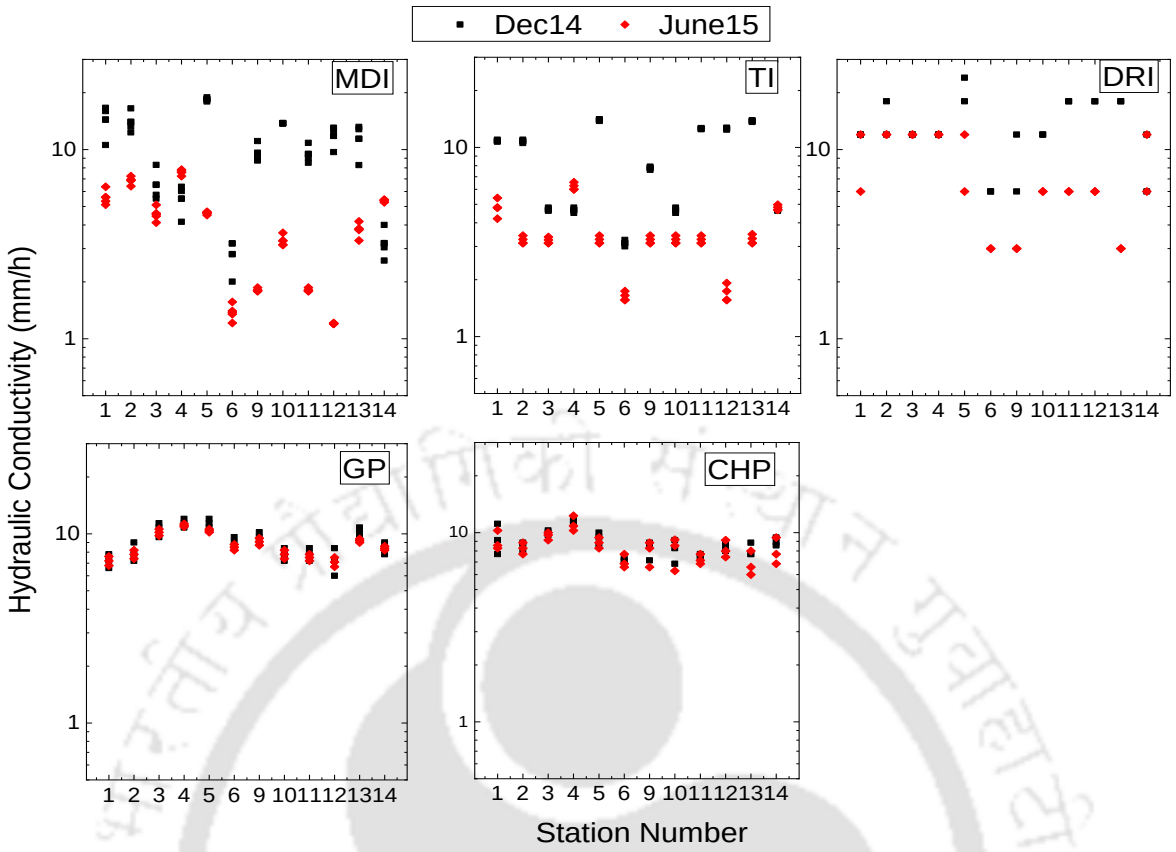

Fig. 4. 12 Hydraulic conductivity (mm/h) measured by infiltrometers and permeameters for two seasons

The repeatability of infiltrometers and permeameters is quantitatively expressed in terms of pooled relative standard deviation (S_{pooled} represented by Eq. 4. 6) of log transformed hydraulic conductivity (log K) (Higgins, et al., 2008; Quan and Zhang, 2003) by considering the measurements made in two different seasons and presented in Fig. 4. 13.

$$S_{pooled} = \sqrt{\frac{(n_1 - 1)s_1^2 + (n_2 - 1)s_2^2}{(n_1 - 1) + (n_2 - 1)}} \qquad (4.\ 6)$$

where, n_1 and n_2 are the numbers of trials for the data sets 1 and 2 (data corresponding to winter and monsoon season as stated earlier), s_1 and s_2 are the relative standard deviation.

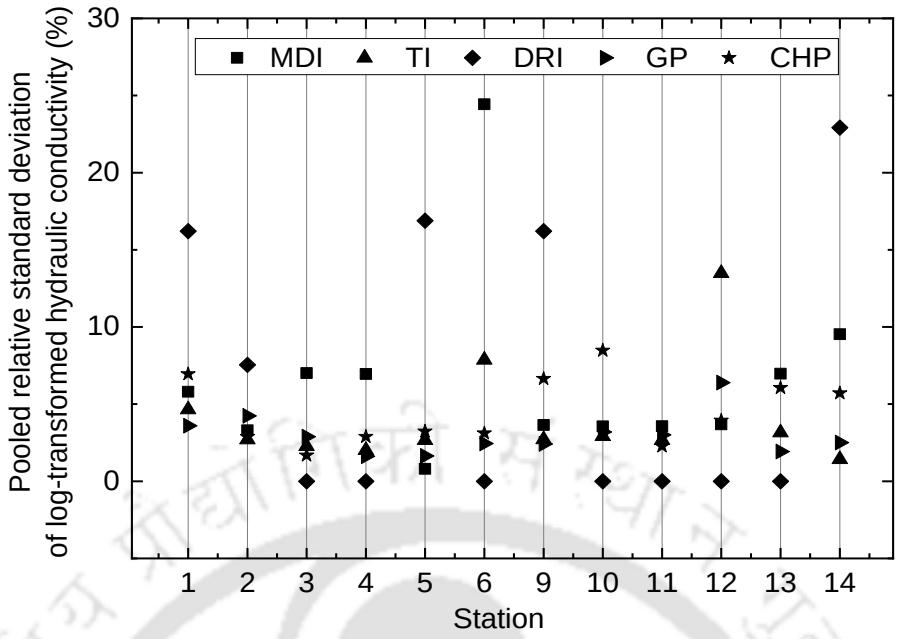

Fig. 4. 13 Repeatability of log transformed hydraulic conductivity (mm/h) measured by infiltrometers and Permeameters

It can be noted that the permeameters and infiltrometers are fairly repeatable with a pooled relative standard deviation less than 10% for the majority of the cases. The statistical results of DRI are not very reliable due to fewer repetitions but have been presented for the sake of completeness. The pooled relative standard deviation was more than 10 % for four stations for DRI. For MDI and TI, station 6 and 10 exhibited more than 10%. The order of performance in terms of pooled relative standard deviation (lower the value, better the performance) are GP < CHP < TI < MDI < DRI.

Another important observation is that the hydraulic conductivity measurements of permeameters for both the seasons matched well. It is well known that the saturated hydraulic conductivity is an invariant parameter for a given soil with a particular pore structure. Since the measurement of GP is performed at some depth (≈ 15 cm) below the ground surface and CHP measurements are performed under controlled dry density (same for both the seasons), it is explicit from the results that the measured hydraulic conductivity undoubtedly corresponds to saturated hydraulic conductivity. Unlike permeameters, the results obtained from infiltrometers are not the same for both the seasons. In the majority of the cases, the infiltration measurements performed in December exhibited higher hydraulic conductivity as compared to June measurements. This observation is similar to those reported in the literature (Morbidelli, et al., 2017). Even for DRI measurements,

which is expected to give saturated hydraulic conductivity, there is a considerable difference in the results obtained for both the seasons. The results indicate that saturated or near saturated hydraulic conductivity measured using infiltrometers do not comply with the condition of invariance as compared to permeameters. This can be due to three reasons: (a) the hydraulic conductivity is determined indirectly based on the cumulative water entry at the ground surface as against the actual flow of water through the soil in the case of permeameters (b) temperature and rain induced drying-wetting cycles altering the surface pore structure (swell-shrinkage) of soil and (c) anthropogenic reasons.

4.3.1. Variability of Hydraulic Conductivity using Different Infiltrometers and Permeameters

The mean of the log transformed hydraulic conductivity, $(\log K)_{mean}$ obtained from infiltrometers and permeameters are compared as shown in Fig. 4. 14. The measurements of disc infiltrometers were comparable with DRI and permeameters for a relatively dry initial state in December 2014. For higher moisture condition (June 2015), $(\log K)_{mean}$ from disc infiltrometers were consistently less than DRI and permeameters. This trend is similar to the results reported in the literature (Morbidelli, et al., 2017).

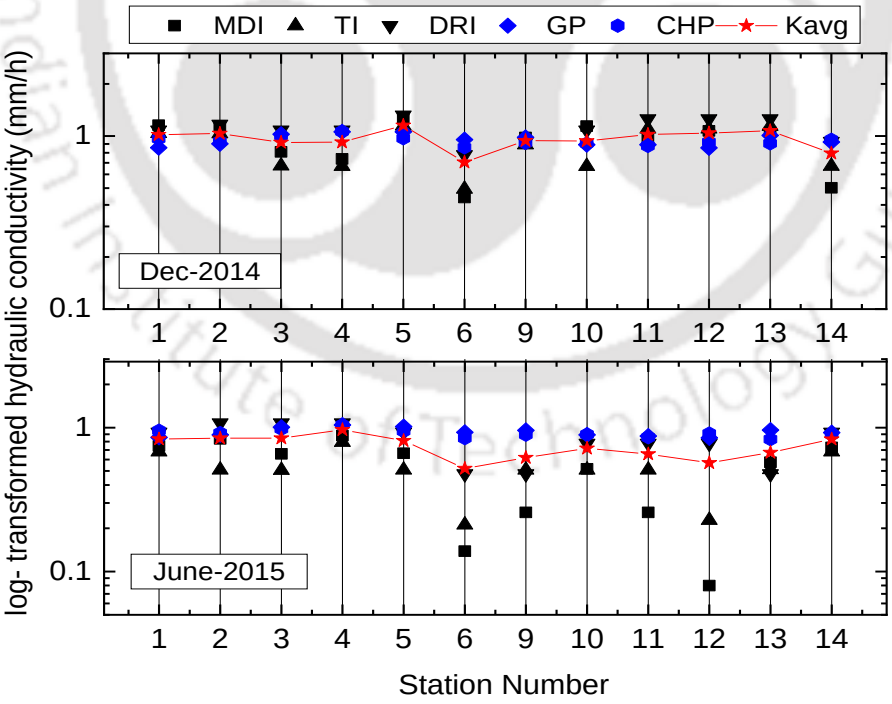

Fig. 4. 14 Comparison of mean of the log transformed hydraulic conductivity measured using infiltrometers and permeameters

As initial moisture content increases, the cumulative infiltration decreases and hence the hydraulic conductivity determined based on the former would result in a lower value as compared to permeameters. Hydraulic conductivity (supposedly saturated) obtained from DRI measurements were found to vary between those of permeameters and disc infiltrometers. This is mainly because the hydraulic conductivity was determined based on the final steady state infiltration rate (for an extended duration of time). The seasonal variations were found to have an insignificant effect on permeameters as shown in Fig. 4. 15.

Principally, the water flow used for the determination of hydraulic conductivity in permeameters occurs through the soil mass as against the entry of water from the ground surface in the case of infiltrometers. The water flow from GP occurs at a depth from the ground surface thereby minimizing the wetting-drying induced effects and unforeseen anthropogenic causes resulting in pore structure changes at the ground surface. However, these factors can have considerable influence on infiltrometer measurements due to its dependence on water entry at the soil surface. The results presented in Fig. 4. 15 corroborates these discussions and bring forth the expected invariant characteristics of field saturated hydraulic conductivity (K_s) for GP. The results of GP compare well with the K_s determined in the lab using CHP for the remolded soil sample with the same initial compaction state as in the field.

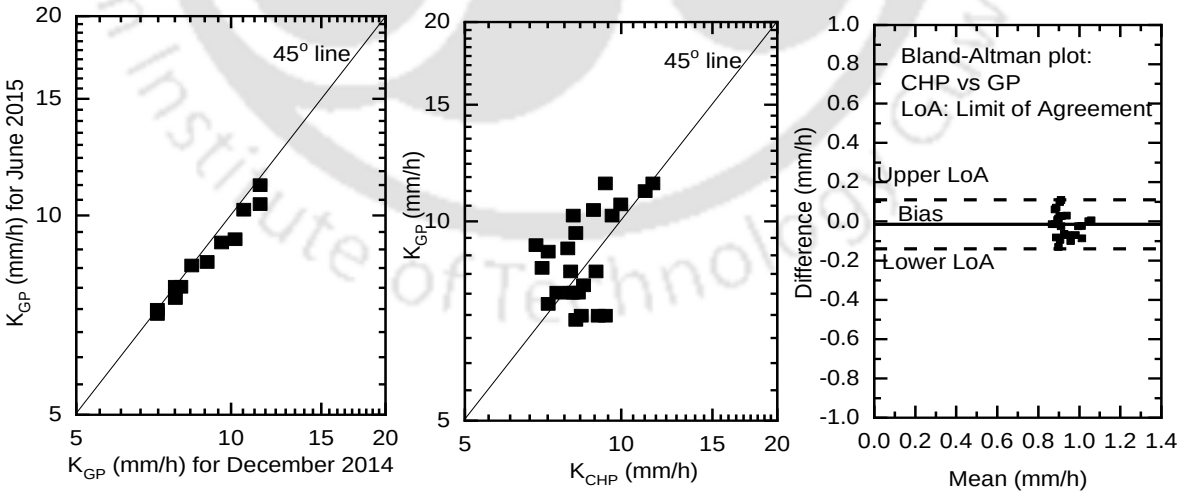

Fig. 4. 15 Seasonal influence on GP measurements and its comparison with CHP

4.3.2. Statistical Analysis using Bland-Altman Plot

The Bland-Altman plot (BAp) is an established graphical statistical method to compare the agreement between two measurement techniques (Brazdzionyte and Macas, 2007). In BAp, the difference between the two methods is plotted on the y-axis, and the mean of two methods are plotted on the x-axis. The mean of the difference between the two methods is defined as bias. The 95 % upper and lower limits of agreement (LoA) is equal to ±1.96 times the standard deviation of the difference. The advantage of BAp is its ability to statistically interpret the data graphically based on how significant is the bias, how wide is the limits of agreement and whether there is an observed trend between difference and the mean (Brazdzionyte and Macas, 2007; Watson and Petrie, 2010). The representation in BAp helps to evaluate the possibility of systematic difference existing between the methods that are compared. This helps to understand whether the difference between two methods is uniform for the whole range of measurements or restricted to a specific range (low, mid or high).

The statistical difference between infiltrometers and permeameters were assessed quantitatively by using the Bland-Altman plot (BAp) as shown in Fig. 4. 16. It can be noted from Fig. 4. 16 that the majority of the data points fall within the limits of agreement. There is a negative bias when disc infiltrometers are compared with DRI while the width of LoA is comparable. For MDI-TI comparison, the bias is close to zero. There is no visible trend existing between difference and mean for all comparisons thereby ruling out any systematic difference between any two infiltrometers. The studies in the literature observed hydraulic conductivity from DRI to be higher than TI (Morbidelli, et al., 2017; Reynolds, et al., 2002; Köhne, et al., 2011; Kodesova, et al., 2010) except for low-permeable soils where the results were found to be similar for DRI and TI methods. This study also observed higher DRI values for high initial moisture condition and comparable results for dry initial state (low-permeable condition). The results indirectly endorse the fact that disc infiltrometer is more appropriate for a low permeable condition, which is similar to the finding reported in the literature (Nestingen, et al., 2018).

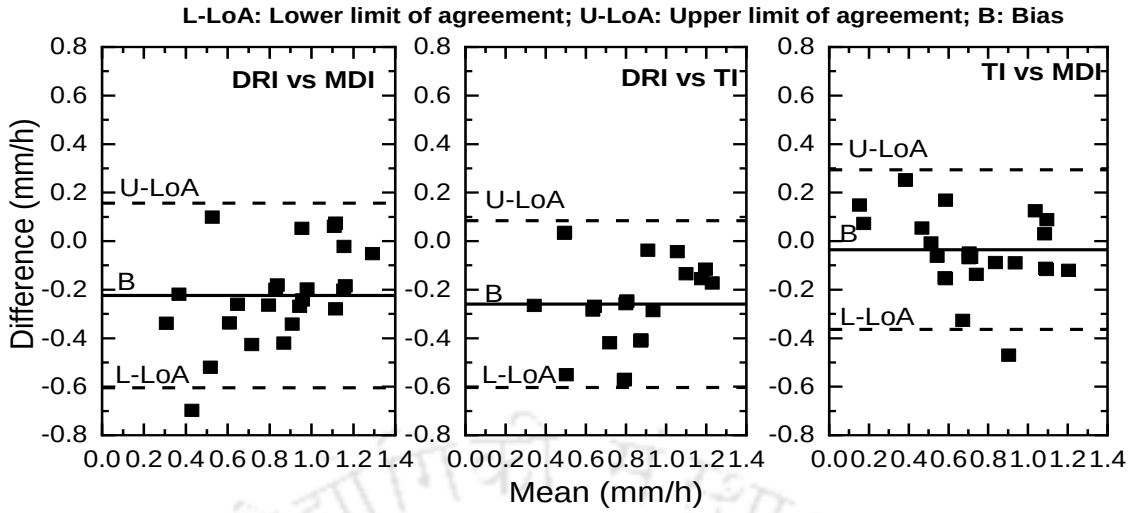

Fig. 4. 16 Bland-Altman plot for statistical comparison of different infiltrometers

The statistical difference between permeameter and the three infiltrometers are presented in Fig. 4. 17. In this comparison, GP is chosen as the reference as it is an established method for determining field hydraulic conductivity. From Fig. 4. 17, it can be visualized that there is a systematic difference between GP and infiltrometers as shown by the increasing trend. Such a systematic difference was not reported previously in the literature. For DRI, the bias is negligible, and several measured data points fall close to zero difference confirming its efficacy in measuring field saturated hydraulic conductivity as compared to disc infiltrometer. The usefulness of DRI for determining saturated hydraulic conductivity was demonstrated under laboratory condition by Nestingen, et al. (2018). Both the disc infiltrometers exhibited negative bias with respect to GP measurements and with very few data points close to zero difference (close to mid-range of the mean) indicating a difference between both the methods. All lower and higher range of mean shows a higher difference with respect to GP measurements. The previous study shows that there is no general consensus in the trend while comparing GP with TI (Morbidelli, et al., 2017) and recommended further investigation for better understanding. Also, the impact of the systematic difference between infiltrometers and GP (despite qualifying LoAs) on various hydrological processes need to be investigated in detail.

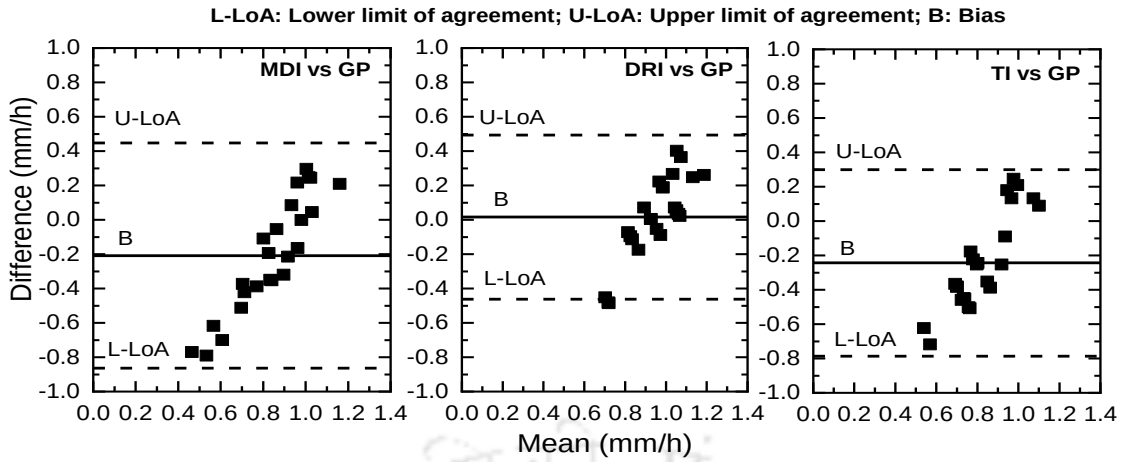

Fig. 4. 17 Bland-Altman plot for statistical comparison between Guelph permeameter and infiltrometers

It is realized from the above discussion that the disc infiltrometer measurements exhibit a negative bias with respect to GP. It is expected that the near saturated hydraulic conductivity corresponding to a minimal tension of 0.5 cm (=0.05 kPa) should be close to the saturated hydraulic conductivity. It can be explained by referring to a conceptual relative hydraulic conductivity curve shown in Fig. 4. 18 for a typical soil with a low air entry value (AEV) close to 10 kPa. It can be noted that the range of tension head in MDI (< 0.6 kPa) and TI (< 2 kPa) is well within the AEV. Theoretically, the hydraulic conductivity corresponding to suction less than AEV should be close to saturated hydraulic conductivity (Fredlund and Rahardjo 1993; Köhne, et al., 2011; Kodesova, et al., 2010). However, the minimal tension (< AEV) set on the disc infiltrometer resulted in near saturated hydraulic conductivity, which is systematically different from GP. The reason for this is not explicit from this study and needs further investigation. Subsequently, an effort was made to explore whether the systematic difference resulted in a statistical correlation between GP and disc infiltrometer measurements. It was noted that the Pearson correlation coefficient (Verbist, et al., 2013) of GP measurements with both the disc infiltrometers were close to 0.1 indicating a very poor correlation. The possibility of such a correlation was not investigated in the literature and needs further investigation with a wide range of soil types.

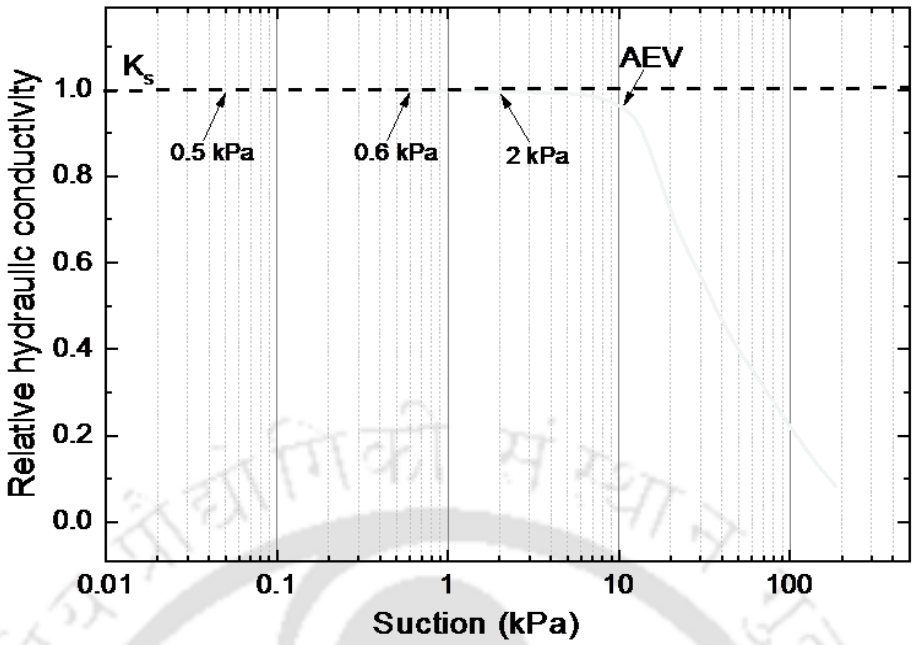

Fig. 4. 18 A conceptual relative hydraulic conductivity curve for a soil having low air entry value close to 10 kPa

4.4 Summary

This chapter compared the measurement of three different infiltrometers: a well-established double ring infiltrometer (DRI), tension disc infiltrometer (TI) and mini disc infiltrometer (MDI) for a river sub-catchment in north-east India. Majority of the studies reported in the literature compared the infiltrometers based on hydraulic conductivity determined indirectly from the infiltrometer response. However, this study adopted the measured infiltration response in terms of initial infiltration (i_i), minimum or final infiltration (i_f) and range of infiltration (i_i-i_f) for comparative assessment. For the same soil type and initial state, there is considerable difference in the measured infiltration rate of different infiltrometers. Owing to these differences, this study further investigated methods for normalizing infiltration rate curves. It was found that $\frac{i-i_f}{i_i-i_f}$ versus $\frac{t}{t_f}$ (t is the time and t_f is final infiltration) is the best form of normalization that alleviates instrument related variabilities. A non-linear asymptotic curve was found to adequately represent the normalized infiltration curve as compared to the Horton form of equation. For a linear relationship with zero intercept, K_{h_0} is observed to be 0.089, 0.173 and 0.125 times i_i, i_f, and $i_i - i_f$, respectively. However, more studies are needed for evolving a

methodology for determining hydraulic parameter from the normalized infiltration rate curves.

Statistical evaluation of the results indicates that hydraulic conductivity determination using all the infiltrometers are fairly repeatable for all the stations and for varying seasons. Statistical comparison of mean hydraulic conductivity performed by t-test indicated that the mean hydraulic conductivity values from MDI and TI are similar for both the seasons and different from DRI values. The hydraulic conductivity determined by MDI and TI are approximately two-thirds of DRI values, which endorses the observation in the literature. For majority of the cases the variability of hydraulic conductivity is within ± 25% of the mean value considering all the infiltrometer measurements. The study clearly demonstrates the usefulness of disc infiltrometers vis-à-vis DRI for rigorous and repeatable measurements for establishing infiltration characteristics at catchment scale.

The statistical difference between infiltrometers and permeameters were quantified using the Bland-Altman plot (BAp). There is a negative bias for disc infiltrometers with DRI, and all the data falls within the limits of agreement (LoA). Comparison of disc infiltrometers exhibited bias close to zero. Both the disc infiltrometers exhibited negative bias with respect to permeameters measurements and a few data points close to zero difference. It was expected that the disc infiltrometer with minimum tension would yield hydraulic conductivity close to saturated hydraulic conductivity. However, hydraulic conductivity determined from disc infiltrometers exhibited a very poor correlation with permeameters. Further studies are required to investigate the reason for the systematic difference in hydraulic conductivity between disc infiltrometers and GP. The impact of such a systematic difference on various hydrological process modeling needs to be studied in detail.

Chapter 5

Spatial and Seasonal Variability of Infiltration Parameters

5.1. General

Soil hydraulic conductivity, which governs the quantity of water entry into the soil is a vital parameter for watershed modeling, irrigation management and waste management (Chahinian, et al., 2006; Mishra, et al., 2003). In this chapter, the spatial and the seasonal variability of soil hydraulic conductivity in the field, determined from infiltration measurements are quantified based on MDI measurements.

5.2. Details of the Field Experiments

The MDI experiments were performed in the study area with extensive spatial measurements at 14 locations (designated as S1 to S14) as discussed in Chapter 3. Experiments were conducted every month, starting from the month of September 2011 to August 2015 for understanding the seasonal variation in the infiltration characteristics. Before performing infiltration measurements, initial gravimetric water content (w) and field dry density (γ) of all the locations were measured according to the procedure mentioned in ASTM D 2216 and ASTM D 6938, respectively. A sequence of MDI measurements was made at a particular location for 4 different tensions, 6, 4, 2 and 0.5 cm. Based on Zhang (1997a) transient state approach, near saturated hydraulic conductivity, K_{h_0} was determined corresponding to each tension head, h_0 as discussed in Chapter 3. The K_{h_0} versus h_0 was extrapolated linearly to $h_0 = 0$ for estimating the saturated hydraulic conductivity, K_s as shown in Fig. 5. 1. For the study area, spatial interpolation was performed by considering MDI measurements at twelve locations and the prediction of K_s was done for two locations. The measured K_s were assigned to each of the sampled points on a GIS platform using ARCGIS, for analyzing the spatial data. These data were geo-referenced to the respective field location and used to generate a statistical surface with numerically interpolated values of K_s for all unknown locations. The spatial prediction of K_s for 2 stations were compared with the measured hydraulic conductivity values for evaluating the accuracy of the five spatial interpolation methods.

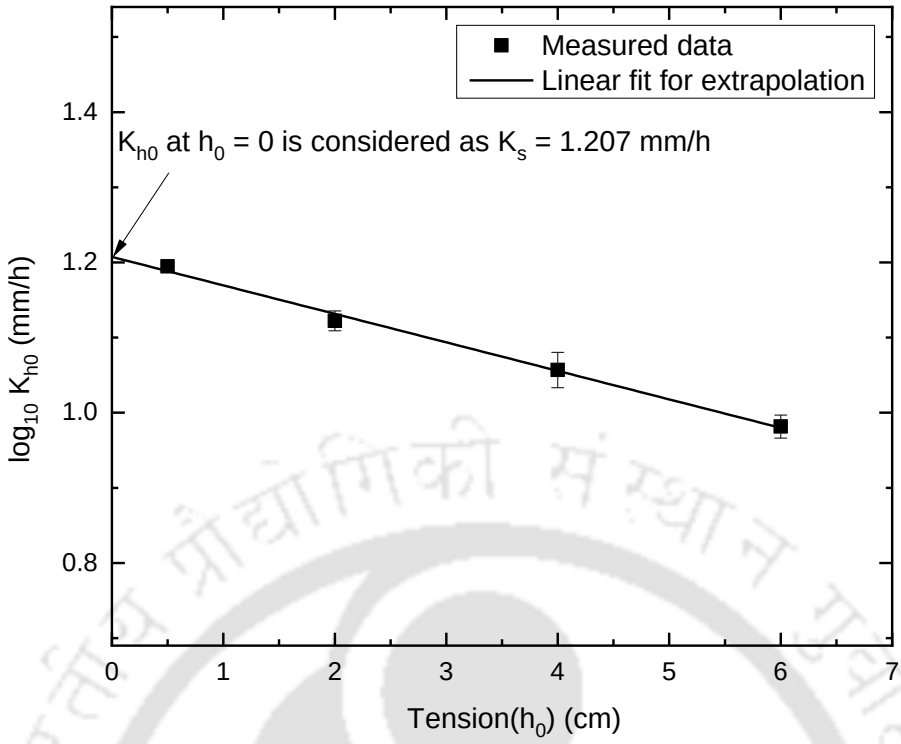

Fig. 5. 1 Determination of saturated hydraulic conductivity

The infiltration rate determined using MDI approached a linear response after exhibiting an initial non-linearity within the duration of testing. The linear response indicates that the infiltration rate has approached a quasi-steady state. It takes around 30-40 minutes for attaining the steady infiltration rate which is different for different stations and suction heads. In the study area, there is wide variation in infiltration characteristics. This may be attributed to the difference in soil type, density and initial water content. The cumulative infiltration versus time response was used to determine hydraulic conductivity by following the procedure mentioned in the Chapter 3. It is understood that for all the external factors remaining same, the saturated hydraulic conductivity is a time invariant parameter of the soil. Therefore, an attempt was made to first evaluate the time invariant response of hydraulic conductivity determined using the MDI for all those months.

5.3. Spatial Variability of Hydraulic Conductivity

Spatial interpolation methods are employed for determining soil hydraulic conductivity at unsampled locations of a catchment based on the point measurements of soil hydraulic conductivity at selected locations (sampled locations) of the catchment (Grayson and Blöschl, 2001). Therefore, it is important for the modelers and planners to

clearly appraise the accuracy of spatial prediction of soil hydraulic conductivity data used as input for hydrologic modeling.

Different spatial interpolation methods have been compared by Li and Heap (2011), which can be used in environmental sciences (Webster and Oliver, 2001) and mining engineering (Journel and Huijbregts, 1978). From the comparative studies among different interpolators, it was observed that the best method varies based on different geological characteristics (Usowicz and Lipiec, 2017). This can be ascertained by the validation of response variables resulting from the interpolated variables (Moyeed and Papritz, 2002; Kravchenko, 2003; Mueller, et al., 2004; Brouder, et al., 2005; Isaaks and Srivastava, 1989). There are not many studies reported in the literature that evaluate the relative performance of different interpolation methods for predicting spatial variability of hydraulic conductivity. Consequently, performing a critical evaluation of five interpolation methods, namely Kriging, Inverse Distance Weighted, Natural Neighbor, Spline and Trend used for the short range spatial prediction of near surface saturated hydraulic conductivity is very significant. The study quantified the variability associated with the prediction of in-situ hydraulic conductivity when different interpolation methods are used. The accuracy of different methods was assessed by comparing the prediction results with the measured hydraulic conductivity in the field.

5.3.1. Spatial Interpolation Methods

This section briefly describes five spatial interpolation methods, namely Inverse distance weighted, Kriging, Natural neighbor, Spline and Trend used in this study for spatial interpolation of soil hydraulic conductivity.

5.3.1.1. Inverse Distance Weighted (IDW) Method

The inverse distance weighted (IDW) method is a deterministic interpolation method based on the surrounding measured values. The method assumes that each measured point has an influence on adjacent points that decreases with distance. Hence, the method assigns greater weights to measurement points close to the prediction point. For interpolation, some specified mathematical formulas are estimated by assigning a weight. The inverse of the distance is raised to a mathematical power (Hutchinson, 1993), and an optimal value for the power is determined by minimizing mean absolute error. In this study, the analysis was carried out using ArcGIS Geostatistical Analyst extension configuration (Wahba, 1990). This interpolation technique determines the values using a

linearly weighted combination to a set of sample points, which does not require prior information. IDW offers a direct estimate of the distribution of uncertainty in the categorical or discrete variable (Moyeed and Papritz, 2002), and hence the most probable values at unsampled locations can be obtained. By identifying the search area, interpolation will use the number of known points within that area. Interpolated points are appraised based on their distance from the known values of sample points. Points that are closer to known values will be more influenced than points that are farther away, which can be described by the following formula:

$$X_P = \frac{\sum_{i=1}^{n} (\frac{x_i}{d_i})}{\sum_{i=1}^{n} (\frac{1}{d_i})} \quad (5.1)$$

where, X_p is the interpolated value, x_i is the sample value at the sample point i, d_i is the distance from the known sample point i to the estimated point; i = 1, 2, 3…. N, the known sample points. The advantage of using IDW is that it can approximate extreme variations and dense sample data points are interpolated with efficacy. The disadvantage is that it is not good for determining extreme values, both maximum and minimum (Mueller, et al., 2004; Brouder, et al., 2005).

5.3.1.2. Kriging Method

Kriging is a statistically optimal interpolator, which minimizes estimation variance when spatial continuity of the variable is known (Mueller, et al., 2004; Babak, 2014). This method produces a predicted surface from a data set of scattered points and optimal interpolator statistically such that, it reduces the variance when the variogram is known (Oliver and Webster, 1990; Robson, 1997). It uses the distance and the difference between known data points for determining unknown values. It also assumes that the direction and distance between the sample data points has a spatial connection, which is thereafter used to describe the variation in the surface (Burrough and McDonnell, 1998). To estimate the output value for every unsampled site, a mathematical function is fitted to an identified number of sample data points within a definite radius. The procedure includes the statistical study of the data, subsequent modeling of variogram and surface construction (Zhang, et al., 1995). The predicted values are determined from the connections between the samples by means of the weighted average method. This method weights the nearby

sample values to develop a prediction for an unsampled site (Burrough, 1987). The general formula used in Kriging method is

$$Z(S_0) = \sum_{i=1}^{N} \lambda_i Z(S_i) \qquad (5.\ 2)$$

where, $Z(S_i)$ is the measured value at the i^{th} location, λ_i is an unknown weight for the measured value at the i^{th} location, $Z(S_0)$ is the predicted value and i =1, 2… N, are the number of measured values.

For modeling the observed semi-variogram, four functions viz., circular, spherical, exponential, and linear were selected in this study (Li, et al., 2000). The choice of the model (designated as K-C, K-S, K-E, and K-L) would affect the prediction of the unknown value. Generally, the curve shape changes considerably near the origin, thereby impacting the prediction. Consequently, the output surface generated is not smooth. Each of the four models mentioned above is intended to appropriate diverse kinds of situations more precisely (Tang, 2002). The advantage of using the kriging method is that it can approximate directional effects, surpasses the lowest and highest point values. However, it does not traverse through any sample point values and as a result, interpolated values become higher or lower than the actual values.

5.3.1.3. Natural Neighbor Method (NNM)

Natural neighbor method (NNM) is an interpolation technique where the value of the unsampled location is set to the value of the nearest data point (Babak, 2014). It is a geometric approximation technique, which uses the natural neighborhood area formulated around each sample point in the data set corresponding to polygonal declustering. Like IDW, the elementary equation of NNM is based on the weighted-average technique. NNM chooses the adjoining nodes, which form a convex hull of the interpolation sample point, then weights their values by equivalent area (Sibson, 1981). The equation for NNM is given by Eq. 5. 3, where the points used to approximate the attribute's (parameter considered) value at location x are the natural neighbors of x.

$$f(x) = \sum_{i=1}^{k} w_i(x) a_i \qquad (5.\ 3)$$

where $f(x)$ is the interpolated function at the point x, i =1,2… k are known sample points, a_i is the attribute of each point in the sample space, $\boldsymbol{w_i(x)}$ is the weight, and each of the neighbor's weight is equal to the natural neighbor coordinate of x related to this neighbor (Ledoux and Gold, 2004). The method can construct precise surface models from sparsely

spread data sets or sample data points, which are spread with irregular density (Boissonnat and Cazals, 2002). The advantage of using NNM is that it can approximate huge numbers of sample data points with efficacy.

5.3.1.4. Spline Method

Spline method (SM) constructs a smooth surface, which precisely traverses through the sample data points while reducing the surface curvature. In this, a mathematical function is fitted to an identified number of adjacent input points where the surface is crossing through the sample data points. This method is good for moderately changing surfaces as it uses slope formulations (Franke, 1982). The mathematical function used for the spline spatial interpolation method is given by Eq. 5. 4,

$$S(x,y) = T(x,y) + \sum_{j=1}^{N} \lambda_j R(r_j) \tag{5. 4}$$

where, N is the number of points, j = 1, 2... N, λ_j are the coefficients, r_j is the distance from the point (x, y) to the j^{th} point.

$T(x, y)$ and $R(r)$ are estimated in accordance with the regularized option as,

$$T(x,y) = a_1 + a_2 x + a_3 y \tag{5. 5}$$

where, a_i are coefficients

$$R(r) = -\frac{1}{2\pi\varphi^2}[\ln(\frac{r\varphi}{2}) + c + B_0(r\varphi)] \tag{5. 6}$$

where, r is the distance, ϕ^2 is the weight parameter, B_0 is the modified Bessel function, c is equal to 0.577215, which is a constant (Mitas and Mitasova, 1988). Spline uses curved lines to calculate sample values. If the weight is more, the values are more adapted to be within the range of the sample data. The advantage of using the spline method is that it can approximate above the highest value and below the lowest value of the sample data points and can also construct a smooth surface. The disadvantage is that it is not good for determining values when the sample data points are adjacent to each other and have huge variations in values (Mitas and Mitasova, 1988).

5.3.1.5. Trend Method

Trend interpolation method (TM) is a statistical technique, which is expressed as a polynomial function for the input sample data points and varies gradually (Chidley and Keys, 1970). The generalized form of the polynomial function is given as Eq. 5. 7,

$$Z = b_0 + b_1 x + b_2 y + b_3 x^2 + b_4 y^2 + ... \quad (5.\ 7)$$

where, Z is the spatially distributed surface variable, and x and y are the locational coordinates, b_i are the coefficients (Hembd and Infanger, 1981). It is an approximate interpolator where the resultant surface seldom traverses through the sample points. This method is mainly useful for recognizing coarse scale pattern from the data. From the sample data points, this interpolation method can perceive trends, which characteristically fluctuate smoothly. The sample data points are fitted with a polynomial equation to the whole surface by least-square regression, which reduces surface variance corresponding to the sample data point values (Kruizinga and Yperlaan, 1978). Subsequently, the surface is obtained such that the sum of the differences of the actual and the predicted values is insignificant for each of the input data.

5.3.2. Comparison of the Spatial Interpolation Methods

The near surface K_s determined at different locations of a given stations were used to evaluate the spatial variability using ArcGIS 10.3.1. Figures 5. 2 and 5. 3 depicts the spatial variability of K_s using different interpolation methods for the stations of the study area. In general, for the study area, K-E, K-S, and IDW portrayed a similar interpolation trend, which is marginally different from K-C and K-L. The NNM and spline procedures depicted a similar trend. However, the TM interpolation results were quite different and more orderly pattern as compared to other methods. Irrespective of the methods adopted, the spatial variability of K_s was found to vary in the same manner as that of the percentage variation of sand fraction depicted in Fig. 3. 5 (b). The sand fraction was predominant varying from 40 to 87% for the study area and as expected, the contours of K_s increased in the same direction as that of sand fraction.

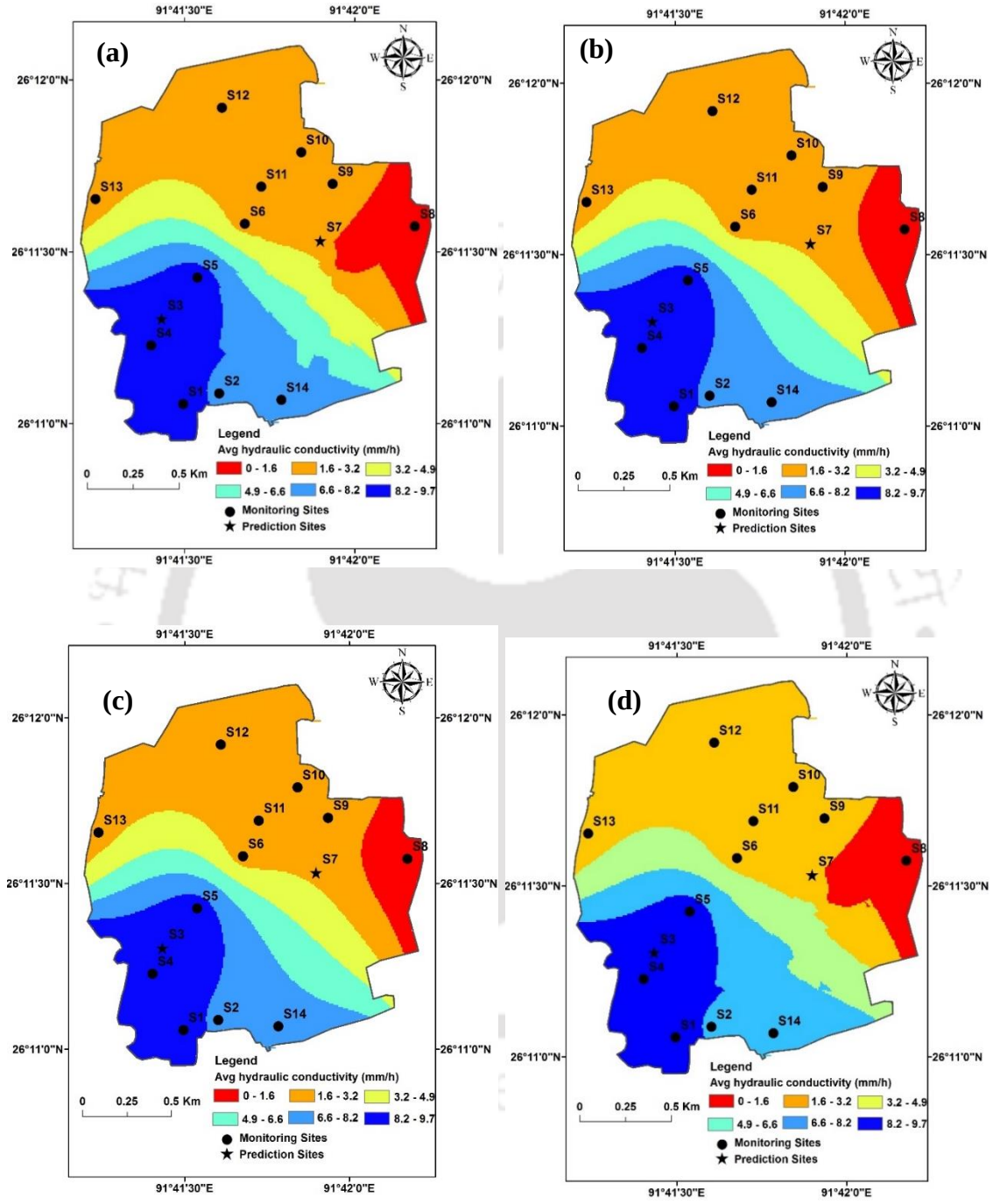

Fig. 5. 2 Spatial prediction of hydraulic conductivity (mm/h) based on different kriging methods (a) circular (b) exponential (c) spherical (d) linear method

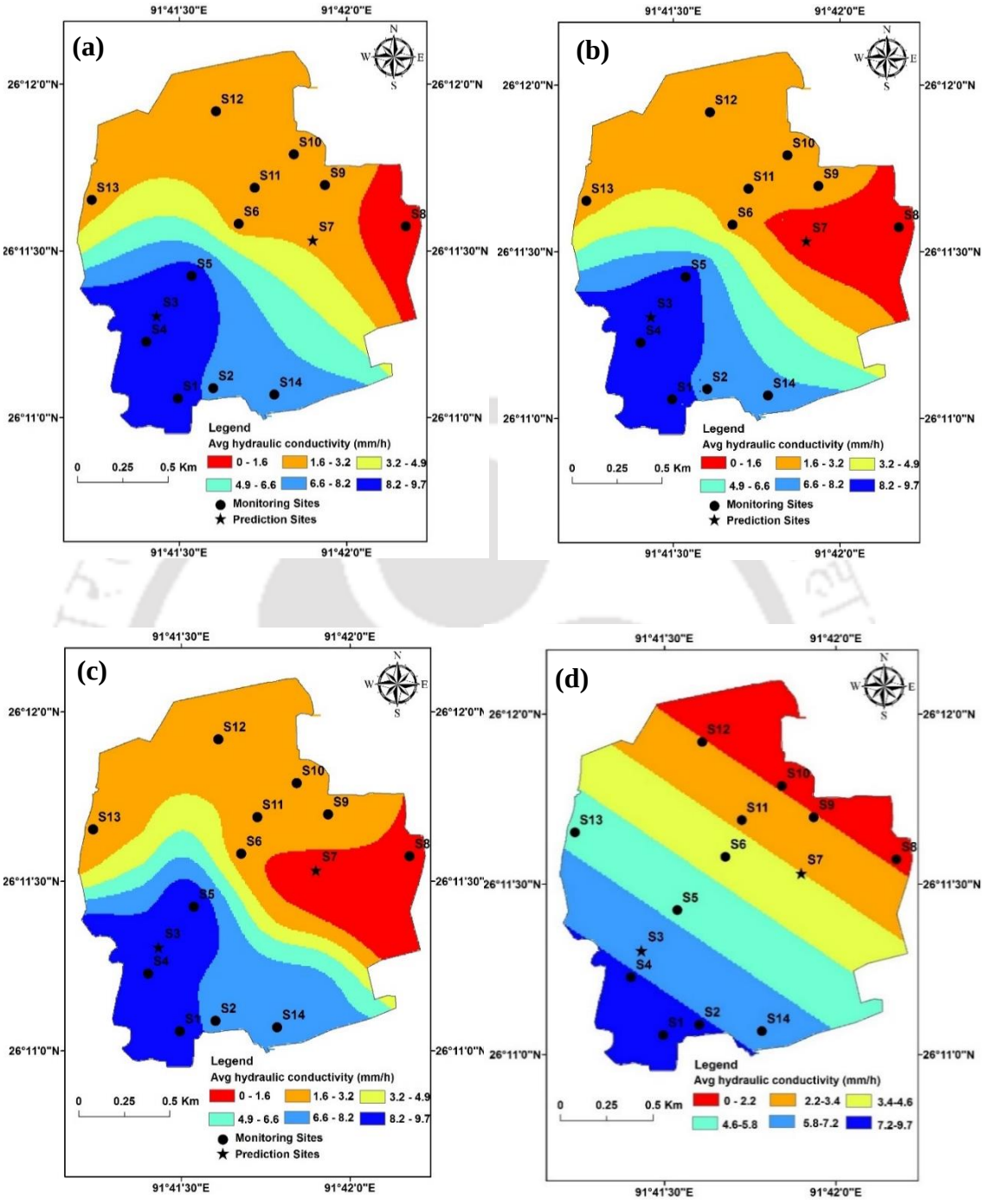

Fig. 5. 3 Spatial prediction of hydraulic conductivity (mm/h) based on (a) IDW, (b) NN method, (c) spline and (d) trend method

For evaluating the efficacy of spatial interpolation methods considered in this study, the K_s estimated from spatial interpolation methods were compared with the measured values for 2 stations (S3 and S7) of the study area. The results of estimation

from different methods are tabulated in Table 5. 1. The values reported in Table 5. 1 were used to determine the root mean square error (RMSE) of the estimated K_s with respect to the measured values and illustrated in Fig. 5. 4. It can be noted from Fig. 5. 4 that K-S, K-L, K-C, K-E and NNM gave comparable RMSE with K-E marginally better than other methods. However, the RMSE of SM was considerably lesser than the other methods indicating its efficacy for spatial prediction of near surface K_s. The SM can model better than other spatial interpolation methods. From Table 5. 1 it can be further noted that the prediction of K_s was found to be more precise for the station with a higher percentage of sand. As the percentage of sand decreased, the spatial prediction of K_s also diminished. The spatial prediction of K_s at station S7 is found to be relatively inferior as compared to other station. This may be attributed to the type of soil (silty soil) and a sudden transition of soil type from sand to silt thereby affecting the accuracy of spatial interpolation. This indicates the predominance of soil type in the prediction of spatial variability of K_s. This observation calls for further investigation to appraise the systematic effect of soil type of spatial interpolation of K_s by considering stations with different soil characteristics. This could not be accomplished in this study because the surface soils in the study area were predominantly constituted of sand.

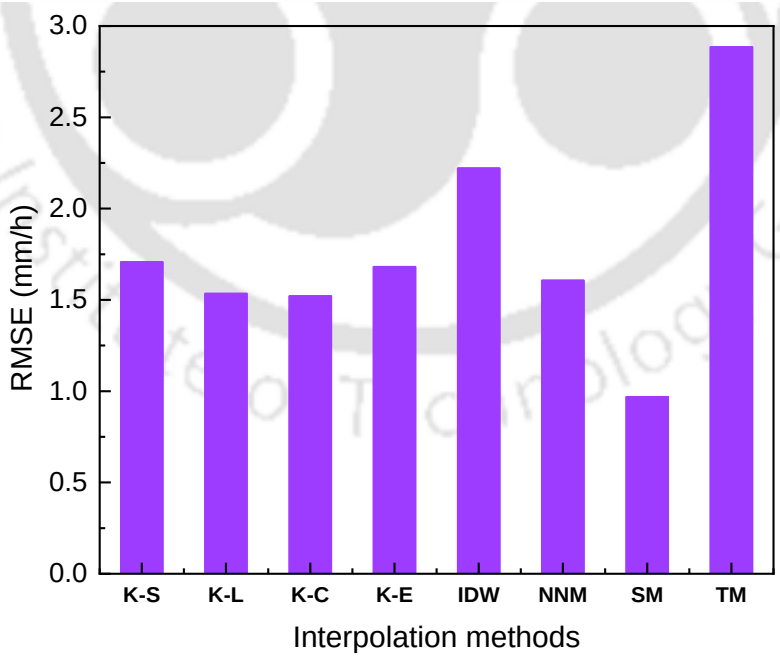

Fig. 5. 4 Evaluation of spatial interpolation methods based on RMSE

Table 5. 1 Actual and predicted hydraulic conductivity (mm/h) using different interpolation methods

Station	Hydraulic conductivity (mm/h)								
	Actual	Interpolated							
		Kriging				IDW	NNM	SM	TM
		K-S	K-L	K-C	K-E				
S3	9.36	9.53	9.51	9.53	9.47	8.01	9.55	6.67	9.61
S7	0.45	2.86	2.62	2.60	2.83	3.29	2.72	3.52	1.80

5.3.3. Spatial Autocorrelation of Hydraulic Conductivity

Spatial autocorrelation is a significant factor in geo-spatial analysis which is measured by both Moran's index (*I*) and Moran's scatterplot (Bivand et.al, 2009). Spatial autocorrelation is advantageous for developing patterns in complex data sets. Spatial autocorrelation is a special case of the spatial correlation function. Like correlation coefficients, its values vary from -1 to 1, though, Moran's *I* measures how one object is similar to others surrounding it. A value of -1 portrays the dispersion perfect i.e. clustering of dissimilar values, 0 signifies no autocorrelation i.e. randomness whereas +1 depicts clustering of similar values (Moran, 1948). Moran's *I* is a characteristic parameter of spatial weight matrices, so the selection of weight functions is very significant for autocorrelation analysis (Getis, 2009). In this study, the data from the 14 stations of the study area is employed for validation. The improved framework of spatial autocorrelation can be applied to all the 14 stations of the study area. The log transformed hydraulic conductivity data are employed for each of the stations as a size measurement, while the distance between any two stations is used as a spatial contiguity measurement.

The calculations of Moran's *I* are based on a weighted matrix w_{ij}. Similarities between units is calculated as the product of the differences between y_i and y_j with the overall mean (Moran, 1948), where *y* represents the hydraulic conductivity.

$$\text{Similarity} = (y_i - \bar{y})(y_j - \bar{y}) \tag{5. 8}$$

where $\bar{y} = \sum_{i=1}^{n} \frac{y_i}{n}$

The Moran's statistic is designed using the basic form, which is divided by the sample variance:

$$S^2 = \frac{\sum (y_i - \bar{y})^2}{n} \tag{5. 9}$$

$$I = \frac{1}{S^2} \frac{\sum_i \sum_j w_{ij}(y_i - \bar{y})(y_j - \bar{y})}{\sum_i \sum_j w_{ij}} \quad (5.10)$$

Therefore, Moran's *I* is the slope in a regression of $\sum_j w_{ij}.(y_j - \bar{y})$ on $(y_i - \bar{y})$ and Moran's scatter plot is depicted based on $[(y_i - \bar{y}), \sum_j w_{ij}.(y_j - \bar{y})]$.

The value at *i* is plotted on the x-axis whereas its spatial lag weighted average of neighboring values are plotted on the y-axis. Then the slope of the linear fit is the Moran's *I* (Moran, 1948). The null hypothesis for the test is that the data is randomly distributed and the alternate hypothesis is that the data is more spatially clustered than any normal expectation. A positive value signifies data is spatially clustered, whereas a negative value shows data is clustered in a competitive way or alternating values with higher degree of spatial heterogeneity. Moron's *I* is a global statistic i.e. a single value for the whole spatial pattern but it does not provide the location of clusters.

The value of Moran's *I* is 0.269, which implies a moderate positive autocorrelation between the stations in the study area. In accordance with the Moran's scatterplot as shown in Fig. 5. 5, spatial autocorrelation can be categorized into four types as the high-high correlation (H-H type: e.g., S1-S5 and S-14) in the first quadrant, the low-high correlation (L-H type: e.g. S13) in the second quadrant, the low-low correlation (L-L type: e.g., S6-S12) in the third quadrant, and the high-low correlation (H-L type: no such stations) in the fourth quadrant (Chen, 2013). In the first and third quadrant, statistically significant cluster of high values (H-H), cluster of low values (LL) can be found. In the second and fourth quadrant outliers can be found in which a high value is surrounded by low values (HL) and a low value is surrounded by high values (LH). In the study area, except the marginal case of S13, in all the other stations, statistically significant clustering can be observed. Spatial autocorrelation identifies concentrations of high values, concentrations of low values, and spatial outliers. Concentration of high values are observed for S1to S5 and S14, which are either sandy or loamy sand. Low values can be found for S6 to S12, which are either loamy or silty and S13 is marginally spatial outlier. The sharpest boundary exists between high and low hydraulic conductivity values of S1 to S5 and S14. In the study area, S13 gives the marginally inconsistent value of hydraulic conductivity in accordance with spatial autocorrelation with unexpectedly higher values of hydraulic conductivity.

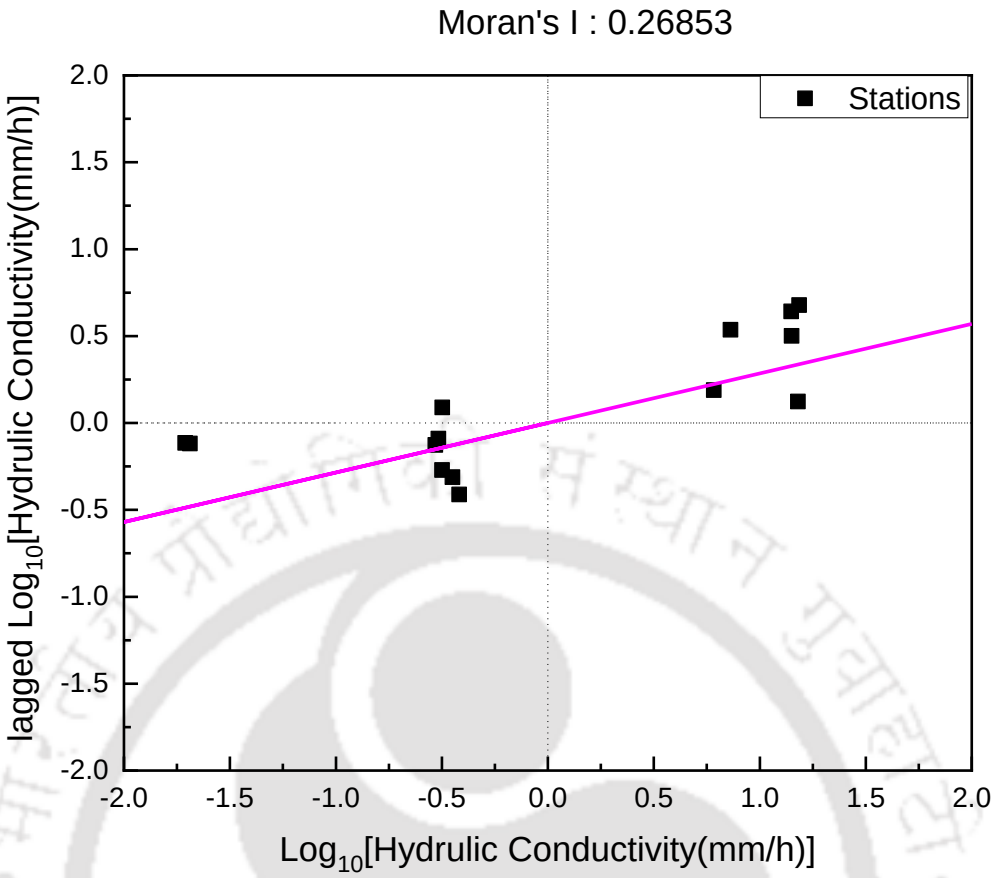

Fig. 5. 5 Moran's scatter plot

5.4. Seasonal Variation of Hydraulic Conductivity

The seasonal variation of hydraulic conductivity is shown in Fig. 5. 6. It can be observed that there is high infiltration from December to February and the highest in the month of December. It decreases from February to June with June exhibiting the lowest infiltration. After June, there is slight increase till October and reaches highest value in December. The pattern of variation of hydraulic conductivity is consistent for all the locations and associated with the initial soil moisture content variation subject to the rainfall pattern of the study area as discussed below.

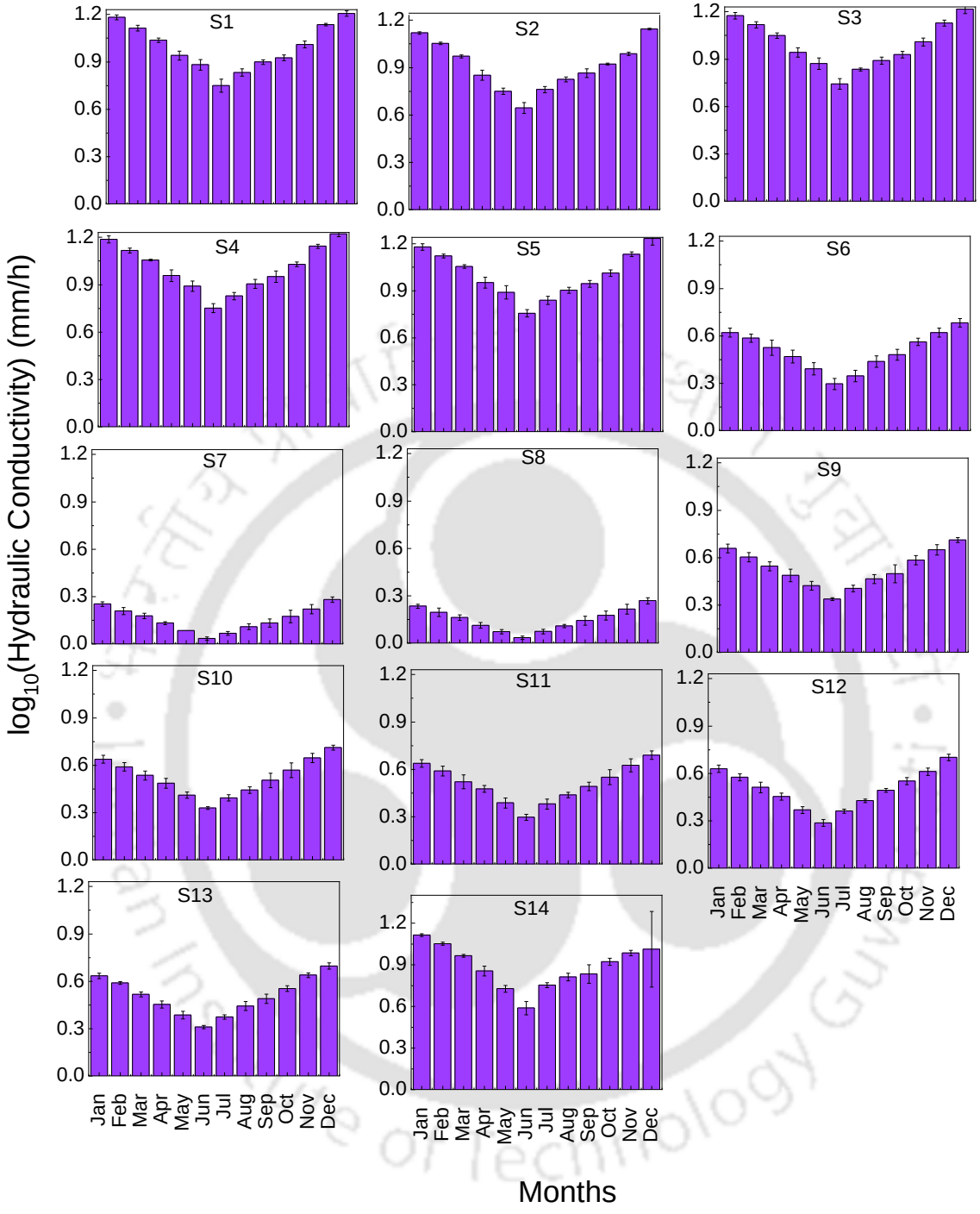

Fig. 5. 6 Monthly variation of hydraulic conductivity (mm/h) at all the stations

5.4.1. Association of Rainfall and Initial Soil Moisture Content with Hydraulic Conductivity

In order to study the interrelationship among the hydraulic conductivity, rainfall and initial moisture content of the soil, the average seasonal variation in the rainfall data

and the initial moisture content from September 2011 to August 2015 are analysed. The monthly variation of the rainfall for four years from the month of September 2011 to August 2015 for the study area is depicted in Fig. 5. 7. It can be inferred from the variation of rainfall that June is the wettest month whereas December is the driest month. In the month of June 318 mm of rainfall occurs and it experiences lowest rainfall in the month of December which is 7 mm. The average seasonal variation in the measured initial moisture content from September 2011 to August 2015 is shown in Fig. 5. 8. Also the spatial variability of the initial moisture content is analysed using ArcGIS 10.3.1 software and depicted in Fig. 5. 9. The results are consistent with the trends observed for the variation of hydraulic conductivity. Maximum rainfall induces high initial moisture content resulting in low hydraulic conductivity.

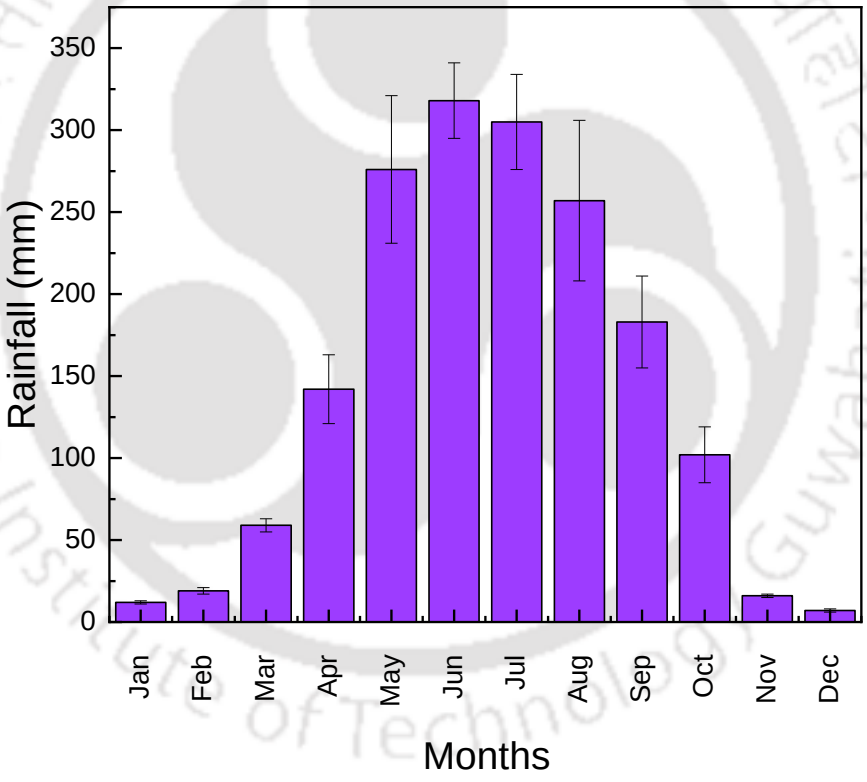

Fig. 5. 7 Monthly variation of average rainfall (mm) for the study area

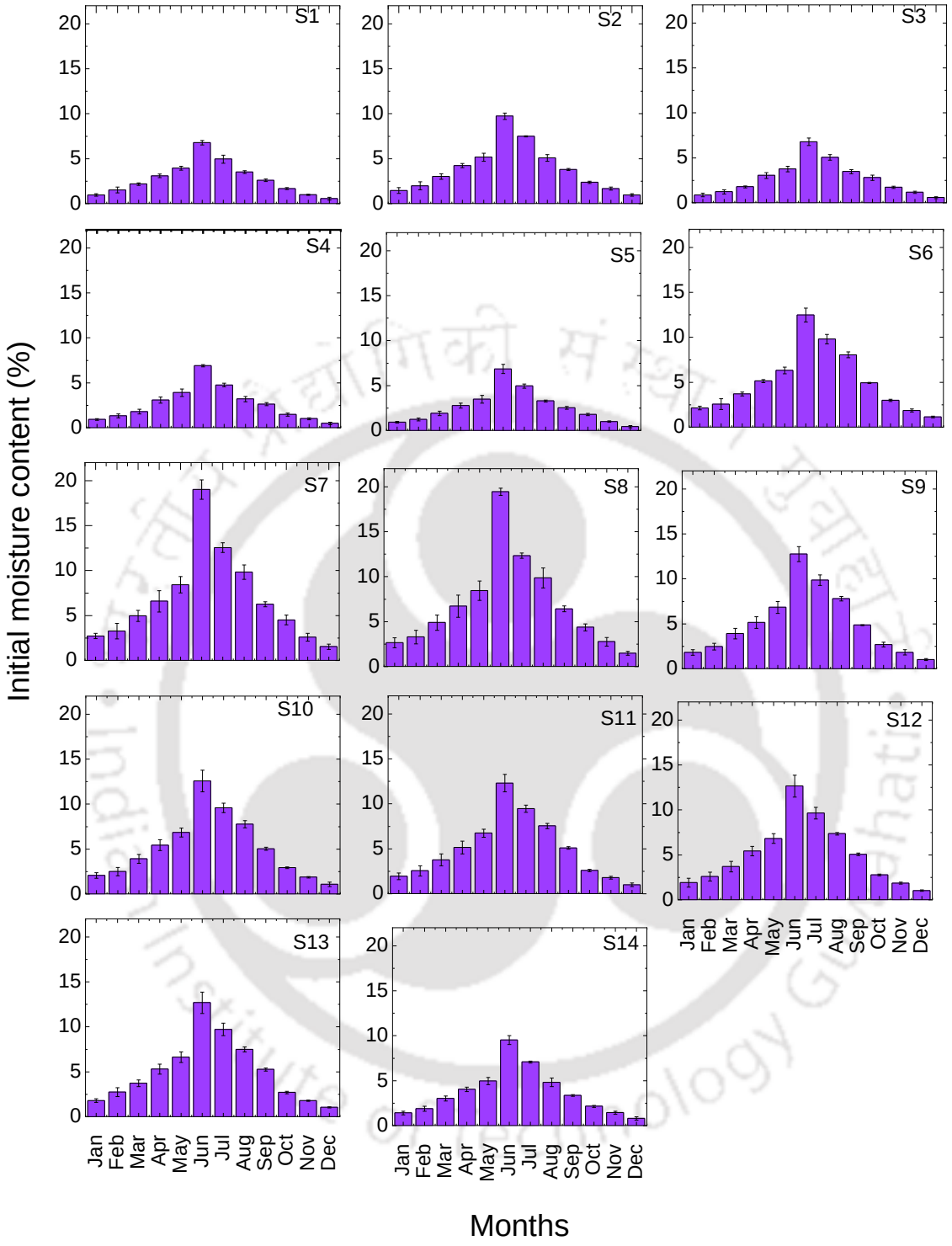

Fig. 5. 8 Monthly variation of initial moisture content (%) for all the stations

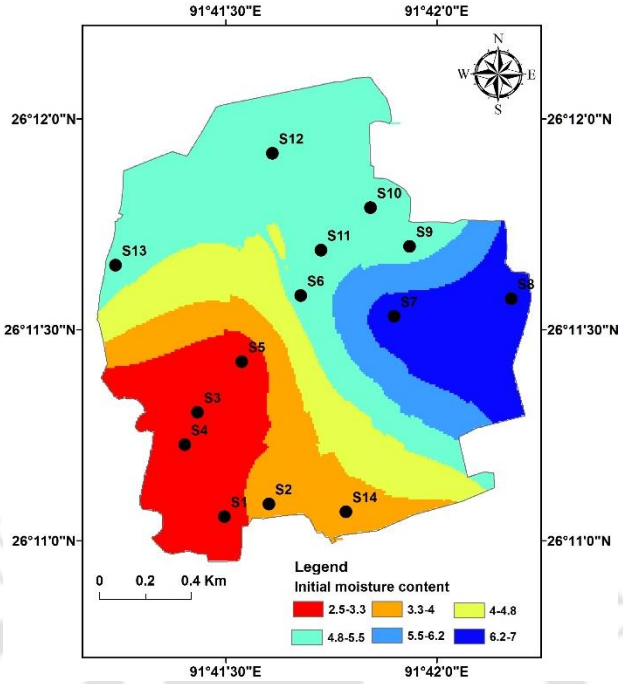

Fig. 5. 9 Spatial variation of initial moisture content (%) for the study area

In statistics, measure of association is used to quantify a relationship between two or more variables. In this study, Pearson's correlation coefficient, Spearman rank-order correlation and Kendall tau were used to measure the strength and significance of association of hydraulic conductivity, initial moisture content and rainfall (Gibbons,1985; Berry and Mielke, 1992; Krieger and Green, 1993; Gibbons, 1993; Kraemer, 2000; Wilcox, 2007). The results of the analysis are listed in Table 5. 2. It can be observed that the rainfall and initial moisture content has a very strong positive correlation and hydraulic conductivity has a strong negative correlation with both rainfall and initial moisture content. Therefore, there is sufficient indication to determine the existence of a significant linear relationship between hydraulic conductivity, initial moisture content and rainfall.

Table 5. 2 Correlation matrix from different methods to measure strength of association

Variable	Pearson's correlation coefficient			Spearman rank-order correlation			Kendall tau		
	Rainfall	IMC	K_s	Rainfall	IMC	K_s	Rainfall	IMC	K_s
Rainfall	1	0.93	-0.94	1	0.99	-1.00	1	0.94	-1.0
IMC	0.93	1	-0.90	0.99	1	-0.99	0.94	1	-0.9
K_s	-0.94	-0.90	1	-1.00	-0.986	1	-1.00	-0.94	1

The mean values from diverse groups with dissimilar conditions are often compared. For a comparison of more than two group means, the one-way analysis of variance (ANOVA) is the suitable method (Venkatesh, et.al., 2013). It considers the relative size of variance amongst group means in comparison with average variance within groups (Green and Salkind, 2010). The 'SS' represents the sum of squares where 'SSB' signifies the sum of squares between groups which is the difference of group means. The 'SSW' signifies sum of squares within groups. The mean of squares between groups (MSB) is then attained by dividing SSB with degrees of freedom. Similarly, the mean of square within groups (MSW) is obtained by dividing SSW with degrees of freedom. The ratio of MSB and MSW which is known to follow the *F* distribution governs how comparatively bigger the difference is between group means in comparison to within the group. For any statistical deduction, the *F* value determined from the observed data needs to be compared with the critical value at an error level of 0.05 in the *F* table known as $F_{critical}$. Larger *F* value suggests that group means are significantly dissimilar with each other in comparison to the difference of the observations within each groups (Green and Salkind, 2010). Larger *F* value than the critical value i.e., $F_{critical}$ indicates that the variations between group means are greater than what would be expected by chance.

In this study, the relationship between hydraulic conductivity and seasonal-spatial factors are examined. The independent variables considered are the seasonal-spatial factors (rainfall and initial moisture content), and the dependent variable is the hydraulic conductivity. Using these variables, it was explored whether a statistical significant relationship existed between hydraulic conductivity and seasonal-spatial factors. Statistical analysis was performed to assess the seasonal and spatial predictability of hydraulic conductivity by testing a set of null hypotheses at the significance level of 5 % by using one-way ANOVA. For quantitative statistical analysis, the log transformed hydraulic conductivity was used. The results of testing HI to H10 hypotheses are presented in Table 5. 3 along with their respective statistical level of significance. The given null hypothesis will be rejected if the corresponding *p* value is less than the significance level of 0.05 with *F* values larger than the critical value. Then the result is interpreted as statistically significant difference among the means of the groups at the error level of 0.05.

Table 5. 3 Results of one-way ANOVA

Hypothesis	Null Hypothesis	F	P values	$F_{critical}$	Decision
H1	There is a statistically significant relationship between the measured monthly log transformed hydraulic conductivity values for all the 12 months	2.279	0.0136	1.851	Reject
H2	There is a statistically significant relationship between the measured monthly log transformed hydraulic conductivity values for the months of November-January	0.487	0.618	3.238	Fail to reject
H3	There is a statistically significant relationship between the measured monthly log transformed hydraulic conductivity values for the months of February-April	0.497	0.612	3.238	Fail to reject
H4	There is a statistically significant relationship between the measured monthly log transformed hydraulic conductivity values for the months of May-July	0.170	0.844	3.238	Fail to reject
H5	There is a statistically significant relationship between the measured monthly log transformed hydraulic conductivity values for the months of August-October	0.653	0.526	3.238	Fail to reject
H6	There is a statistically significant relationship between the measured monthly log transformed hydraulic conductivity values for all the stations of the study area	69.065	0.000002	1.7845	Reject
H7	There is a statistically significant relationship between the measured monthly log transformed hydraulic conductivity values for sandy soils of the study area	0.0185	0.997	2.817	Fail to reject

H8	There is a statistically significant relationship between the measured monthly log transformed hydraulic conductivity values for loamy soils of the study area	0.137	0.983	2.354	Fail to reject
H9	There is a statistically significant relationship between the measured monthly log transform hydraulic conductivity values for silty soils of the study area	0.047	0.830	4.301	Fail to reject
H10	There is a statistically significant relationship between the measured monthly log transformed hydraulic conductivity values for loamy sand soils of the study area	0.140	0.712	4.301	Fail to reject

H1 and H6 results indicate that there is as statistically significant difference among the means of the groups of log transformed hydraulic conductivity values as the observed *F* value is larger than the critical value. Hence the result may be interpreted as statistically significant difference among the means of the groups at the error level 0.05. The result suggests the rejection of the null hypothesis that all the group means are the same, and coincidently supports that at least one group mean differs from other group means.

It is clear from the Table 5. 3 that the monthly log transformed hydraulic conductivity values are statistically similar seasonally but not annually. Hydraulic conductivity for the study area can be ascertained for four seasons independently. Similarly, the monthly log transformed hydraulic conductivity values are statistically similar for a particular soil but not for the study area as a whole. Therefore, hydraulic conductivity determination for a particular study area has to incorporate seasonal and soil aspects in it. Hence an attempt was made to assess the effect of both seasonal and spatial factors on log transformed hydraulic conductivity values using a 2-way ANOVA with repetition. The statistical output is shown in Table 5. 4 which shows that the spatial variation is a significant aspect of the log transformed hydraulic conductivity values, whereas seasonal variation did not reach statistical significance at 0.05 alpha level. Statistical output for 2-way ANOVA for assessing the effect of interaction between the spatial and seasonal factors is non-significant at 0.05 alpha level.

Table 5. 4 Results of two-way ANOVA

Hypothesis	Null Hypothesis	F	P values	$F_{critical}$	Decision
H1	There is no statistically significant variation within the measured monthly log normal hydraulic conductivity values for the months of November-January	3.86	0.006	1.704	Reject
H2	There is no statistically significant variation within the measured monthly log normal hydraulic conductivity values for all the stations with sandy soils of the study area	0.48	0.618	3.238	Fail to reject
H3	There is no statistically significant variation within the measured monthly log normal hydraulic conductivity values for the months of November-January and all the stations with sandy soils of the study area	3.51	0.014	1.851	reject

5.5. Summary

The efficacy of different interpolation methods for estimating the spatial variability of near surface saturated hydraulic conductivity, K_s was evaluated. Five spatial interpolation methods, namely Kriging, Inverse Distance Weighted, Natural Neighbour, Spline and Trend methods were used for spatial predictions of K_s. The study indicated that with sudden change in soil characteristics and soil compaction state, the accuracy of all methods decreases. For a small study area with a higher number of point measurements, Kriging with exponential, spherical functions and inverse distance weighted methods of spatial interpolation portrayed a similar trend. The trend method interpolation results were quite different and more orderly pattern as compared to other methods for the study area. The spatial variability of K_s was found to be in the same pattern as that of the percentage variation of the sand fraction for the study area.

Based on the root mean square error (RMSE), it was noted that Kriging with circular, spherical, exponential and linear function and natural neighbour method gave comparable RMSE with Kriging-exponential method marginally better than others. The RMSE of spline method was considerably lesser than the other methods. It was further

noted that the prediction of K_s was found to be more precise for the station with a higher percentage of sand. As the percentage of sand decreased, the spatial prediction of K_s also diminished. This indicates the predominance of soil type in the prediction of spatial variability of K_s, which needs to be investigated further.

The results presented in this study attempted to evaluate the time varying response of hydraulic conductivity determined using the MDI for four consecutive years within the study area. It was evident that all the 14 stations have a consistent pattern of hydraulic conductivity variation with time (seasonal). From January to June the hydraulic conductivity values were found to decrease and increase from June to December. The trend was associated with the rainfall and initial soil moisture variation. It was observed that the hydraulic conductivity has a strong negative association with both rainfall and initial moisture content. The Moran's index infers a moderate positive autocorrelation between the stations in the study area. Another finding from the spatial autocorrelation is that the difference in hydraulic conductivity values are negatively associated with distances. For adjacent stations having the same soil types, less differences in hydraulic conductivity values are observed.

Chapter 6

Role of Measurement Time and Equations for Determining Hydraulic Conductivity

6.1. General

This chapter critically evaluates the appropriateness of different mathematical equations for determining hydraulic conductivity based on disc infiltrometer measurements. The first section of this chapter presents a detailed discussion on steady and transient mathematical equations for determining hydraulic conductivity and the last section deals with the influence of short term and long term MDI measurements on hydraulic conductivity determination.

6.2. Mathematical Equations for Determining Hydraulic Conductivity

There are several well-established mathematical equations for determining near surface hydraulic conductivity in the field (Angulo-Jaramillo, et al., 2000). Researchers have proposed short term transient methods and long term steady state methods for analyzing disc infiltrometer data (Ankeny, et al., 1991; Logsdon and Jaynes, 1993; Jacques, et al., 2002; Angulo-Jaramillo, et al., 2000, 2016). These methods adopt different assumptions, mathematical formulations and boundary conditions for estimating hydraulic characteristics (David and César, 2009; Haverkamp, et al., 1994; Reynolds, et al., 2002). This may lead to the variability in the determination of surface hydraulic conductivity using MDI (Verbist, et al., 2013). MDI measures near saturated hydraulic conductivity $\left(K_{h_0}\right)$ corresponding to a negative pressure head $\left(h_0\right)$ applied at the ground surface. The variabilities in the hydraulic conductivity depending on the measurement techniques are appraised in the literature (Verbist, et al., 2013). However, there is no conclusive recommendation on the appropriateness of any particular measurement methodology. It is mainly due to the lack of reference true value for hydraulic conductivity in the field (Morbidelli, et al., 2017). Researchers have carried out studies to evaluate different physically based, semi-empirical and empirical infiltration equations in different types of soil (Hsu, et al., 2002; Mishra, et al., 2003; Chahinian, et al., 2006; Sihag, et al., 2017). However, there are not many studies that critically evaluate the appropriateness of

different mathematical equations for determining hydraulic conductivity based on MDI measurements under identical field conditions and different seasons.

The primary objective of this chapter is to evaluate nine popular mathematical equations that can be used to determine hydraulic conductivity based on MDI measurements performed at 14 stations within a sub catchment of north-east India for two different seasons. A well established Guelph permeameter (GP) was used as the reference for saturated hydraulic conductivity (K_s) measurement in the field (Salverda and Dane, 1993; Reynolds and Elrick, 1985; Bagarello and Giordano, 1999; Morbidelli, et al., 2017). Some of the mathematical equations considered in this study determine K_{h_0} instead of K_s . For such cases, K_{h_0} measured at a water head h_0 lower than zero was extrapolated to h_0 equal to zero for determining K_s as discussed in Section 5.2 and as shown in Fig. 5. 1. From the past research works, it was observed that Wooding-Gardner, Weir's Refinement, van- Genuchten Zhang (vG-Z), Ankeny (A), and Haverkamp (H) equations are appropriate mathematical equations that can be used for analyzing MDI results for the field conditions.

Infiltration beneath the MDI is governed by axisymmetric three-dimensional water flow into an initially unsaturated porous medium. For a given field condition, MDI measures cumulative infiltration with time for a specific time interval. This raw data is analyzed using different steady state and transient mathematical equations for determining K_{h_0} . The details of mathematical equations considered in this study are briefly discussed as follows.

6.2.1. Wooding-Gardner Equation (W-G)

According to Wooding (1968), the steady-state flux, q_{h_0} entering into the soil at a tension head h_0 , from a shallow circular pond of radius r_0 , can be approximated by a three-dimensional axisymmetric infiltration equation (Eq. 6. 1):

$$q_{h_0} = K_{h_0}\left[1 + 4\lambda_c / (\pi r_0)\right] \tag{6. 1}$$

where $\lambda_c = 1/\alpha$ c, is the macroscopic capillary length, and K_{h_0} is the near saturated hydraulic conductivity which is a function of h_0 . The first term of Eq. 6. 1 represents the one-dimensional vertical infiltration below the disc under gravity. The second term designates the lateral spread under the capillary matric force. The Gardner (1958)

exponential function for the estimation of hydraulic conductivity (K_{h_0}) can be expressed as,

$$K_{h_0} = K_s \exp(\alpha_c h_0) \quad \text{, when } h_0 \le 0 \tag{6. 2}$$

where K_s is the saturated hydraulic conductivity.

Combining both Wooding's and Gardner equations, K_s can be determined by Eq. 6. 3.

$$Q_{h_0} = \pi r^2 K_s \exp(\alpha_c h_0)\left(1+\frac{4}{\pi r \alpha_c}\right) \tag{6. 3}$$

where Q_{h_0} is the steady-state flow rate under a given tension h_0. The unknowns in this equation are K_s and α_c, which can be estimated by conducting infiltration measurements with a fixed disc radius and multiple negative pressure heads (Wang, et al., 1998).

6.2.2. Weir's Refinement Method (W-R)

For water flow from a small surface source such as MDI disc, Weir (1987) observed that Wooding's approximate solution might not be representative. The flow rate and the infiltrometer disc radius, r_0 were normalized into the following dimensionless form:

$$Q^* = \frac{\alpha_c}{r_0 K_s \exp(\alpha_c h_0)} Q_{h_0} \tag{6. 4}$$

$$r^* = \frac{1}{2}\alpha_c r_0 \tag{6. 5}$$

Wooding's relationship was modified as,

$$Q^* = 4 + 2\pi r^* \tag{6. 6}$$

For, $r^* < 0.4$, Weir (1987) found that Eq. 6. 6 may not be precise and thereby proposed an alternative estimate for Q^* given by Eq. 6. 7.

$$Q^* = \frac{4\pi \sin^2(r^*)}{r^*\pi \sin(r^*)\cos(r^*) + 2r^* \sin^2(r^*)\ln(r^*) - 1.073(r^*)^3} \tag{6. 7}$$

The experimental fitting parameter α_c is determined from the known steady-state flow rates at two tensions h_1 and h_2 using Eq. 6. 8.

$$\alpha_c = \frac{\ln\left[Q(h_2)/Q(h_1)\right]}{h_2 - h_1} \tag{6. 8}$$

The saturated hydraulic conductivity can be estimated by Weir's equation as

$$K_s = \frac{\alpha_c}{r_0}\exp\left(-\alpha_c h_1\right)\frac{Q\left(h_1\right)}{Q^*} \tag{6. 9}$$

6.2.3. van-Genuchten - Zhang Method (vG-Z)

Zhang (1997a) proposed a method for determining near saturated hydraulic conductivity, K_{h_0} from the measured cumulative infiltration versus the square root of the time response of relatively dry soil. The measured result was fitted with a second-order polynomial equation for determining the hydraulic conductivity and sorptivity of the soil. Zhang (1997a) used simulated data of cumulative infiltration under the disc infiltrometer for the determination of constants C_1 and C_2 . The near saturated hydraulic conductivity K_{h_0} and sorptivity S_{h_0} was estimated by

$$K_{h_0} = \frac{C_2}{A_2} \tag{6. 10}$$

$$S_{h_0} = \frac{C_1}{A_1} \tag{6. 11}$$

where A_1 and A_2 are the dimensionless coefficients. Using numerous numerical experiments, the empirical relationships were established for A_1 and A_2 as functions of soil retention parameters, infiltrometer parameters, and initial water content (Zhang and van Genuchten, 1994; Zhang, 1997a). The dimensionless coefficients alter with the total infiltration time, although, the variation becomes insignificant as infiltration time increases and the coefficients can be treated as constants. By considering van Genuchten (1980) soil water retention function, the coefficients are given by the following equations:

$$A_1 = \frac{1.4b^{0.5}\left(\theta_0 - \theta_i\right)^{0.25}\exp\left[3\left(n-1.9\right)\alpha h_0\right]}{\left(\alpha r_0\right)^{0.15}} \tag{6. 12}$$

$$A_2 = \frac{11.65\left(n^{0.1}-1\right)\exp\left[2.92\left(n-0.19\right)\alpha h_0\right]}{\left(\alpha r_0\right)^{0.91}} \qquad n \geq 1.9 \tag{6. 13}$$

$$A_2 = \frac{11.65\left(n^{0.1}-1\right)\exp\left[7.5\left(n-0.19\right)\alpha h_0\right]}{\left(\alpha r_0\right)^{0.91}} \qquad n < 1.9 \tag{6. 14}$$

n and α represents the van Genuchten soil parameters, $h_0(<0)$ is the pressure head of the infiltrometer, r_0 is the radius of the infiltrometer, θ_0 is the water content at h_0, θ_i is the initial water content, b is the parameter equal to 0.55. The van Genuchten parameters for different soil texture can be obtained from Carsel and Parrish (1988).

6.2.4. White and Sully Method (W-S)

White and Sully (1987) proposed a method to determine the value of α_c in Gardner (1958) exponential hydraulic conductivity function (Eq. 6. 2) as follows:

$$\alpha_c = \frac{\left(\theta_{h_0} - \theta_n\right)(K_{h_0} - K_n)}{bS_{h_0}^2} \tag{6. 15}$$

where S_{h_0}, θ_{h_0} and K_{h_0} is the sorptivity, moisture content and hydraulic conductivity at pressure head h_0, θ_n and K_n are the initial moisture content and the corresponding hydraulic conductivity and b is a shape factor. Linking Eqs. 6.15 and 6.1 with an assumption that K_n is insignificant, White, et al. (1992) proposed the equation:

$$K_{h_0} = q_{h_0} - \frac{4bS_{h_0}^2}{(\theta_{h_0} - \theta_n)\pi r_0} \tag{6. 16}$$

where q_{h_0} is the flow rate at steady state for pressure head h_0, S_{h_0} was determined from early time cumulative infiltration versus square root of the time response of MDI by following vG-Z method (Eq. 6. 11), θ_{h_0} is obtained from the soil surface instantly after the measurement, θ_n is determined before the measurement, and b is taken as 0.55.

6.2.5. Simunek-Wooding Method (S-W)

Simunek, et al. (1998) presumed that in the interval between two adjacent heads, the parameter α_c in Gardner (1958) exponential hydraulic conductivity function was constant. This assumption was used to find out the hydraulic conductivity in the middle of the interval between two successive heads, h_i and h_{i+1}. The parameter α_c was given as,

$$\alpha_c = \frac{\ln \frac{q_{i+1}}{q_i}}{h_{i+1} - h_i} \qquad i = 1\ldots, \text{n-1} \tag{6. 17}$$

The average steady state infiltration rate can be described as:

$$q_{h_0} = \sqrt{q_{i+1} \times q_i + 1} \qquad i = 1\ldots, \text{n-1} \tag{6. 18}$$

Then the near saturated hydraulic conductivity, K_{h_0} was estimated as,

$$K_{h_0} = \frac{q_{h_0}}{1 + \frac{4}{r_0 \alpha_c}} \tag{6. 19}$$

6.2.6. Ankeny Method (A)

Ankeny, et al. (1991) proposed a multiple head method for the determination of near saturated hydraulic conductivity using two consecutive tension heads. The parameter α_c in Gardner (1958) exponential hydraulic conductivity function was estimated by,

$$\alpha_c = \frac{\ln \frac{Q_{h_1}}{Q_{h_2}}}{h_1 - h_2} \tag{6. 20}$$

where Q_{h_1} and Q_{h_2} are the steady-state fluxes at h_1 and h_2, respectively.

Corresponding to two tension heads, $h_0 = h_1$ and h_2, two values of K_{h_0} can be obtained as

$$K_{h_1} = \frac{Q_{h_1}}{\pi r_0^{\,2} + \frac{4r_0}{\alpha_c}} \tag{6. 21}$$

$$K_{h_2} = \frac{Q_{h_2}}{\pi r_0^{\,2} + \frac{4r_0}{\alpha_c}} \tag{6. 22}$$

6.2.7. Zhang Method-I (Z-I)

Zhang (1998) suggested a procedure to reduce the time for field infiltrometer experiments drastically which do not require steady-state infiltration rates but infiltration data at any time by modifying Ankeny, et al. (1991) procedure. In this method, the correction factors were proposed as follows:

$$f_1 = 1 + \frac{0.4431 r_0 \left(\theta_1 - \theta_i\right)^{0.5}}{\left(K_{h_1} \lambda t_1\right)^{0.5}} - 0.216 \exp\left[-\frac{4.01 K_{h_1} \lambda t_1}{\left(\theta_1 - \theta_i\right) r_0^{\,2}}\right] \tag{6. 23}$$

$$f_2 = 1 + \frac{0.4431 r_0 \left(\theta_2 - \theta_i\right)^{0.5}}{\left(K_{h_2} \lambda t_2\right)^{0.5}} - 0.216 \exp\left[-\frac{4.01 K_{h_2} \lambda t_2}{\left(\theta_2 - \theta_i\right) r_0^{\,2}}\right] \tag{6. 24}$$

where K_{h_1} and K_{h_2} are the hydraulic conductivity values and θ_1 and θ_2 are the final water contents at tensions $h_0 = h_1$ and h_2 respectively, θ_i is the initial water content, Q_1 and Q_2 are the measured flux at infiltration time t_1 and t_2, and λ is the macroscopic capillary length, which are unknowns. The modified method in the matrix form can be expressed as:

$$\begin{bmatrix} f_1\pi r_0^2 & 0 & 4f_1 r_0 K_{h_1} \\ 0 & f_2\pi r_0^2 & 4f_2 r_0 K_{h_2} \\ 0.5\Delta h & 0.5\Delta h & K_{h_2} - K_{h_1} \end{bmatrix} \begin{bmatrix} K_{h_1} \\ K_{h_2} \\ \lambda \end{bmatrix} = \begin{bmatrix} Q_{h_1} \\ Q_{h_2} \\ 0 \end{bmatrix} \quad (6.25)$$

where Q_{h_1} and Q_{h_2} are the measured flux at infiltration time t_1 and t_2 for tension h_1 and h_2. Matrices are nonlinear because the coefficients are functions of the unknowns K_{h_1}, K_{h_2} and λ. A Picard iteration with an incremental solution technique was used to solve the nonlinear equations assuming the initial approximate solution (Zhang, 1998).

6.2.8. Zhang Method –II (Z-II)

Zhang (1997b) proposed the infiltration model of the disc infiltrometers which is known as the second method of Zhang as,

$$I = C_1\sqrt{t} + C_2 t \quad (6.26)$$

where I is the cumulative infiltration, C_1 and C_2 are parameters and t is the time.

The relationship for infiltration rate *i* is derived as:

$$i = 0.5C_1 t^{-0.5} + C_2 \quad (6.27)$$

If the steady-state infiltration rate $i_s = C_2$, then

$$f = \frac{Q}{Q_s} = \frac{i}{i_s} = 1 + 0.5\frac{C_1}{C_2} t^{-\frac{1}{2}} \quad (6.28)$$

where Q_s is the steady-state flow rate.

For the tensions h_1 and h_2, the correction factors f_1 and f_2 can be expressed as,

$$f_1 = \frac{Q_1}{Q_{1s}} = 1 + 0.5\frac{C_{11}}{C_{12}} t_1^{-\frac{1}{2}} \quad (6.29)$$

$$f_2 = \frac{Q_2}{Q_{2s}} = 1 + 0.5\frac{C_{21}}{C_{22}} t_2^{-\frac{1}{2}}. \quad (6.30)$$

Fitting Zhang (1997b) equation to cumulative infiltration data from *0* to t_1 for tension h_1 and *0* to t_2 for tension h_2, the coefficients C_{11}, C_{12}, C_{21} and C_{22} were determined. In accordance with the first method of Zhang, t_1 and t_2 can be any infiltration time. Using known values of f_1 and f_2 for any definite time, the hydraulic conductivity can be found out by Zhang (1998) as follows:

$$K_{h_1} = \frac{\frac{Q_1}{f_1}}{\pi r_0^2 + 4\pi r_0} \tag{6. 31}$$

$$K_{h_2} = \frac{\frac{Q_2}{f_2}}{\pi r_0^2 + 4\pi r_0} \tag{6. 32}$$

6.2.9. Haverkamp Method (H)

Haverkamp, et al. (1994) developed a physically based quasi-exact equation describing the three-dimensional unsaturated cumulative infiltration (I) curve for disc infiltrometers expressed as

$$\frac{2(K_{h_0} - K_n)^2}{S_{h_0}^2} t = \frac{2}{1-\beta} \frac{(K_{h_0} - K_n)}{S_{h_0}^2} \left\{ I - K_n t - \left[\frac{\gamma S_{h_0}^2}{r_0(\theta_{h_0} - \theta_n)} \right] t \right\}$$
$$- \frac{1}{1-\beta} ln \left(\left\{ e^{\frac{2\beta(K_{h_0} - K_n)}{S_{h_0}^2}} \left\{ I - K_n t - \left[\frac{\gamma S_{h_0}^2}{r_0(\theta_{h_0} - \theta_n)} \right] t \right\} + (\beta - 1) \right\} \beta^{-1} \right) \tag{6. 33}$$

where r_0 is the radius of the disc, θ_n and θ_{h_0} are the initial and final volumetric water content respectively, S_{h_0} is the sorptivity, and γ is the proportionality constant, K_{h_0} and K_n are the soil hydraulic conductivity values corresponding to θ_{h_0} and θ_n, respectively, and β is a shape constant.

Haverkamp, et al. (1994) assumed K_n to be negligible and simplified the above equation for short to a medium time interval as,

$$I = C_1 \sqrt{t} + C_2 t \tag{6. 34}$$

$$\text{where, } C_1 = S_0; C_2 = \frac{2-\beta}{3} K_{h_0} + \frac{\gamma S_{h_0}^2}{r_0(\theta_{h_0} - \theta_n)} \tag{6. 35}$$

Using this expression, Vandervaere, et al. (2000a) suggested the differentiated linearization (DL) method to infer soil hydraulic properties using linear regression. The DL method is only applicable for short to medium time and the validity of this method is questioned when the capillary forces are predominant (Angulo-Jaramillo et al., 2000). The technique consists of differentiating it with respect to the square root of time which gives,

$$\frac{dI}{d\sqrt{t}} = C_1 + 2C_2\sqrt{t} \qquad (6.\ 36)$$

Plotting the $\frac{dI}{d\sqrt{t}}$ term as a function of $\sqrt{t}$ gives C_1 as the intercept and C_2 as the slope of the corresponding regression lines. Haverkamp, et al. (1999, 2005) proposed an average value of 0.75 for γ and 0.6 for β. Knowing C_1 and C_2 from the DL method (Eq. 6. 36) K_{h0} is obtained by using Eq. 6. 35. The summary of all the equations, its designation, different parameters and initial conditions required for the calculation of hydraulic conductivity are listed in Table 6. 1.

6.3. Hydraulic Conductivity Determined using Mathematical Equations from Steady and Transient State Infiltration

The MDI and GP measurements reported in chapter 4 are used for the mathematical analysis. The critical evaluation of different mathematical equations used for determining hydraulic conductivity from the measured results of MDI necessitates a reliable reference value. In this study, GP was considered as the reference because it is an established method for measuring field K_s. Most of the mathematical equations (except Wooding-Gardner and Weir's refinement method) evaluated in this study gives near saturated hydraulic conductivity for which there is no independent reference value. Therefore, K_{h_0} corresponding to different tension heads (h_0) obtained from MDI was linearly extrapolated to estimate the field saturated hydraulic conductivity at $h_0 = 0$ as discussed in Section 5.2 and as depicted in Fig. 5. 1. It can be noted that the variation in K_{h_0} corresponding to h_0 of 0.05 kPa to 0.6 kPa (or 0.5 cm to 6 cm) is linear (Zhang, 1997a) and hence the linear extrapolation to $h_0 = 0$ is justified. For statistical analysis, the hydraulic conductivity was log transformed based on the understanding that hydraulic conductivity generally follows log-normal distribution (Bouwer, 1969; Nielsen, et al., 1973; Buckland, 1988). The K_s estimated from the results of MDI using different mathematical equations are compared

with GP measurements for all the stations and two seasons as shown in Fig. 6. 1. Owing to the marginal standard deviation of these measurements, the error bars are not shown in the figure.

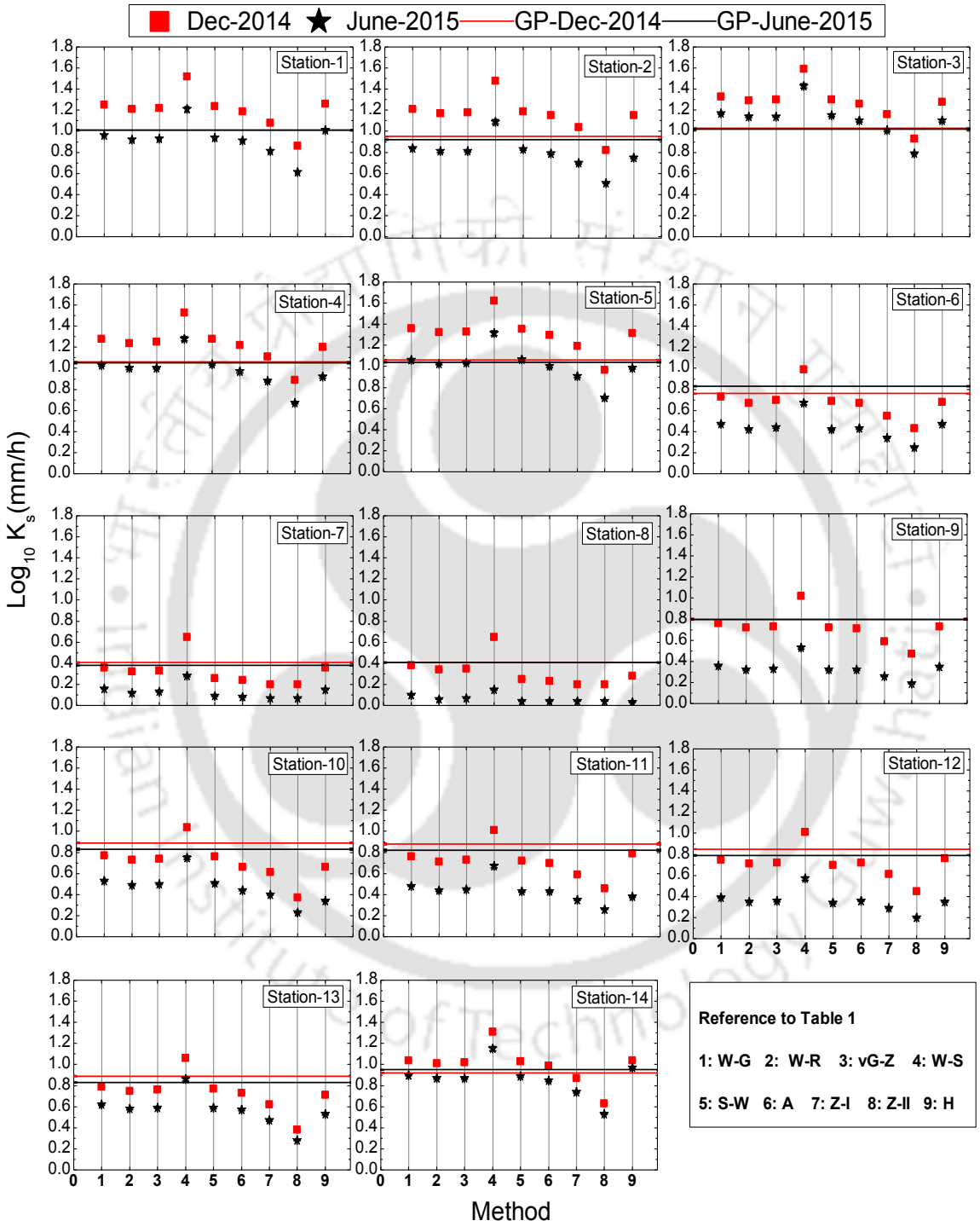

Fig. 6. 1 Comparison of saturated hydraulic conductivity (mm/h) determined from MDI and GP

Table 6. 1 Parameters and initial conditions for different equations

S. No.	Equation	Equation Parameters			Parameters		Reference
					Near Saturated Hydraulic Conductivity	Saturated Hydraulic Conductivity	
1	W-G	α_c, λ_c			Wooding Eq. (Eq.6. 1)	Gardner Eq. (Eq. 6. 2)	Gardner (1958); Wooding (1968)
2	W-R	$\alpha_c = \frac{\ln\left[Q(h_2)/Q(h_1)\right]}{h_2 - h_1}$ $\lambda_c = 1/\alpha_c$			Weir Eq. (Eq. 6. 4)	Gardner Eq. (Eq. 6. 2)	Weir (1987); Gardner (1958); Wang, et al. (1998)
3	vG-Z	n	Sand	2.68	vG-Z (Eq.6. 10)	Extrapolation method	Zhang (1997a); van Genuchten (1980)
			Loam	1.56			
			Silt	1.37			
		α_c	sand	0.145			
			Loam	0.036			
			Silt	0.016			
4	W-S	$\alpha_c = \frac{(\theta_{h_0} - \theta_n)(K_{h_0} - K_n)}{bS_{h_0}^2}$ $\lambda_c = 1/\alpha_c$			White Eq (Eq.6. 16)	Extrapolation method	White and Sully (1987); White, et al. (1992)
5	S-W	$\alpha_c = \frac{\ln \frac{q_{i+1}}{q_i}}{h_{i+1} - h_i}$			$K_{h_0} = \frac{q_{h_0}}{1 + \frac{4}{r_0 \alpha_c}}$	Extrapolation method	Simunek, et al. (1998)
6	A	$\alpha_c = \frac{\ln \frac{Q_{h1}}{Q_{h2}}}{h_1 - h_2}$			$K_{h_1} = \frac{Q_{h_1}}{\pi r^2 + \frac{4r}{\alpha_c}}$	Extrapolation method	Ankeny, et al. (1991)
7	Z-I	$K_{h_1}, K_{h_2}, \lambda_c$			Zhang matrix form (Eq.6. 25)	Extrapolation method	Zhang (1998)
8	Z-II	$K_{h_1}, K_{h_2}, \lambda_c$			Zhang Eq. (Eqs. 6. 31 and 6. 32)	Extrapolation method	Zhang (1997b)
9	H	γ	0.75		Differential linearization method (Eq.6. 36)	Extrapolation method	Haverkamp, et al. (1994, 1999, 2005); Vandervaere, et al. (2000a)
		K_n	0				
		β	0.6				

It is evident that the K_s measurements of GP for both the seasons match well indicating the invariant behaviour of K_s for a particular soil and pore structure. Unlike GP, the results from MDI are not the same for both the seasons thereby violating the condition of invariance.

The MDI measurements in December gave higher K_s as compared to June even though the difference between two seasons is well within one order of magnitude. It may be noted that the GP measurements were performed at a depth of 15 cm below the ground surface whereas MDI measurements were performed on the ground surface. The major reason for the difference in K_s (from MDI) corresponding to different seasons can be attributed to the higher sensitivity of MDI measurements to surface pore structure changes with seasons as compared to GP. In general, the observations in Fig. 6. 1 indicates that the mathematical equations can be divided into three sets. The first set of equations include W-G, W-R, vG-Z, S-W, A, and H listed in Table 6. 1 gave comparable K_s based on the MDI measurements. The K_s from the second set of equations Z-I and Z-II is lesser and third set of equation W-S is higher as compared to first set. It is worth noting that the first set includes both steady state and transient equations for determining K_s. From the initial observation, it is difficult to comment on the comparison of K_s determined from different equations with GP results. It can be noted that for some stations, first set of equations performed reasonably well depending on the season. Statistical analysis was performed in the ensuing section for better understanding of the comparisons of K_s determined from mathematical equations with GP measurements.

6.3.1. Variability in Hydraulic Conductivity

The statistical difference between K_s determined from GP and different mathematical equations (using MDI results) were assessed quantitatively by using Bland-Altman plot (BAp) as shown in Fig. 6. 2, where each panel refers to a single equation applied to all the stations and seasons. Bland-Altman plot is an established graphical statistical method to compare the agreement between two measurement techniques (Brazdzionyte and Macas, 2007).

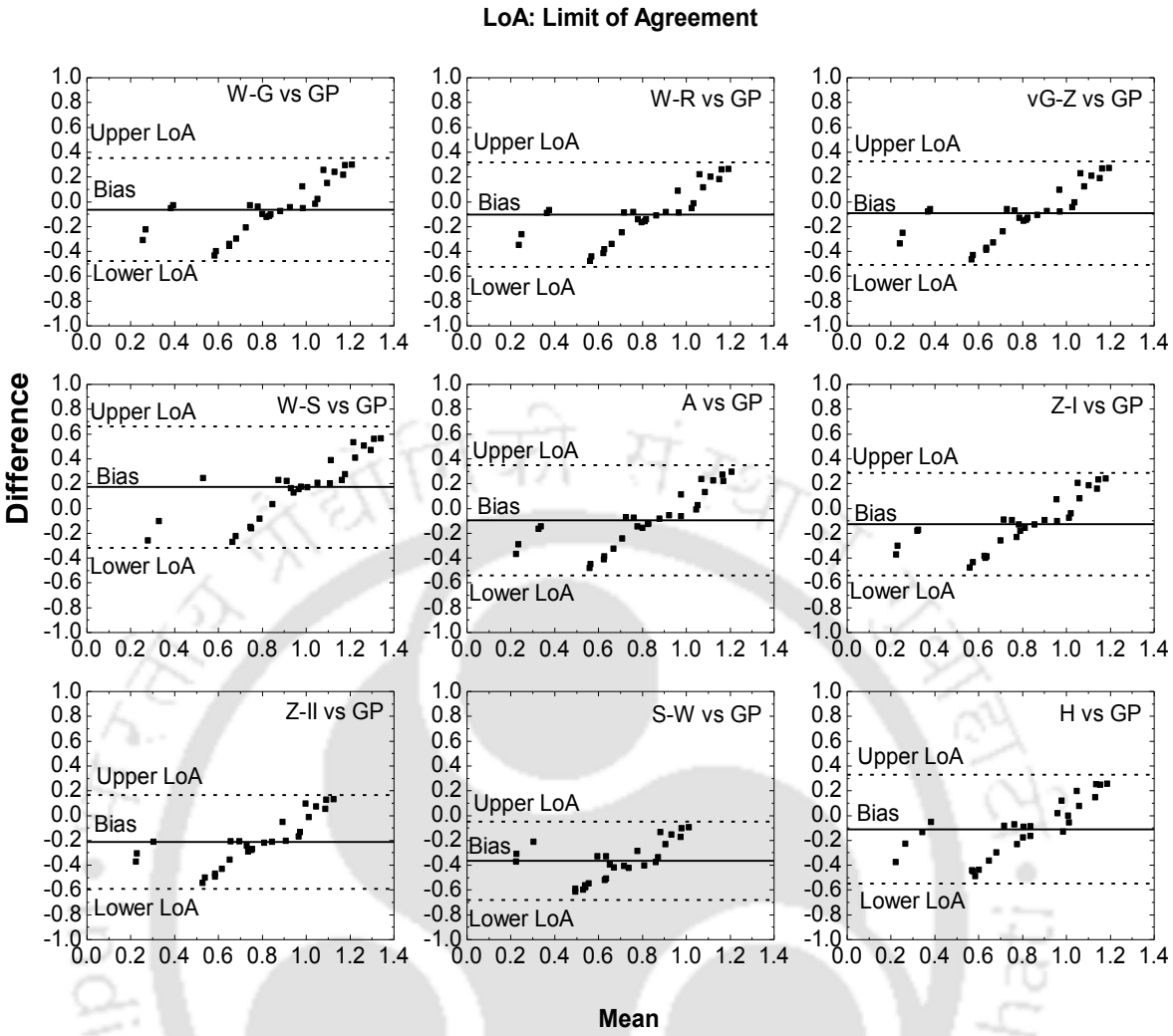

Fig. 6. 2 Bland-Altman plot for statistical comparison between K_s determined from Guelph permeameter and different equations (based on MDI)

In this plot, the difference between MDI and GP is plotted on the Y-axis and mean of the two methods are plotted on the X-axis. In Fig. 6. 2, "bias" is the mean of the difference between the two methods. The 95 % upper and lower limits of agreement (LoA) is equal to ±1.96 times the standard deviation of the difference between the two methods. The BAp helps to compare two methods based on the magnitude and direction of the bias, width of LoA and whether there is any systematic trend between the difference and the mean. It is understood that the K_s comparisons with minimal bias and LoA can be considered to be better. The details of parameters for BAp for different equations are listed in Table 6. 2.

It can be noted from Fig. 6. 2 that the majority of the data points falls within the LoA. With GP as the reference method, LoA indicates the total error of a given mathematical equation (Krouwer, 2002) used for determining K_s. Smaller LoA means the majority of the data falls within smaller error limit. It is noted that LoA is comparable for the majority of the mathematical equations considered with maximum LoA for W-S and minimum for S-W. However, LoA alone may not be sufficient for deciding the appropriateness of the equations. The bias between the two data sets also needs to be considered. Among all the equations, W-S versus GP is having a positive bias, which means that W-S overestimated K_s as compared to GP. The three equations W-G, vG-Z and A exhibited minimum bias (<0.1) with GP. For a better understanding, LoA is plotted with respect to bias as shown in Fig. 6. 3. Based on Fig. 6. 3, it can be noted that there is not much of difference in LoA for all the equations considered. At the same time, there is a wider range of bias exhibited by these equations. Considering both LoA and bias, K_s determined by equations W-G, W-R, vG-Z, A and H is found to compare well with the results of GP.

Table 6. 2 Statistical analysis of hydraulic conductivity determined using different equations

S. No.	Method	Bias (mm/h)	Lower LoA	Upper LoA	Width of LoA	Pearson Coefficient	p-value
1	W-G	-0.063*	-0.479	0.353	0.832	0.86	0.0037
2	W-R	-0.103	-0.524	0.319	0.843	0.86	0.0020
3	vG-Z	-0.092*	-0.508	0.324	0.832	0.86	0.0023
4	W-S	*0.173*	-0.316	0.661	0.977	0.84	0.0513
5	S-W	-0.365	-0.680	-0.050	0.630	0.81	0.0033
6	A	-0.096*	-0.539	0.348	0.887	0.88	0.0003
7	Z-I	-0.126	-0.539	0.287	0.826	0.88	0.0003
8	Z-II	-0.211	-0.59	0.169	0.759	0.86	0.0004
9	H	-0.109	-0.549	0.331	0.880	0.84	0.0032

*Bias is close to zero; italics value shows the postive bias and bold values indicate failed to reject the null hypothesis (p>0.05)

It can be noted further from Fig. 6. 2 that there is a systematic difference in K_s determined from equations and GP results. There is a visible increase in difference with the mean for all the equations and the trends are quite consistent. For mid-range of mean, the difference is centred around bias. For those methods with low bias, this means that

mid-range values of K_s determined from equations exhibited a better comparison with GP results as compared to the higher and lower range of K_s. The definition of low, mid and high range of K_s is entirely dependent on the data from this study. The impact of the systematic difference of K_s determined from different equations and GP measurements on the modeling of various hydrological processes is not clear from this study and need to be investigated in detail.

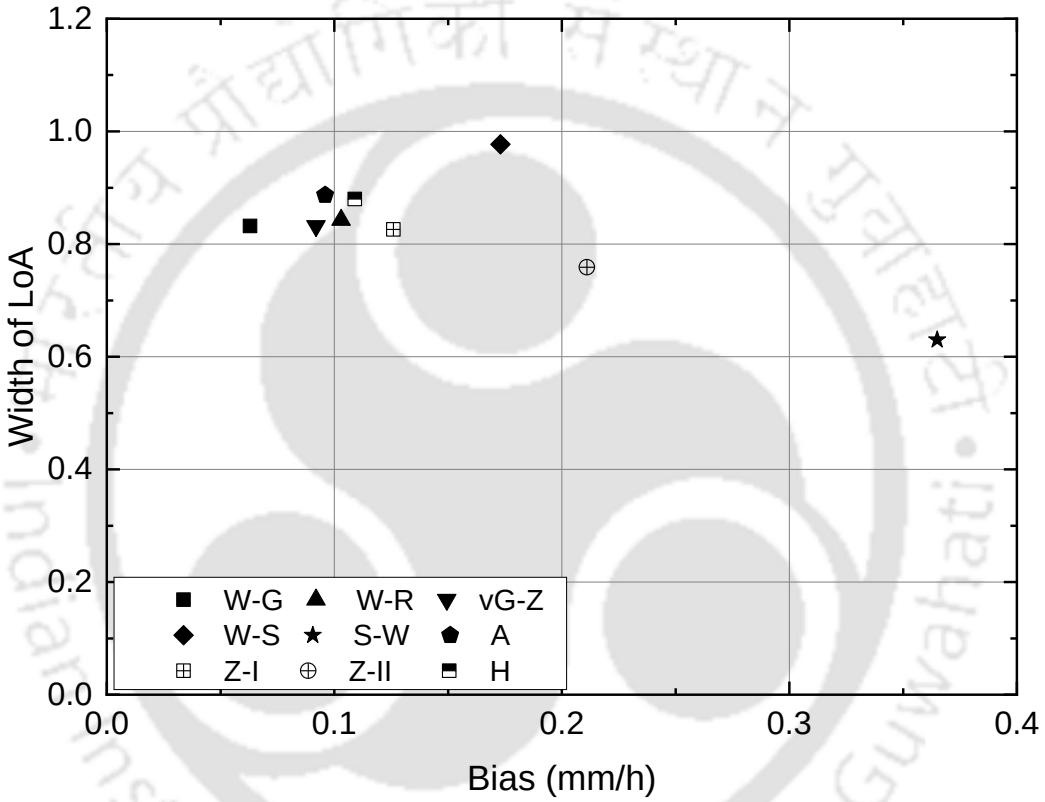

Fig. 6. 3 Limit of agreement versus bias plot for K_s determined from different mathematical equations

An effort was made to explore the correlation between K_s from different equations and GP measurements. The details of the Pearson correlation coefficient (Verbist, et al., 2013) and the *p*- values are listed in Table 6. 2. It can be noted that the Pearson correlation coefficient was found to vary between 0.81-0.88, indicating a fair correlation. However, it is difficult to adjudge the effectiveness of equations in determining K_s based on the Pearson correlation coefficient. In the case of White and Sully (W-S) method, even though

the Pearson coefficient was 0.84, the bias and the *p*-value (from Pearson correlation) indicated a marginal comparison of K_s with GP.

For cross verifying the observations from BAp, a comparison diagram was plotted between K_s determined by different equations and GP measurements as shown in Fig. 6. 4. It can be observed that the equations W-G, W-R, vG-Z, S-W, A, Z-II and H gave the majority of K_s values within 25% variation. The results from BAp indicated a subset of this group of equations, which performed better.

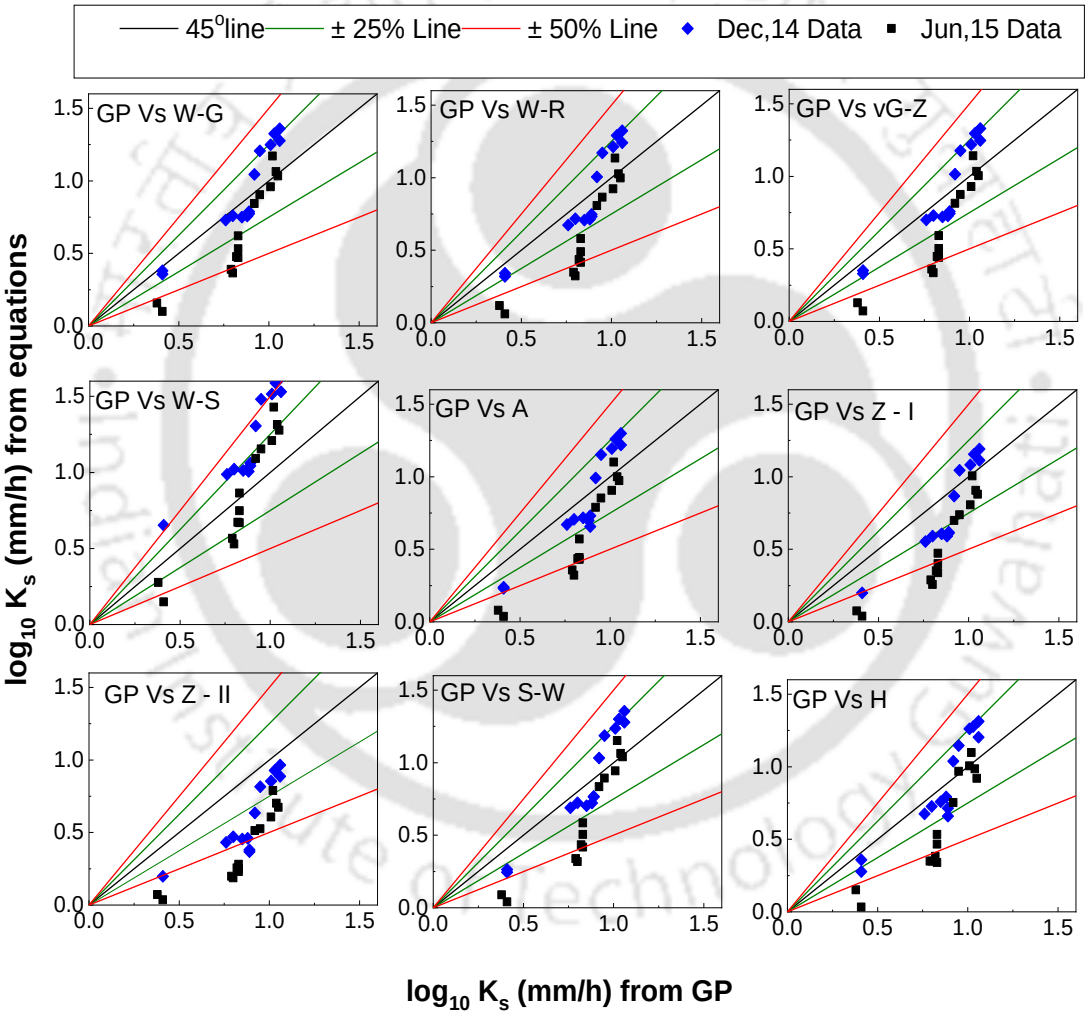

Fig. 6. 4 Comparison of hydraulic conductivity estimated from MDI and GP measurements

Similar to the finding from Fig. 6. 2, it can be noted that the mid-range of K_s exhibited a better match between equations and GP. A few of the December data exhibited

overestimation and July data showed underestimation in the higher and lower range of K_s , respectively. The Root Mean Square Error (RMSE) of all the equations were estimated by considering GP as the reference value of K_s and are illustrated in Fig. 6. 5.

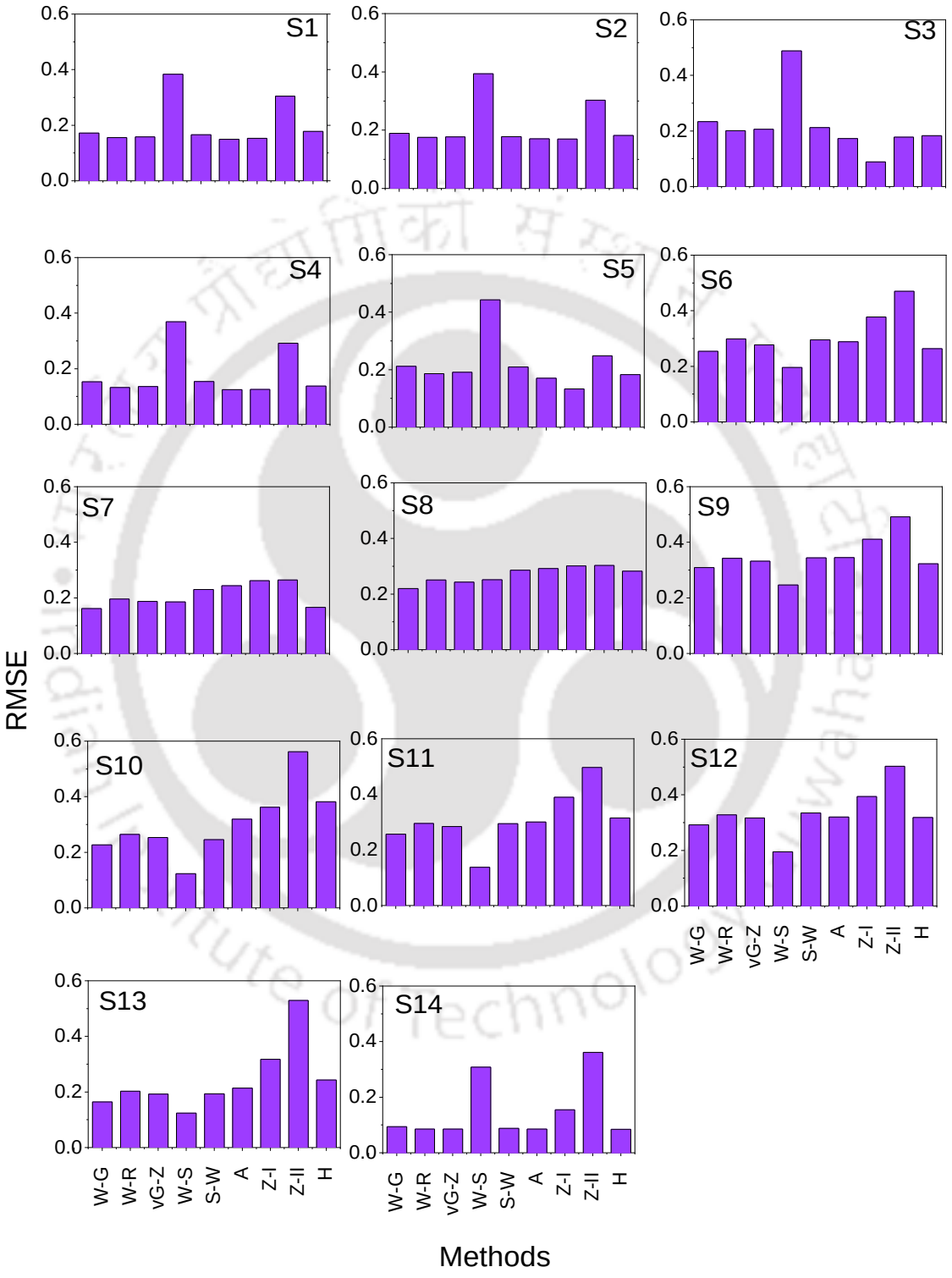

Fig. 6. 5 RMSE of saturated hydraulic conductivity estimated from different mathematical equations based on MDI results

In general, W-S, Z-I, and Z-II equations were found to perform poorly in different locations considered in this study. For silt dominant stations S7 and S8, RMSE of all equations were found to be comparable. The above discussion reveals the fact that different mathematical equations can induce variability in K_s for the same measured data of MDI.

Based on all the statistical procedures, the smallest subset of equations identified by BAp (W-G, W-R, vG-Z, A and H) is recommended for estimating near surface hydraulic conductivity based on MDI results. Among the equations, W-G, W-R and A are based on the Wooding's steady state formulations whereas vG-Z and H are transient methods. The steady state equations that determined K_s directly (W-G and W-R) was found to be superior to those which relied on extrapolation (W-S, S-W, Z-I, and Z-II). The equations W-G and W-R is entirely dependent on the measured results of MDI and do not depend on any estimated soil parameters. The results from W-G and W-R were found to be similar, thereby ruling out the influence of small disc radius of MDI on hydraulic conductivity determination based on W-G (Weir, 1987) for the soils considered in this study. For transient state equations (vG-Z and H), extrapolation of K_{h_0} to K_s was found to yield satisfactory results. The adequacy of vG-Z equation indicates that neglecting the effect of sorptivity in *K* determination was not erroneous for the soils in the study area. The W-S equation was found to grossly overestimate K_s as compared to GP measurements. This can be attributed to the overestimation of the sorptivity parameter used in W-S equation (Jacques, et al., 2002). According to Zhang (1997a), the accuracy of sorptivity is less for smaller measurement duration. The factors f_1 and f_2 used in Z-I and Z-II equations would have resulted in the underestimation of K_s as compared to GP measurements.

6.4. Influence of Short Term and Long Term MDI Measurements on Hydraulic Conductivity Determination

It may be noted that there are no recommended code provisions for the measurement and analysis procedure of MDI. Due to the small water reservoir of MDI, it is mostly applicable for short term measurements. The details of the methd of analysis folowed in this analysis is explained in the following sub sections.

6.4.1. Methods of Analysis for Short-Term and Long-Term MDI Measurements

In the absence of any specified method of analysis, the general user community tends to adopt the manufacture specified procedure and method of analysis for all practical purpose. The manufacturer specified method is based on the rigorous numerical analysis performed by Zhang (1997a). The method describes transient infiltration and it is based on the two-term infiltration model by Philip (1957) as discussed in Sub section 2.2.3. The transient approach of Zhang (1997a) was applied to the short-term (< 50 minutes)) and long-term (240 minutes) data series marked as A and B, respectively, in Fig. 6.6.

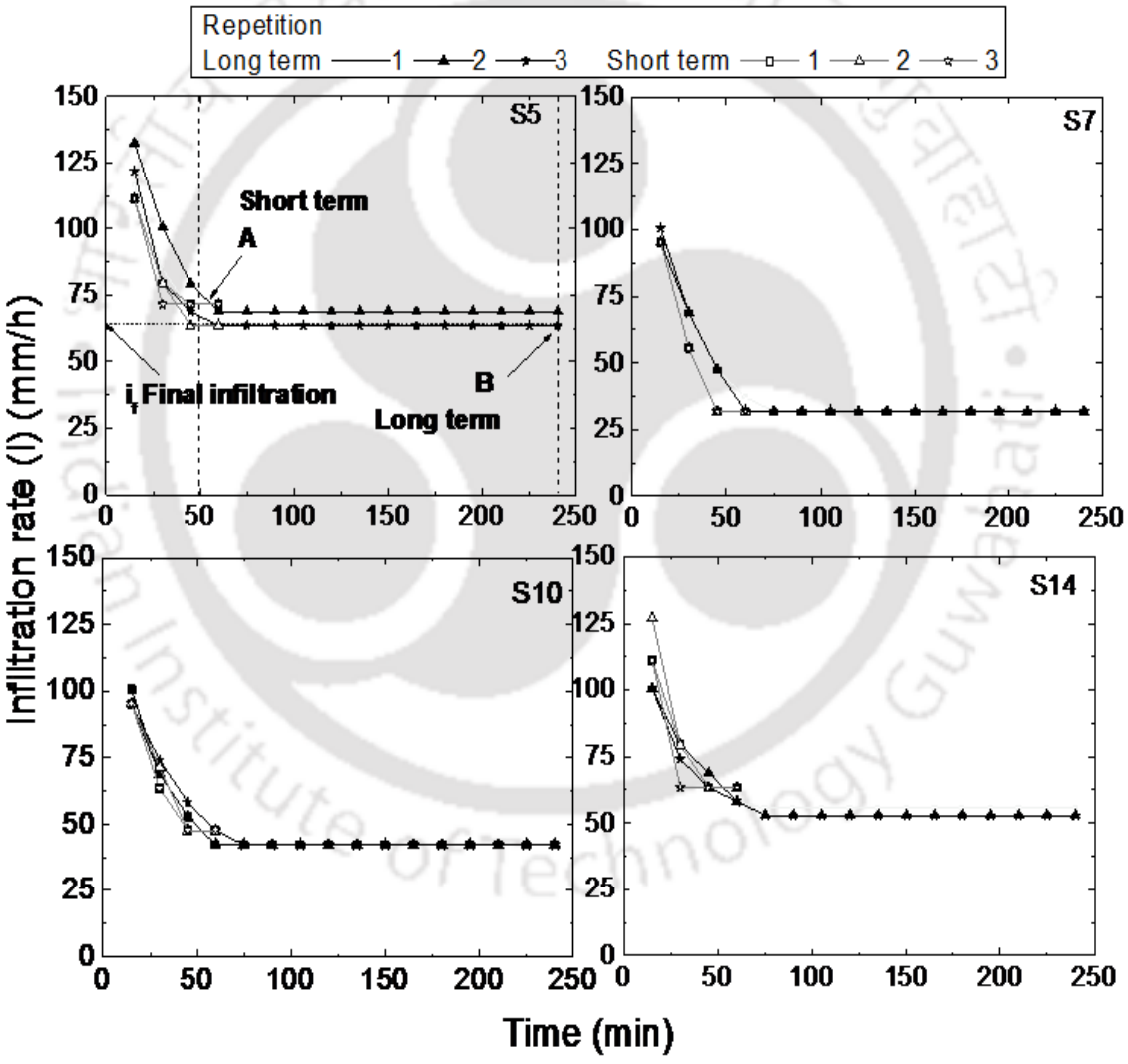

Fig. 6. 6 Typical infiltration rate curves from MDI for tension head 2 cm

Figure 6.6 also depicts the repeatability of MDI measurements for selected stations for a tension head of 2 cm and it can be noted that the MDI measurements are fairly repeatable. Zhang's method follows transient approach and hence the infiltration measurement time may have influence on K_{h0} determination. The comparative analysis by applying Zhang's method to data series A (short-term transient) and B (long-term quasi steady state) would help to understand the bias, if any, associated with the infiltration measurement time on K_{h0} determination. These methods of K_{h0} determination are tabulated in Table 6. 3 as N_1 and N_2 for data series A and B, respectively. Further, the K_{h0} obtained from N_1 and N_2 was used to determine K_s by extrapolating the value of K_{h0} for zero tension and designated as S_1 and S_2.

Table 6. 3 Methods of analysis for determining near saturated and saturated hydraulic conductivity using MDI results

Near saturated hydraulic conductivity (K_{h0})			Saturated hydraulic conductivity (K_s)		
Method	Desig-nation	Remark	Method	Desig-nation	Remark
1	N_1	Zhang's approach short-term data (A in Fig. 6.6)	1	S_1	K_s from N_1 extrapolated to $h_0 = 0$
2	N_2	Zhang's approach long-term data (B in Fig. 6.6)	2	S_2	K_s from N_2 extrapolated to $h_0 = 0$
3	N_3	Haverkamp's approach (short-term data A)	3	S_3	Wooding-Gardner equation using steady state discharge
4	IH_h	Final infiltration rate from hyperbolic method (extrapolation of short-term data A)	4	S_4	K_s from N_4 extrapolated to $h_0 = 0$
5	IM_h	Final infiltration rate from measured results (long-term data B)	5	$IH_{h=0}$	Final infiltration rate from hyperbolic method extrapolated to $h_0 = 0$
			6	$IM_{h=0}$	Final infiltration rate from measured results extrapolated to $h_0 = 0$

In the Table 6. 3, N and S corresponds to the method of analysis used for near saturated hydraulic conductivity and saturated hydraulic conductivity, respectively. The steady-state flux, q_{h0} entering into soil at a tension head h_0, from a shallow circular pond of radius r_0, can be approximated by a three-dimensional axisymmetric infiltration equation (Wooding, 1968) given by Eqs. 3.1 to 3.5. The steady-state discharge Q_{h_0} was used to determine K_s and designated as method S_3 in Table 6. 3.

The quasi-exact equation proposed by Haverkamp, et al. (1994) (denoted by Eq. 6. 33) was used to determine determining K_{h_0} by following the differentiated linearization (DL) method (Vandervaere, et al., 2000a). Unlike Zhang's method, this method considers the effect of sorptivity on the determination of K_{h0}. The K_{h0} was determined by considering short-term infiltration data measured using MDI and designated as N_3. The results from N_3 was used to determine K_s by the method of extrapolation and designated as S_4 in Table 6. 3.

The short-term measured data (< 50 minutes) as shown by data series A is Fig. 6.6 was used to determine final infiltration rate (i_f) by hyperbolic method (Al-Shamrani, 2005; Huang, et al., 2014; Chung, et al., 2014). In this method, it is assumed that the infiltration rate (i) versus time (t) response follows a rectangular hyperbola expressed by Eq. 6. 37. Equation 6. 38 indicates that when time t tends to ∞, the final infiltration rate i_f is equal to the constant m. Accordingly, the Eq. 6. 38 is expressed in linear form as given by Eq. 6. 39. Figure 6. 7 corresponds to MDI measurement of station 5 of the study area for a tension head of 0.5 cm. When a straight line is fitted to this data, the slope is given by 1/m. The inverse of the slope (m) is therefore equal to i_f. Therefore, i_f corresponding to different tension head was determined and this method is designated as IH_h in Table 6. 3. Further, the ratio *t/i* was plotted as a function of time as shown in Fig. 6. 7(b).

$$i = \frac{mt}{k+t} \tag{6. 37}$$

$$i = \frac{m}{\frac{k}{t}+1} \tag{6. 38}$$

$$\frac{t}{i} = \frac{k}{m} + \frac{t}{m} \tag{6. 39}$$

where, *k and m* are parameters of hyperbola equation.

In addition, the parameters *k* and *m* was used to extrapolate the short-term data A to long-term data for 4 hours as shown in Fig. 6. 7(a). The van Genuchten-Zhang method was applied to the extrapolated data from hyperbolic method for estimating K_{h_0} corresponding to different tension head for the method IH_h. These values were further extrapolated to tension head zero to obtain K_s and this method is designated as $IH_{h=0}$ in Table 6. 3. Therefore, both i_f and K_{h_0} was determined based on short-term data by following hyperbolic method.

The measured infiltration rate versus time data from MDI for 240 minutes (data B) was used to determine the quasi steady state final infiltration rate i_f (shown in Fig. 6.6). In this study, this was directly considered as K_{h0} and designated as IM_h and the extrapolated value corresponding to zero tension from IM_h was considered as K_s (designated as $IM_{h=0}$) in Table 6. 3. The following section deals with the analysis of above mentioned methods for understanding the short-term and long-term MDI measurements on hydraulic conductivity determination (K_{h0} and K_s).

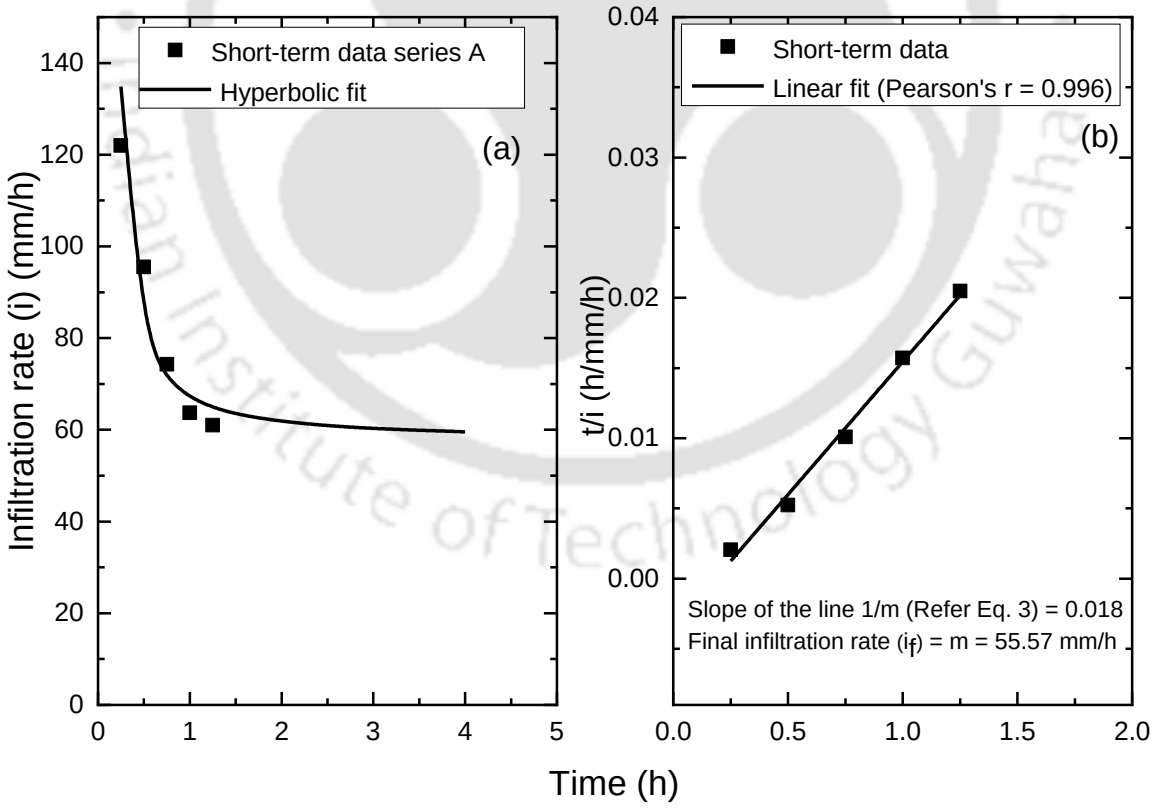

Fig. 6. 7 (a) Hyperbolic fit to short-term MDI data and (b) determination of final infiltration rate from MDI measurement of station 5 for tension head 0.5 cm

6.4.2. Discussion on Short-Term and Long-Term Data Analysis

The measured short-term and long-term MDI data as discussed above were used in conjunction with different transient and steady state mathematical procedures for determining the variability in near saturated (K_{h_0}) and saturated (K_s) hydraulic conductivity corresponding to identical conditions. Figure 6. 8 compares K_{h_0} determined by Zhang's method for short-term and long-term measured data designated as N_1 and N_2, respectively, in Table 6. 3.

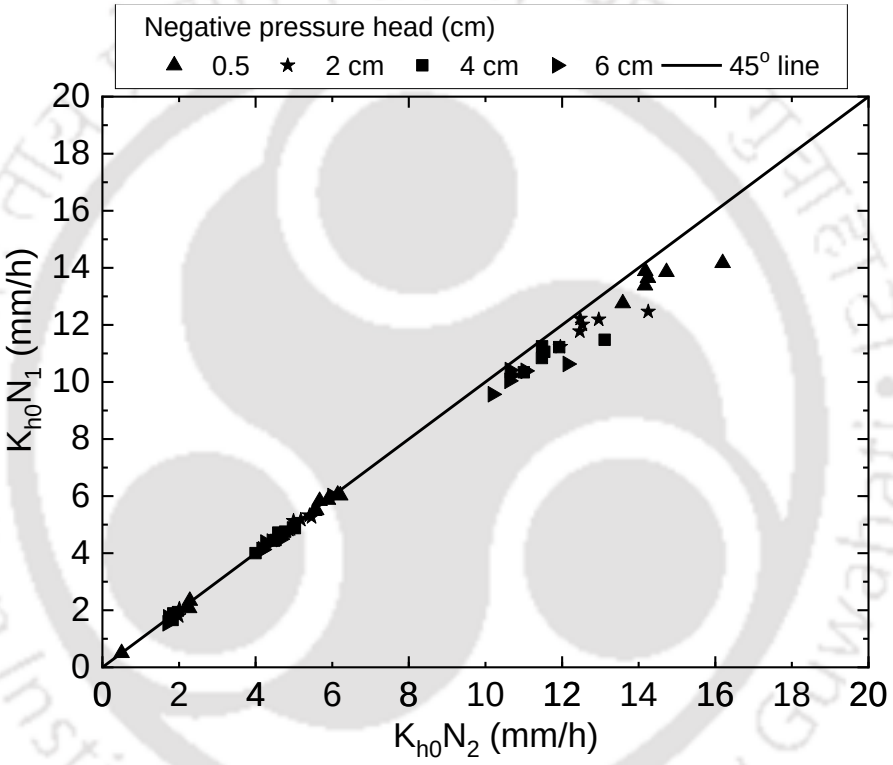

Fig. 6. 8 Comparison of near saturated hydraulic conductivity obtained from short-term and long-term MDI measurements and Zhang's method of analysis

The data include MDI measurements corresponding to four different negative pressure heads at 14 locations in the study area. The aim of this comparison is to evaluate whether the applied negative pressure head influence K_{h_0} determination. It is explicit that the applied tension head do not have much influence on K_{h_0} determination. For the range of K_{h_0} < 8 mm/h, both N_1 and N_2 results in the same value, and for K_{h_0} > 8 mm/h, N_1 marginally underestimates as compared to N_2. A higher K_{h_0} corresponds to a drier initial

state of the soil and higher infiltration. It may be noted that the effect of sorptivity will be more pronounced for soils with low initial water content and for short time duration. Zhang's approach does not consider the effect of sorptivity on K_{h_0} determination. It is understood that the variation of dimensionless coefficients (Eqs. 6.12 to 6.14) involved in the determination of K_{h_0} can be treated as constants as duration of infiltration time increases. Therefore, combined influence of sorptivity and short term measurement would have resulted in a marginal underestimation of K_{h_0} N_1.

The near surface saturated hydraulic conductivity K_s obtained based on the K_{h_0} from $N_1$and N_2 (designated as S_1 and S_2, respectively in Table 6. 3) was compared with field saturated hydraulic conductivity measured at the same location using a Guelph permeameter as shown in Fig. 6. 9. It can be noted that the K_s from the methods S_1 and S_2 do not compare well with the GP measurements. As the range of K_s increases, the deviation is found to be more. There are both under and over estimation of K_s from S_1 and S_2 and majority of the data are within 50 % variability as compared to GP. There is no specific advantage for long term and short term data (A and B) when K_s from MDI based on Zhang's method was compared with GP. Such an under and over estimation of MDI results with reference to field saturated hydraulic conductivity are reported in the literature (Nestingen, et al., 2018).

The variability can be attributed to the combination of various factors such as (a) the methodology followed for K_{h_0} and K_s estimation from MDI measurements, (b) MDI measurements are based on water entry into the soil whereas GP is based on water permeation within the soil, (c) soil surface characteristics influence MDI measurement significantly, whereas the influence would be considerably less for GP (measurement depth is 15 cm below ground surface), (d) the variation of MDI with reference to GP will be site-specific as noted in the comparison presented in Fig. 6. 9 (both under and over estimation), and can be due to both soil structure and soil type prevalent at the measurement location. The individual contribution of these factors could not be ascertained from the present study, and needs experimentation with controlled known boundary conditions in the field for further investigation.

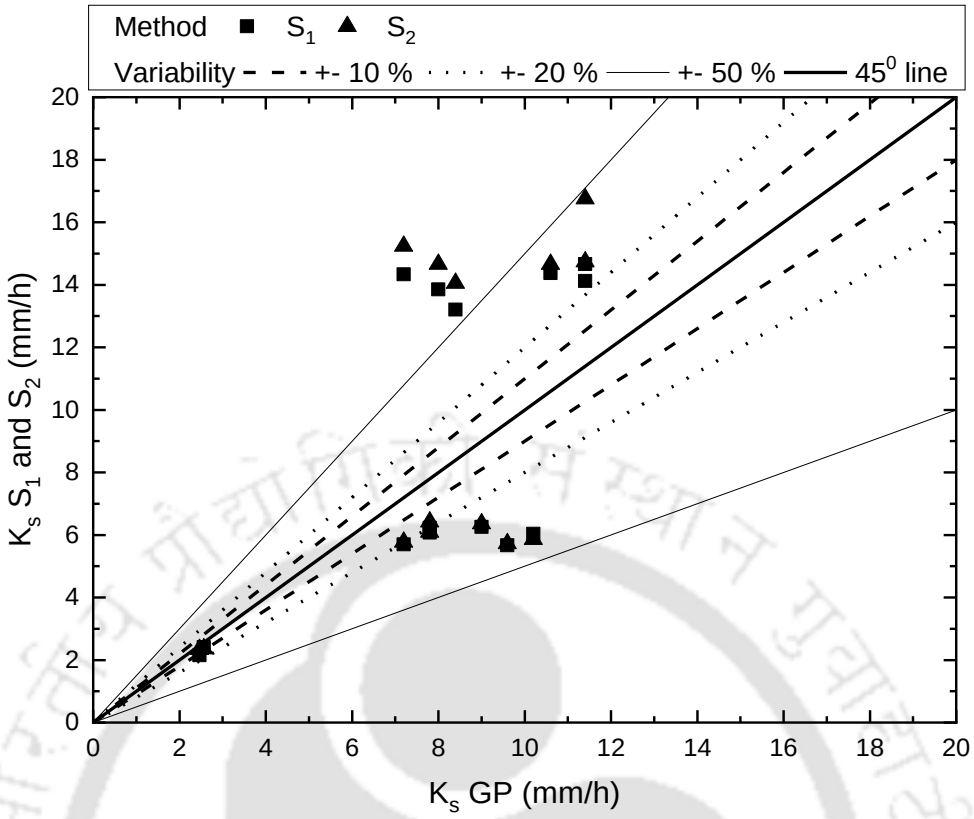

Fig. 6. 9 Comparison of saturated hydraulic conductivity obtained from S_1 and S_2 (Table 6. 3) and Guelph permeameter

The Wooding-Gardner equation (Eq. 6. 3) gives K_s from MDI measurements. Since method S_3 is a steady state method, the long term measured data from MDI was used. This was compared with S_1, S_2 data and GP measurements for the study area as shown in Fig. 6. 10. It may be noted that Gardner's α determined by two head approach in S_3 was found to be less sensitive for soils present in the study area. Hence, the resulting K_s from S_3 method was found to be comparable for different locations of the study area. It is explicit that the K_s determined by steady state approach (S_3) is considerably greater than Zhang's transient method (S_1 and S_2) and GP measurements. To prove this point, Pearson's correlation coefficient "r" was determined and reported in parenthesis as shown in Fig. 6. 10. A poor correlation was exhibited by S_3-GP relationship whereas a better correlation was noted for S_1, S_2 methods with S_3. Similar to the factors stated above, GP measurements at a depth portrayed a lower K_s as compared to the surface K_s obtained by method S_3 based on MDI measurements.

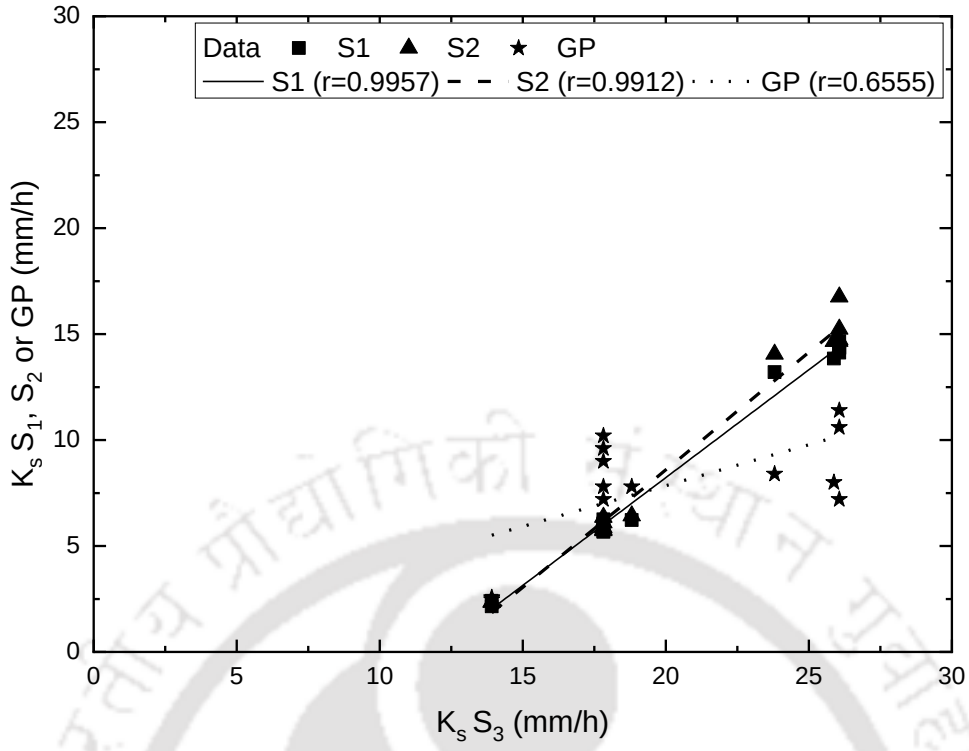

Fig. 6. 10 Comparison of saturated hydraulic conductivity obtained from S_3 with S_1, S_2 and Guelph permeameter

Figure 6. 11 depicts the comparison of Zhang's method (N_1 and N_2) with Haverkamp's transient analysis based on data series A (denoted by N_3 in Table 6. 3). It can be noted that K_{h_0} from N_1 and N_2 matches well with Haverkamp's analysis for K_{h_0} < 16 mm/h for the type of soils found in the study area. For K_{h_0} > 16 mm/h, Zhang's analysis was found to underestimate the values as compared to Haverkamp's method irrespective of the data series A and B. The mismatch is for higher values of K_{h_0}, which corresponds to low initial moisture content where the influence of sorptivity is maximum (Angulo-Jaramillo, et al., 2016). It may be noted here that N_1 and N_2 do not account for sorptivity for K_{h_0} determination as compared to Haverkamp method (N_3).

The K_s obtained indirectly from N_3 (designated as S_4) was compared with S_1, S_2 and GP as shown in Fig. 6. 12. It can be noted that the majority of the comparison of S_4 with S_1 and S_2 falls within 20 % variability but exceeds more than 50 % variability for GP. It is clear from previous discussion and Fig. 6. 12 that the measurement data from MDI is more influential in the determination of K_{h_0} and K_s than the analysis procedure itself. This is the reason why the trends reported in Fig. 6. 9 and Fig. 6. 12 are similar.

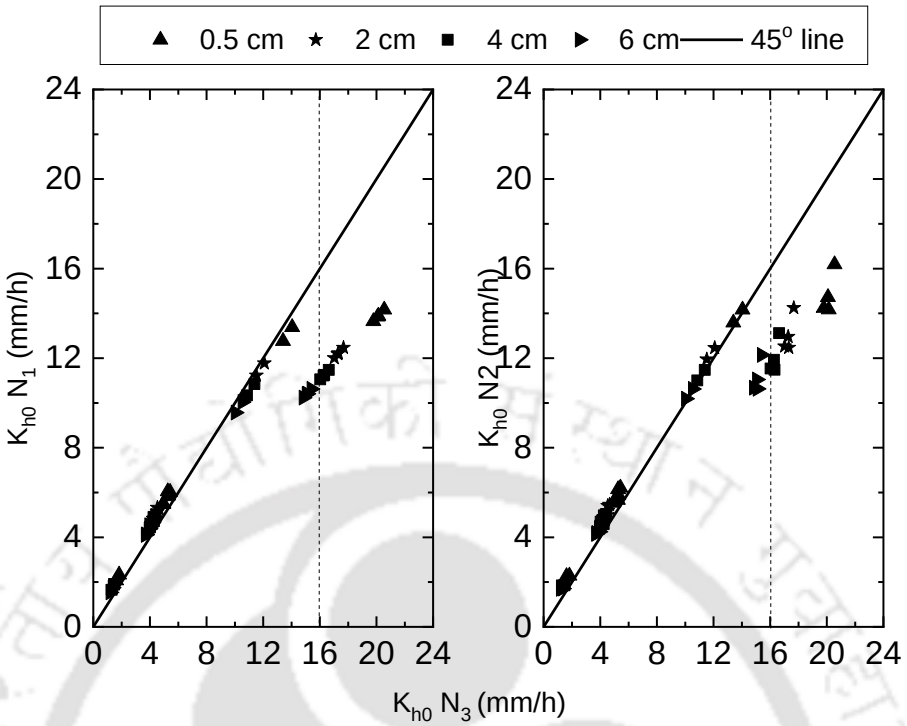

Fig. 6. 11 Comparison of near saturated hydraulic conductivity obtained from Zhang's method (N_1 and N_2 in Table 6. 3) and Haverkamp method (N_3)

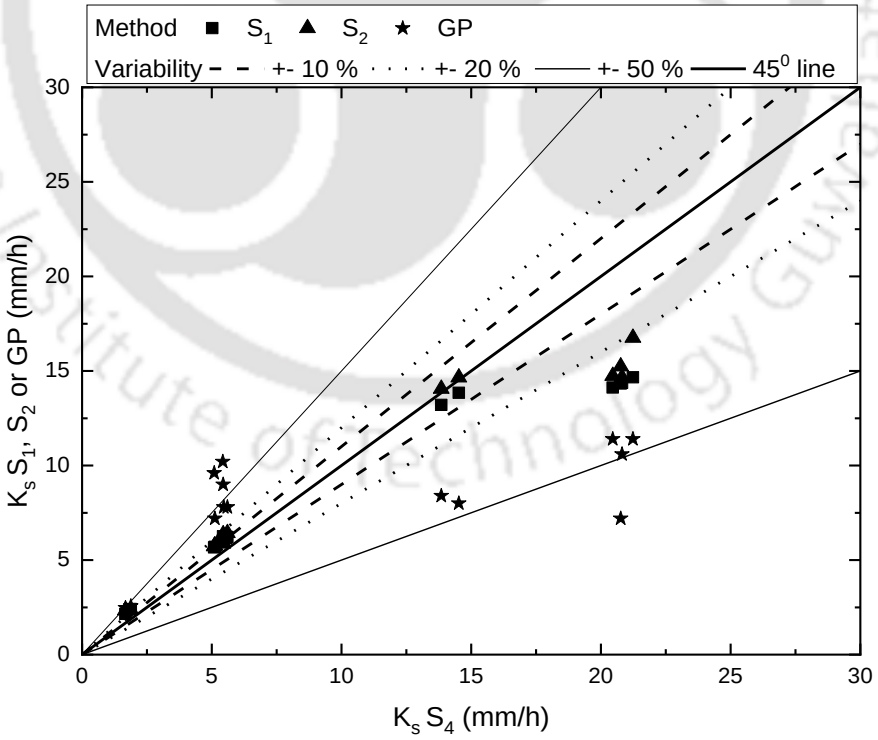

Fig. 6. 12 Comparison of saturated hydraulic conductivity obtained from Zhang's method (S_1, S_2 in Table 6. 3) and GP with Haverkamp method (S_4)

The final infiltration rate (i_f) was estimated from short-term data using hyperbolic method (as discussed in Sub section 6.4.1) corresponding to different tension head. These i_f were compared with K_{h_0} determined from N_1 and N_2 as shown in Fig. 6. 13. It can be noted that there is no comparison between K_{h_0} determined from N_1 and N_2 and i_f estimated from hyperbolic method. Hence, no relationship was attempted between these attributes. However, an effort was made to find the factor R1, which is defined as the ratio of K_{h_0} N_2 to the i_f estimated from IH_h and the results are tabulated in Table 6. 4. It can be noted that there is a distinct value of R1 for different soil type observed in the study area. The values of R1 is not sensitive to the applied tension pressure head and hence it was averaged. The average R1 for sand and loamy sand is comparable and hence considered to be the same. As the soil texture becomes finer, the R1 values reduces.

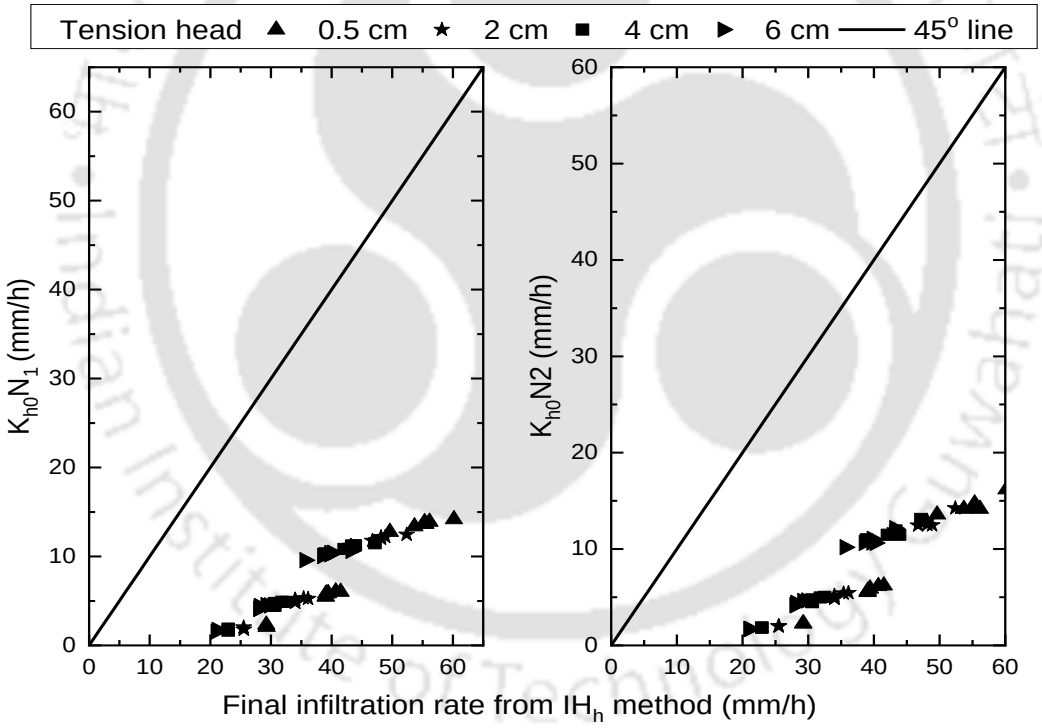

Fig. 6. 13 Comparison of near saturated hydraulic conductivity obtained from Zhang's method (N_1, N_2 in Table 6. 3) with final infiltration rate estimated by hyperbolic method (IH_h)

Table 6. 4 Ratio of K_{h_0} determined from N_2 and final infiltration rate estimated from IH_h

Station No.	Soil	Ratio R1 = $\frac{K_{h0}\text{determined from N2}}{\text{Final infiltration rate estimated from IH}_h}$				Average R1	Average R1 based on soil
		Tension head (cm)					
		0.5	2	4	6		
S1	S	0.266	0.269	0.275	0.278	0.27	0.27
S3		0.252	0.255	0.261	0.264	0.26	
S4		0.256	0.260	0.265	0.269	0.26	
S5		0.268	0.271	0.278	0.281	0.27	
S2	LS	0.263	0.266	0.272	0.275	0.27	
S14		0.273	0.276	0.283	0.286	0.27	
S6	L	0.151	0.152	0.156	0.157	0.15	0.15
S9		0.141	0.143	0.146	0.148	0.15	
S10		0.149	0.152	0.155	0.157	0.15	
S11		0.149	0.151	0.154	0.156	0.15	
S12		0.143	0.144	0.147	0.149	0.15	
S13		0.145	0.146	0.150	0.151	0.15	
S7	Si	0.077	0.078	0.079	0.081	0.08	0.08
S8		0.078	0.078	0.080	0.081	0.08	

S: Sand; LS: Loamy sand; L: Loam; Si: Silt

The factor R1 was applied to the i_f estimated from IH_h and again compared with K_{h_0} determined from N_2 as shown in Fig. 6. 14. It can be noted that there is an excellent match between K_{h_0} determined from N_2 and factored i_f from IH_h method by using the soil specific factor R1 listed in Table 6. 4. This indicates a clear possibility of determining K_{h_0} from i_f estimated by hyperbolic method based on short term data A in Fig. 6.6. The i_f values need to be factored using the soil specific values of R1 reported in Table 6. 4. The values of factor R1 could be obtained for only four soil textures: sand, loamy sand, loam and silt based on the soil type available in the study area. Further studies are needed to the determine the values of R1 for other soil textures.

In addition, vG-Zhang approach was applied to the estimated curve (long-term) based on hyperbolic method for determining K_{h_0} and compared with N_1 and N_2 as shown in Fig. 6. 15. As expected, it can be noted that the long term data (N_2) matched well as compared to N_1 with the K_{h_0} determined from hyperbolic method. This observation endorses the fact that the hyperbolic method can be used to generate the long-term infiltration data based on the short-term measurements from MDI.

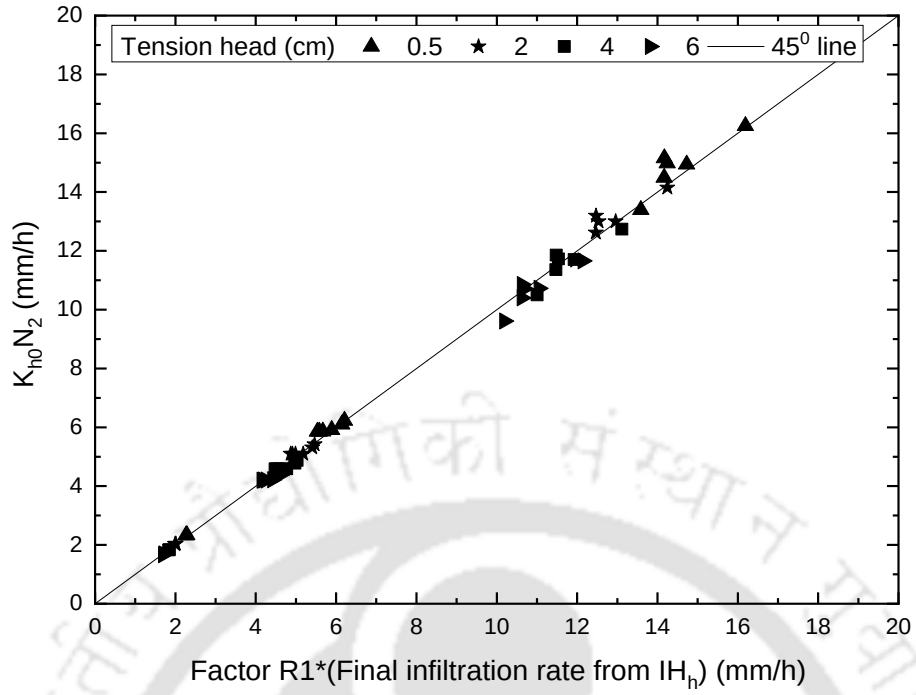

Fig. 6. 14 Comparison of near saturated hydraulic conductivity obtained from N_2 and factored final infiltration rate estimated from IH_h

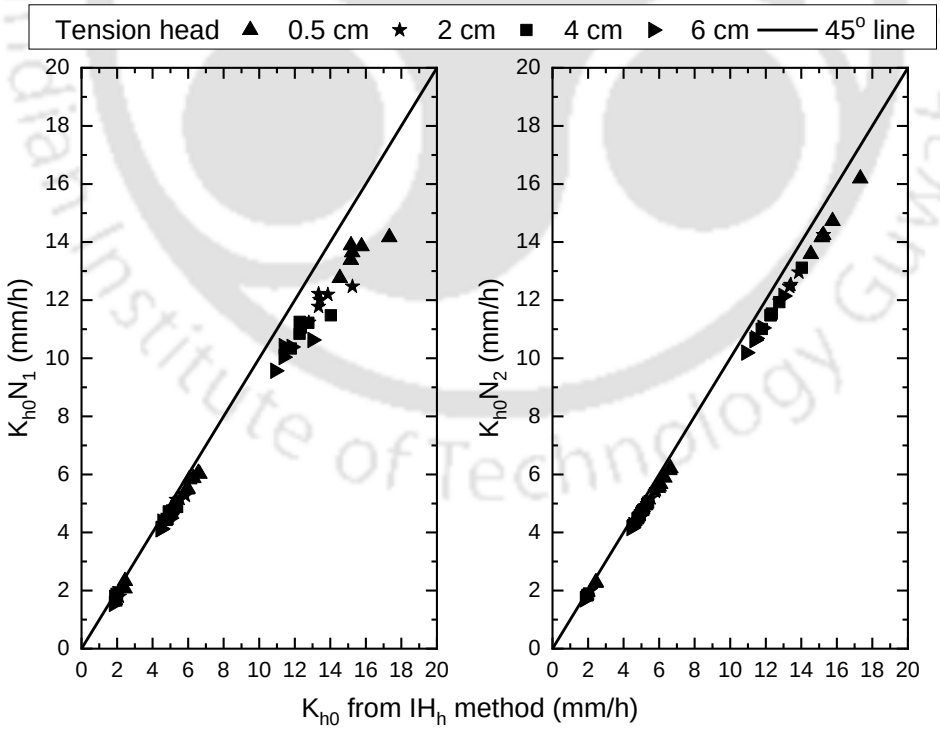

Fig. 6. 15 Comparison of near saturated hydraulic conductivity obtained from Zhang's method (N_1, N_2 in Table 6. 3) and hyperbolic method (IH_h)

The K_{h_0} from hyperbolic method was used to determine saturated hydraulic conductivity and was compared with the results of S_2 and GP as shown in Fig. 6. 16. It can be noted that there is an excellent match between K_s obtained from hyperbolic method and S_2 while there is high variability with GP data. This again endorses the previous finding that hyperbolic method can be used to extrapolate the short-term data to obtain long term response. Further, effort was made to explore relationship between K_s from hyperbolic method and final infiltration rate (i_f) estimated from hyperbolic method. The results are shown in Fig. 6. 17. It can be noted that there is a good linear relationship between K_s from hyperbolic method and final infiltration rate estimated from hyperbolic method with Pearson's correlation equal to 0.9856. This empirical relationship can be used to estimate near surface K_s from short term measurements of MDI by knowing i_f from hyperbolic method. However, this relationship is valid for i_f > 30 mm/h.

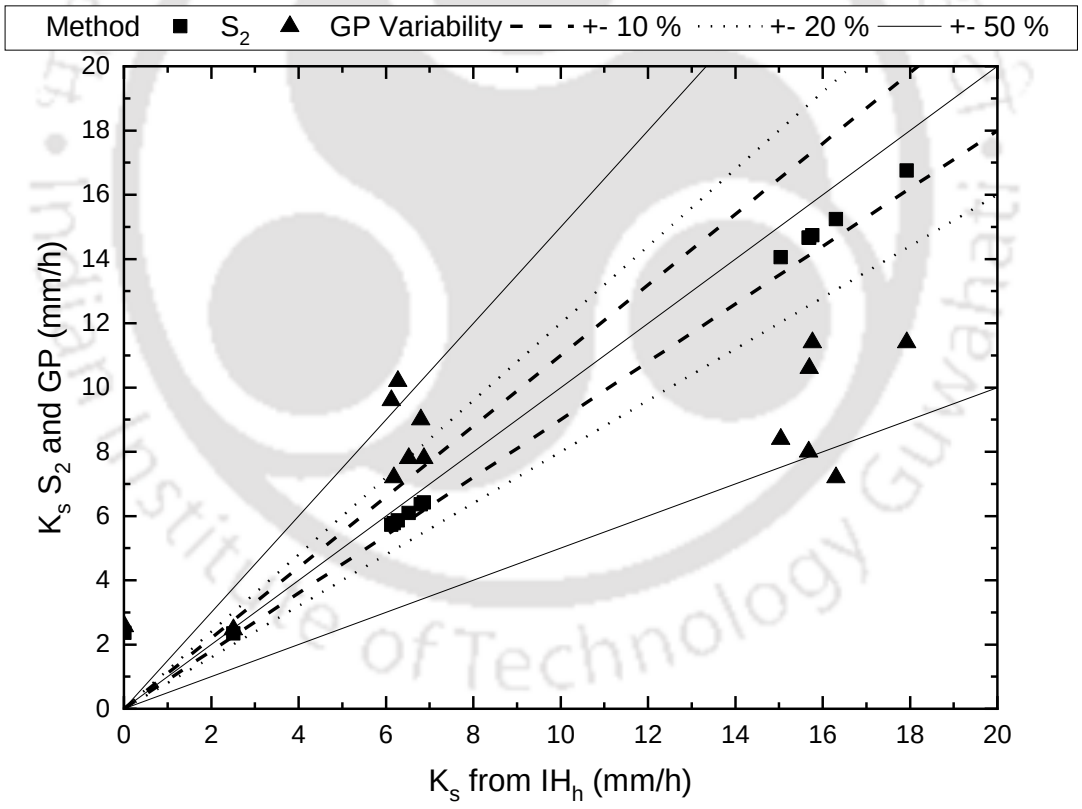

Fig. 6. 16 Comparison of saturated hydraulic conductivity obtained from Zhang's method (S_2), GP with hyperbolic method (IH_h)

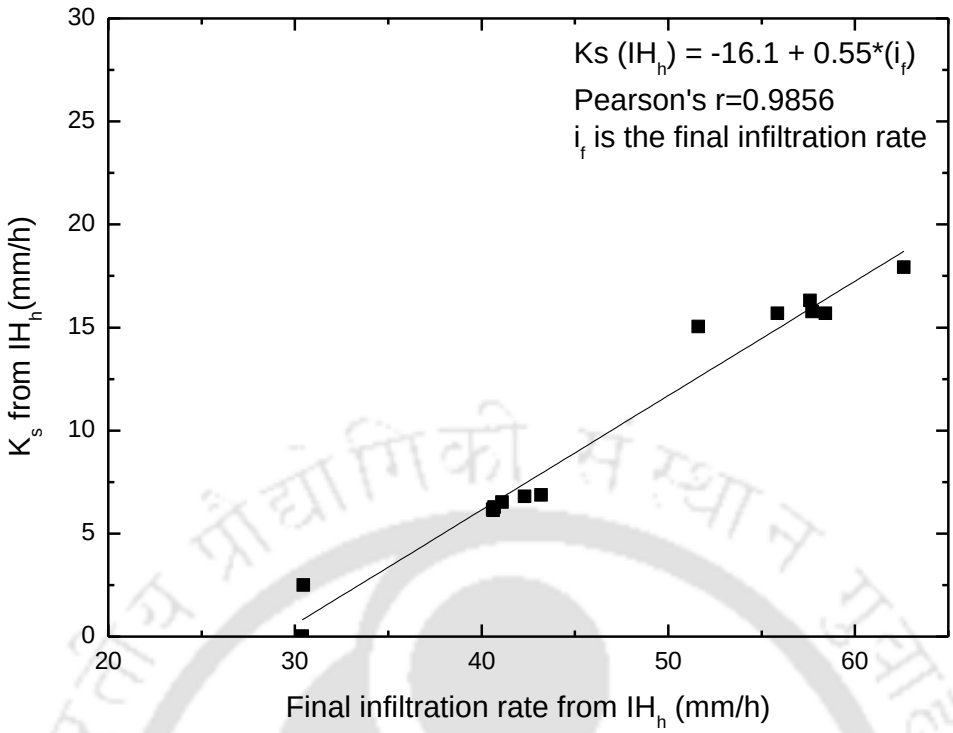

Fig. 6. 17 Relationship between saturated hydraulic conductivity and final infiltration rate (i_f) obtained from hyperbolic method (IH_h)

The estimated i_f from hyperbolic method based on the short term data (data A in Fig. 6. 6) was validated with the long term (data B in Fig. 6. 7) measured i_f from MDI as depicted in Fig. 6.18. For completeness, the extrapolated i_f to zero pressure head ($IH_{h=0}$ and $IM_{h=0}$ in Table 6. 3) are also shown in Fig. 6.18. It can be noted that the estimated and measured i_f matches well with the former marginally underestimated as compared to the measured values. This again reinforces the fact that hyperbolic method is quite effective in estimating the final infiltration rate from the short term measured data of MDI. Both estimated and measured i_f can be factored by R1 for determining K_{h_0} indirectly from short term MDI measurements as explained before.

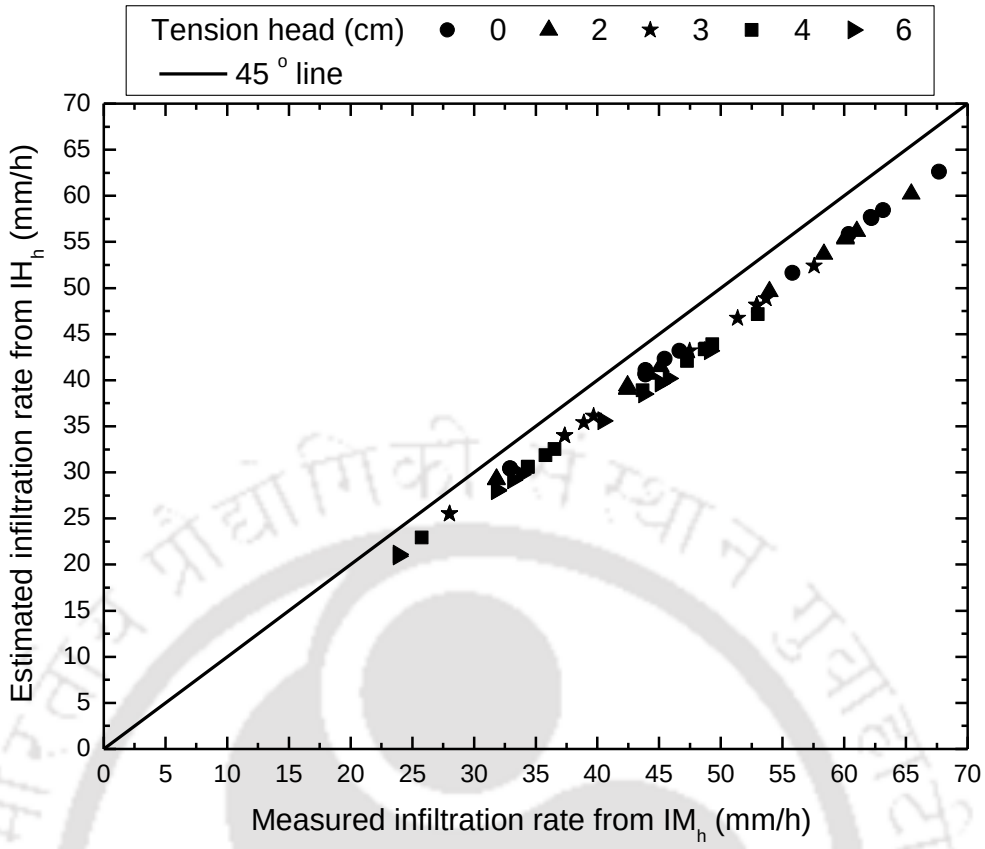

Fig. 6. 18 Comparison of estimated final infiltration rate from hyperbolic method with measured final infiltration rate from MDI

6.5. Summary

This study performed a critical evaluation of nine mathematical equations for determining near surface saturated hydraulic conductivity (K_s) based on mini disc infiltrometer (MDI) measurements corresponding to different field conditions. A well established Guelph permeameter (GP) was used as a reference measurement for K_s in the field. The nine equations considered in this study include Wooding-Gardner (W-G), Weir's Refinement (W-R), van- Genuchten Zhang (vG-Z), White and Sully (W-S), Simunek-Wooding (S-W), Ankeny (A), Zhang method -I (Z-I), Zhang method -II (Z-II) and Haverkamp (H). The statistical difference between K_s determined from GP and different mathematical equations (using MDI results) were assessed quantitatively by using Bland-Altman plot (BAp), Pearson correlation coefficient and root mean square error (RMSE). Analyzing the limits of agreement (LoA) and bias used in BAp, it was noted

that, K_s determined by W-G, W-R, vG-Z, A, and H equations compared well with the results of GP.

The final section of this chapter deals with the investigation on the influence of short-term and long-term MDI measurements on hydraulic conductivity determination. Five different approaches were studied for near saturated (K_{h0}) and saturated hydraulic conductivity (K_s) determination. Zhang's method of analysis using short-term and long-term measured data gave identical results for K_{h_0} < 8 mm/h and marginal variation for K_{h_0} > 8 mm/h for the type of soils in the study area. The variation was attributed to the non-consideration of sorptivity effect and short duration of measurement for relatively dry state of the soil. The K_s determined based on Zhang's method using short-term and long-term data did not compare well with the independent measurement using Guelph permeameter (GP) and exhibited both under and over estimation. A poor correlation was exhibited by K_s determined from steady-state Wooding-Gardner equation as compared to Zhang's method and GP.

The K_{h_0} from Zhang's method matched well with Haverkamp's analysis for K_{h_0} < 16 mm/h and underestimate for K_{h_0} > 16 mm/h irrespective of short-term or long-term data. The mismatch was again attributed to the non-consideration of sorptivity in Zhang's analysis as compared to Haverkamp's method. This study demonstrated the prediction of final infiltration rate (i_f) from short-term data using a rectangular hyperbolic method. It was shown that the estimated i_f compared well with measured i_f from long-term measured data. A method was developed by defining a soil specific factor for estimating K_{h_0} based on i_f obtained from hyperbolic analysis of short-term data. A good comparison was noted between K_s obtained from hyperbolic method and Zhang's method while there was high variability with GP data. The empirical linear relationship between K_s from hyperbolic method and final infiltration rate estimated from hyperbolic method can be used to estimate near surface K_s from short-term measurements of MDI. The relationship is valid for i_f > 30 mm/h.

Chapter 7

Laboratory Investigation on the Relationship and Sensitivity of Initial Compaction State on Near Saturated Hydraulic Conductivity

7.1. General

Infiltration is primarily influenced by soil type and initial compaction conditions (dry density and water content). However, there are not many studies that investigates the relationship and sensitivity of initial compaction state on infiltration characteristics of soils. Recent developments such as portable mini disc infiltrometer (MDI) permits controlled, non-destructive and non-intrusive infiltration experiments in the laboratory. Using this possibility, the study formulated a statistically significant multiple-linear regression (MLR) to quantitatively investigate the relationship between near saturated near surface hydraulic conductivity K_{h_0} and initial compaction state (dry density, γ and gravimetric water content, w) with and without negative pressure head (h_0). Also, an artificial neural network (ANN) model was developed for predicting the hydraulic conductivity by knowing the initial compaction state and particle size fraction of a particular soil. As such, this chapter discusses the association between initial compaction conditions with the near saturated hydraulic conductivity attained from infiltration responses for different types of soils including both cohesionless and cohesive soils.

7.2. Material and Methods

7.2.1. Soil Characterization

In this study, cohesionless sand, a cohesive natural lateritic hill soil (red soil), a silty and a loam soil were selected. The soils were characterized for their basic geotechnical characteristics and the results are summarized in Table 7. 1. The soils were classified as SP, CL, MH and ML based on Unified Soil Classification System (USCS) as stated in ASTM D 2487, where, SP stands for poorly graded sand, CL for lean clay of low plasticity, MH for high plasticity silt and ML for low plasticity silt. Specific gravity (G) of soil is determined based on ASTM D 854 and particle-size distribution was determined in accordance with ASTM D 7928-17.

Table 7. 1 Soil characteristics of the selected soils

Soil Type	Particle size fraction (%)			USCS*	Specific Gravity (G_s)	van Genuchten parameters	
	Sand	Silt	Clay			α	n
Sand	95	5	0	SP	2.55	0.145	2.68
Red soil	30	32	38	CL	2.72	0.059	1.48
Silt	23	56	21	MH	2.62	0.016	1.37
Loam	27	42	31	ML	2.68	0.036	1.56

7.2.2. Experimental Setup

Two PVC cylindrical molds of 20 cm diameter and 30 cm height were fabricated with and without bottom drainage provision for performing controlled MDI infiltration measurements on compacted soil samples shown in Fig 7.1. A rammer of 1.7 kg was used to impart the required compaction energy to the soil sample. The soils were compacted at a target γ of 1.4 g/cm^3, 1.6 g/cm^3 and 1.8 g/cm^3. The target water content of the soil varied from air dried, 2%, 4%, 8%, 12%, 16% and 20 % for sand and air dried, 2%, 10%, 20%, 25%, 30% and 35 % for red soil, silt and loam. Determination of K_{h_0} could not be performed for those samples having initial state of the sample close to full saturation. The required mass of air dried soil sample was mixed with calculated quantity of water to obtain desired water content. The soil sample was packed in the mold in three layers by giving equal number of blows on each layer. The number of blows depends on the desired state of compaction for a particular soil and was determined by trial and error. The weight of soil filled in the cylinder was noted and the bulk density was determined. The water content of the compacted soil was measured by oven drying method (ASTM D 2216), and the γ of the sample was determined. This was done to verify whether the achieved compaction state was identical to the targeted values. Remolded samples were opted in this study as against the field samples for achieving homogeneous samples of known compaction states. Field core samples may result in heterogeneity in terms of compaction state, which is not known and will not serve the purpose for which this study is performed.

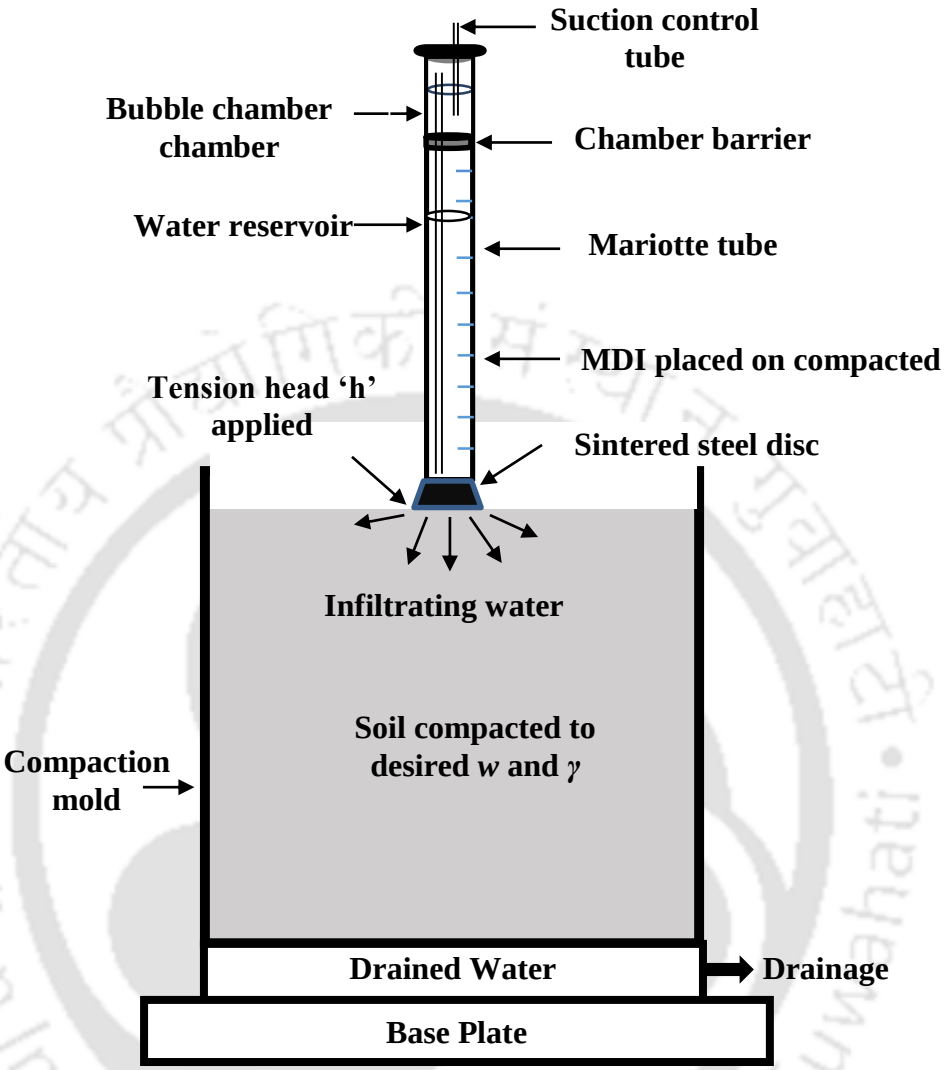

Fig. 7. 1 Experimental set up

For each compacted state of the soil, MDI measurements were performed for suction head 0.5, 2, 4 and 6 cm corresponding to with and without bottom drainage. All the experiments were repeated four times for ensuring the authenticity of the results obtained. The results were used to develop a relationship between hydraulic conductivity as a function of compaction state and applied tension head (h_0). It may be noted that the initial condition of the soil sample was kept identical for every suction head. In total, 544 sets of measurements were performed for sand and 512 for red soil, silt and loam respectively.

7.2.3. Determination of Hydraulic Conductivity

The size of the laboratory mold in which the soil is compacted was fixed such that there is no boundary effect on MDI measurements. Trial experiments were performed to verify no boundary effect on near surface near saturated hydraulic conductivity (K_{h_0}) determination. Afer preparing the MDI, it was placed on the soil surface and water was allowed to infiltrate. The volume of water that infiltrates into the soil at different time interval was measured for plotting cumulative infiltration (cm) versus time response.

The near saturated hydraulic conductivity K_{h_0} from three-dimensional infiltration response was determined by the transient approach proposed by Zhang using the Eq. 3. 6 (Section 3.2.3). The required water retention parameters corresponding to van Genuchten (1980) model was obtained based on the USDA textural classifaction as proposed by Carsel and Parrish (1988) and as recommended by the manufacturer of MDI. From the literataure (Angulo-Jaramillo, et al., 2016), it was observed that there is a possibility of error in C_2 determination because of the influence of sorptivity on K_{h_0} determination, which is not accounted in Zhang's method (Smettem, et al., 1994). However, for all practical purpose and as a first hand estimate, Zhang's method was found to be suitable for analysing MDI measurements (Angulo-Jaramillo, et al., 2016). It is worth mentioning here that Dohnal, et al. (2010) has demonstrated that Zhang (1997a) method is the most reliable method for determining hydraulic conductivity from MDI results for soils having van Genuchten parameter *n* greater than 1.35. It may be noted that the value of *n* for soils considered in this study is greater than 1.35 as listed in Table 7. 1, which justifies the use of Zhang's method.

In spite of the above justification for Zhang's method, this study attempted to understand the influence of sorptivity on K_{h_0} determination. There is a possibility of improper estimation of K_{h_0} as the soil becomes dry where in the effect of soil suction and sorptivity increases. For this reason, re-analysis of MDI results was performed using the physically based two-term cumulative infiltration model proposed by Haverkamp, et al. (1994). This model accounts for the influence of sorptivity on the estimation of K_{h_0} (Angulo-Jaramillo, et al., 2016). Haverkamp, et al. (1994) developed a quasi-exact equation describing the three-dimensional unsaturated cumulative infiltration curve for disc infiltrometers. The three-dimensional cumulative infiltration for short to medium time

can be determined by using Eq. (6. 34), in which the values of C_1 and C_2 are given by Eq. 6. 35.

Table 7. 2 and 7. 3 summarizes the statistical parameters for the repeatability of the near saturated hydraulic conductivity of the soil (K_{h_0}) measurements using MDI for sand (SA) and red soil (RS), respectively. These statistical parameters include arithmetic mean (AM), standard deviation (SD) and coefficient of variation (CV) for selected compaction states and suction. All the sets of measurements exhibited similar statistical trends and hence for the sake of brevity not all the results are listed in Tables 7. 2 and 7. 3.

Table 7. 2 Statistical parameters for the repeatability of near saturated hydraulic conductivity (mm/h) measurement for sand

Sr. No.	Drainage condition	Dry Density (g/cm^3)	Water content (%)	Suction (cm)	AM (mm/h)	SD	CV (%)
1	without drainage	1.4	4	0.5	18	0.24	1.2
2				6	12	0.36	2.8
3			12	0.5	12	0.3	2.3
4				6	12	0.24	2.1
7		1.6	2	0.5	18	0.36	2.5
8				6	12	0.18	1.4
9			12	0.5	12	0.48	4.3
10				6	6	0.06	0.4
11		1.8	2	0.5	12	0.06	0.4
12				6	6	0.3	3.4
13			6	0.5	12	0.12	1.4
14				6	6	0.18	4.3
16	with drainage	1.4	12	6	12	0.3	2.0
17		1.6	0	0.5	12	0.6	1.4
18				6	12	0.12	0.8
20			2	6	12	0.12	0.9
22		1.8	2	6	12	0.3	2.7
24			6	6	6	0.12	3.5

AM - Arithmetic mean; SD - Standard deviation and CV- Coefficient of variation

The results indicate that the measurements performed using MDI is repeatable for the soils and compaction state considered in this study. The coefficient of variation is less than 5 % for all the MDI measurements. This is an encouraging statistical trend for the K_{h_0} measurements, which is considered to be a highly variable parameter in the literature (Vrettas and Fung, 2015). The high repeatability is the result of controlled compaction and

homogeneity of soil samples considered in this study. The K_{h_0} corresponding to with and without bottom drainage conditions is depicted in Fig. 7.2. It is explicit that the influence of bottom drainage condition on K_{h_0} determination using MDI is negligible. This indicates that the three dimensional wetting front beneath MDI is not influenced by bottom drainage condition for the test duration considered in this study.

Table 7. 3 Statistical parameters for the repeatability of near saturated hydraulic conductivity (mm/h) measurement for red soil

Sr. No.		Dry Density (g/cm^3)	Water content (%)	Suction (cm)	AM (mm/h)	SD	CV (%)
1	without drainage	1.4	4	0.5	10.2	0.42	4.0
2				6	8.4	0.12	1.1
3			12	0.5	7.2	0.18	2.4
4				6	7.8	0.24	3.2
7		1.6	2	0.5	7.2	0.12	1.3
8				6	6.6	0.06	0.6
9			12	0.5	6.6	0.36	5.5
10				6	5.4	0.18	3.1
11		1.8	2	0.5	4.8	0.12	2.8
12				6	4.2	0.12	3.3
13			6	0.5	9.0	0.06	0.6
14				6	8.4	0.01	0.1
15	with drainage	1.4	12	0.5	1.3	0.02	1.5
16				6	1.0	0.002	0.3
20		1.6	2	6	3.9	0.16	4.2
21		1.8	2	0.5	3.2	0.04	1.2
22				6	2.6	0.02	0.6
23			6	0.5	1.4	0.01	0.9
24				6	0.7	0.02	2.8

AM - Arithmetic mean; SD - Standard deviation and CV- Coefficient of variation

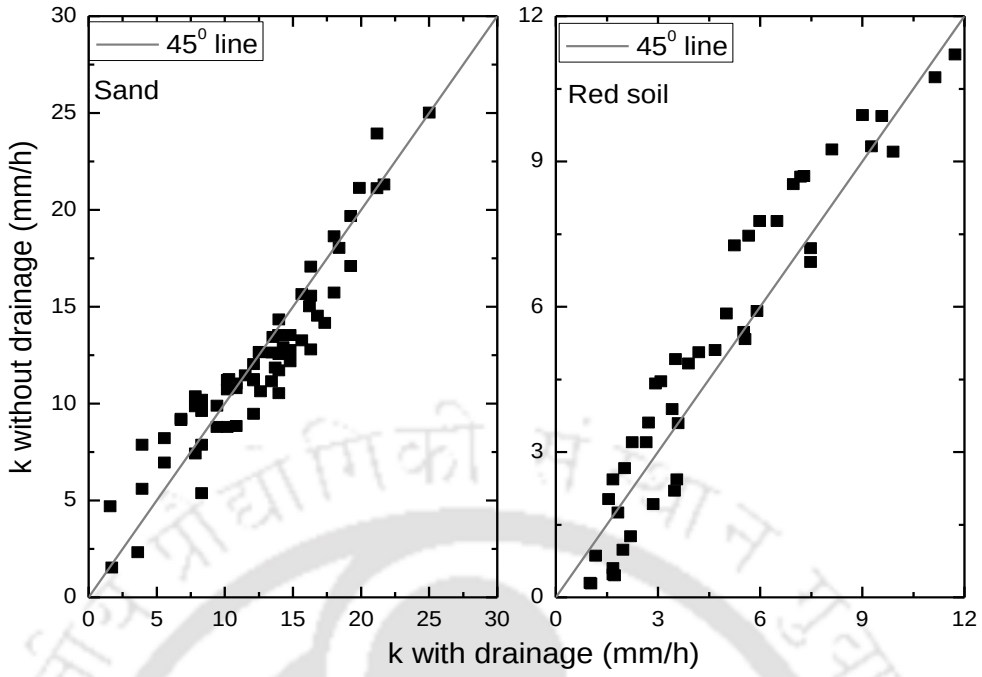

Fig. 7. 2 Comparison of near saturated hydraulic conductivity (K_{h_0}) with and without bottom drainage

To understand the effect of sorptivity, the K_{h_0} values determined based on Haverkamp's (considering sorptivity) and Zhang's analysis (not considering sorptivity) were compared for soils SA and RS as depicted in Figs. 7.3 and 7.4, respectively. It can be noted that the K_{h_0} obtained from Haverkamp's and Zhang's methods of analysis compares well for K_{h_0} values less than 15 mm/h for sand and 8 mm/h for red soil. Beyond this prescribed value, the Zhang's method marginally underestimates K_{h_0} as compared to Haverkamp's method. It is explicit from the figures that the mismatch is for higher K_{h_0} values, which corresponds to relatively low initial water content of the sample. It is known that the influence of sorptivity is predominant for low water content. This means that the underestimation of K_{h_0} from Zhang's analysis for relatively dry state of the soil can be attributed to the non-consideration of sorptivity effect for both the soils. However, it is worth mentioning that the mismatch between Haverkamp's and Zhang's methods of analysis is well within 10% variability for both the soils as indicated in Figs. 7.3 and 7.4. Even though it is understood that the role of sorptivity is prominent for low water content, it is not clear from the literature about the degree of saturation of the soil for which the

effect is more prominent on K_{h_0} determination. Further analysis of initial state of the soil shows that the average degree of saturation for SA is 20 % and for RS is 30 % below which the sorptivity is found to influence K_{h_0} determination.

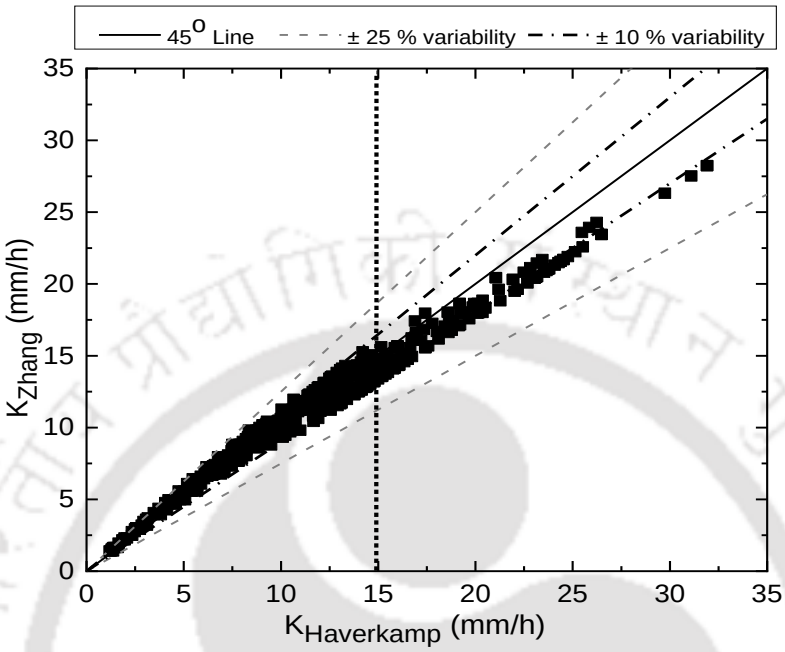

Fig. 7. 3 Comparison of hydraulic conductivity determined using Haverkamp and Zhang equations for sand

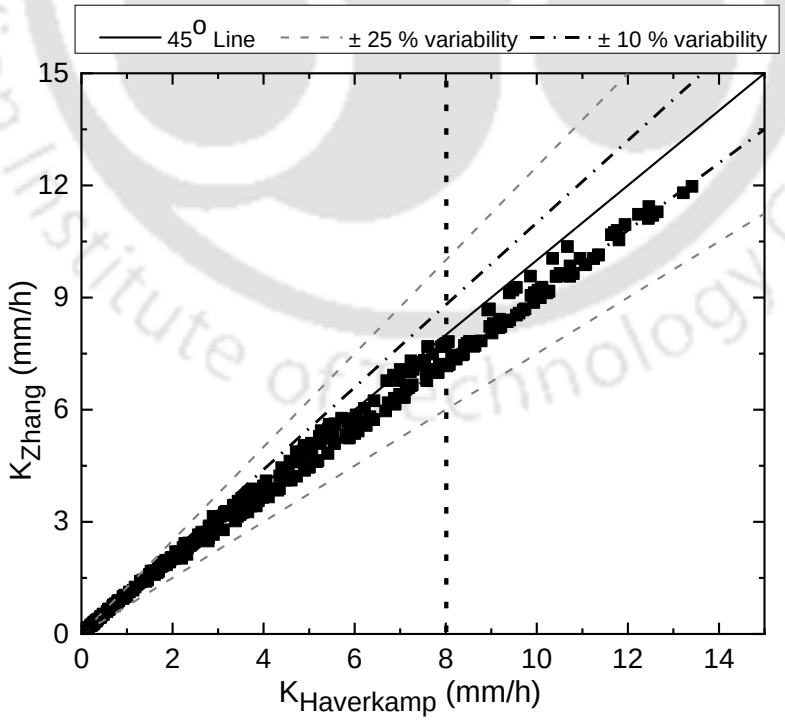

Fig. 7. 4 Comparison of hydraulic conductivity determined using Haverkamp and Zhang equations for red soil

Figure 7.5 exhibits the variation of K_{h_0} with initial compaction state for soils SA and RS, for infiltration measurements performed at 0.5 and 6 cm tension. For a particular *w*, the infiltration and K_{h_0} decreased with an increase in γ. For a particular γ, the K_{h_0} determined from infiltration measurements decreased with an increase in initial water content for both the soils and the trends are consistent for all the cases considered in this study. For a higher initial water content, the measured infiltration was less and hence the K_{h_0} determined based on the former is also less. It can be noted from the literature that a drier initial state of the soil has high suction and hence low unsaturated hydraulic conductivity (Fredlund and Rahardjo, 1993). However, a drier soil absorbs more water at the boundary due to which the infiltration and K_{h_0} is higher.

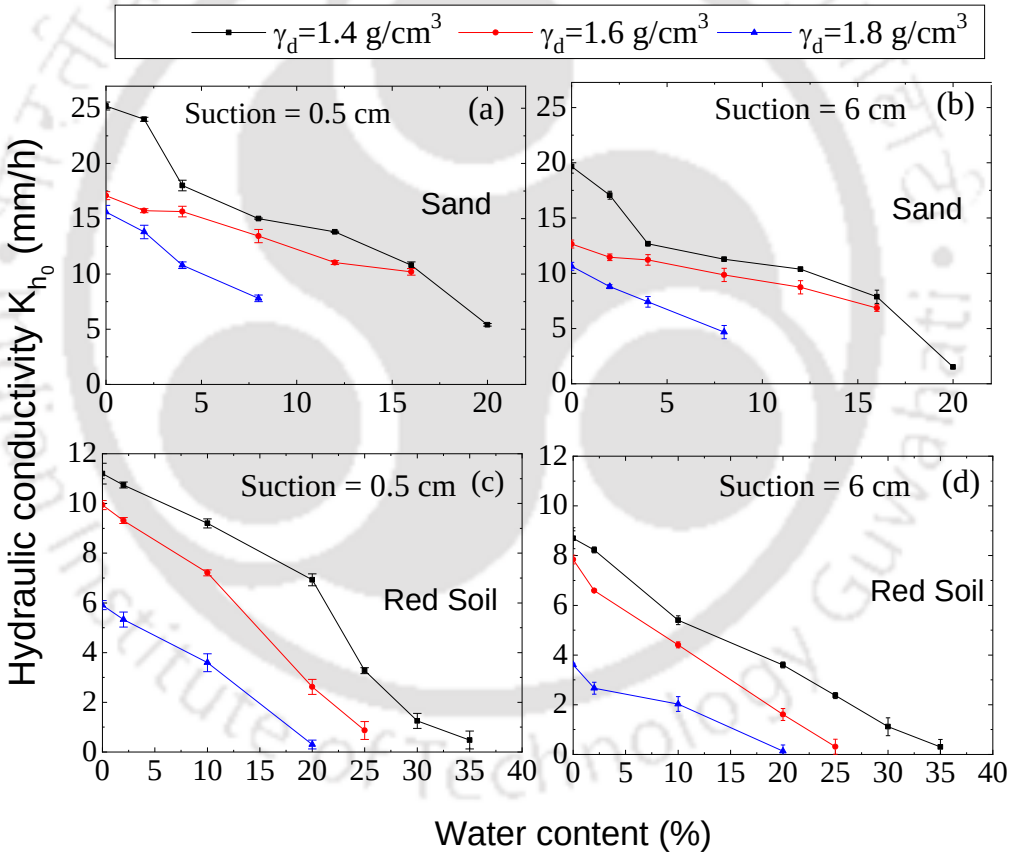

Fig. 7. 5 Variation of hydraulic conductivity with initial compaction for sand (a, b) and red soil (c, d)

There are several studies that investigates the variation of hydraulic conductivity (measured based on flow through soils as in the case of permeameters) for different initial compaction states (Assouline, et al., 1997; Zhang, et al., 2006), there are not many studies

for the near surface, near saturated hydraulic conductivity based on infiltration measurements. This aspect can only be investigated through controlled infiltration measurements as in the present study. The K_{h_0} determined from infiltration measurements is more appropriate and mandatory for any hydrologic modelling related to irrigation, drainage, artificial recharge and flooding where the surface K_{h_0} is more important.

Owing to the importance of surface hydraulic conductivity, an effort is made in this study to investigate the relationship between K_{h_0} and initial compaction state (γ and w) for cohesionless and cohesive soil considered in this study. Such relationships are rarely reported in the literature essentially due to the paucity of controlled infiltration measurements with fully known initial compaction conditions. This was possible in this study due to the use of MDI on a laboratory compacted samples allowing infiltration measurements on samples with known compaction state. This is not always possible in the field measurements due to the inherent factors affecting homogeneity of soil compaction state.

7.3. Relationship of Initial Compaction State on Near Saturated Hydraulic Conductivity Using Multiple Linear Regression (MLN) Analysis

As a simple first hand estimation, a multiple linear regression (MLR) analysis was performed to investigate the quantitative relationship and sensitivity of initial compaction condition (γ and w) and h_0 on K_{h_0} for a particular soil where sand and red soil were selected. The general form of the MLR is expressed as

$$y = \alpha_0 + \alpha_1 x_1 + \alpha_2 x_2 + \alpha_3 x_3 ..... + \alpha_k x_k + e \qquad (7.1)$$

where y is the variable to be predicted (K_{h_0} in this case) and x_i is the predictor variables. The coefficients $\alpha_1, ..., \alpha_k$ measure the effect of each predictor after considering the effect of all other predictors in the model. The coefficients measure the marginal effects of the predictor variables. 400 different sets of values were used for MLR.

The adequacy of the regression equation was quantified using R-square value. For more than one independent variables, adjusted R-square is used, which is adjusted for the number of predictors in the model (McCardle, 2003; Cramer, 1987; Ohtani, 1994). A higher the adjusted R-square indicates better representation of the model to the fitted

data. The adequacy of the model was checked using 100 independent measured values of K_{h0} (for sand and red soil).

7.3.1. Results of MLR model for Near Saturated Hydraulic Conductivity

A simple multiple-linear regression (MLR) equation was formulated with and without considering boundary negative pressure head for both Zhang's and Haverkamp's approach to understand its influence. The coefficients of all the cases of MLR equation obtained from the present study is listed in Table 7. 4.

Table 7. 4 Multiple linear regression equation for hydraulic conductivity of sand and red soil

Soil type	Method of analysis	Equation without considering h_0	Adjusted R^2	Equation considering h_0	Adjusted R^2
Sand	Zhang	K_{h_0} =-0.73 w-18.54 γ +45.97	0.75	K_{h_0} =-0.73 w-18.54 γ - 0.87 h_0 + 48.7	0.88
	Haverkamp	K_{h_0} = -0.89 w-19.83 γ +49.46	0.79	K_{h_0} =-0.89 w-19.83 γ - 0.88 h_0 + 52.21	0.89
Red soil	Zhang	K_{h_0} =-0.25 w-11.83 γ +26.13	0.81	K_{h_0} =-0.25 w-11.86 γ - 0.45 h_0 +27.58	0.90
	Haverkamp	K_{h_0} = -0.28 w-12.75 γ +28.28	0.83	K_{h_0} =-0.28 w-12.75 γ - 0.47 h_0 +29.74	0.91

K_{h_0} – hydraulic conductivity; w – initial water content; γ– initial dry density, h_0 – applied disc tension

The adequacy of the MLR equation was validated by independent infiltration measurements performed on both soils. Figures 7.6 and 7.7 depicts the comparison of measured and estimated K_{h_0} for sand and red soil, respectively. It can be noted that majority of the measured and estimated K_{h_0} falls within ±25 % variability and encouraging number of data within 10 % variability. Further, statistical analysis was performed to assess the predictability of MLR equation by testing a set of null hypotheses as listed in Table 7. 5 at the significance level of 0.05.

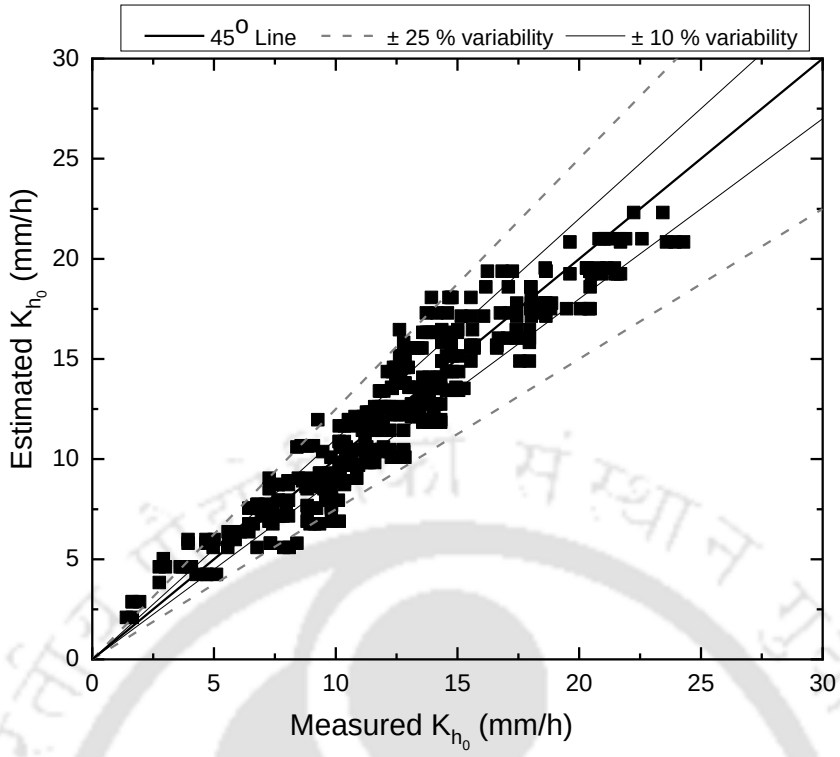

Fig. 7. 6 Comparison of measured and estimated near saturated hydraulic conductivity for sand

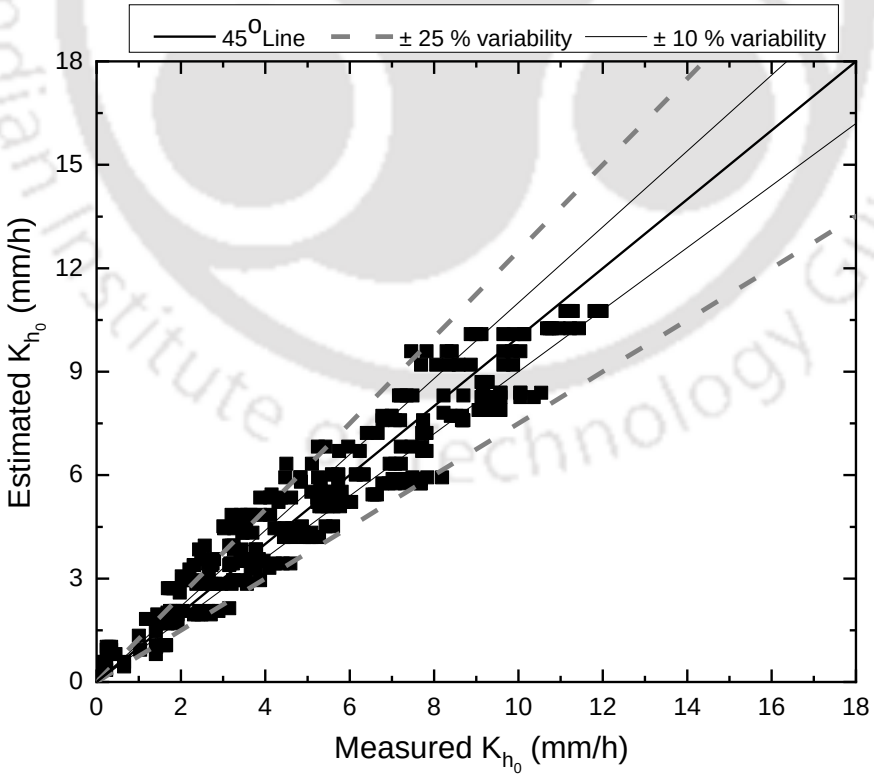

Fig. 7. 7 Comparison of measured and estimated near saturated hydraulic conductivity for red soil

Kruskul-Wallis Hypothesis testing with the significance level of 0.05 was conducted to establish statistical difference between measured and estimated K_{h_0} values. The results of testing HI and H2 hypotheses are presented in Table 7. 5 along with their respective statistical level of significance. The stated null hypothesis is rejected if the corresponding *p* value is less than 0.05. The results tabulated in Table 7. 5 shows that *p* value is greater than 0.05 for both the soils considered in this study and hence fail to reject the null hypothesis. This means that the estimated K_{h_0} is not statistically different from measured results, which is an encouraging result for practical applications.

Table 7. 5 Kruskul-Wallis Hypothesis testing

Hypothesis	Null Hypothesis	*p* values	Decision
H1	none of the measured hydraulic conductivity values differ significantly from the estimated values obtained from MLR equation for sand	0.99	Fail to reject
H2	none of the measured hydraulic conductivity values differ significantly from the estimated values obtained from MLR equation for red soil	0.82	Fail to reject

The developed relationship will be handy for predicting near saturated near surface hydraulic conductivity based on infiltration measurements by knowing the initial compaction condition of the soil, which is relatively simple and more certain than K_{h_0} measurements. For a highly variable parameter like K_{h_0} (Lee, et al., 2016; Assouline, 2013), such MLR can be a good first hand estimate for various field applications where actual infiltration measurements cannot be performed. Such relationship can also be employed for determining infiltration for a known γ and w determined remotely for inaccessible sites. However, the generality of such MLR need to be established by testing wide variety of soils.

7.3.2. Sensitivity Analysis of MLR Equation

The influence of input parameters w, γ and h_0 on K_{h_0} was quantified by sensitivity index determined by one-at-a-time measure (Saraiva, et al., 2017). According to the methodology explained in Saraiva, et al. (2017), method of difference is adopted for determining sensitivity index, which is based on the difference between system response (y_{ij}) and the base solution (β) for a particular parameter variation. For y_{ij}, i varies from 1 to

k, where *k* is the total number of parameters and *j* = 1 to *n*, where *n* is the number of equidistant sample points which is kept same for all the parameters. The sensitivity indices $S_{d(xi)}$ is given by Eq. 7. 2, where x_i is the parameter.

$$S_{d(xi)} = \frac{\sum_{j=1}^{n} S_{ij}}{n} \tag{7. 2}$$

where *i* and *k* remains same as explained above, S_{ij} is the partial sensitivity indices for the *j*th sample point of the curve x_i given by Eq. 7. 3.

$$S_{ij} = \frac{\left|y_{ij} - \beta\right|}{\sum_{i=1}^{k} \left|y_{ij} - \beta\right|} \tag{7. 3}$$

The results from Eqs. 7.2 and 7.3 is used to develop quantitative representation of sensitivity index of each parameter considered in this study (*w*, γ and *h*). This method helps to evaluate how sensitive the parameters are for the same percentage variation.

Figure 7.8 exhibits spider diagram (Saraiva, et al., 2017) which forms the basis of method of difference for illustrating the sensitivity of parameters. Spider diagram represents the output variation (in this case, value of K_{h_0}) for a given percentage variation in the input parameters considered one at a time (*w*, γ and h_0). The reference value of K_{h_0} (measured value) corresponding to a reference value of input parameters is shown in the figure. The spider graph offers a first-hand graphical information on the sensitivity of parameters. Only two cases were considered here one each of sand and red soil with and without considering h_0. It can be noted that spider graph presents a consistent representation of parameter sensitivity where in K_{h_0} determination is highly sensitive to γ, followed by *w* and h_0. Other cases of spider diagram present the same information and is not presented here for the sake of brevity.

The results from the spider diagram was used to determine sensitivity index S_d (Eq. 7. 5) for all the multiple-linear regression equations considered in this study as shown in Fig.7.9. The quantitative values of sensitivity index clearly indicate that the initial dry density (γ) has significant influence on K_{h_0} determination for all the cases considered in this study for both the soils. The sensitivity of h_0 is marginally more than *w* for three cases. However, for all practical purpose, the sensitivity of *w* and h_0 can be considered comparable. The results clearly indicate the importance of the knowledge of initial

compaction state of soil for determining infiltration characteristics in addition to the scale effects reported in the literature (Rasoulzadeh and Fatemi, 2011).

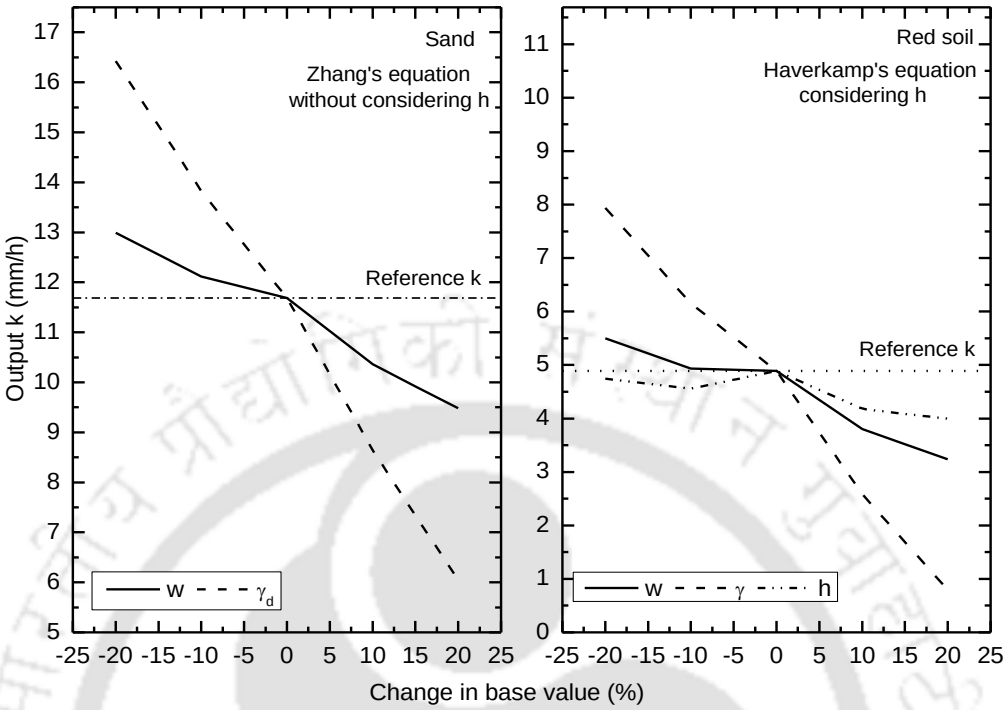

Fig. 7. 8 Spider graph relevant to method of difference

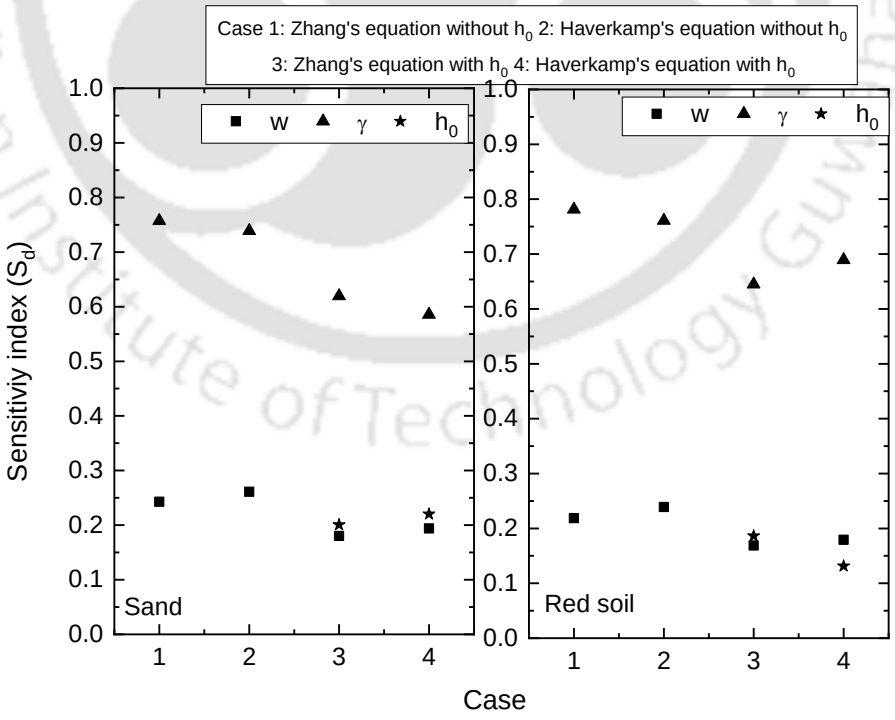

Fig. 7. 9 Sensitivity index of different input parameters for near saturated hydraulic conductivity equations

7.4. Relationship of Initial Compaction State on Near Saturated Hydraulic Conductivity Using ANN

Neural networks are data mining assemblies comprising artificial neurons in a multifaceted architecture to establish correlation between the inputs parameters and the outputs parameters (Das, et al., 2011; Mishra, et al., 2016). Training a network contains an iterative procedure through which the network gives the appropriate inputs along with a precise output for each of the inputs. After effective training, the training set has been learned with the learning weights are marginally attuned during each iteration and the training cycle concluded until the suitable weights have been established (Das, et al., 2012).

In the study, ANN was performed to correlate surface hydraulic conductivity as a function of soil fractions (sand, silt and clay) and initial compaction condition (dry density and water content) for a particular soil. The boundary pressure head which was applied at the bottom disc was also considered as an independent variable in the study. The data required for this analysis was generated using controlled laboratory experiments conducted in loam, silt, red soil and sand sample. 544 different sets of values were used for ANN model for sand samples whereas for red soil, silt and loam samples 512 sets of values were used respectively.

In the study, ANN toolbox accessible with MATLAB v 2015A has been used for the establishment of the association between the hydraulic conductivity and soil fractions, initial compaction conditions and pressure head applied at the bottom disc (MathWorks, 2001). The network was constructed and trained via different learning algorithms. In the study, a multilayer feed-forward-back-propagation network supported by Levenberg–Marquardt's learning rule had been used as it was the most efficient and accurate in determining the optimal point compared to other algorithms as shown in Fig. 7. 10 with the lowest mean square errors (MSE) with 6 neurons or nodes. The maximum possible iterations had been set to 50,000 where the progress in consecutive learning iterations was estimated by means of MSE, as expressed in Eq. 7. 4.

$$MSE = \frac{1}{N_d}\sum_{i=1}^{N}\left(O_s - O_A\right)^2 \qquad (7.\ 4)$$

where O_S and O_A were the simulated and predicted values respectively of the same unit and N_d was the total number of units. As evident from Fig. 7. 10, the number of nodes in the hidden layer was optimum to have a least MSE. Consequently, the network structure

has been used in the study includes a 6-6-1 architecture with six nodes in the input layer, six nodes in the hidden layer and one node in the output layer as shown in Fig. 7. 11. In the present network, nonlinear tan-sigmoid transfer function was used for all the nodal connectors.

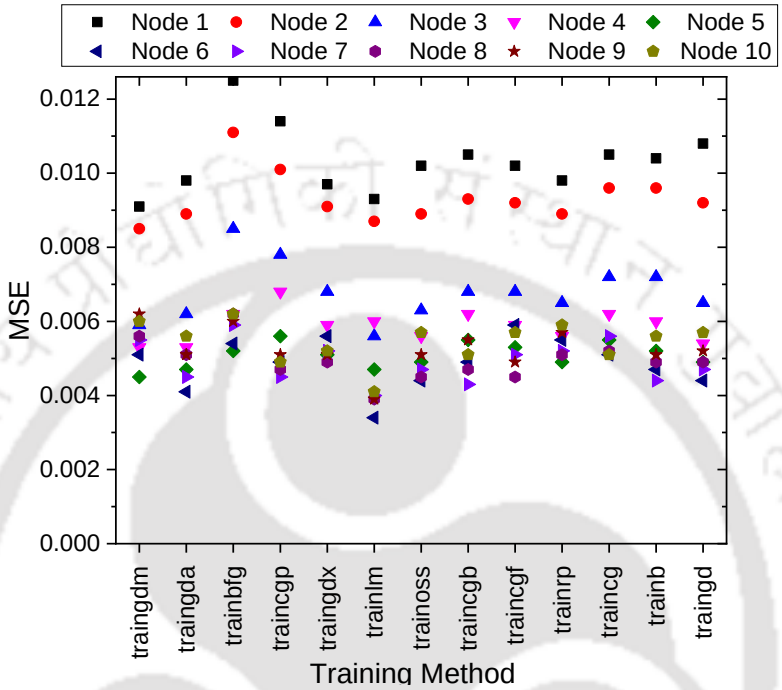

Fig. 7. 10 Training program of hidden layer transfer functions with MSE data

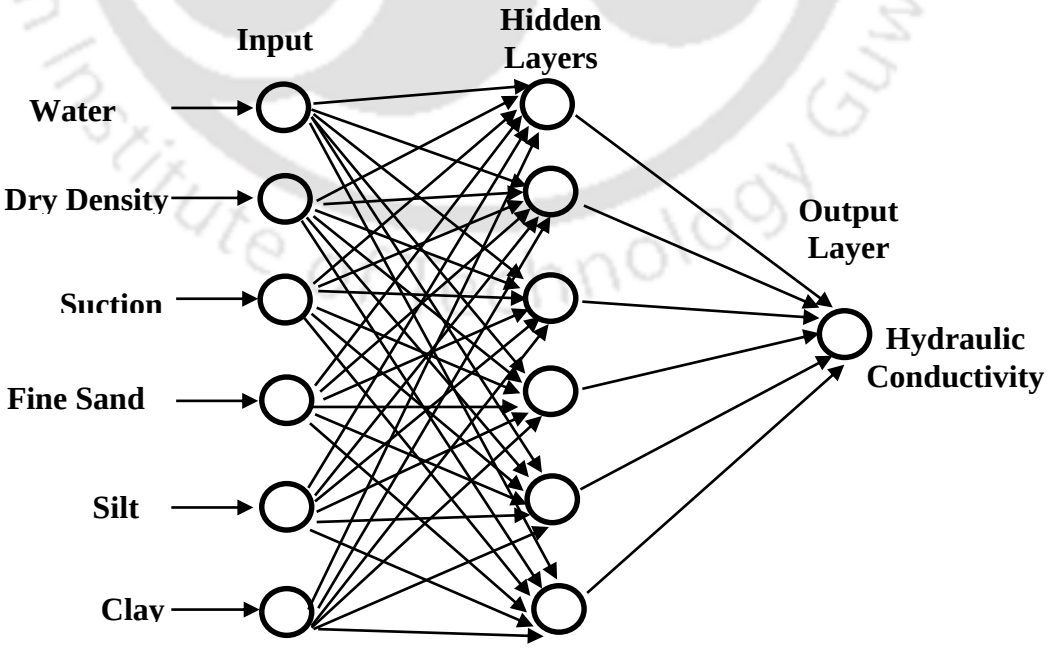

Fig. 7. 11 Structure of the Neural Network

7.4.1. Normalization of Input and Output

The normalization was carried out using the following expression given by Eq. 7. 5:

$$S_j^n = 2\frac{S_j^a - S_j^{\min}}{S_j^{\max} - S_j^{\min}} - 1 \qquad (7.\ 5)$$

where S_j^n and S_j^a were the j^{th} values of input or output before and after normalization respectively whereas S_j^{max} and S_j^{min} are the maximum and minimum values of all before normalization. With the normalization process the raw data of inputs and outputs had been normalized between -1 and 1.

7.4.2. Number of Hidden Neurons

In the study, an analysis was carried out to find out the optimal number of nodes essential in the hidden layer. It was evident from the Fig. 7. 10 that the lowest MSE was in the case of Levenberg–Marquardt's training function with 6 nodes in the hidden layer. Hence, a 6-6-1 ANN architecture had been employed with six input nodes (initial water content, dry density, applied suction at the bottom disc of MDI, sand fraction, silt fraction and clay fraction) with one output node (hydraulic conductivity) and six hidden nodes as shown in Fig. 7.11.

7.4.3. Overview and Performance of the ANN Architecture

The architecture of the ANN can adapt its performance in accordance with the specific problem. Consequently, ANN has the ability to apprehend effective configuration from a particular dataset which is known as training where the connection weights of nodes alter methodically to provide the preferred results (Das, et al., 2012). The foremost objective of the training is to find the ideal connection weights which would produce minimum MSE (Ghaboussi et.al., 1994; Demuth and Hagan, 1996). In this study, the partition of samples for training, testing and validation was carried out in accordance with the conservative practice which is shown in Table 7. 6. The training parameters are listed in Table 7. 7 and the optimum connection weights attained from the training was set aside for testing and validation phases. The training process was persistent until the error is lowest in testing dataset (Viji, et al., 2013).

Table 7. 6 Number of samples used in various performances

Sr. No.	Performance	Number of Samples
1	Training	1456
2	Testing	312
3	Validation	312

Table 7. 7 Training parameters in the study

Sr. No.	Training parameters	Magnitudes and Selection
1	Training function	trainlm
2	Transfer function Hidden layer	tansig
3	Transfer function Output layer	tansig
4	Performance function	mse
5	Error after learning	0.001
6	Epochs	50,000
7	Number of neurons in input layer	6
8	Number of hidden layers	1
9	Number of neurons in hidden layer	6
10	Number of output layers	1

Validation checks indicated the number of successive iterations that the validation performance fails to reduce. With number of stopping criteria was used concurrently, the training phase was supposed to end when any of the criteria is met. In the training phase, the coefficient of correlation R^2 was 0.984, which indicates a solid association between predicted and simulated results underlining the optimal training of the neural network. The connection weights from this stage could be attained as a result of the training which were then used in the testing and validation stages along with the conforming biases as tabulated in Table 7. 8 to 7. 10. The trained neural network along with its optimal connection weights, was used for the testing stage to assess the capability of prediction for the model. The testing stage had depicted in Fig. 7. 12, a high correlation coefficient R^2 of 0.987 offers an endorsement that the trained ANN model had greater prediction capacity. Afterwards, the trained neural network considered the validation dataset which was not used till now neither in training nor in testing stage. The validation phase was suitable to test the appropriateness of the neural network model. Figure 7. 12 demonstrated outstanding matching with R^2 of 0.987 between simulated and predicted values emphasizing the greater performance of the 6-6-1 ANN architecture. The development of training was reviewed for the three stages training, testing and validation by plotting the deviation of MSE with the concluded number of epochs, as shown in Fig. 7.13. In the

study, the usefulness of the trained network was tested on the basis of the training statistics with the recorded data of coefficient of correlation R^2. As the values of R^2 fluctuated from 0.984 to 0.987, the ANN was optimally trained and the network structure had outstanding competence of prediction.

Table 7. 8 Input-Hidden Connection Weights

Hidden / Input	A	B	C	D	E	F
1	-0.181	-3.050	-6.359	3.883	0.505	-4.198
2	-0.550	-2.828	-1.600	0.547	-0.004	-3.802
3	1.924	0.049	-0.295	0.285	0.268	0.038
4	-0.167	1.296	-1.033	-2.241	-0.386	-0.145
5	0.100	0.752	2.477	0.581	0.262	-0.337
6	-0.708	0.294	1.688	0.435	-1.079	-0.505

Table 7. 9 Output-Hidden Connection Weights

	Hidden					
	A	B	C	D	E	F
Output	-0.190	2.044	0.435	-0.850	-0.436	-1.676

Table 7. 10 Biases obtained after training phase

Biases	
Hidden layer	Output layer
1.986	-0.608
-0.785	
-2.264	
3.687	
0.045	
-1.681	

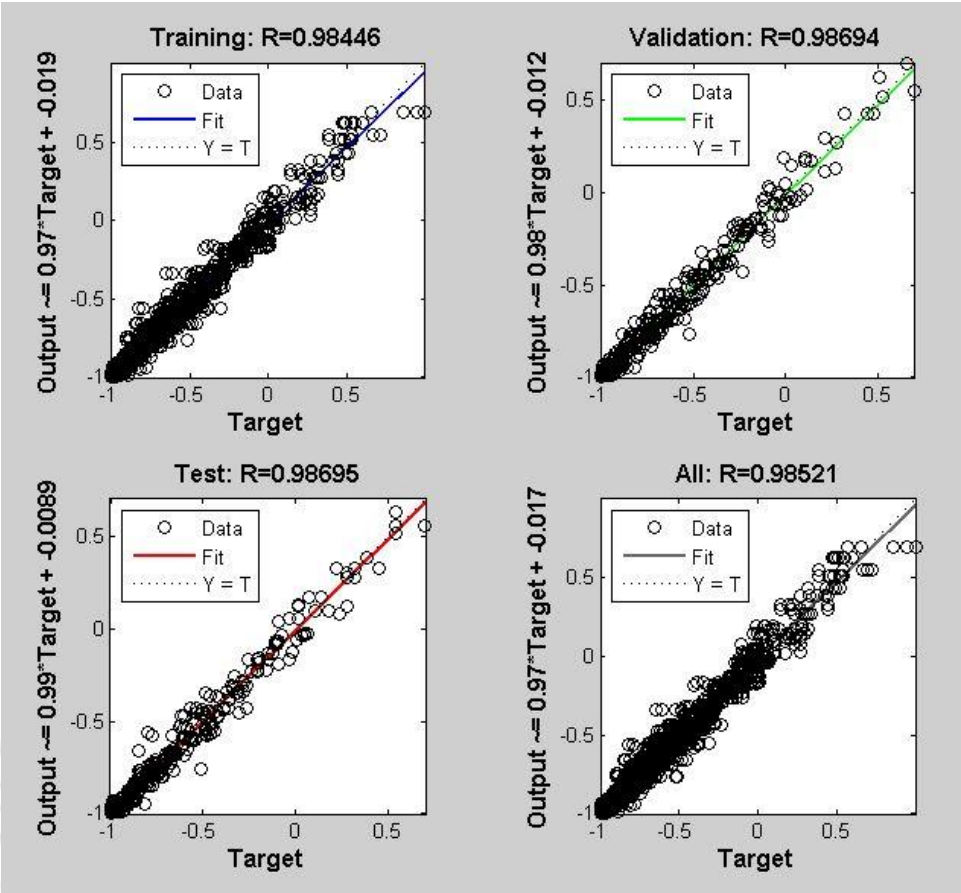

Fig. 7. 12 Capability of neural structure for training, Testing and Validation phase

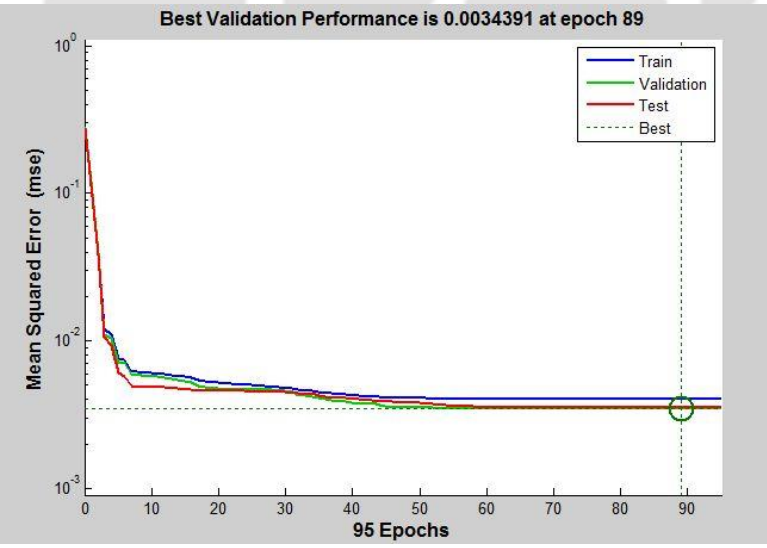

Fig. 7. 13 Comparison of MSE

7.4.4. Sensitivity of ANN Model

Sensitivity analysis is significant for the selection of influencing input variables so as to provide their ranking in accordance with their importance. There are different ways to ascertain the contributory input variables (Olden, et al., 2004; Das, et al., 2010; Mishra, et al., 2016). Among them, garson's algorithm was used in this study to find the importance of inputs (Garson, 1991; Olden et.al., 2004**)**. In the case of Garson's algorithm, initially the input-hidden and hidden-output weights were separated, and the absolute values of the weights was used to distinguish the rank of input parameters (Garson, 1991). In the approach, the product of the input–hidden and hidden–output connection weights were considered. The result is a ranking of the input variables based on their absolute values, also provide the idea whether the outputs are having a direct or inverse relation with different input parameters (Olden et.al., 2004).

$$Input_X = \sum_{Y=A}^{F} \frac{|Hidden_{XY}|}{\sum_{Z=1}^{6} |Hidden_{ZY}|} \quad (7.\ 6)$$

Accordingly, the above expression represents the estimation of variable importance for predictor variable X (where X = 1–6), using the weights connecting each of the input neurons Z (where Z = 1–6) to each of the hidden neurons N (where N = 1–6), and the latter to the single output neuron. The result of the sensitivity analysis conducted with the Garson's method to deliver the importance ranking to the input parameters was shown in Table 7. 11.

Table 7. 11 Sensitivity index for near saturated hydraulic conductivity by Garson's algorithm (based on ANN)

S. No.	Input	Importance	Importance (%)	Rank
1	Water content	2.105	35.1	1
2	Dry density	1.112	18.5	2
3	Suction	0.709	11.8	5
4	Sand	0.765	12.8	4
5	Silt	0.527	8.8	6
6	Clay	0.782	13.0	3

It is obvious from the Table 7. 11 that initial water content was the most significant input parameter with maximum impact on the variations in prediction for the Garson's

algorithm method. It was followed by the other input parameters according to their impact dry density, clay and sand fraction, applied suction and silt fraction in case of Garson's algorithm in that oder.

7.4.5. ANN Prediction Equation for Near Saturated Hydraulic Conductivity

A model equation was framed with the weights and biases acquired from trained ANN. The mathematical equation linking the input variables and the output could be expressed as (Goh et.al., 2005; Das and Basudhar, 2008),

$$K_n = f_{sig}\left\{b_0 + \sum_{k=1}^{h}\left[w_k \times f_{sig}\left(b_{hk} + \sum_{i=1}^{m} w_{ik} X_i\right)\right]\right\} \quad (7.\ 7)$$

where K_n was the normalized output variable, f_{sig} is the sigmoid transfer function, b_0 is the bias at the output layer; W_k is the connection weight between k^{th} node of hidden layer and the output node, b_{hk} is the bias at the k^{th} node of the hidden layer, m is the number of input variables, h is the number of nodes in the hidden layer, W_{ik} is the connection weight between i^{th} layer of input and k^{th} node of hidden layer, X_i is the normalized input variables.

With the values of the connection weights and biases tabulated in Table 7. 8 to 7. 10 and subsequent expression was framed where w represents the first input parameter initial water content, γ represent second input parameter dry density, h_0 represents the third input parameter applied suction, s represents fourth input parameter sand fraction, si represents the fifth input parameter silt fraction and c represents the sixth input parameter clay fraction,

$$A_1 = 1.986 - 0.181\,w - 0.550\,\gamma + 1.924\,h_0 - 0.167\,s + 0.1\,si - 0.708\,c \quad (7.\ 8)$$

$$A_2 = -0.785 - 3.050\,w - 2.828\,\gamma + 0.049\,h_0 + 1.296\,s + 0.752\,si + 0.294\,c \quad (7.\ 9)$$

$$A_3 = -2.264 - 6.359\,w - 1.600\,\gamma - 0.295\,h_0 - 1.033\,s + 2.477\,si + 1.688\,c \quad (7.\ 10)$$

$$A_4 = 3.687 + 3.883\,w + 0.547\,\gamma + 0.285\,h_0 - 2.241\,s + 0.581\,si + 0.435\,c \quad (7.\ 11)$$

$$A_5 = 0.045 + 0.505\,w - 0.004\,\gamma + 0.268\,h_0 - 0.386\,s + 0.262\,si - 1.079\,c \quad (7.\ 12)$$

$$A_6 = -1.681 - 4.198\,w - 3.802\,\gamma + 0.038\,h_0 - 0.145\,s - 0.337\,si - 0.505\,c \quad (7.\ 13)$$

$$B_1 = -0.190 \times \frac{e^{A_1} - e^{-A_1}}{e^{A_1} + e^{-A_1}} \quad (7.\ 14)$$

$$B_2 = 2.044 \times \frac{e^{A_2} - e^{-A_2}}{e^{A_2} + e^{-A_2}} \quad (7.15)$$

$$B_3 = 0.435 \times \frac{e^{A_3} - e^{-A_3}}{e^{A_3} + e^{-A_3}} \quad (7.16)$$

$$B_4 = -0.850 \times \frac{e^{A_4} - e^{-A_4}}{e^{A_4} + e^{-A_4}} \quad (7.17)$$

$$B_5 = -0.436 \times \frac{e^{A_5} - e^{-A_5}}{e^{A_5} + e^{-A_5}} \quad (7.18)$$

$$B_6 = -1.676 \times \frac{e^{A_6} - e^{-A_6}}{e^{A_6} + e^{-A_6}} \quad (7.19)$$

$$C_1 = -0.608 + B_1 + B_2 + B_3 + B_4 + B_5 + B_6 \quad (7.20)$$

$$K_n = \frac{e^{C_1} - e^{-C_1}}{e^{C_1} + e^{-C_1}} \quad (7.21)$$

The K_n value as acquired from Eq. 7. 21 was in between −1 and 1 and that required to be denormalized as,

$$K_{h_0} = 0.5(K_n + 1)\ (K_{\max} - K_{min}) + K_{min} \quad (7.22)$$

where, K_{max} and K_{min} were the maximum and minimum value respectively of the dataset

7.5. Summary

This study investigated the possible relationship and sensitivity of initial compaction condition of soil on the near saturated near surface hydraulic conductivity (K_{h_0}) determined by minidisc infiltrometer (MDI). The coefficient of variation was found to be less than 5 % for MDI measurements proving its repeatability for the controlled compaction and homogeneous soil samples considered in this study. The three dimensional wetting front beneath MDI was not influenced by the bottom drainage condition for the test duration considered in this study. It can be noted that the K_{h_0} obtained from Haverkamp's and Zhang's methods of analysis compares well for lower K_{h_0} values less than 15 mm/h for cohesionless soil and 8 mm/h for cohesive soil. For both the soils, the Zhang's method marginally underestimates K_{h_0} (within 10 %) as compared to Haverkamp's method for higher K_{h_0} values, which corresponds to low initial water content of the sample (sorptivity is predominant). The variation of K_{h_0} from Zhang's analysis may be attributed to the non-consideration of sorptivity effect for both the soils. The average

degree of saturation was 20 % and 30 % for cohesionless and cohesive soil, respectively, for which sorptivity was found to influence K_{h_0} determination. For a particular initial gravimetric water content (w), the infiltration and K_{h_0} decreased with an increase in dry density (γ). For a particular γ, the K_{h_0} determined from infiltration measurements decreased with an increase in w for both the soils and the trends are consistent for all the cases considered in this study. A drier soil absorbs more water at the soil surface due to which the infiltration and K_{h_0} is higher.

A simple multiple-linear regression (MLR) equation was formulated with and without considering boundary negative pressure head (h_θ) for both Zhang's and Haverkamp's approach to investigate the relationship between K_{h_0} and initial compaction state (γ and w) for cohesionless and cohesive soil considered in this study. The adequacy of the MLR equation was validated by independent infiltration measurements performed on both soils. The relationship between estimated K_{h_0} from MLR and measured results was found to be statistically significant, which is an encouraging result for practical applications. It is believed that such MLR can be a good first hand estimate for various field applications where actual infiltration measurements cannot be performed. However, the generality of such MLR need to be established by testing wide variety of soils. The developed MLR was used to study the sensitivity of input parameters (w, γ and h_θ) on K_{h_0} by using spider diagram and method of difference. The quantitative values of sensitivity index clearly indicate that the initial dry density (γ) has significant influence on K_{h_0} determination for all the cases considered in this study. The sensitivity of w and h_θ is much less than γ and can be considered comparable.

The study also explored the effect of soil type, applied suction and initial compaction state of soil on the hydraulic conductivity(K_{h_0}) based on ANN model estimated on controlled MDI measurements carried out in the laboratory. Unlike linear regression model, the sensitivity analyses (Garson's algorithm) based on ANN model indicated that K_{h_0} determined from MDI is more sensitive to initial water content followed by dry density. The ANN model with the six input parameters was the optimal model based on the statistical parameters and correlation coefficient for training and testing data set.

Chapter 8

Numerical Flow Simulation Beneath Infiltrometers

8.1. General

There is substantial advancement in the theoretical understanding and mathematical formulation of water flow and solute transport in the vadose zone with quite a few analytical solutions. However, there is a need to cross verify the validity of input hydraulic parameters from the database for simulating infiltration beneath infiltrometers. In this chapter, the flow processes beneath different infiltrometers were numerically simulated using Hydrus 2D software. Also, controlled experiments with instrumentation were conducted under controlled condition to understand the flow processes beneath a mini disc infiltrometer (MDI).

8.2. Field Experiments

The infiltration tests conducted at 14 locations in the study area for June 2014, December 2014 and June 2015 using mini disc infiltrometer (MDI), tension infiltrometer (TI), and double ring infiltrometer (DRI) were utilized for the numerical simulation of flow beneath infiltrometers. Initial gravimetric water content (w) and field dry density (γ) of all the stations were determined before the infiltration experiments in accordance with ASTM D 2216 and ASTM D 6938, respectively. The infiltration tests were conducted in the field using MDI and TI measurements corresponding to 2 different tensions, 6 and 0.5 cm for all the locations and DRI measurements were conducted with a ponding head of 8 cm. The details of the field experiments are already discussed in Chapter 3.

8.3. Numerical Simulation Using HYDRUS 2D

The numerical simulation of flow beneath infiltrometers requires the solution of the Richards' equation (Richards, 1931; Chow, et al., 1988), which describes water flow in a variably saturated soil. These solutions use soil hydraulic parameters and do not require measured infiltration data. The factors influencing the soil hydraulic properties are the soil type, soil structure, soil compaction state and the saturation state of the soil matrix (Schuhmann, et al., 2011). The numerical flow simulation beneath infiltrometers was performed using HYDRUS 2D software, which numerically solves Richard's equation for

water flow through soil using Galerkin type finite element scheme.

8.3.1. Direct Simulation Using HYDRUS

The governing flow equation for simulating the flow beneath the infiltrometers can be described by the non-linear Richard's equation given by Eq. 8. 1 (Warrick, 1992).

$$\frac{\partial\theta}{\partial t}=\frac{1}{R}\frac{\partial}{\partial R}\left(RK(h)\frac{\partial h}{\partial R}\right)+\frac{\partial}{\partial z}\left(K(h)\frac{\partial h}{\partial z}\right)-\frac{\partial K(h)}{\partial z} \tag{8. 1}$$

where *h* is the pressure head; θ is the volumetric water content; *z* and *R* are the vertical and radial coordinates respectively, and *K(h)* is the unsaturated hydraulic conductivity function.

The soil hydraulic functions such as *θ(h)* and *K(h)* in Eq. 8. 2 are non-linear functions of *h* and can be expressed in terms of soil water retention parameters in accordance with the statistical pore size distribution model of Mualem (1976) (Mualem, 1976; van Genuchten, 1980)

$$\theta(h)=\begin{cases}\theta_r+\dfrac{\theta_s-\theta_r}{\left[1+|\alpha h|^n\right]^m}, h<0\\ \theta_s, h\geq 0\end{cases} \tag{8. 2}$$

$$K(h)=\mathrm{K_s}\,S_e^l\left[1-\left(1-S_e^{1/m}\right)^m\right]^2 \tag{8. 3}$$

$$m=1-\frac{1}{n}, n>1 \tag{8. 4}$$

where θ_r and θ_s is the residual and saturated water content respectively; K_s is the saturated hydraulic conductivity; S_e is the effective saturation; n is the pore-size distribution index; l is the pore-connectivity parameter and α is the parameter representing air entry value in soils.

The above van Genuchten-Mualem's model consists of 6 independent parameters, $\theta_r,\theta_s,K_s,n,l$ and α where n,l and α are empirical parameters affecting the shape of the hydraulic function. The van Genuchten water (v-G) retention model parameters (Mualem, 1976; van Genuchten, 1980) are given by Carsel and Parrish (1988) as listed in Table 8. 1.

By knowing the pressure head imposed by different infiltrometers at the boundary, hydraulic parameters for different soil types (Table 8. 1), and measured values of θ_s and K_s from the field or lab (as discussed in section 3.3), the direct flow simulation was

performed using Hydrus 2D. The results of direct simulation give cumulative infiltration with time response beneath infiltrometer. A comparison of the simulation results with measured infiltration curves help to understand the adequacy of the hydraulic parameters listed in Table 8. 1.

Table 8. 1 Hydraulic parameters of van Genuchten model for different soils (Carsel and Parrish, 1988)

Soil Type	θ_r	θ_s	α	n (cm^{-1})	K_s (cm/min)	l
Sand	0.045	0.43	0.145	2.68	0.4950	0.5
Loamy sand	0.057	0.41	0.124	2.28	0.2432	0.5
Sandy loam	0.065	0.41	0.075	1.89	0.0737	0.5
Loam	0.078	0.43	0.036	1.56	0.0173	0.5
Silt	0.034	0.46	0.016	1.37	0.0042	0.5
Silt loam	0.067	0.45	0.020	1.41	0.0075	0.5
Sandy clay loam	0.100	0.39	0.059	1.48	0.0218	0.5
Clay loam	0.095	0.41	0.019	1.31	0.0043	0.5
Silty clay loam	0.089	0.43	0.010	1.23	0.0012	0.5
Sandy clay	0.100	0.38	0.027	1.23	0.0020	0.5
Silty clay	0.070	0.36	0.005	1.09	0.0003	0.5
Clay	0.068	0.38	0.008	1.09	0.0033	0.5

8.3.2. Inverse Simulation Using HYDRUS

The hydraulic parameters from the database (Table 8. 1) may not be always representative of the soils encountered in the study area. These parameters were estimated by performing the inverse flow simulation of infiltration test. In this study, the model parameters α and n were determined by performing inverse simulation using HYDRUS 2D. By considering measured cumulative infiltration data, the model parameters α and n were estimated using Levenberg-Marquardt parameter estimation technique (Marquardt, 1963) by minimizing the objective function, Φ (Simunek, et al., 1998), which is given by Eq. 8. 5,

$$\phi(\mathrm{b,q,p}) = \sum_{j=1}^{m_q} v_j \sum_{i=1}^{n_{qj}} w_{ij} \left[\breve{g}_j(\mathrm{x,t_i}) - \mathrm{g_j(x,t_i,b)} \right]^2 + \sum_{j=1}^{m_p} \bar{v}_j \sum_{i=1}^{n_{pj}} \bar{w}_{ij} \left[\breve{p}_j(\theta_i) - p_j(\theta_i, b) \right]^2 + \sum_{j=1}^{n_b} \hat{v}_j \left[\breve{b}_j - bj \right]^2 \quad (8.5)$$

where the first term on the right-hand side represents deviations between the measured and calculated space-time variables (e.g., observed pressure heads, water contents, and/or concentrations at different locations and/or time in the flow domain, or the actual or cumulative flux versus time across a boundary of specified type). In this term, m_q is the number of different sets of measurements, n_q is the number of measurements in a particular measurement set, represents specific measurements at time for the j^{th} measurement set at location $\boldsymbol{x}$ (r, z), are the corresponding model predictions for the vector of optimized parameters $\boldsymbol{b}$ (θr , θs , α, n, Ks, ...), and v_j and $w_{i,j}$ are weights associated with a particular measurement set or point respectively. The second term of Eq. 8. 5 represents differences between independently measured and predicted soil hydraulic properties (e.g., retention, $\theta(h_0)$ and/or hydraulic conductivity, $K(\theta)$ or $K(h_0)$ data), while the terms $m_p, n_{pj}, \breve{p}_j(\theta_i), p_j(\theta_i, b), \bar{v}_j$ and $\bar{w}_{ij}$ have similar meanings as for the first term but now for the soil hydraulic properties. The last term of Eq. 8. 5 represents a penalty function for deviations between prior knowledge of the soil hydraulic parameters, and their final estimates, b_j, with n_b being the number of parameters with prior knowledge and representing pre-assigned weights.

The objective function Φ can be expressed for an arbitrary combination of selected variables, q as (Simunek and van Genuchten, 1996),

$$\phi(b,q) = \sum_{j=1}^{M}\left(v_j \sum_{i=1}^{N_j} w_{ij}\left[q_j(t_i) - q_j^*(t_i,b)\right]^2 \right) \qquad (8.\ 6)$$

where, optimised parameter vector $b = \{\alpha, n, Ks\}$, M is the number of sets of measurements, Nj is the number of measurements in an individual set, $q_j(t_i)$ is explicit measurement for the j^{th} measurement set at time t_i, $q_j^*(t_i,b)$ is the conforming prediction for parameter vector b, and v_j and w_{ij} are weights connected with a set of measurements j and a measurement i within set j respectively.

In this study, three parameters were optimized (Ks, n, and α) as part of the inverse simulation. The suggested values for a specific soil type in accordance with the van Genuchten model are given as initial estimate for the unknown parameters α, n and measured values from the field are used as an initial estimate for parameter Ks. The values of other parameters such as θ_s is obtained from the field, θ_r as suggested by van Genuchten model (Simunek and van Genuchten, 1996; AnguloJaramillo, et al., 2016) and l is taken as 0.5 (Simunek and van Genuchten, 1996).

8.4. Numerical Simulation Results

The direct simulation of the infiltration was carried out using HYDRUS 2D for MDI, TI, and DRI for measurements in the field. The magnitude of the transport domain was chosen in such a way that the outer boundaries had no influence on flow simulation within the domain. The boundary conditions adopted for direct simulation and details of the mesh are depicted in Fig. 8.1. A mesh convergence study was performed to ensure that there is no influence of mesh size on the simulation results.

The simulation results of cumulative infiltration were compared with the measured cumulative infiltration for all the 14 locations of the study area and presented in Fig. 8.2 for MDI. It can be noted that for stations S2, S5, S11, S13, and S14, the simulated and measured results matched well. Among them, S2 and S14 have loamy sand, S5 has sandy and S11 and S13 have loamy soils. For both locations having loamy sand, the simulated and measured results are identical whereas for both the locations having silty soils, the simulated results are overestimated. Out of four locations having sandy soils, the simulated results are underestimated in three cases, while for S5, it is matching well. Similarly, out of the six locations having loamy soils, the simulated results are overestimated in the case of S6, S10 and S12, identical for S11 and S13 and underestimated for S9. Such inconsistencies can be attributed to a particular value of the parameters used from the database. Additionally, it can be noted that the seasonal variation has minimal influence on the results.

The comparison of simulated and measured cumulative infiltration obtained from TI is shown in Fig. 8.3. It can be observed from Fig. 8.3 that except S6, there is a significant difference between the measured and simulated results for all the stations. The seasonal influence was also found to be more for comparison of TI measurements. The major difference between MDI and TI is the aerial footprint of measurements. A wider measurement area of TI may influence measurements due to the presence of macro, micro cracks and seasonal influence as compared to MDI. Figure 8. 4 depicts the measured and simulated cumulative infiltration for DRI measurements. It can be observed that the results matched well except for station S1.

From the above Figs. 8.2 to 8.4, it can be concluded that there is variation in the cumulative infiltration from direct simulation and the experimental data from the field tests. These inconsistencies between the numerically simulated and experimental results can be due to the inappropriate soil hydraulic parameters α and n, values based on soil

texture, specifically for disc infiltrometer analysis. The van Genuchten parameters α and n has a substantial impact in defining the shape of the soil hydraulic functions.

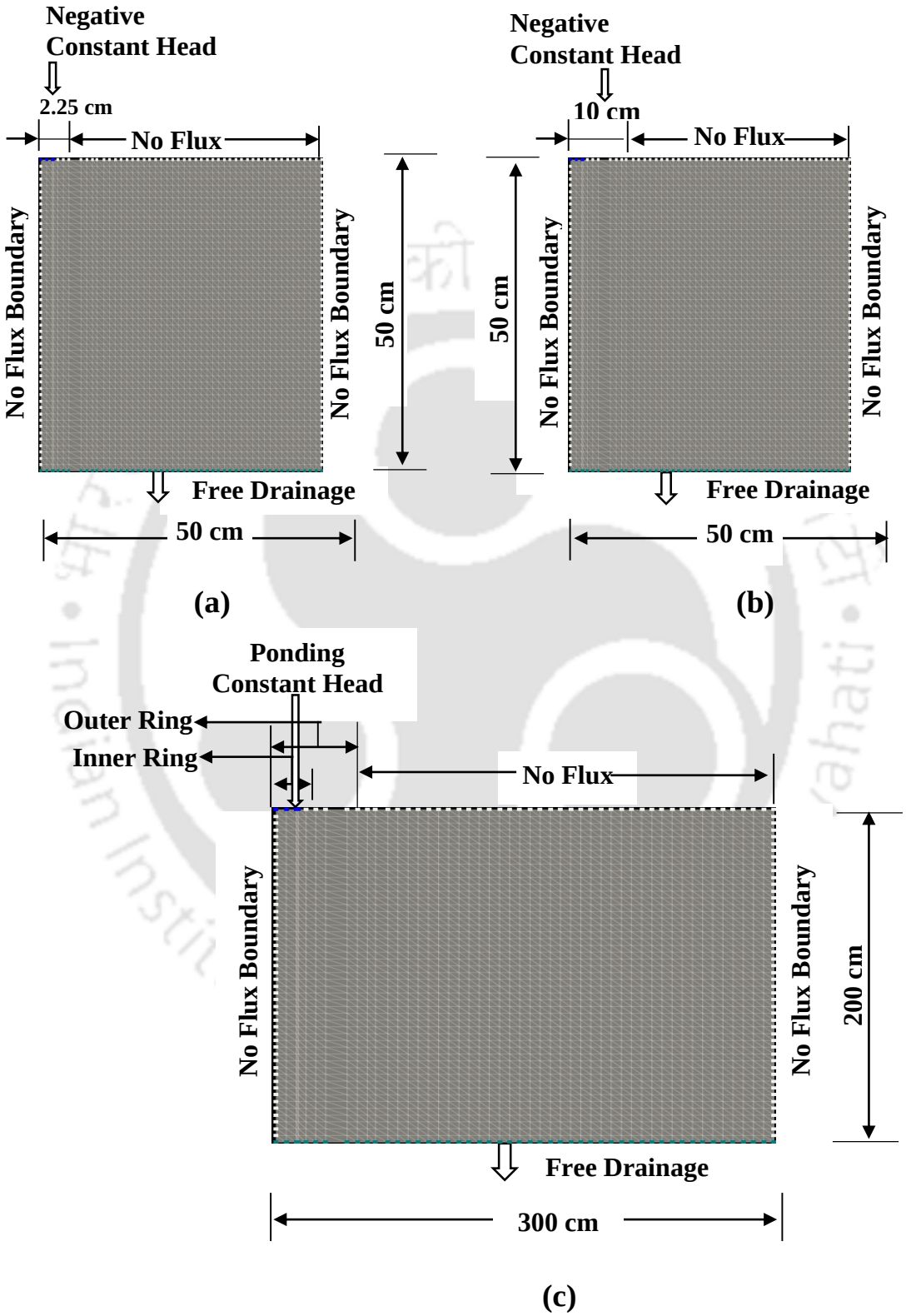

Fig. 8. 1 Axisymmetric HYDRUS simulation domain and boundary conditions for (a)MDI (b) TI and (c) DRI

The direct simulation using the values of the van Genuchten parameters α and n based on the soil texture, underestimated and overestimated results in case of MDI and TI. Hence, for studying the influence of these parameters on the infiltration simulation, an inverse analysis was conducted for MDI to estimate the optimized values of van Genuchten parameters α and n for different types of soils in the study area. The values of the parameters α and n obtained from the inverse simulation are presented in Table 8. 2.

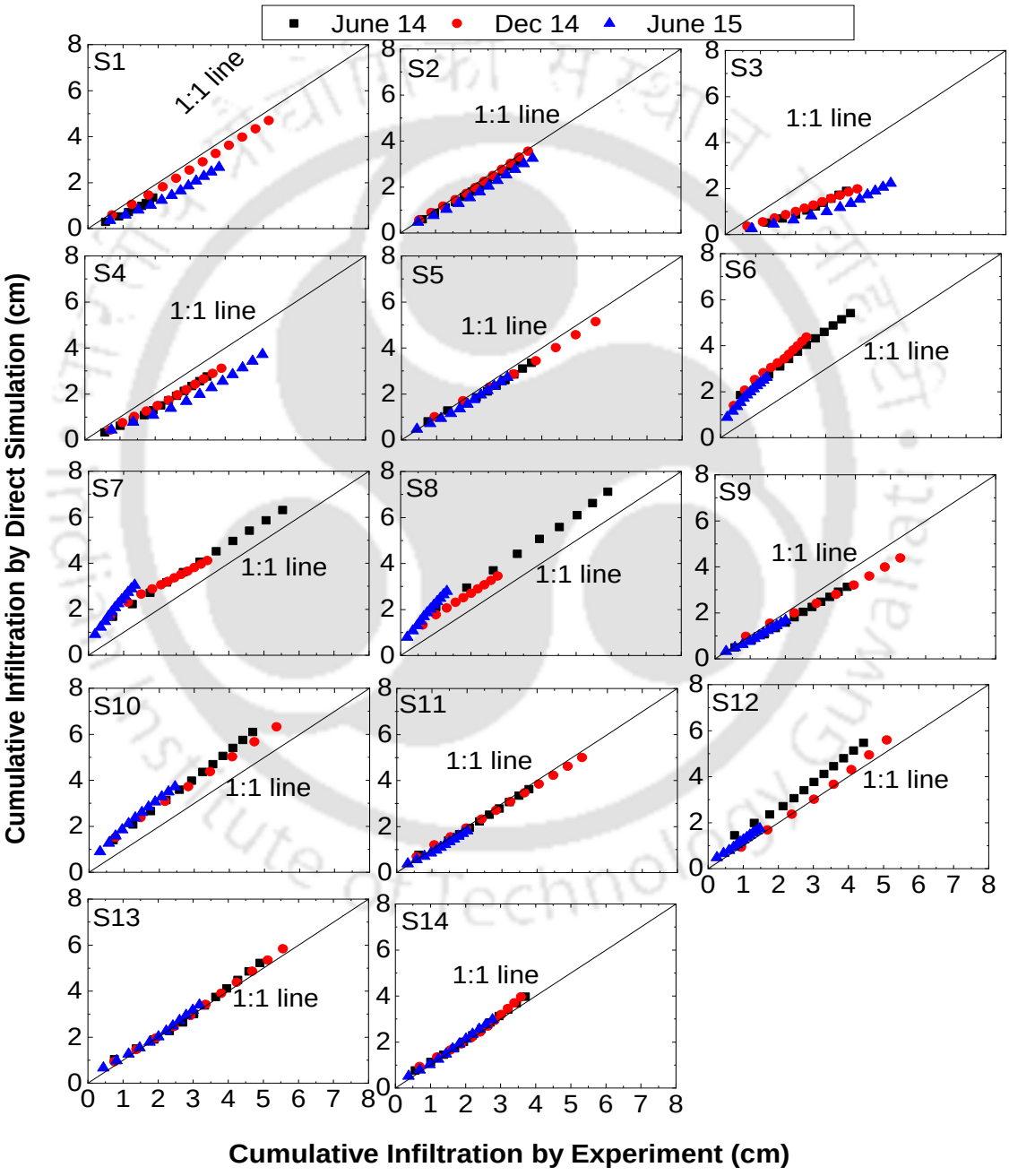

Fig. 8. 2 Comparison of cumulative infiltration obtained from direct simulation and field experiments for MDI

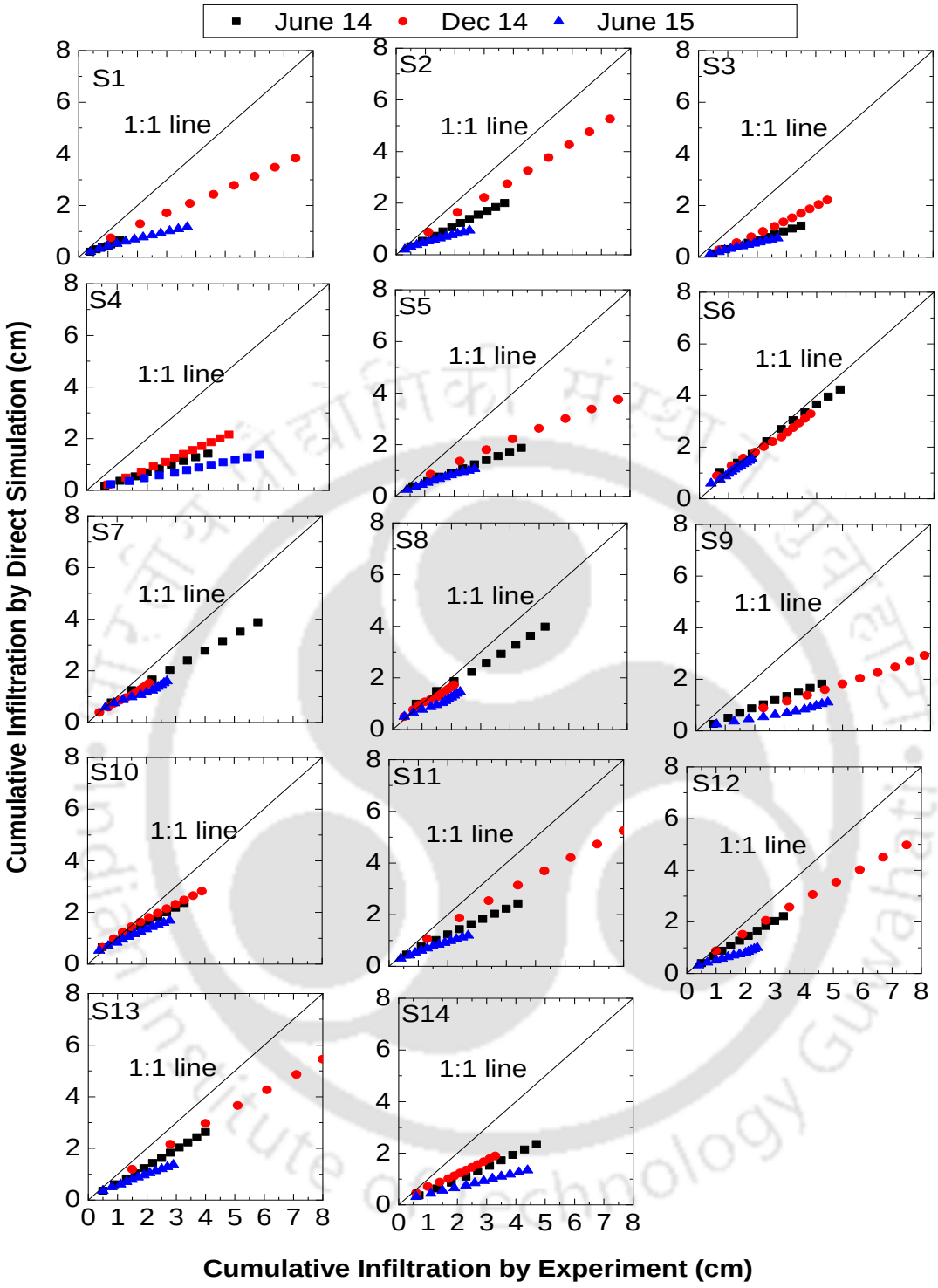

Fig. 8. 3 Comparison of cumulative infiltration obtained from direct simulation and field experiments for TI

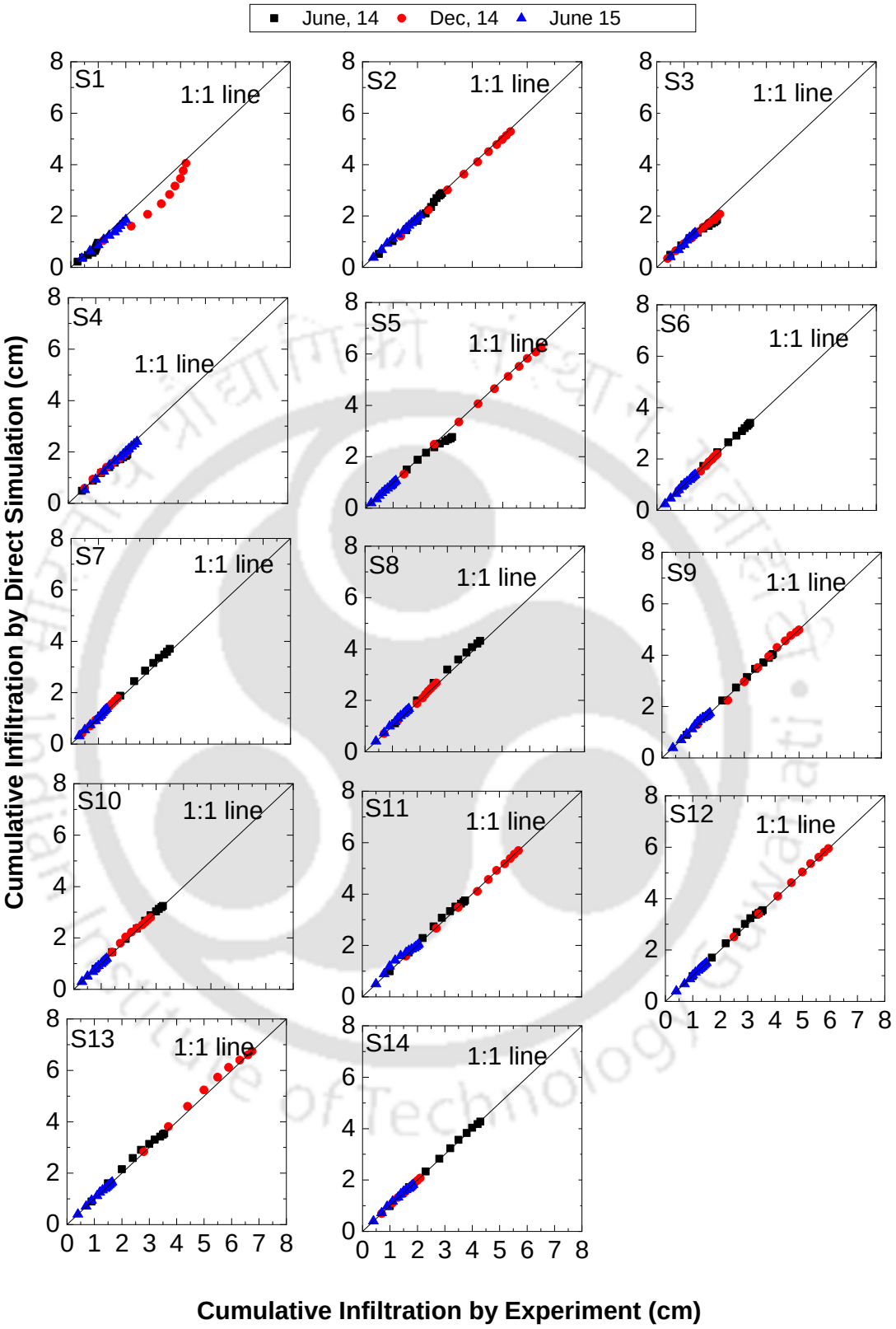

Fig. 8. 4 Comparison of cumulative infiltration obtained from direct simulation and field experiments for DRI

Table 8. 2 Details of the vG parameters based on soil texture and inverse analysis for MDI at suction 0.5 cm

Station	Type of soil	van Genuchten model parameters							
		Carsel and Parrish (1988)		June 15		Dec 14		June 14	
		n_{van}	α_{van}	n_{inv}	α_{inv}	n_{inv}	α_{inv}	n_{inv}	α_{inv}
S1	Sand	2.68	0.145	7.160	0.129	5.263	0.110	6.258	0.127
S2	Loamy Sand	2.28	0.124	3.830	0.220	3.130	0.193	3.760	0.209
S3	Sand	2.68	0.145	3.830	0.220	3.251	0.185	3.772	0.201
S4	Sand	2.68	0.145	4.506	0.181	3.758	0.169	4.167	0.177
S5	Sand	2.68	0.145	2.391	0.114	2.510	0.114	2.385	0.112
S6	Loam	1.56	0.036	2.945	0.002	3.201	0.014	2.547	0.008
S7	Silt	1.37	0.016	1.111	0.002	1.147	0.020	1.100	0.008
S8	silt	1.37	0.016	1.154	0.002	1.214	0.015	1.126	0.007
S9	Loam	1.56	0.036	1.717	0.045	1.589	0.041	1.735	0.048
S10	Loam	1.56	0.036	1.352	0.001	1.514	0.013	1.319	0.007
S11	Loam	1.56	0.036	1.616	0.034	1.656	0.031	1.506	0.039
S12	Loam	1.56	0.036	1.369	0.014	1.488	0.011	1.348	0.021
S13	Loam	1.56	0.036	1.468	0.027	1.589	0.023	1.425	0.032
S14	Loamy Sand	2.28	0.124	2.473	0.129	2.073	0.1	2.324	0.125

The variations of van Genuchten parameters α and n for the four types of soils in the study area with season, different applied tension heads and with different infiltrometers are depicted in Figs. 8.5 to 8.7. Figure 8.5 indicates how the van Genuchten parameters α and n changes seasonally for different soil types. It is evident from the Fig. 8.5 that there is no significant temporal variations of the van Genuchten parameters α and n. Such a verification is important because cumulative infiltration is influenced by seasonal variation. However, such variations are not sensitive to the variation in van Genuchten parameters estimated from infiltration measurements. In Fig. 8.6, it was deliberated how the van Genuchten parameters α and n varies with the soil types for different applied suctions of 0.5 cm and 6 cm. It can be seen that there is no visible difference in the van Genuchten parameters α and n corresponding to different tension heads.

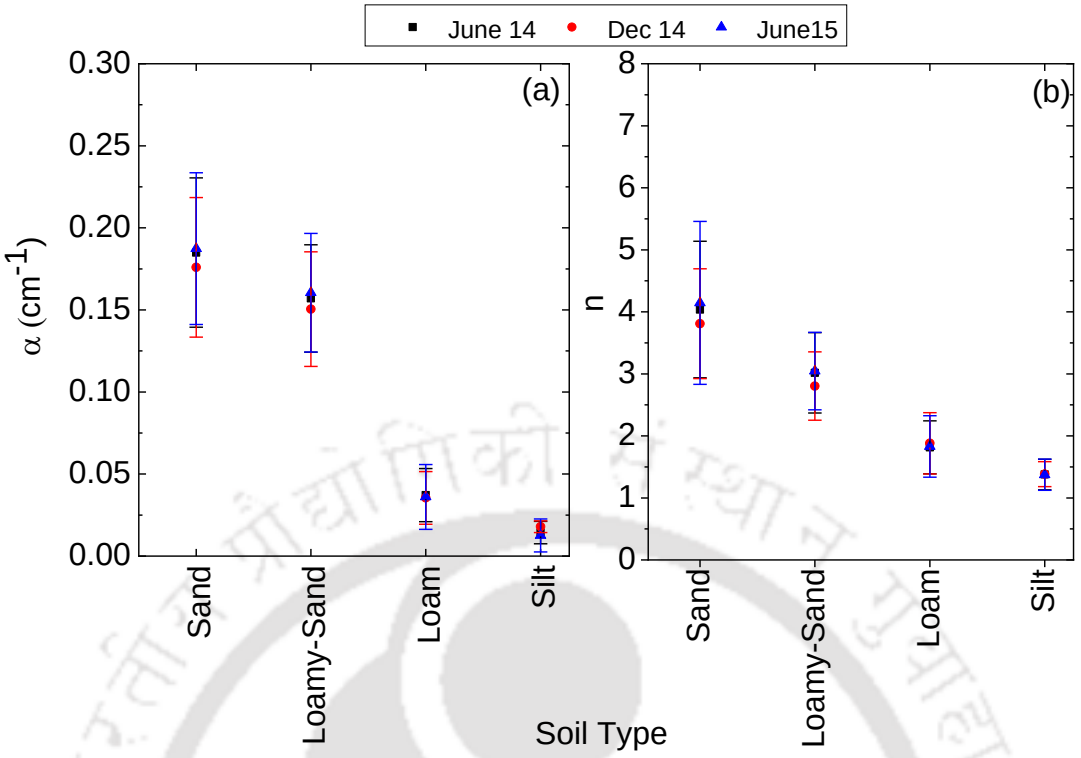

Fig. 8. 5 Seasonal changes in (a) α and (b) n with different seasons for different soils

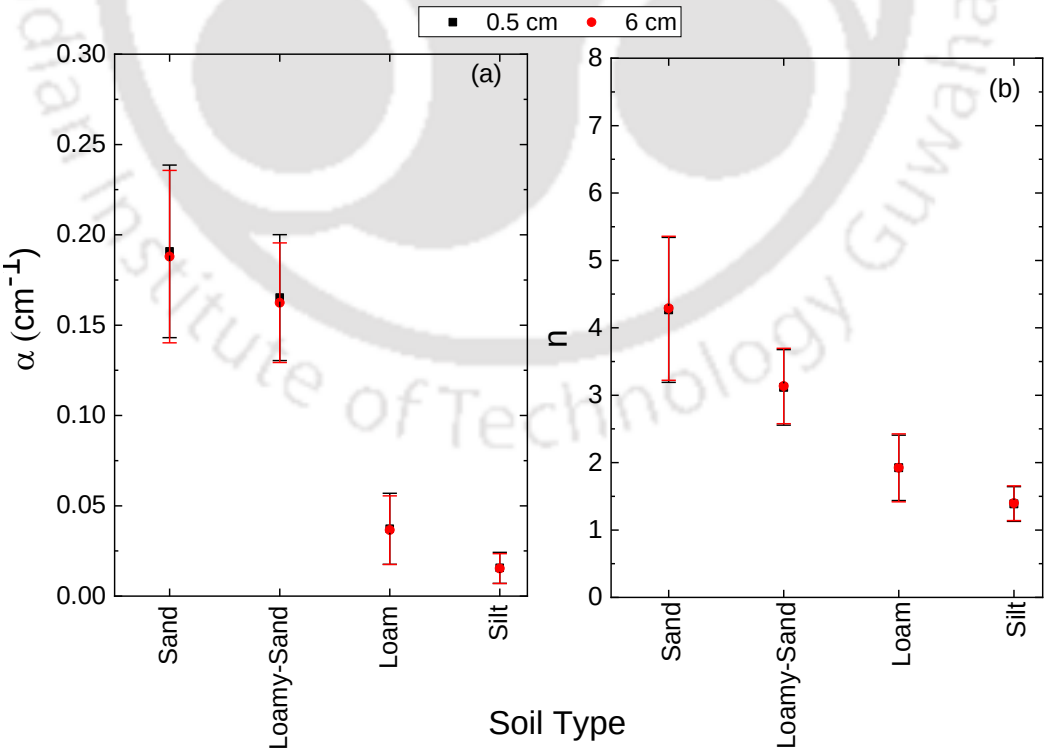

Fig. 8. 6 Changes in (a) α and (b) n with soil types corresponding to suction heads

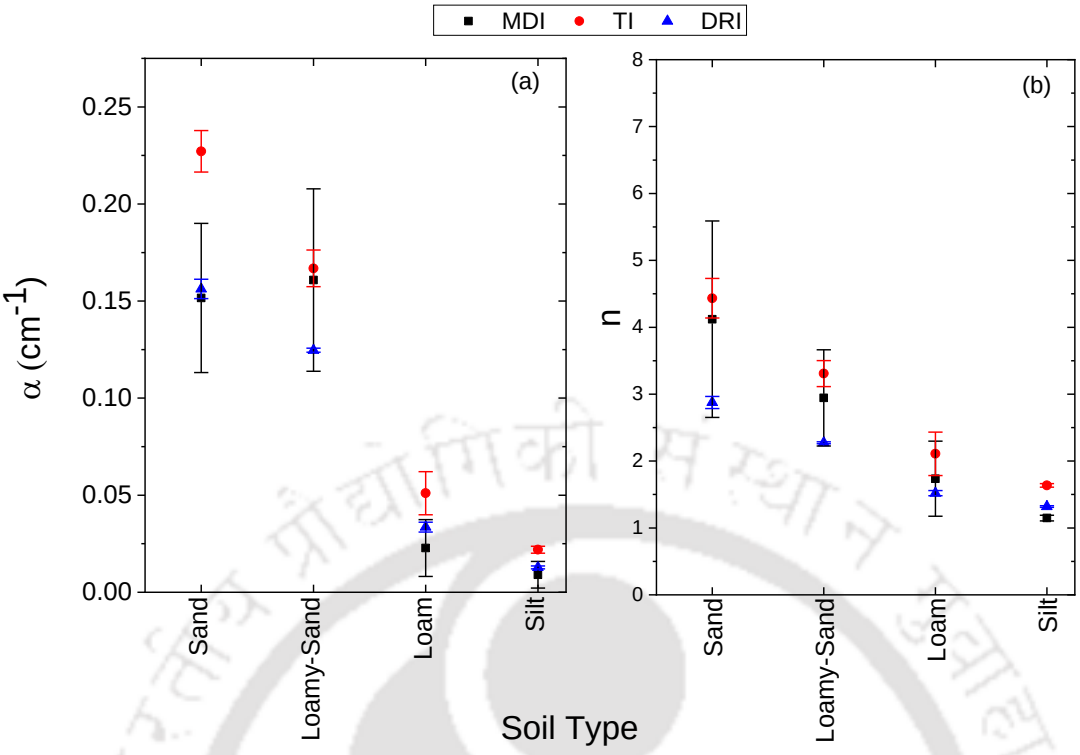

Fig. 8. 7 Variation in (a) α and (b) n for MDI, TI and DRI

Figure 8.7 presented how the van Genuchten parameters *α* and *n* fluctuates with the soil types for the different infiltrometers MDI, TI and DRI. There is difference in van Genuchten parameters estimated from three infiltrometers with TI exhibiting higher values as compared to other infiltrometers. For all the cases (Figs. 8.5 to 8.7), the expected deviation in parameters is significant for sand and minimal for silt texture. The van Genuchten parameters obtained using inverse simulation for different soil textures were found to exhibit variability. Therefore, a range of optimized hydraulic parameters α and n are proposed and the same ate listed in Table 8. 3. It was noted that the values of van Genuchten parameters based on soil texture are within the range of optimized hydraulic parameters determined through inverse simulation. It is also noted that the values of shape parameter *n* exhibit marginal variability with respect to the season as well. This is mainly due to the sensitivity of the cumulative infiltration on soil surface structural changes based on which α and n are optimized.

Table 8. 3 The range of optimized hydraulic parameter α and n obtained using inverse simulation with MDI at suction 0.5 cm

Soil type	Stations	α_{van} (texture)	α_{inv}	n_{van} (texture)	n_{inv}
Sand	1,3,4,5	0.145	0.11-0.22	2.68	2.39-7.16
Loamy Sand	2,14	0.124	0.1-0.22	2.28	2.07-3.83
Loam	6,9,10,11,12,13	0.036	0.001-0.129	1.56	1.35-2.94
Silt	7,8	0.016	0.002-0.02	1.37	1.11-2.94

The hydraulic conductivity ($\log_{10} K_{avg}$) values from the field experiments are listed in Table 8. 4 whereas the values from the numerical modeling are listed in Table 8. 5. A comparison of the results show that for all the infiltrometers the results are matching well. This indicates that van Genuchten parameters α and n do not influence hydraulic conductivity determination infiltrometers.

Table 8. 4 Hydraulic conductivity (mm/h) determined using various infiltrometers

Station No.	$\log_{10}(K_{avg})$								
	June 2014			Dec 2014			June 2015		
	MDI	TI	DRI	MDI	TI	DRI	MDI	TI	DRI
S1	0.168	0.161	0.478	1.153	1.035	1.078	0.748	0.957	0.954
S2	0.686	0.478	0.778	1.145	1.033	1.256	0.837	0.918	1.079
S3	0.632	0.477	0.781	0.810	0.672	1.079	0.659	0.983	1.079
S4	0.673	0.605	0.778	0.737	0.668	1.079	0.881	1.047	1.079
S5	0.667	0.605	0.776	1.266	1.145	1.381	0.664	0.947	0.954
S6	0.584	0.677	0.778	0.441	0.494	0.778	0.140	0.648	0.477
S7	0.813	0.825	1.078	0.194	0.198	1.077	0.079	0.576	0.301
S8	0.793	0.722	1.079	0.252	0.198	1.077	0.079	0.617	0.301
S9	0.591	0.605	0.778	0.981	0.891	1.080	0.258	0.898	0.477
S10	0.658	0.477	0.776	1.139	0.668	1.080	0.518	0.903	0.778
S11	0.641	0.605	0.781	0.975	1.100	1.257	0.258	0.860	0.778
S12	0.574	0.520	0.778	1.070	1.100	1.255	0.080	0.913	0.778
S13	0.658	0.477	0.778	1.052	1.139	1.256	0.576	0.836	0.477
S14	0.801	0.659	1.081	0.502	0.670	1.0805	0.730	0.903	0.954

Table 8. 5 Hydraulic conductivity (mm/h) estimated using inverse analysis

Station No.	$\log_{10}(K_{avg})$								
	June 2014			Dec 2014			June 2015		
	MDI	TI	DRI	MDI	TI	DRI	MDI	TI	DRI
S1	0.163	0.153	0.475	1.151	1.01	1.08	0.741	0.95	0.951
S2	0.682	0.471	0.780	1.144	1.01	1.26	0.829	0.91	1.077
S3	0.611	0.471	0.780	0.78	0.671	1.08	0.65	0.98	1.077
S4	0.662	0.6	0.780	0.724	0.671	1.08	0.872	1.01	1.077
S5	0.66	0.6	0.780	1.261	1.11	1.38	0.662	0.94	0.951
S6	0.597	0.671	0.780	0.463	0.49	0.78	0.15	0.642	0.475
S7	0.828	0.819	1.08	0.209	0.195	1.08	0.9	0.57	0.300
S8	0.806	0.716	1.08	0.262	0.195	1.08	0.9	0.613	0.300
S9	0.587	0.6	0.780	0.977	0.89	1.08	0.253	0.893	0.475
S10	0.665	0.471	0.780	1.148	0.671	1.08	0.53	0.9	0.780
S11	0.641	0.6	0.780	0.975	1.07	1.26	0.253	0.85	0.780
S12	0.579	0.5	0.780	1.069	1.07	1.26	0.08	0.91	0.780
S13	0.661	0.471	0.780	1.054	1.11	1.26	0.577	0.83	0.475
S14	0.802	0.653	1.08	0.503	0.671	1.08	0.731	0.9	0.951

The optimized parameters from inverse simulation are found to vary within a range for different soil types. For the same soil type, the variability of α and n estimated from the inverse analysis was found to be significant as against a particular value based on texture. This indicates the necessity to perform actual measurements at the site, wherever possible, as against using the hydraulic parameters based on texture. For understanding the influence of this, there is a need to carry out controlled experiments in the laboratory for understanding the influence of soil hydraulic parameters as discussed in the following sections.

8.5. Controlled Experimental Simulation of Flow Process Beneath MDI

Controlled experiments in the laboratory were performed for the four homogeneous soils, sand, clay loam (red soil), silt and loam using MDI. van Genuchten–Mualem model soil hydraulic properties were estimated using inverse simulation in Hydrus 2D. The details of the experimental set up used in the study are discussed below.

8.5.1. Experimental Setup

For performing the controlled experiments using MDI, a PVC cylindrical mould with a diameter of 30 cm and height equal to 50 cm was used. A rammer of 1.7 kg was

used to impart the necessary compaction to the soil sample. The particular soil sample was air dried and the required mass was compacted in three layers with equal number of blows using the rammer. The bulk density of the soil was determined from the weight of the soil filled in the cylinder. The infiltration experiments were conducted using MDI corresponding to suction of 0.5 cm on all the four soil samples. The measured results were used to plot cumulative infiltration versus square root of time response, based on which infiltration parameters C_1 and C_2 were computed.

8.5.2. Different Sensors Used

The moisture content and the soil suction was measured with time at different depths using sensors such as 5TM ECH2O moisture sensors and T5 miniature tensiometers respectively as shown in Fig. 8.8. Five moisture sensors were used in the experiment along with three tensiometers. Among the five moisture sensors, three were placed at the top (15 cm), middle (25 cm) and bottom (35 cm) from soil surface on one side of the PVC mould. Other two were placed both sides of the MDI horizontally, and three tensiometers were placed at the top (15 cm), middle (25 cm) and bottom (35 cm) from soil surface on the diametrically opposite side of the PVC mould. The T5 tensiometer can measure suction less than 100 kPa, which is adequate for sand, the same may not hold good for other soils of fine texture (Stannard, 1994; Samjstrla and Harrison, 1998; Malaya and Sreedeep, 2016). Therefore, the relationship between suction and water content obtained from WP4 suction measurements were used to extrapolate suction greater than 100kPa. There is an assumption here that the soil exhibits negligible hysteresis. This is mainly because MDI experiments are wetting phenomenon while WP4 measurements corresponds to drying. From the measurements, the variation of soil suction with the time was obtained for a given cumulative infiltration beneath MDI.

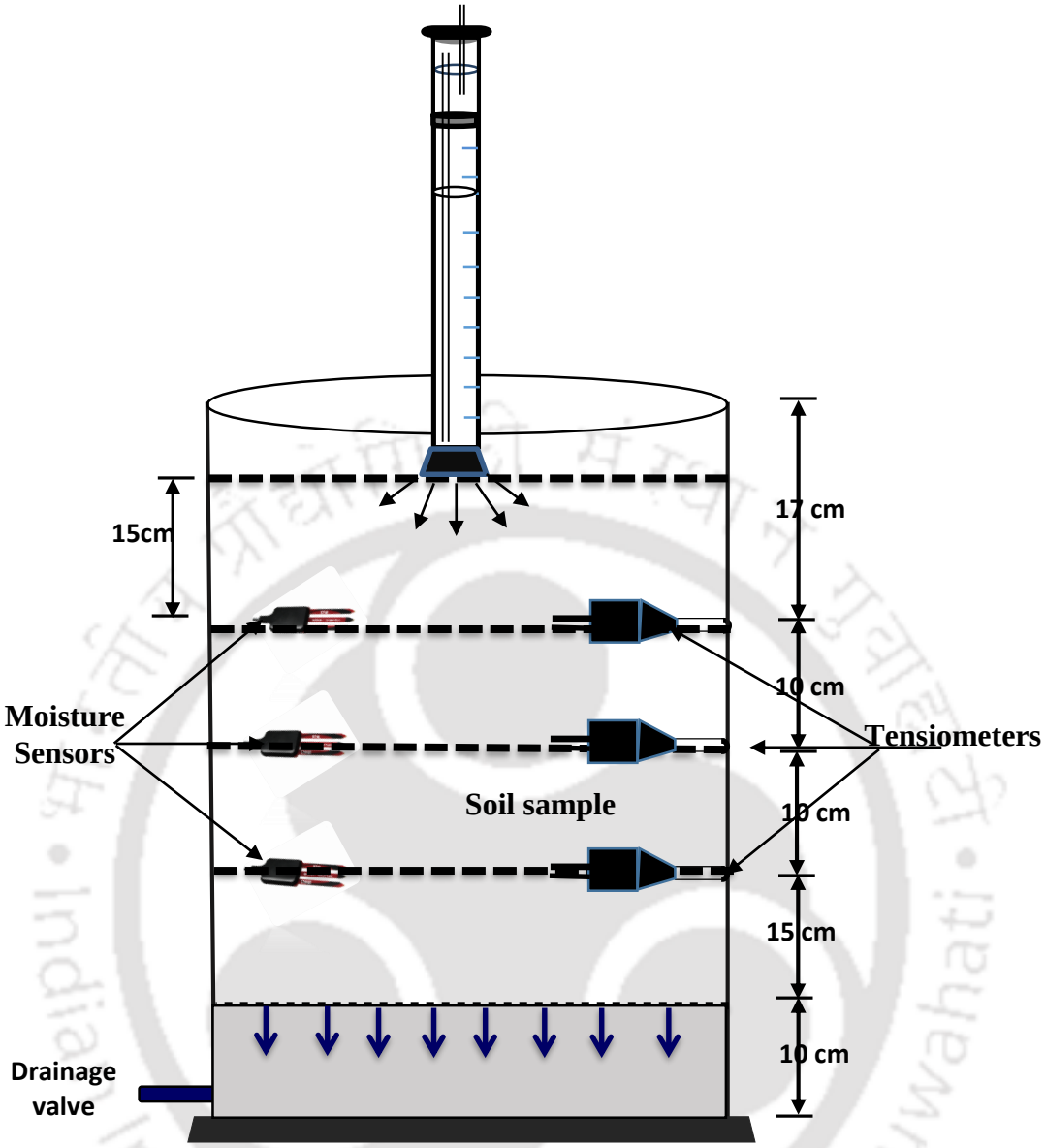

Fig. 8. 8 Setup for controlled laboratory column study

8.5.2.1. Calibration of ECH2O moisture sensors

The volumetric water content of the soil was measured using 5TM sensors, and it is based on the dielectric constant of the soil. Different soils have different electrical properties. There are variations in the output of the ECH2O sensors due to soil bulk density, mineralogy, texture and salinity of that particular soil. Therefore, soil- specific calibration for 5TM ECH2O sensors was performed to ensure accuracy in volumetric water content measurements. For calibration, a PVC cylindrical mould with a diameter of 20 cm and height equal to 20 cm was used, as depicted in Fig. 8.9.

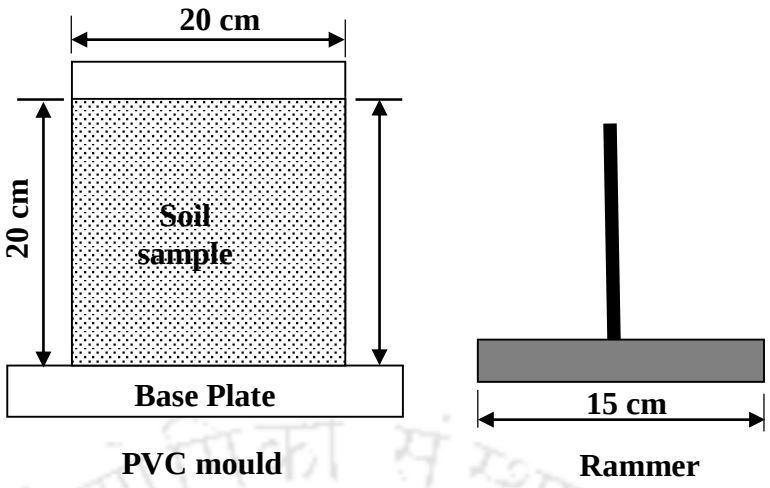

Fig. 8. 9 Details of the mould used for laboratory infiltration experiments

Different dry densities and target water contents (air dried, 5%, 10%, 15%, and 20 %) were used for calibration of sand. Similarly, to conduct the calibration of red soil, silt and loam sample, three different dry densities (γ_1, γ_2, γ_3) and different targeted water contents (air dried, 10%, 20%, 30%, and 40 %) were used. The soil sample was packed in a PVC mould in three layers with an equal number of blows using the rammer. The weight of the soil, which was filled in the cylinder was noted, and the bulk density was determined. Sample with same water content has been compacted to three different dry densities (γ_1, γ_2, γ_3) with the number of blows equal to 5, 10 and 20 blows.

The dry density of compacted samples was computed using the known values of the water content and bulk density. A scatter plot was prepared with the output of the sensors on the x-axis and computed volumetric water content on the y-axis which was used to develop a mathematical calibration relationship. The computed water content (θ_{comp})is the true reference value, which is obtained from the known mass-volume relationship as given by Eq. 8. 7.

$$\theta_{comp} = \frac{w\gamma}{\gamma_w} \qquad (8.\ 7)$$

where w is the moisture content; γ is the dry density of soil and γ_w is the unit weight of water

The new calibration curves for sand, red soil, silt and loam are depicted in Fig. 8. 10. In Fig 8. 10, the raw data is the output from the sensor. A second order polynomial

was fitted to evolve a calibration equation for calculating θ from the known values of raw data. The computed and observed moisture content is depicted in Fig. 8. 11.

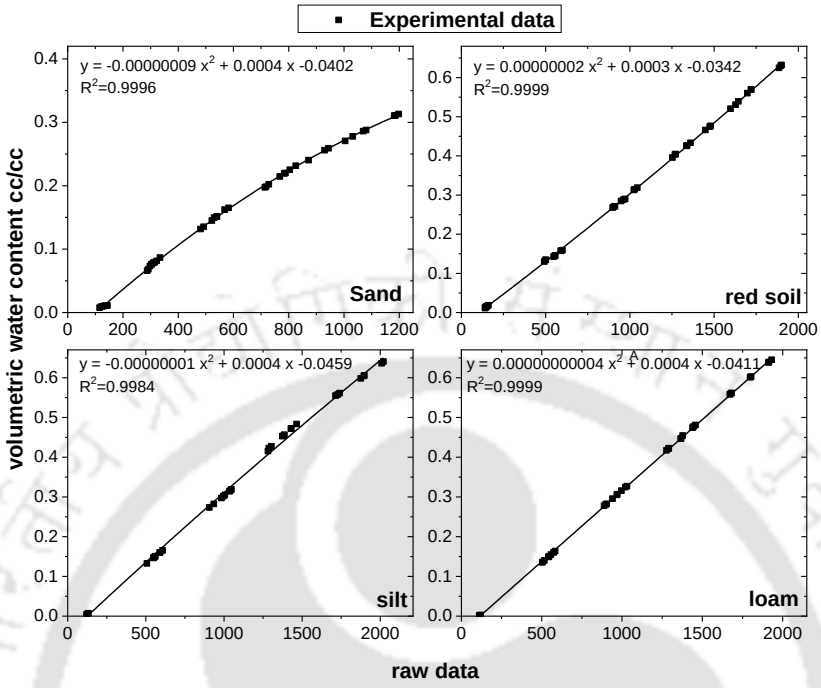

Fig. 8. 10 Calibration curve of ECH2O moisture sensors

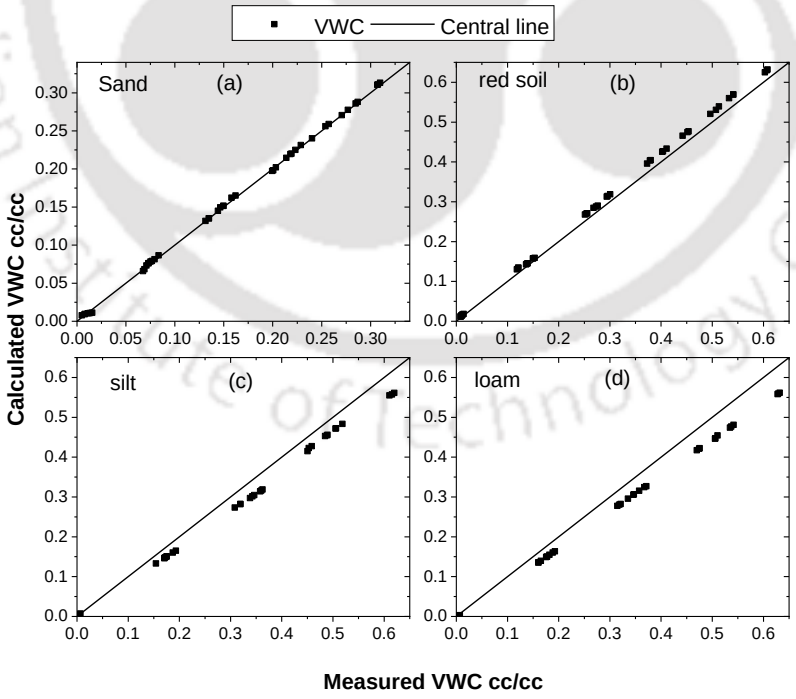

Fig. 8. 11 Comparison of measured and the calculated volumetric water content (a) Sand (b)Red soil (c) Silt and (d) Loam

8.5.2.2. Tensiometer

A miniature tensiometer is used in laboratory experiments to determine the soil suction (Tarantino and Tombolato, 2005; Malaya and Sreedeep, 2016). As the moisture content of the soil changes, the suction also changes (Lu and Likos, 2004). The variation of soil suction with the moisture content is defined as the soil water characteristic curve (SWCC) of that particular soil. In very dry soil, suction dominates, and the gravity term becomes negligible (El-Ehwany, 1990).

8.5.2.3. WP4 Dew point Potentiameter

The dew point potentialmeter (WP4) is used to determine SWCC for suction>100 kPa. It may be noted that the WP4 measurements are more precise for suction greater than 1000kPa (Petry and Jiang, 2007). The detailed methodology adopted in dew point potentiometer is discussed in ASTM 6836. For red soil, silt and loam soils, soil suction above 100 kPa were obtained indirectly from SWCC established using WP4 and observed water content during experiments.

8.5.3. Discussion on Controlled Experimental Results

The variation of the soil suction with time at different layersduring MDI infiltration are depicted in Fig. 8. 12. Both fine-grained and coarse-grained soils were affected by soil suction, but the particle size of the soil controls the magnitude of suction. Smaller particles such as silt, generated a higher suction than that generated by larger sand particles. It was also quite evident from all the soils that the decrease in soil suction was more drastic initially, which was more prominent for the fine grained soils such as red soil, silt, and loam.

The volumetric moisture content responses were recorded, and the same is depicted in Fig. 8. 13. Initially, as the soil was very dry, moisture content was close to zero. With increase in time, the degree of saturation of the soil increased from the top to bottom of the mould as the wetting front moved down. In due course of time, when soil approach near saturation the moisture content attained close to the porosity value of that particular soil at that particular dry density. As expected, coarse-grained soils like sand drained faster than the fine grained soils due to which moisture content increased rapidly for sand. Similar to the observations in Fig. 8.12, the increase in moisture content was more drastic initially, and it was more prominent for the coarse grained soils. It was noted that the

sensors at the same depth exhibited constant measurements, which ensures the repeatability of the observation.

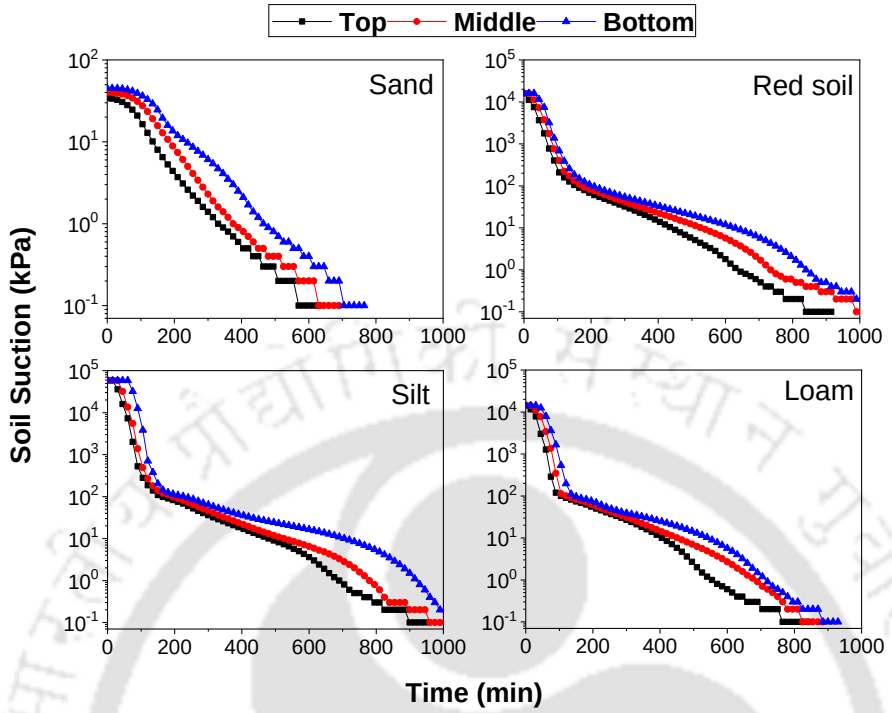

Fig. 8. 12 Variation of soil suction with time at different levels of the soil column (a) Top (b) Middle (c) Bottom

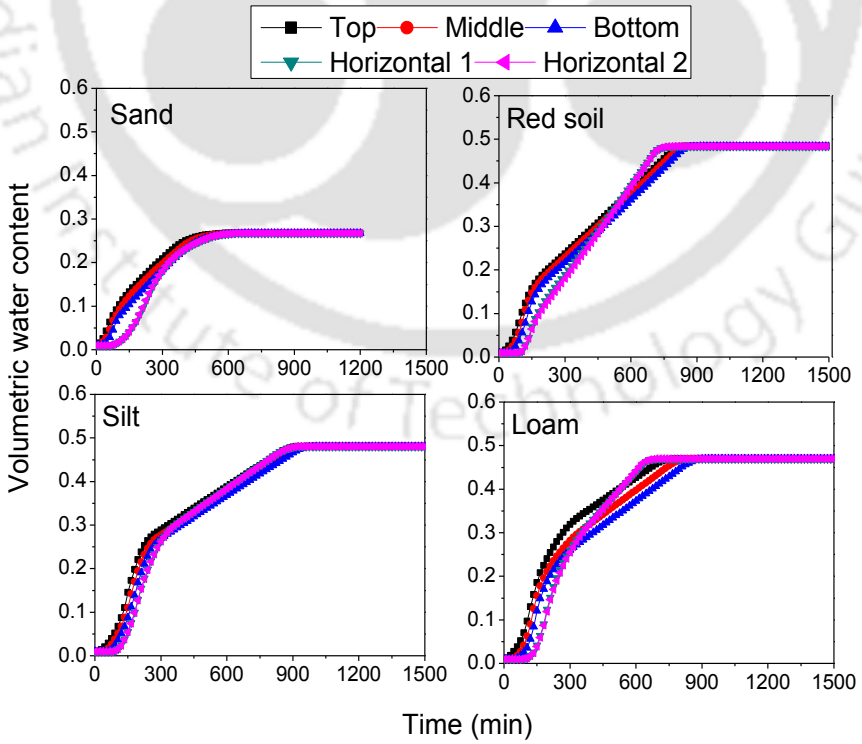

Fig. 8. 13 Variation of volumetric water content with time from the five moisture sensors

Experiments were conducted with a zero-flux boundary condition at the sides and free drainage conditions at the bottom of the soil column. The cumulative infiltration data was obtained using MDI corresponding to a tension of 0.5 cm for sand, red soil, silt and loam soils. Experiments were repeated thrice for all the soils. Initially, the amount of drained water was less and gradually increased. When the soil approached near saturation, the amount of drained water became reasonably constant.

Volumetric water content responses from the five moisture sensors were recorded. Also, from the three tensiometers and WP4 results, soil suction responses were obtained. The SWCC was obtained based on MDI wetting front by plotting suction with volumetric water content for same time duration as depicted in Fig. 8. 14.

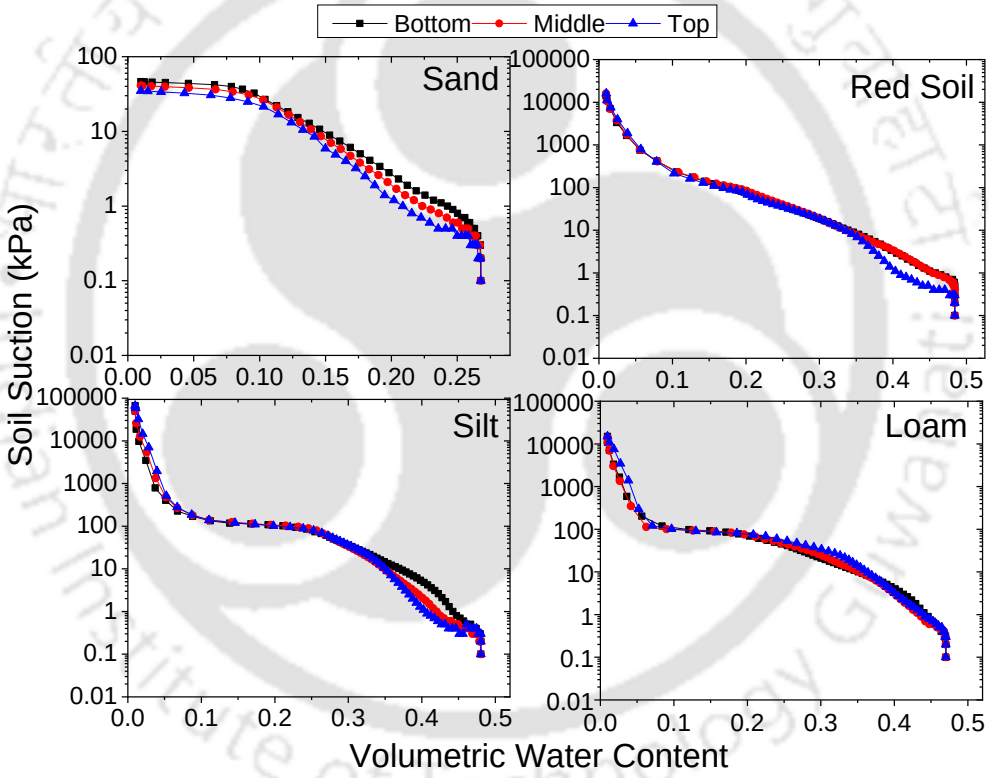

Fig. 8. 14 SWCC obtained from sensor measurements during Infiltration

Figure 8. 14 shows the SWCC for four types of soils which was used to predict the soil water storage and field capacity. As the sand include primarily capillary binding, it released maximum water at higher potentials, whereas red soil, loam, and silt with adhesive binding, released water at lower potentials. Near saturated hydraulic

conductivities for each of the measurements at tension 0.5 cm was evaluated and is listed in Table 8. 6.

Table 8. 6 Hydraulic conductivity values (mm/h) for various types of soils

Soil Type	Hydraulic conductivity values (mm/h)		
	Trial 1	Trial 2	Trial 3
Sand	20.1	18.8	20.9
Red soil	4.7	4.7	4.9
Silt	3.6	3.8	3.2
Loam	4.7	4.4	4.9

8.6. Numerical Simulation Results Using Hydrus 2D

Numerical simulation of flow below MDI was carried out using HYDRUS 2D for the controlled laboratory experiments. During the simulation, the transport domain was chosen in such a way that the outer boundaries did not disturb the flow field located within the domain. The selected transport domain was then discretized as a finite element mesh. The domain adjacent to the disc had smaller mesh sizes compared to domain away from it and is shown in Fig. 8. 1(a).

The infiltration test was conducted with the set up depicted in Fig. 8. 8 and a sequence of MDI measurements was obtained for tension corresponding to 0.5 cm for all the four types of soils viz. sand, red soil, loam and silt. The infiltration tests were repeated three times corresponding to each of the 4 types of soils. The first repetition of cumulative infiltration results for tension of 0.5 cm obtained from MDI are depicted in Fig. 8. 15. These plots compare the direct simulation results obtained by using values of hydraulic parameters from van Genuchten model with the experimental cumulative infiltrations. From the Fig. 8. 15, it is evident that in case of sand and loamy soil, it is marginally underestimated whereas for the red soil and silt, not much variation is observed.

The cumulative infiltration response of MDI was used to estimate the van Genuchten hydraulic parameters by inverse analysis. These estimated values were used to determine SWCC. The SWCC, so obtained was compared with the measured SWCC obtained from sensors (Section 8.6) as depicted in Fig. 8. 16. It can be noted that except for sand there is a reasonable match between simulated and measured SWCC. For more clarity the comparison of simulated and observed soil suction and volumetric water content are carried out and the same are plotted in Fig. 8. 17 and 8. 18. It can be observed from these figures that there is a difference between the simulated and the observed values in

the case of sand and in all the other cases not much variation is observed. It may be attributed to the values used in for the soil hydraulic properties based on the Carsel and Parrish (1988).

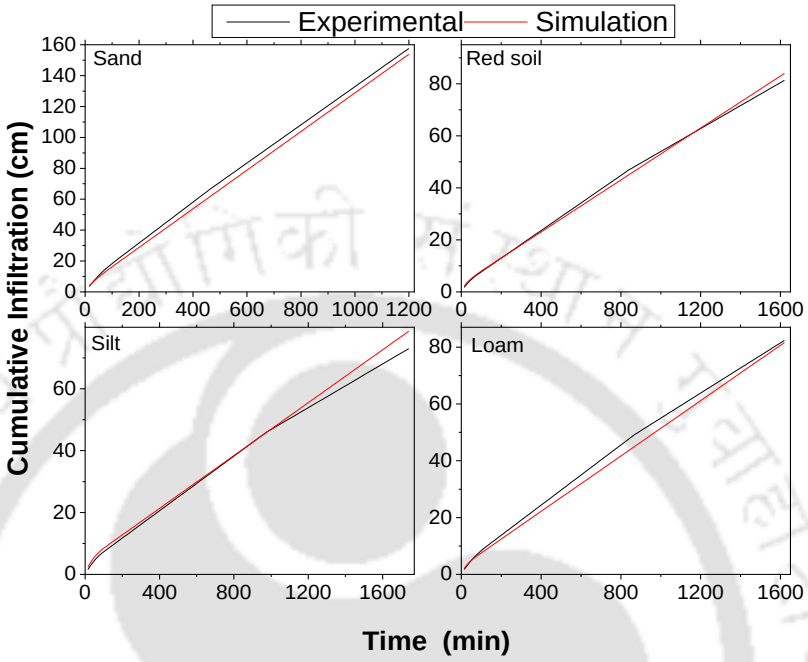

Fig. 8. 15 Cumulative infiltration curve using MDI with 0.5 cm tension

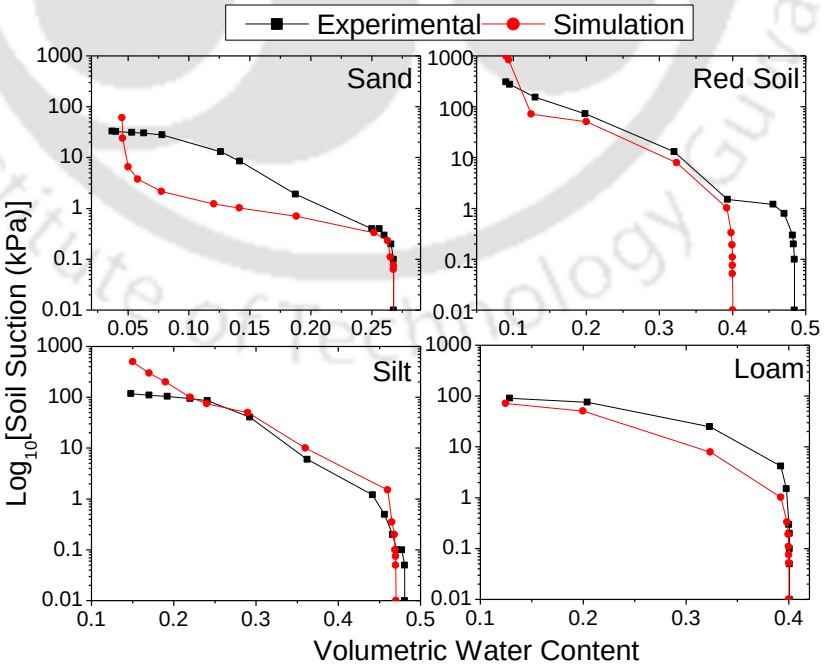

Fig. 8. 16 Comparison of numerical and experimental soil suction (kPa) versus volumetric water content response

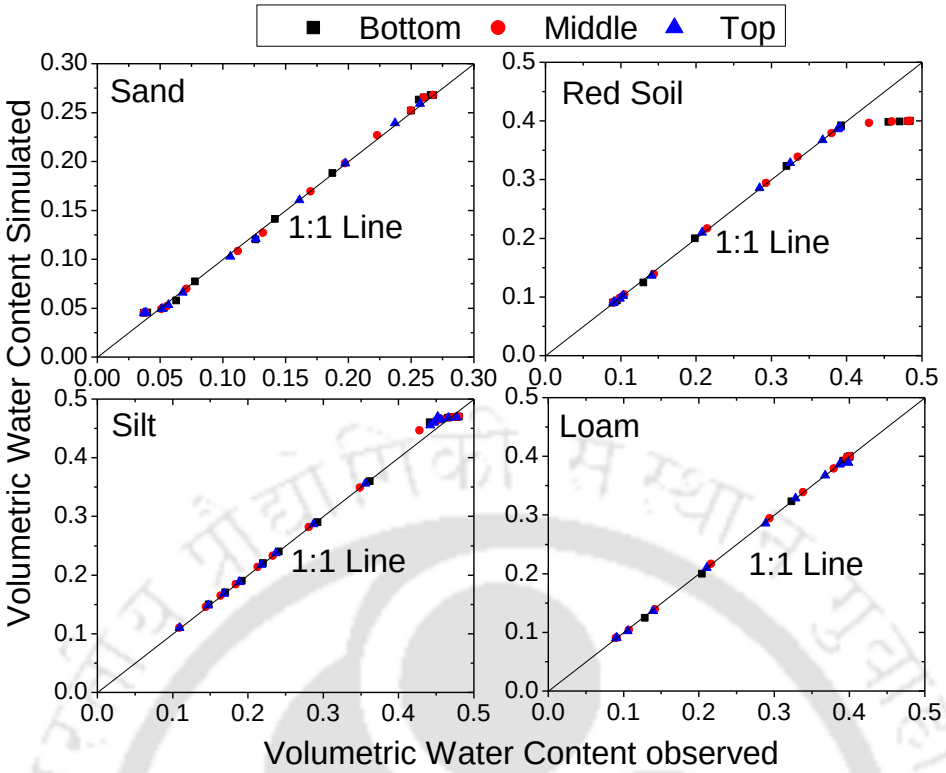

Fig. 8. 17 Comparison of observed and simulated volumetric water contents

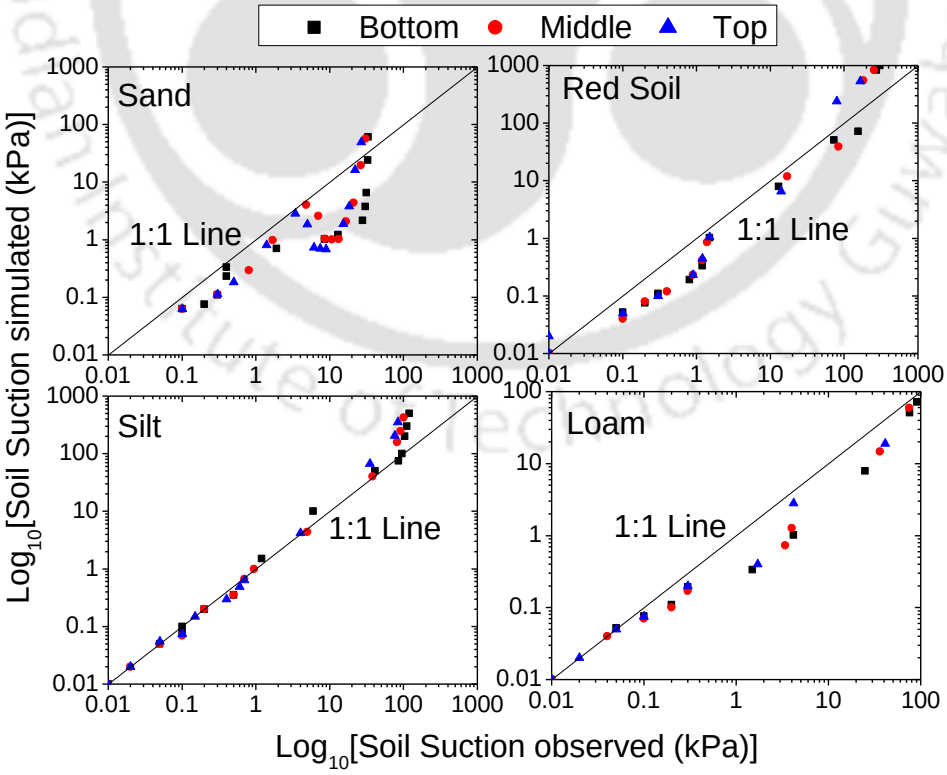

Fig. 8. 18 Comparison of observed and simulated soil suction (kPa)

8.7. Summary

This chapter deals with the comparison of measured and simulated infiltration in the field and under controlled laboratory conditions. From the field study, it was noted that the van Genuchten hydraulic parameters exhibited a wide range as against the value based on soil texture. It was noted that van Genuchten hydraulic parameter values were within the range obtained from the inverse analysis for soil types considered in this study. The observation from laboratory MDI measurements shows that SWCC estimated from MDI measurements compares reasonably well with the measured SWCC at different depth of the column experiment for all soils considered in this study, except sand texture. This endorses the validity of hydraulic parameters obtained from MDI, which was not studied using controlled experiments previously.

Chapter 9

Conclusions and Future Scope of Work

9.1. General

This chapter enlists the important conclusions derived from this study followed by major contributions. The last part of this chapter discusses the future scope of work.

9.2. Conclusions

1. A comparative analysis of two tension disc infiltrometers (Tension infiltrometer (TI) and mini disc infiltrometer (MDI)) and conventional double ring infiltrometer (DRI) was performed in the field for two different seasons. For the same soil type and initial state, the measured infiltration rate response was entirely different for disc infiltrometers and DRI.
2. This study proposed a normalized procedure and asymptotic curve for representing infiltration rate measured using different infiltrometers. The proposed normalization would alleviate instrument related variabilities while comparing infiltration measurements performed using different infiltrometers under various conditions.
3. The mean hydraulic conductivity values from both MDI and TI was found to be approximately half to two-thirds of DRI values. This observation is consistent with the Philip parameter A (Philip, 1957), which was reported to be close to 0.30 reported in the literature (Sharma, et al., 1980; Christianson, et al., 2016) and 0.67 as reported in Youngs (1968).
4. The initial water content at the measurement stations exhibited a negative correlation with hydraulic conductivity determined from infiltrometer. The particle size fraction was found to have statistically insignificant correlation with hydraulic conductivity.
5. The near saturated near surface hydraulic conductivity (K_{h_0}) exhibited a positive correlation with all the infiltration characteristics. The K_{h_0} was observed to be 0.089, 0.173 and 0.125 times initial infiltration rate (i_i), final infiltration rate (i_f) and range of infiltration rate ($i_i - i_f$), respectively.
6. This study further quantified the statistical difference of hydraulic conductivity determined from infiltrometers and permeameters by using Bland-Altman plot. There

is a systematic difference between permeameters and infiltrometers as shown by the increasing trend. Both the disc infiltrometers exhibited negative bias with the permeameters with very few data points close to zero difference.

7. The efficacy of five interpolation methods (Kriging, Inverse Distance Weighted, Natural Neighbour, Spline and Trend) for estimating the spatial variability of near surface saturated hydraulic conductivity, K_s was evaluated. It was noted that the Spline method gave a better spatial prediction as compared to other methods. The prediction of K_s was found to be more precise for those stations with a higher percentage of sand. A sudden transition of soil type from sand to silt was found to influence the accuracy of spatial prediction.
8. A critical evaluation of nine mathematical equations used for determining near surface saturated hydraulic conductivity (K_s) from mini disc infiltrometer (MDI) measurements corresponding to different field conditions were performed. It was established that K_s determined by Wooding-Gardner, Weir's Refinement, van Genuchten-Zhang, Ankeny and Haverkamp equations compared well with the measured values in the field.
9. The influence of short-term and long-term MDI measurements on hydraulic conductivity determination was explored. Zhang's method of analysis using short-term and long-term measured data gave identical results for K_{h_0} < 8 mm/h and marginal variation for K_{h_0} > 8 mm/h for the type of soils in the study area.
10. This study demonstrated the estimation of final infiltration rate (i_f) from short-term data using a rectangular hyperbolic method. A distinct factor R1 was determined for estimating K_{h_0} based on i_f obtained from hyperbolic method for i_f > 30 mm/h.
11. This study investigated the possible relationship and sensitivity of initial compaction condition of soil on K_{h_0} determined by MDI. The Zhang's method marginally underestimates K_{h_0} (within 10 %) as compared to Haverkamp's method for higher K_{h_0} values, which was attributed to the effect of sorptivity.
12. A simple multiple-linear regression (MLR) equation was formulated with and without considering boundary negative pressure head (h_0) for both Zhang's and Haverkamp's approach to investigate the relationship between K_{h_0} and initial compaction state (γ and w) for cohesionless and cohesive soil. The quantitative values of sensitivity index

clearly indicate that the initial dry density (γ) has significant influence on K_{h_0} determination for all the cases considered in this study. The sensitivity of w and h_0 was much less than γ and comparable.

13. Unlike linear regression model, the sensitivity analyses (Garson's algorithm) based on non-linear ANN model indicated that K_{h_0} determined from MDI is more sensitive to initial water content followed by dry density. The ANN model incorporated the effect of soil type as well.
14. The study performed controlled laboratory studies with sensor measurements for investigating the flow beneath MDI. The volumetric water content determined from MDI measurements were found to compare with the measured values. This endorses the validity of hydraulic parameters obtained from MDI which was not studied using the using controlled experiments.
15. From the field study, it was noted that the van Genuchten hydraulic parameters exhibited a wide range as against the value based on soil texture. It was noted that van Genuchten hydraulic parameter values based on texture were within the range obtained from the inverse analysis for soil types considered in this study.

9.3. Major Contributions from This Study

1. Extensive comparison among different infiltrometers and permeameters for hydraulic characterization in the field. Based on this, a normalized infiltration rate equation was proposed for minimizing the instrument related bias.
2. Evaluation of equation for determining hydraulic conductivity using MDI.
3. Evaluation of equation for spatial prediction of hydraulic conductivity determined using MDI.
4. Investigated the effect of short-term and long-term MDI measurements on hydraulic conductivity determination.
5. Proposed rectangular hyperbolic method for estimating final infiltration rate from short-term measurements. A soil-specific empirical relation was developed for determining near saturated hydraulic conductivity from final infiltration rate.
6. A multi-linear regression and ANN model was developed through controlled laboratory measurements for studying the relationship and sensitivity of near saturated hydraulic conductivity on initial compaction state.
7. Controlled and instrumented laboratory study for investigating the flow beneath MDI.

9.4. Future Scope of This Study

1. Further studies are needed to evolve a procedure for determining hydraulic conductivity from the normalized infiltration rate curve proposed in this study.
2. Extensive infiltration studies are needed with different types of soil and initial conditions to propose a generalized equation (similar to the one proposed in this study) to correlate infiltration characteristics (initial infiltration rate, final infiltration rate and range of infiltration rate) with K_{h_0}.
3. The impact of the systematic difference between infiltrometers and permeaemeters on various hydrological processes need to be investigated in detail.
4. The predominance of soil type on the prediction of spatial variability of hydraulic conductivity needs to be studied further.
5. The usefulness of rectangular hyperbolic method needs to be demonstrated with other types of soils than the one considered in this study.
6. The proposed ANN model needs further modifications by considering larger database with wide variety of surface soils. Based on the extensive database, alternate artificial intelligence techniques can be used for developing the predictive model for near surface near saturated hydraulic conductivity.

References

Ahuja, L. R. (1976), "Measurement hydrologic properties of soil with a double ring infiltrometer and multiple depth tensiometers," *Soil Science Society of America Journal*, 40(4), 494–499.

Al-Shamrani, M.A. (2005), "Applying the hyperbolic method and Ca/Cc concept for settlement prediction of complex organic-rich soil formations", *Engineering Geology*, 77, 17 – 34.

Alagna, V., Bagarello, V., Di Prima, S., Giordano, G., and Iovino, M. (2016), "Testing infiltration run effects on the estimated water transmission properties of a sandy-loam soil", *Geoderma*, 267, 24–33.

Alagna, Bagarello, Di Prima, Guaitoli, Iovino, Keesstra, Cerdà and Artemi (2019), "Using Beerkan experiments to estimate hydraulic conductivity of a crusted loamy soil in a Mediterranean vineyard", *Journal of Hydrology and Hydromechanics*, 67(2), 191-200.

Alizadehtazi, B., DiGiovanni, K., Foti, R., Morin, T., Shetty, N.H., Montalto, F.A. and Gurian, P.L. (2016), "Comparison of Observed Infiltration Rates of Different Permeable Urban Surfaces Using a Cornell Sprinkle Infiltrometer", *Journal of Hydrologic Engineering ASCE*, 21(7). 06016003.

Angulo-Jaramillo, R., Vandervaere, J.-P., Roulier, S., Thony, J.-L., Gaudet, J.-P., and Vauclin, M. (2000), "Field measurement of soil surface hydraulic properties by disc and ring infiltrometers: A review and recent developments", *Soil and Tillage Research*, 55, 1–29.

Angulo-Jaramillo, R., Elrick, D., Parlange, J. Y., Gerard-Marchant, P., and Haverkamp, R. (2003), "Analysis of short-time single-ring infiltration under falling-head conditions with gravitational effects", *Hydrology Days Proc.*, 16–23.

Angulo-Jaramillo, R., Bagarello, V., Iovino, M., and Lassabatere, L. (2016), "Infiltration Measurements for Soil Hydraulic Characterization", *Springer International Publishing*, 43–180.

Ankeny, M. D., Ahmed, M., Kaspar, T. C., and Horton, R. (1991), "Simple field method for determining unsaturated hydraulic conductivity," *Soil Science Society America Journal*, 55, 467-470.

Assouline, S., Tavares-Filho, J., and Tessier, D., (1997), "Effect of Compaction on Soil Physical and Hydraulic Properties: Experimental Results and Modeling", Soil *Society of America Journal*, 61, 390-398.

Assouline, S. (2013), "Infiltration into soils: Conceptual approaches and solutions.", *Water Resources Research*, 49, 1755–1772.

ASTM D 3385 (2009), "Standard Test Method for Infiltration Rate of Soils in Field Using Double-Ring Infiltrometer", *ASTM International*, West Conshohocken, PA.

ASTM D 2487 (2011), "Standard Practice for Classification of Soils for Engineering Purposes (Unified Soil Classification System)", *ASTM International, West Conshohocken, PA.*

ASTM D 854 (2014), "Standard Test Methods for Specific Gravity of Soil Solids by Water Pycnometer", *ASTM International*, West Conshohocken, PA.

ASTM D 6938 (2015), "Standard Test Methods for In-Place Density and Water Content of Soil and Soil-Aggregate by Nuclear Methods (Shallow Depth)", *ASTM International, West Conshohocken, PA.*

ASTM D 5856 (2015), "Standard Test Method for Measurement of Hydraulic Conductivity of Porous Material Using a Rigid-Wall, *Compaction-Mold Permeameter", ASTM International*, West Conshohocken, PA,

ASTM D 7928 (2017), "Standard Test Method for Particle-Size Distribution (Gradation) of Fine-Grained Soils Using the Sedimentation (Hydrometer) Analysis", *ASTM International*, West Conshohocken, PA.

ASTM D 2216 (2010), "Standard Test Methods for Laboratory Determination of Water (Moisture) Content of Soil and Rock by Mass. *ASTM International*, West Conshohocken, PA.

ASTM D 698 (2012), "Standard Test Methods for Laboratory Compaction Characteristics of Soil Using Standard Effort" *ASTM International*, West Conshohocken, PA.

ASTM D 6836 (2016), "Standard Test Methods for Determination of the Soil Water Characteristic Curve for Desorption Using Hanging Column, Pressure Extractor, Chilled Mirror Hygrometer, or Centrifuge", *ASTM International*, West Conshohocken, PA.

Babak, O. (2014), "Inverse distance interpolation for facies modeling", *Stoch Environ Res Risk Assess*, 28, 1373–1382.

Bagarello, V., and Giordano, G. (1999), "Comparison of procedures to estimate steady flow rate in field measurement of saturated hydraulic conductivity by the Guelph permeameter method", *J. Agric. Eng. Res*. 74, 63–71.

Bagarello, V., Di Prima, S., and Iovino, M. (2014), "Comparing alternative algorithms to analyze the beerkan infiltration experiment", *Soil Sci. Soc. Am. J.* 78(3), 724-736.

Bean, E.Z., Hunt, W.F., and Bidelspach, D.A. (2007), "Field survey of permeable pavement surface infiltration rates", *Journal of Irrigation and Drainage Engineering,* 133(3), 249–255.

Berry, K. J., and Mielke, P. W. (1992), "A family of multivariate measures of association for nominal independent variables", *Educational and Psychological Measurement, 52*(1), 41-55.

Beven, K., and Binley, A. (1992), "The future of distributed models: model calibration and uncertainty prediction", *Hydrological Processes,* 6, 279–298.

Bivand, R.S., Muller, W., and Reder, M. (2009), "Power calculations for global and local Moran's I", *Computational Statistics and Data Analysis,*53, 2859–2872.

Bodhinayake, W., Si, B.C., and Noborio, K. (2004), "Determination of hydraulic properties in sloping landscapes from tension and double-ring infiltrometers", *Vadoze Zone Journal,* 3(3), 964–970.

Boissonnat, J.D., and Cazals, F. (2002), "Smooth surface reconstruction via natural neighbor interpolation of distance functions", *Computational Geometry,* 22,185–203.

Bouwer, H. (1969), "Planning and interpreting soil permeability measurements" *J. Irrig. Drain. Div., Proc. Am. Soc. Civil Eng.,* 95(3), 391-402.

Bouwer, H. (1986), "Intake rate: Cylinder infiltrometer - Methods of soil analysis. Part 1, A. Klute, ed., 2nd Ed.", *American Society of Agronomy and Soil Science Society of America (ASA and SSSA), Madison, WI,* 825–844.

Brazdzionyte, J., and Macas, A., (2007), "Bland-Altman analysis as an alternative approach for statistical evaluation of agreement between two methods for measuring hemodynamics during acute myocardial infarction," *Medicina (Kaunas),* 43(3), 208-214.

Brebbia, C.A., and Walker, S., (1980), "Boundary Element Techniques in Engineering," *Newnes–Butterworths, London,* 210.

Brouder, S.M., Hofmann, B.S., and Morris, D.K. (2005), "Mapping soil pH: accuracy of common soil sampling strategies and estimation techniques", *Soil Sci Soc Am J*, 69, 427–442.

Brown, R. A., and Borst, M. (2014), "Evaluation of surface infiltration testing procedures in permeable pavement systems", *Journal of Environmental Engineering*, 140 (3), 04014001.

Buckingham, E. (1907), "Studies on the movement of soil moisture", *U.S. Dept. Agr. Bur. Soils Bull.* 38.

Buckland, G.D. (1988), "Graph for estimating field scale hydraulic conductivity sampling requirements", *Can. Agric. Eng.*, 30, 323-324.

Burgy, R. H., and Luthin, J. N. (1956), "A test of the single-ring and double-ring types of infiltrometers."*Trans. Am. Geophys. Union*, 37(2), 189–191.

Burian, S., Nix, S., Durrans, S., Pitt, R., Fan, C., and Field, R. (1999), "Historical development of wet-weather flow management", *Journal of water resource planning and management, ASCE*, 125, 1(3), 3-13.

Burrough, P.A. (1987), "Principles of Geographical Information Systems for Land Resources Assessment", *Clarendon Press*, Oxford, 147 – 165.

Burrough, P.A., and McDonnell, R.A. (1998), "Principles of Geographical Information Systems", *Oxford University Press*, Oxford, 333.

Carsel, R. F. and Parrish R. S. (1988), "Developing joint probability distribution of soil water retention characteristics," *Water Resources Research*, 24, 755-769.

Chahinian, N., Moussa, R., Andrieux, P., and Voltz, M. (2006), "Accounting for temporal variation in soil hydrological properties when simulated surface runoff on tilted plots*", Journal of hydrology*, 326, 135-152.

Chen, Y. (2013), "New Approaches for Calculating Moran's Index of Spatial Autocorrelation" *PLoS ONE*, 8(7), e68336.

Chidley, T.R.E., and Keys, K.M. (1970), "A Rapid Method of Computing Areal Rainfall", *Journal of Hydrology*, 12, 15-24.

Cho, C.M. (1971), "Convective transport of ammonium with nitrification in soil," *Canadian Journal of Soil Science*, 51(3), 339–350.

Chow, V.T., Maidment, D.R., and Mays, L.W. (1988), "Applied Hydrology", *McGraw-Hill*, USA.

Christianson, R.D., Hutchinson, S.L., and Brown, G.O. (2016), "Curve Number Estimation Accuracy on Disturbed and Undisturbed Soils" *Journal of Hydrologic Engineering*, 21(2), 04015059.

Chu, X., and Marino M. A. (2005), "Determination of ponding condition and infiltration into layered soils under unsteady rainfall", *Journal of Hydrology*, 313, 195-207.

Chung, S.G., Kweon, H.J., and Jang, W.Y. (2014), "Hyperbolic Fit Method for Interpretation of Piezocone Dissipation Tests, *Journal of Geotechnical and Geoenvironmental Engineering*, 140(1), 251-254.

Constantz, J., Herhelrath, W.N., and Murphy, F. (1988), "Air encapsulation during infiltration," *Soil Science society of America Journal*, 52, 10-16.

Corradini, C., Melone, F., and Smith, R.E. (2000), "Modeling local infiltration for a two layered soil under complex rainfall pattern", *Journal of Hydrologic Engineering, ASCE*, 237, 58-73.

Cramer, J. S. (1987), "Mean and variance of R^2 in small and moderate samples", *Journal of Econometrics*, 35, 253-266.

Dagadu, J. S., and Nimbalkar, P.T. (2012), "Infiltration studies of different soils under different soil conditions and comparison of infiltration models with field data", *International Journal of Advanced Engineering Technology*, 3(2), 154-157.

Das, S.K., and Basudhar, P.K. (2008), "Prediction of residual friction angle of clays using artificial neural network", *Engineering Geology*, 100, 142–145

Das SK, Samui, P., Sabat, A.K., and Sitharam, T.G. (2010), "Prediction of swelling pressure of soil using artificial intelligence technique", *Environ Earth Sci.,* 61, 393–403.

Das, S.K., Samui, P., and Sabat, A.K. (2011), "Application of artificial intelligence to maximum dry density and unconfined compressive strength of cement stabilized soil", *Geotech Geol Eng.*, 29, 329–342.

Das, S.K., Samui, P., and Sabat, A.K. (2012), "Prediction of field hydraulic conductivity of clay liners using an artificial neural network and support vector machine", *Int J Geomech,* 12, 606–611.

David, M. F., César, G., C. (2009), "New method for monitoring soil water infiltration rates applied to a disc infiltrometers", *Journal of Hydrology*, 379, 315-322.

De Luca, D.L., and Cepeda, J.M. (2016), "A procedure to obtain analytical solutions of 1D Richards' equation for infiltration in two-layered soils", *J. Hydrol. Engg.* 21(7), 04016018.

Demuth, H.B., and Hagan, M.T. (1996), "Neural network design", *PWS Publishing Company*, Boston.

Di Prima, S., Concialdi, P., Lassabatere, L., Angulo-Jaramillo, R., Pirastru, M., Cerdà, A., and Keesstra, S. (2018), "Laboratory testing of Beerkan infiltration experiments for assessing the role of soil sealing on water infiltration", *Catena*, 167, 373-384.

Dirk, S. M., Carlson, D. D., Cherkauer, D. S., and Malik, P. (1999), "Scale dependency of hydraulic conductivity in heterogeneous media," Ground Water, 37(6), 904–919.

Dohnal, M., Dusek, J., and Vogel, T. (2010), "Improving Hydraulic Conductivity Estimates from Minidisk Infiltrometer Measurements for Soils with Wide Pore-Size Distributions", *Soil Science Society of America Journal*, 74(3), 804–811.

El-Ehwany, M. and Houston, S. L. (1990) "Settlement and Moisture Movement in Collapsible Soils," *Journal of Geotechnical Engineering*, 7, 162-167.

Elrick, D.E., Reynolds, W.D., and Tan, K.A. (1989), "Hydraulic conductivity measurements in the unsaturated zone using improved well analyses", *Ground Water Monit. Rev.*, 9(3), 184-193.

Elrick, D.E., and Reynolds, W.D. (1992), "Methods of analyzing constant head well permeameter data", *Soil Sci. Soc. Am. J.*, 56, 320-323.

Elrick, D. E., Parkin, G. W., Reynolds, W. D., and Fallow, D. J., (1995), "Analysis of early-time and steady-state single-ring infiltration under falling head conditions", *Water Resour. Res.*, 31(8), 1883–1893.

Fatehnia, M., Tawfiq, K., and Ye, M. (2016), "Estimation of saturated hydraulic conductivity from double-ring infiltrometer measurements", *European Journal of Soil Science*, 67 (2), 135-147.

Faybishenko, B. (1999), "Comparison of laboratory and field methods for determining the quasi-saturated conductivity of soils," *Proceedings of the International workshop on characterization and measurement of Unsaturated porous media*, 279-292.

Fodor, N., Sándor, R., Orfanus, T., Lichner, L., and Rajkai, K. (2011), "Evaluation method dependency of measured saturated hydraulic conductivity", *Geoderma*, 165, 60–68.

Fok, Y.S. (1970), "One-dimensional infiltration into layered soils", *Journal of Irrigation and Drainage Div*ision, 96(2), 121-129.

Franke, R. (1982), "Smooth Interpolation of Scattered Data by Local Thin Plate Splines", *Computer and Mathematics with Applications*, 8(4), 273–281.

Fredlund, D.G., and Rahardjo, H. (1993), "Soil Mechanics for Unsaturated Soils", *John Wiley and Sons, Inc.*

Gadi, V. K. Tang, Y. R. Das, A. Monga, C. Garg, A. Berretta, C. and Sahoo, L. (2017), "Spatial and temporal variation of hydraulic conductivity and vegetation growth in green infrastructures using infiltrometer and visual technique," *Catena*, 155, 20-29.

Gardner, W. (1958), "Some steady-state solutions of the unsaturated moisture flow equation with application to evaporation from a water table". Soil Sci., 85, 228 – 232.

Garg, A., Li, J., Hou, J., Berretta, C., and Garg, A. (2017), "A new computational approach for estimation of wilting point for green infrastructure", *Measurement,* 111, 351–358.

Garson, G.D. (1991), "Interpreting neural-network connection weights", *Artif Intell Expert*, 6(7), 47–51.

Getis, A. (2009), "Spatial weights matrices", *Geographical Analysis* 41 (4), 404–410.

Ghaboussi, J., Sidarta, D.E., and Lade, P.V. (1994), "Neural network based modelling in geomechanics. In: Computer methods and advances in geomechanics", Rotterdam *Publishing*, Balkema, 153–164.

Gibbons, J. A. (1985), "Shrinkage formulas for two nominal level measures of association", *Educational and Psychological Measurement, 45*(3), 551-566.

Gibbons, J. D. (1993), "Nonparametric measures of association", *Thousand Oaks, CA: Sage Publications.*

Goh, A.T.C., Kulhawy, F.H., and Chua, C.G. (2005), "Bayesian neural network analysis of undrained side resistance of drilled shafts", *Journal of Geotechnical and Geo-Environmental Engineering. ASCE*, 131(1), 84–93.

Grayson, R., Blöschl, G. (2001), "Spatial Patterns in Catchment Hydrology: Observations and Modelling", *Cambridge University Press.*

Green, S. B., and Salkind, N. J. (2010), "Using SPSS for Windows and Macintosh: Analyzing and Understanding Data (5th ed.)", *Pearson Education, Inc.* Upper Saddle River, NJ.

Hachum, A.Y., and Alfaro, J.F. (1980), "Rain infiltration into layered soils: Prediction", *Journal of Irrigation and Drainage Division*, 106(4), 311-319.

Hanks, R.J., and Bowers, S.A. (1962), "Numerical solution of the moisture flow equation for infiltration into layered soils", *Soil Science Society of America Journal*,26, 530-534.

Haverkamp, R., Ross, P. J., Smettem, K., R., J., and Parlange, J. Y., (1994), "Three–dimensional analysis of infiltration from the disc infiltrometers", *Water Resource Research*, 30, 2931-2935, https://doi.org/10.1029/94WR01788.

Haverkamp, R., Arrúe, J., Vandervaere, J., Braud, I., Boulet, G., Laurent, J., Taha, A., Ross, P., Angulo-Jaramillo, R. (1996), "Hydrological and thermal behaviour of the vadose zone in the area of Barrax and Tomelloso (Spain): Experimental study, analysis and modeling" *Project UE n. EV5C-CT 92*, 00–90.

Haverkamp, R., Bouraoui, F., Zammit, C., Angulo-Jaramillo, R., and Delleur, J.W. (1999), "Soil properties and moisture movement in the unsaturated zone - In J.W. Delleur (ed.)", *The handbook of groundwater engineering*, 2931–2935, CRC, Boca Raton, FL.

Haverkamp, R., Leij, F, Fuentes, C., Sciortino, A., Ross, P. (2005), "Soil Water Retention", *Soil Science Society of America Journal - SSSAJ*. 69.

Hayashi, M., and Quinton, W. L. (2004), "A constant-head well permeameter method for measuring field-saturated hydraulic conductivity above an impermeable layer" *Can. J. Soil Sci.* 84, 255–264.

Hembd, J., and Infanger, C.L. (1981), "An Application of Trend Surface Analysis to a Rural-Urban Land Market", *Land Economics, University of Wisconsin Press*, 57(3), 303-332.

Higgins, J. P. T., White, I. R., and Anzures-Cabrera, J., (2008), "Meta-analysis of skewed data: Combining results reported on log-transformed or raw scales," *Statistics in Medicine*, 27(29), 6072-6092.

Hillel, D., and Gardner, W.R. (1970), "Measurement od unsaturated conductivity and diffusivity by infiltration through an impending layer", *Soil Science*, 109, 149-153.

Hillel, D., (1998), "Environmental Soil Physics", *Academic Press*, 771.

Homolák, M., Capuliak, J., Pichler, V., and Lichner, L. (2009), "Estimating hydraulic conductivity of a sandy soil under different plant covers using minidisk infiltrometer and a dye tracer experiment", *Biologia*, 64(3), 600–604.

Hornung, U., and Messing, W. (1981), "Simulation of two-dimensional saturated/unsaturated flows with an exact water balance*," In: Verruijt, A., Barends, F.B.J. (Eds.), Flow and Transport in Porous Media, Balkema, Rotterdam*, 91–96.

Hsu, S. M., Ni, C. F., and Hung, P.F. (2002), "Assessment of Three Infiltration Formulas based on Model Fitting on Richards Equation ", *Journal of Hydrologic Engineering, ASCE*, 7(5), 373-379.

Huang, C.-C., Hsieh, H.-Y., and Hsieh, Y.-L. (2014), "Hyperbolic models for a 2-D backfill and reinforcement pullout", *Geosynthetics International*, 21(3), 168 – 178.

Hutchinson, M.F. (1993), "On thin plate splines and kriging. In: Tarter ME, Lock MD (eds) Computing and science in statistics", University *of California, Berkeley*

Indian Standard Methods of Tests for Soils, (1975), IS: 2720 (Part XXIX), *Bureau of Indians Standards.*

Isaaks, E.H., and Srivastava, R.M. (1989), "An introduction to applied geostatistics" *1st edn, Oxford University Press, New York*

Jacques, D., Mohanty, B.P., and Feyen, J. (2002), "Comparison of alternative methods for deriving hydraulic properties and scaling factors from single-disc tension infiltrometer measurements", *Water Resources Research*, 38(7), 25-1-25-14.

Jiang, G., Noonan, M., J., Buchan, G., D., and Smith, N. (2005), "Transport and deposition of *Bacillus subtilis* through an intact soil column", *Australian Journal of Soil Research*, 43(6), 695-703.

Journel, A.G., and Huijbregts, C.J. (1978), "Mining Geostatistics", *Academic Press*, 600.

Kodesova, R., Simunek, J., Nikodem, A., and Jirku, V. (2010), "Estimation of the dual permeability model parameters using tension disk infiltrometer and Guelph permeameter," *Vadoze Zone Journal*, 9, 213-225.

Köhne, J.M., Alves Júnior, J., Köhne, S., Tiemeyer, B., Lennartz, J., Kruse (2011), "Double-ring and tension infiltrometer measurements of hydraulic conductivity and mobile soil regions," *Pesquisa Agropecuária Tropical*, 41, 336-347.

Kostiakov, A. N. (1932), "On the dynamics of the coefficient of water-percolation in soils and on the necessity for studying it from a dynamic point of view for purposes of amelioration", *Transactions Congress International Society for Soil Science*, 6th, Moscow, Part A: 17-21.

Kraemer, H. C. (2000), "Measures of association", *In Encyclopedia of psychology, American Psychological Association*, 5, 135-139.

Kravchenko, A.N. (2003), "Influence of spatial structure on accuracy of interpolation methods*", Soil Sci Soc Am J,* 67, 1564–1571.

Krieger, A. M., and Green, P. E. (1993), "Generalized measures of association for ranked data with an application to prediction accuracy" *Journal of Classification, 10*(1), 93-114.

Krouwer, J.S. (2002), "Setting performance goals and evaluating total analytical error for diagnostic assays", *Clin Chem*, 48(6),919–927.

Kruizinga, S., and Yperlaan, G.J. (1978), "Spatial Interpolation of Daily Total of Rainfall", *Journal of Hydrology*, 36, 65-73.

Kumar, S., Sekhar, M., Reddy, D.V., and Mohan Kumar, M.S. (2010), "Estimation of soil hydraulic properties and their uncertainty: comparison between laboratory and field experiment", *Hydrological Processes*, 24(23), 3426–3435.

Lassabatère, L., Angulo-Jaramillo, R., Soria Ugalde, J.M., Cuenca, R., Braud, I., and Haverkamp, R. (2006), "Beerkan estimation of soil transfer, parameters through infiltration experiments – BEST", *Soil Sci. Soc. Am. J.*, 70, 521-532.

Lassabatere, L., Di Prima, S., Angulo-Jaramillo, R., Keesstra, S., and Salesa, D. (2019), "Beerkan multi-runs for characterizing water infiltration and spatial variability of soil hydraulic properties across scales", *Hydrological Sciences Journal*, 64(2), 165-178.

Latorre, B., Moret-Fernández, D., and Peña, C. (2013), "Applications and Challenges Estimate of soil hydraulic properties from disc infiltrometer three-dimensional infiltration curve: theoretical analysis and field applicability", Procedia Environmental Sciences, 19, 580 – 589.

Latorre, B., Peña, C., Lassabatere, L., Angulo-Jaramillo, R., and Moret-Fernández, D. (2015), "Estimate of soil hydraulic properties from disc infiltrometer three-dimensional infiltration curve: Numerical analysis and field application", *Journal of Hydrology*, 527, 1-12.

Ledoux, H., and Gold, C.M. (2004), "An efficient natural neighbour interpolation algorithm for geoscientific modeling", *In Developments in Spatial Data Handling—11th International Symposium on Spatial Data Handling, Edited by: Fisher, P. F. Berlin: Springer*, 97–108.

Lee, R. S., Welker, A. L., and Traver, R. G. (2016), "Modeling Soil Matrix Hydraulic Properties for Variably-Saturated Hydrologic Analysis", *Journal of Sustainable Water in the Built Environment*, 2(2).

Li, X., Chen, G., and Lu, L. (2000), "Comparison of spatial interpolation methods", *Advances in Earth Sciences*, 15 (3), 260 -265.

Li, J., and Heap, A.D. (2011), "A review of comparative studies of spatial interpolation methods in environmental sciences: Performance and impact factors", Ecological *Informatics*, 6, 228–241.

Lin, R. F., and Wei, K. Q. (2006), "Tritium profiles of pore water in the Chinese loess unsaturated zone: Implications for estimation of ground-water recharge", Journal *of Hydrology*, 328(1), 192–199.

Loaiciga, H. A., and Huang, A. (2007), "Ponding Analysis with Green-and-Ampt Infiltration", *Journal of Hydrologic Engineering, ASCE*, 109(1), 62-70.

Logsdon, S. D., and Jaynes, D. B., (1993), "Methodology for Determining Hydraulic Conductivity with Tension Infiltrometers," *Soil Science Society of America Journal*, Vol. 57, 1426-1431.

Lu, N., and Likos, W.J. (2004)," Unsaturated Soil Mechanics". *John Wiley and Sons, Inc*., 417-459.

Luna-Saez, D., Sanchez-Reyes, C., and Munozpardo, J. (2005), "Methods for measuring field-saturated hydraulic conductivity", *Tecnología y Ciencias Del Agua, Jiutepec*, 20(2), 95-107.

Malaya, C., and Sreedeep, S. (2016), "Evaluation of Different Laboratory Procedures for Determining Suction–Water Content Relationship of Cohesionless Geomaterials", *J. Mater. Civ. Eng.*, 28(2), 04015123.

Marshall, T.J., and Stirk, G.B. (1950), "The effect of lateral movement of water in soil on infiltration measurements", *Australian Jour.Agr. Research*, 1, 253-265.

Marquardt, D.W. (1963), "An algorithm for least squares estimation of nonlinear parameter", *Journal of Society Ind. Applied Math*, 11, 431-441.

MathWorks (2001), "Matlab user's manual -Version 2015A", *The MathWorks, Inc*., Natick.

McCardle, B. H. (2003), "Lines, models, and errors: Regression in the field", *Limnology and Oceanography*, 48, 1363-1366.

McKenzie, N., Coughlan, K., and Cresswell, H. (2002), "Soil Physical Measurement and Interpretation for Land Evaluation", *CSIRO Publishing*.

Merino-Martín, L. , Commander, L., Mao, Z., Stevens, J., C., Miller, B., P., Golos, P., J., Mayence, C., E., and Dixon, K. (2017), "Overcoming topsoil deficits in restoration of semiarid lands: Designing hydrologically favourable soil covers for seedling emergence", *Ecological Engineering*, 105, 102–117.

METER Environment (2018), "Minidisk Infiltrometer User's Manual", *METER Environment*, Pullman, USA 24.

Mezencev, V. J. (1948), "Theory of formation of the surface runoff", *Meteorologiae Hidrologia*, 3, 33-40.

Mishra, A.K., Kumar, B., and Dutta, J. (2016), "Prediction of hydraulic conductivity of soil bentonite mixture using hybrid-ANN approach", *J Environ Inf.*, 27(2), 98–105.

Mishra, S.K., Tyagi, J.V., and Singh, V.P. (2003), "Comparison of infiltration models", *Hydrol. Process.* 17(13), 2629–2652.

Mitas, L., and Mitasova, H. (1988), "General Variation Approach to the Interpolation Problem", *Computer and Mathematics with Applications*, 16 (12), 983–992.

Moran, P.A.P. (1948), "The interpretation of statistical maps", *Journal of the Royal Statistical Society, Series B*, 37(2), 243–251.

Morbidelli, R., Saltalippi, C., Flammini, A., Cifrodelli, M., Picciafuoco, T., Corradini, C., and Govindaraju, R.S. (2017), "In situ measurements of soil saturated hydraulic conductivity: Assessment of reliability through rainfall–runoff experiments," *Hydrological Processes*, 31, 2017, 3084–3094.

Moret-Fernández, D., and González-Cebollada, C. (2009), "New method for monitoring soil water infiltration rates applied to a disc infiltrometers, Journal *of Hydrology*, 379, 315–322.

Moyeed, R.A., and Papritz, A. (2002), "An empirical comparison of kriging methods for nonlinear spatial point prediction", *Math Geol* 34, 365–386.

Mualem, Y. (1976), "A new model for predicting the hydraulic conductivity of unsaturated porous media", *Water resources research*, 12(3), 513-522.

Mubarak, I., Mailhol, J.C., Angulo-Jaramillo, R., Ruelle, P., Boivin, P., and Khaledian, M., (2009b), "Temporal variability in soil hydraulic properties under drip irrigation", *Geoderma*, 150, 158–165.

Mueller, T.G., Pusuluri, N.B., Mathias, K.K., Cornelius, P.L., Barnhisel, R.I., and Shearer, S.A. (2004), "Map quality for ordinary kriging and inverse distance weighted interpolation*", Soil Sci Soc Am J,* 68, 2042– 2047.

Munoz-Carpena, R., Regalado, C.M., Alvarez-Benedi, J., and Bartoli, F. (2002), "Field evaluation of the new Philip-Dunne permeameter for measuring saturated hydraulic conductivity, *Soil Sci.*, 167 (1), 9–24.

Nestingen, R. P. E., Asleson, B. C., Gulliver, J. S. Hozalski, R. M. and Nieber, J. L. (2018), "Laboratory Comparison of Field Infiltrometers," *Journal of Sustainable Water in the Built Environment*, 4 (3), 201804018005.

Neuman, S.P. (1973), "Saturated-unsaturated seepage by finite elements," *Proceedings of ASCE, Journal of Hydraulics*, 2233–2250.

Nielsen, D. R., Biggar, J.W., and Erh, K. T. (1973), "Spatial variability of field-measured soil-water properties," *Hilgardia*, 42, 215- 260.

Ohtani, K., (1994), "The density function of R^2 and $\overline{\mathbf{R^2}}$ and their risk performance under asymmetric loss in misspecified linear regression models", *Economic Modelling*, 11, 463-71.

Olden, J.D., Joy, M.K., and Death, R.G. (2004), "An accurate comparison of methods for quantifying variable importance in artificial neural networks using simulated data", *Ecological Modelling*, 178, 389–397.

Oliver, M.A., and Webster, R. (1990), "Kriging: a method of interpolating for geographical information system", *International Journal of Geographical Information System*, 4(3), 313 - 332

Petry, T. M., and Jiang, C. P. (2007), "Soil Suction and Behavior of Chemically Treated Clays", *Transportation Research Record*, *2026*(1), 30–38.

Philip, J. (1957), "The theory of infiltration: 4. Sorptivity and algebraic infiltration equations", *Soil sci*, 84, 257–264.

Philip, J.R. (1969), "Theory of infiltration", *Advances in Hydro science*, 5, 215-305.

Pitt, R., Chen, S.E., Clark, S.E., Swenson, J., and Ong, C.K. (2008), "Compaction's impacts on Urban Storm-Water Infiltration", *Journal of irrigation and drainage engineering*, 134(5), 652-658.

Pitt, R., Lantrip, J., Harrison, R., Henry, C.L., Xue, D., and O'Connor T.P. (1999), "Infiltration through Disturbed Urban Soils and Compost-Amended Soil Effects on Runoff Quality and Quantity", *USEPA*, Washington DC.

Pollalis, E. and Valiantzas, J. (2014), "Isolation of a 1D Infiltration Time Interval under Ring Infiltrometers for Determining Sorptivity and Saturated Hydraulic Conductivity: Numerical, Theoretical, and Experimental Approach," *J. Irrig. Drain Eng.*, 04014050.

Qashu, H.K. (1969), "Infiltration and Water Depletion in Lysimeters", *Soil Sci. Soc. Amer. Proc.*, 33, 775-778.

Quan, H., and Zhang, J., (2003), "Estimate of standard deviation for a log-transformed variable using arithmetic means and standard deviations," *Statistics in Medicine*, 22, 2723-2736.

Raoof, M., Sadraddini, A. A., Nazemi, A.H., and Marofi, S. (2009), **"**Estimating saturated and unsaturated hydraulic conductivity and sorptivity coefficient in transient state in sloping lands," *Journal of Food, Agriculture & Environment*, 7(3, 4), 861-864.

Rasoulzadeh, A., and Fatemi, M., (2011), "Scaling of cumulative infiltration curves using pedotransfer functions", *International Conference on New Technology of Agricultural Engineering (ICAE 2011), IEEE*, China.

Revol, P., Clothier, B.E., Mailhol, J.C., Vachaud, G., and Vauclin, M. (1997), "Infiltration from a surface point source and drip irrigation 2. An approximate time-dependent solution for wet-front position", *Water Resour Res.*, 33(8),1869–1874.

Reynolds, W. D., and Elrick, D. E. (1990), "Ponded infiltration from a single ring. I: Analysis of steady state flow", *Soil Sci. Soc. Am. J.*, 54(5), 1233–1241.

Reynolds, W. D., and Elrick, D. E. (1991), "Determination of Hydraulic Conductivity Using a Tension Infiltrometer," *Soil Science Society of America Journal*, 55 (3), 633-639.

Reynolds, W. D., Elrick, D. E. and Clothier, B.E. (1985), "The constant head well permeameter: Effect of unsaturated flow", *Soil Sci.*, 139, 172–180.

Reynolds, W.D., and Elrick, D.E. (1985), "In situ measurement of field-saturated hydraulic conductivity, sorptivity and α-parameter using the Guelph permeameter", *Soil Sci.*, 140, 292-302.

Reynolds, W.D., Elrick, D.E., and Youngs, E.G. (2002), "Single-ring and double-or-concentric-ring infiltrometer. In: Dane, JH; Topp, GC (Eds.). Methods of soil analysis", *Soil Sci. Soc. Am.*, 821-826.

Richards, L. A. (1931), "Capillary conduction through porous mediums", *Physics 1,* 313-318.

Richards, L.A., Gardner, W.R., and Ogata, G. (1956), "Physical processes in determining water loss in soil", *Soil Sci. Soc. Am. Proc*., 20, 310-314.

Robson, S.M. (1997), "Spherical methods for spatial interpolation: review and evaluation", *Cartography and Geographic Information System*, 24(1),3-20.

Romano, N., Brunone, B., and Santini, A. (1998), "Numerical analysis of one-dimensional unsaturated flow in layered soils", *Advances in Water Resource*, 21, 315-324.

Ronayne, M.J., Houghton, T.B., and Stednick, J.D. (2012), "Field characterization of hydraulic conductivity in a heterogeneous alpine glacial till", *J Hydrol,* 458–459,103–109.

Salverda, A.P., and Dane, J.H., (1993), "An examination of the Guelph permeameter for measuring the soil's hydraulic properties", *Geoderma Elsevier*, 57(4), 405–421.

Samani, Z., Cheraghi, A., and Willardson, L. (1989), "Water movement in horizontally layered soils." *J. Irrig. Drain. Eng.*, 115(3), 449–456.

Samjstrla, A. G., and Harrison, D. S. (1998), "Tensiometer for soil moisture measurements and irrigation scheduling." Dept. of Agricultural and Biological Engineering, Florida Cooperative Extension Service, Institute of Food and Agricultural Sciences, Univ. of Florida, Gainesville, FL.

Saraiva, J. P., Lima, B. S., Gomes, V. M., Flores, P. H. M., Gomes, F. A., Assis, A. O., Reis, M. R. C., Araujo, W. R. H., Abrenhosa, C., and Calixto, W. C. (2017), "Calculation of sensitivity index using one-at-a-time measures based on graphical analysis", *18th International Scientific Conference on Electric Power Engineering (EPE), IEEE*, 17-19 May 2017, Czech Republic.

Schuhmann, R., KöNiger, F., Emmerich, K., Stefanescu, E., and Stacheder, M. (2011), "Determination of hydraulic conductivity based on (soil)-moisture content of fine grained soils." *Hydraulic conductivity-issues, determination and applications, InTech. Rijeka,* 165-188.

Serrano, S.E. (1990), "Modeling Infiltration in hysteretic soils", *Advances in Water Resource*, 13(1), 12-23.

Sharma, M. L., Gander, G.A., and Hunt, C.G. (1980), "Spatial variability of infiltration in a watershed", *Journal of Hydrology,* 45(1-2), 101-122.

Sibson, R. (1981), "Interpolating Multivariate Data: Chapter 2: A Brief Description of Natural Neighbor Interpolation", *John Wiley & Sons,* New York.

Sihag, P., Tiwari, N.K., and Ranjan, S. (2017), "Estimation and inter-comparison of infiltration models", *Water Sci,* 31(1),34–43.

Simunek, J., and van Genuchten, M.T. (1996), "Estimating soil hydraulic properties from tension disc infiltrometer data by numerical inversion." *Water Resour. Res.*,32, 2683–2696.doi: 10.1029/96WR01525.

Simunek, J., van Genuchten, M. T., Gribb, M. M. and Hopmans J. W. (1998), "Parameter estimation of unsaturated soil hydraulic properties from transient flow processes," *Soil & Tillage Research,* 47, 27-36.

Smettem, K. R.J., Parlange, J. Y., Ross, P. J., and Haverkamp, R. (1994), "Three dimensional analysis of infiltration from the disc infiltrometer - A capillary-based theory", *Water Resour. Res.,* 30, 2925-2929, https://doi.org/10.1029/94WR01787.

Smith, R.E (1972), "The Infiltration Envelope: Results from a Theoretical Infiltrometer", *Journal of Hydrology,* 17, 1-21.

Springer, P.E., and Cundy, T.W. (1987), "Field-scale evaluation of infiltration parameters from soil texture for hydrologic analysis", *Water Resources Research,* 23(2), 325–334.

Srivastava, R., and Yeh, J.T.C. (1991), "Analytical solutions for one-dimensional, transient infiltration towards water table in homogeneous and layered soils", *Water Resource Research,* 27, 753-762.

Stannard, D. I. (1994), "Tensiometers—Theory, construction, and use", *Geotech. Test. J.*, 15(1), 48–58.

Stauffer, F., and Dracos, T. (1986), "Experimental and numerical study of water and solute infiltration in layered porous media", *Journal of Hydrologic Engineering, ASCE,* 84,9-34.

Swartzendruber, D., and Olson, T. C. (1961a), "Model study of the double ring infiltrometer as affected by depth of wetting and particle size," *Soil Sci.*, 92(4), 219–225.

Swartzendruber, D., and Olson, T. C. (1961b), "Sandy-model study of buffer effects in the double ring infiltrometer," *Soil Sci. Soc. Am. Proc.*, 25(1), 5–8.

Tang, Y.B. (2002), "Comparison of semivariogram models for Kriging monthly rainfall in eastern China", *Zhejiomj University Science,* 3(5), 584- 590.

Tarantino, A., and Tombolato, S., (2005), "Coupling of hydraulic and mechanical behaviour in unsaturated compacted clay," *Géotechnique,* 55 (4), 307-317.

Tension Infiltrometer, 2825K1 Tension Infiltrometer, *Soil moisture Equipment Corporation, USA.*

Touma, J., Voltz, M., and Albergel, J. (2007), "Determining soil saturated hydraulic conductivity and sorptivity from single ring infiltration tests," *Eur. J. Soil Sci.*, 58(1), 229–238

Tricker, A. S. (1978), "Infiltration cylinder—some comments on its use," *Journal of Hydrology*, 36(3–4), 383–391.

Usowicz, B., and Lipiec, J. (2017), "Spatial variability of soil properties and cereal yield in a cultivated field on sandy soil", *Soil and Tillage Research*, 174, 241-250.

Valiantzas, J.D. (2010), "New linearized two-parameter infiltration equation for direct determination of conductivity and sorptivity," *Journal of Hydrology*, 384 (1-2) 1–13.

van Dam, J., C., and Feddes, R., A., (2000), "Numerical simulation of infiltration, evaporation and shallow groundwater levels with the Richards equation", Journal *of Hydrology*, 233, 72-85.

van Genuchten, G., Mallants, D., Ramos, J., Deckers, J.A., and Feyen, J. (1996), "Estimating Infiltration parameters from basic soil properties", *Hydrological processes*, 10, 687-701.

Van Genuchten, M.T. (1980), "A closed-form equation for predicting the hydraulic properties of unsaturated soils", Soil *Science Society America Journal*, 44, 892-898.

Vanderlinden, K., Gabriels, D., and Giráldez, J.V. (1998), "Evaluation of infiltration measurements under olive trees in Córdoba", *Soil Tillage Res.*, 48, 303–315.

Vandervaere, J. P., Vauclin, M., and Elrick, D. E. (2000a), "Transient flow from tension infiltrometers I. The two-parameter equation", *Soil Science Society of America Journal*, 64 (4), 1263–1272.

Vandervaere, J. P., Vauclin, M., and Elrick, D. E. (2000b), "Transient Flow from Tension Infiltrometers II. Four Methods to Determine Sorptivity and Conductivity", *Soil Science Society of America Journal*, 64, 1272–1284.

Venkatesh, V., Brown, S., and Bala, H. (2013), "Bridging the qualitative-quantitative divide: Guidelines for conducting mixed methods research in information systems", *MIS Quarterly*, 37,21-54.

Verbist, K., Torfs, S., Cornelis, W., M., Oyarzún[c], R., Soto, G. and Gabriels, D. (2010), " Comparison of Single- and Double-Ring Infiltrometer Methods on Stony Soils," *Vadose Zone Journal*, 9(2), 462-475.

Verbist, K.M.J., Cornelis, W.M., Torfs, S., and Gabriels, D. (2013), "Comparing Methods to Determine Hydraulic Conductivities on Stony Soils", *Soil Sci. Soc. Am. J.*, 77, 25-42.

Viji, V.K., Lissy, K.F., Sobha, C., and Benny, M.A. (2013), "Predictions on compaction characteristics of fly ashes using regression analysis and artificial neural network analysis" *Int J Geotech Eng*. 7(3), 282–291.

Vrettas, M., D., and Fung, I.Y. (2015), "Toward a new parameterization of hydraulic conductivity in climate models: Simulation of rapid groundwater fluctuations in Northern California", *Journal of Advances in Modeling Earth Systems*, 7, 2105–2135.

Wagenet, R.J., Biggar, J.W., Nielsen, D.R. (1976), "Analytical solutions of miscible displacement equations describing the sequential microbiological transformations of urea, ammonium and nitrate", *Research Report no. 6001, Department of Water Science and Engineering*, University of California, Davis, 53.

Wahba, G. (1990), "Spline models for observational data. In: CBMSNSF regional conference series in applied mathematics", *Society for Industrial and Applied Mathematics*, Philadelphia, 169.

Wang, D., Yates, S.R., Lowery, B., and van Genuchten, M. T. (1998), "Estimating soil hydraulic properties using tension infiltrometer with varying disc diameters," *Soil Science*, 163(5), 356-361.

Wang, Q.J., Horton, R., and Fan, J. (2009) "An Analytical Solution for One-Dimensional Water Infiltration and Redistribution in Unsaturated Soil", *Pedosphere*, 19(1), 104-110.

Warrick, A.W. (1992), "Models for disk infiltrometers", *Water Resour. Res.*, 28(5), 1319–1327.

Warrick, A.W., and Nielsen, D.R. (1980) "Spatial Variability of Soil Physical Properties in the Field, In D. Hillel, (ed.) Applications of Soil Physics ed.", *Academic Press*, New York.

Watson, P. F., and Petrie, A., (2010), "Method agreement analysis: A review of correct methodology," *Theriogenology*, 73, 1167-1179.

Webb, B.W., Clack, P. D., and Walling, D. E. (2003), "Water–air temperature relationships in a Devon river system and the role of flow," *Hydrological Processes*, 17(15), 2003, 3069–3084.

Webster, R., and Oliver, M. (2001), "Geostatistics for Environmental Scientists*", John Wiley & Sons, Ltd, Chichester*, 271.

Weir. G.J. (1987), "Steady infiltration from small shallow circular ponds", *Water Resources Research*, 23(4), 733–736.

Whisler, F.D., and Klute, A. (1966), "Analysis of infiltration into stratifies soil columns", *Proceed IAHS symposium on water in the unsaturated flow*, Wageningen, The Nederland, 451-470.

Whitaker, A., Alila, Y., Beckers, J. and Toews, D. (2003), "Application of the distributed hydrology soil vegetation model to Redfish Creek, British Columbia: Model evaluation using internal catchment area", *Hydrol. Proc*. 17, 199–224.

White, I., and Sully, M.J. (1987), "Macroscopic and Microscopic capillary length and time scales from field infiltration", *Water resource Research*, 23, 1514-1522.

White, I., Sully, M. J., and Perroux K. M. (1992), "Measurement of surface-soil hydraulic properties: Disc permeameters, tension infiltrometers, and other techniques*," Advances in Measurement of Soil Physical Properties: Bringing Theory in to Practice, Madison, Wisconsin, USA, soil science society of America*.

Wilcox, R. R. (2007), "Local measures of association: Estimating the derivative of the regression line". *British Journal of Mathematical and Statistical Psychology*, 60, 107-117.

Woltemade, C.J. (2010), "Impact of Residential Soil Disturbance on Infiltration Rate and Stormwater Runoff", *Journal of the American Water Resources Association*, 46,700-711.

Wooding, R.A. (1968), "Steady infiltration from large shallow circular pond", *Water Resource Research*, 4, 1259-1273.

Wu, L., Pan, L., Roberson, M. J., and Shouse, P. J. (1997), "Numerical evaluation of ring infiltrometers under various soil conditions," *Soil Sci.*, 162(11), 771–777.

Xu, X., Lewis, C., Liu, W., Albertson, J.D., and Kiely, G. (2012), "Analysis of single-ring infiltrometer data for soil hydraulic properties estimation: comparison of BEST and Wu methods", *Agricultural Water Management*, 107, 34–41.

Yamsani, S., K., Sreedeep, S., and Rakesh, R.R. (2016), "Frictional and Interface Frictional Characteristics of Multi-Layer Cover System Materials and Its Impact on Overall Stability". *International Journal of Geosynthetics and Ground Engineering*, 2, 23.

Yilmaz, D., Lassabatère, L., Angulo-Jaramillo, R., Deneele, D., Legret, M. (2010), "Hydrodynamic characterization of basic oxygen furnace slag through an adapted BEST method", *Vadose Zone Journal*, 9, 1-10.

Youngs, E.G. (1968), *"*An estimation of sorptivity for infiltration studies from moisture moment considerations*" Soil Science Society of America Journal*, 106(3), 157-163.

Zhang, C., Chen, B., and Wu, L. (1995), "Geographic Information System", *Higher Education Press*, Beijing, 71 – 79.

Zhang, R. (1997a), "Determination of soil sorptivity and hydraulic conductivity from the disk infiltrometer." *Soil Science Society of America Journal*, 61, 1024-1030.

Zhang, R. (1997b), "Infiltration models for the disk infiltrometer." *Soil Science Society of America Journal*, 61, 1597-1603.

Zhang, R. (1998), "Estimating soil hydraulic conductivity and macroscopic capillary length from the disk infiltrometer," *Soil Science Society of America Journal*, 62, 1513-1521.

Zhang, R. and van Genuchten, M.T. (1994), "New models for unsaturated soil hydraulic properties", *Soil Sci*., 158, 77-85.

Zhang, S., Grip, H., and Lovdahl, L. (2006), "Effect of soil compaction on hydraulic properties of two loess soils in China", *Soil and Tillage Research*, 90, 117–125.

Zhou, S. M., Warrington, D., N., Lei, T.-W., Lei, Q.-X., and Zhang, M.-L. (2015), "Modified CN Method for Small Watershed Infiltration Simulation", *Journal of Hydrological Engineering*, 20(9), 04014095.

Zienkiewicz, O.C., Pareck, C.J. (1970), "Transient field problems: two-dimensional analysis by isoperimetric finite element," *International Journal for Numerical Methods in Engineering 2*, 61–71.

List of Publications

Journals

Published

1. Ghosh, B., and Sreeja, P. (2019), "Effect of Initial Compaction State on Near-Saturated Hydraulic Conductivity", Journal of Irrigation and Drainage, ASCE, 145(12), 1-10. 04019028.
2. Ghosh, B., Sreeja, P., and Yamsani, S.K. (2019), "Evaluation of infiltrometers and permeameters for measuring hydraulic conductivity", ACEM-ASTM, 8(1), 308-321.
3. Ghosh, B., and Sreeja, P. (2019), "A critical evaluation on the variability induced by different mathematical equations on hydraulic conductivity determination using disc infiltrometers", Acta Geophysica, 67(3), 863-877, https://doi.org/10.1007/s11600-019-00266-6.
4. Ghosh, B., and Sreeja, P. (2019), "An appraisal on the interpolation methods used for predicting spatial variability of field hydraulic conductivity", Water Resources Management, Springer, 33(6), 2175-2190. DOI: 10.1007/s11269-019-02248-1.
5. Ghosh, B., and Sreeja, P. (2019), "A critical evaluation of measurement induced variability in infiltration characteristics for a river sub-catchment", Measurement, 132, 47–59. DOI: 10.1016/j.measurement.2018.09.018.
6. Naik, A. P., Ghosh, B., and Sreeja P. (2019), "Estimating soil hydraulic properties using mini disc infiltrometer", ISH Journal of Hydraulic Engineering, Taylor and Francis, 25, (1), 62-70.

Under Review

1. Ghosh, B., and Sreeja, P. "Estimation procedure for near surface hydraulic conductivity based on disc infiltrometer measurements", Journal of Hydrologic Engineering, ASCE.

Conferences

1. Naik, A. P., Ghosh, B., and Sreeja P. (2017), "Estimating soil hydraulic properties using mini disc infiltrometer", HYDRO, Dec. 8-10, CWPRS, Pune, India.
2. Ghosh, B., and Sreeja, P. (2016), "Influence of drainage conditions on infiltration characteristics determined using disc infiltrometers", 21st International conference on

Hydraulics, Water Resources, Coastal Engineering, HYDRO, Dec. 8-10, CWPRS, Pune, India.

3. Ghosh, B., and Sreeja, P. (2014), "Comparative study of double ring and tension infiltrometers to measure infiltration properties and hydraulic conductivity", 19th International conference on Hydraulics, Water Resources, Coastal and Environmental Engineering, Dec. 18-20, Manit, Bhopal, India.